Assessment of synthetic chalcones as cancer chemopreventive agents

By

Hiba Abbas Jasim

A thesis submitted in partial fulfilment of the requirements of Liverpool John Moores University for the degree of Doctor of Philosophy

October 2019

Dedication

To the place where the writing was initiated

My country

"Mesopotamia" Iraq

To my family

Mom and Dad

Brothers and Sisters

Acknowledgements

First and foremost, thanks to **Allah** for all your blessings, guidance and help in giving me the health and strength to complete this thesis.

This work will not have been possible without a financial support of **The Iraqi Ministry of Higher Education and Scientific Research** and its representative in the United Kingdom **the Iraqi Cultural Attaché** in London through **The College of Education for Pure Sciences- University of Anbar-Iraq**.

PhD is a rewarding but challenging journey, which would not be possible without the help of many people. I would like to express my deep and sincere gratitude to my supervisors, **Dr Kenneth Ritchie, Prof Satyajit Sarker** and **Dr Sharon Moore** for the constant support that helped to develop my scientific thinking and guidance throughout my candidature. They have built and directed an environment that granted me an opportunity to learn and practise research skills, meet and collaborate with brilliant researchers, and transfer the long journey of PhD to a great experience.

Special thanks to Prof Randolph Arroo and Dr Ketan Ruparelia (De Montfort Universit) for suppling chalcones generously and Prof Roland Wolf (University of Dundee, UK) for providing ARE32 cell line.

I would also like to address my sincere gratitude to the staff of the School of Pharmacy and Biomolecular Sciences for their assistance and help in diverse ways. Specially, Dr Kehinde Ross and Dr Adam Richardson for their assistance with the PCR. I would also like to thank Dr Amos Fatokun, Dr Lutfun Nahar and Dr Darren Sexton for their encouragements and assistance. Any lab work will not done without a lab Research Support Group, so I would like to thank Dr Daniel Graham, Dr John Hall, Dr Jerry Bird, Dr Nicola Browning, Dr Nicola Dempster and Miss Jennifer Thomson for providing

assistance and training during my work in the laboratories, and Ms Angela Lewis for her help and support. I really appreciate all of security staff for their help and patient.

Special thanks go to Georgiana Zavoianu (Liverpool John Moores University) and Dr Farooq Aljubouri (Al-Nahrain University, Iraq) for the training and helping in cell culture. I would like to thank my friends and colleagues Afaf, Shaymaa, Sushmita, Sarayut, Stephanie, Mujtaba, Samare, Ruqayah, Nashwa, and Ruba at Liverpool John Moores University. It has been such a pleasure and a privilege to work with you all.

I would also like to thank my Parents, **Dr Abbas Aldhaibani** and **Widad Al-Rawi**, my brother, **Dr Mohammed** and sisters **Saba and Sura**, who have always supported, encouraged and believed in me, in all my present and future endeavours.

Last but not the least; I would like to give special thanks to my brother, **Dr Omar Aldhaibani** for his continuous moral support throughout my PhD. This journey cannot be completed without his patient, support and encouragement.

ABSTRACT

Cigarette smoking acts as a key source of lung cancer, where the carcinogen malondialdehyde (MDA) produced from cigarette increases the DNA damage. To reduce the carcinogenic effect of MDA researchers are using natural or synthetic compounds as chemopreventive agents to minimise or prevent cancer. In the current research a library of synthetic chalcones were investigated, which were synthesised and kindly gifted by Prof Arroo from De Montfort University (DMU). These chalcones are categorised based on their chemical structures such as alkoxyl group (17 chalcones), methylene-dioxy group (13 chalcones), and methylene-dioxin group (1 chalcone). Nuclear factor erythroid 2-related factor 2 (Nrf2)- antioxidant response element (ARE) pathway play an important role in chemoprevention due to induction of antioxidant defence gene like NQO1 by detoxifying and reducing oxidative stress.

To investigate whether the chalcones can switch on NRF2-ARE pathway, 31 synthetic chalcones were evaluated for (i) their toxicity using thiazolyl blue tetrazolium bromide (MTT) assay, and (ii) chemopreventive activity by luciferase fold induction using luciferase assay through the AREc32 reporter cell line, which includes a luciferase gene linked with ARE drive gene. The results showed that twelve chalcones have induced luciferase around 2-16 fold induction as a consequence of the switch on the Nrf2-ARE pathway. Thereafter, the selected chalcones were investigated for their ability as lung chemopreventive agents against MDA through lung normal cell line MRC-5 and cancer cell line MRC-5 SV2. Firstly, the non-toxic concentrations of chalcones in MRC-5 and MRC-5 SV2 have determined by MTT assay, then the non-toxic concentration of chalcones was examined for their ability to induce NQO1 protein, as a prototype of antioxidant enzymes, in both lung cell lines using Western blot assay. The results showed that chalcones DMU-2210, 1122, 1103 and 2265 were consequently found to be capable

of increasing NQO1 protein level at 24 h in both the cell lines. Also, these twelve chalcones were then examined for their ability to prevent the toxicity of MDA. The results revealed that DMU-1113, 2265, 2210, 2267, 1103, 1122 and 1119 could reduce the toxicity of MDA in MRC-5 cells. However, the DMU-1113, 1122, 2207, 1103, 1119 and 2265 were lead to inhibit the growth of MRC-5 SV2 cells in present of MDA.

The chalcones capable of NQO1 induction and reduction of MDA toxicity were then chosen to continue with the project in cytogenetic and molecular biology. Specifically, chalcones DMU-2210, 1122 and 1103, were chosen as a representative selection of the different activities noted in the library as a whole. They were examined for their ability to reduce the generation of reactive oxygen species (ROS) using intracellular ROS assay and protect DNA against damage by MDA using the comet assay. The results indicated that the three chalcones could reduce ROS levels and also DNA damage by MDA. In addition, the three chalcones were examined for their ability to induce *NRF2* gene expression and consequently *NQO1* gene expression using qPCR protocol, with DMU-1122 and 1103 being capable of this. Finally, to verify the hypothesis that chalcones can prevent MDA induced toxicity due to the switching on of the Nrf2 pathway, *NRF2* gene was knocked down. This was confirmed by qPCR and Western blot protocols through pre-treated MRC-5 cell line with chalcones then MDA, the results showed the *NRF2* gene was successfully knocked down. Simultaneously, MTT assay was used to confirm the chemopreventive activity of chalcones against MDA in MRC-5 knocked down *NFR2* gene. The MTT results showed that DMU-1122 and 2210 could retain the capacity to prevent MDA induced cell toxicity in the absence of *NRF2*. Consequently, it could be inferred that chalcones are capable of inducing other antioxidant defence pathways crucial in the prevention of MDA toxicity.

TABLE OF CONTENTS

LIST OF FIGURES

LIST OF TABLES

LIST OF SCHEMES

LIST OF ABBREVIATIONS

Δ	Delta
ω	Omega
λ	Lambda
$^{\bullet}$OH	Hydroxyl radical
µl	Microlitre
µM	Micromolar
$^{1}O_2$	Singlet oxygen
4-HNE	4-Hydroxy-2-nonenal
6-Oxo-M$_1$dG	3-(2-Deoxy-*β*- d -erythropentofuranosyl)-pyrimido[1,2-f]purine-6,10(3H,5H)-dione
8-OxodG	8-Oxo-7,8-dihydro-2′-deoxyguanosine
α	Alfa
αT-O$^{\bullet}$	α-tocopherol radical
αT-OH	α-tocopherol, Vitamin E
A	Adenine
Am	Ampere
AhR	Arylhydrocarbon receptor
ALT	Alanine aminotransferase
AMPK	AMP-activated protein kinase
ANOVA	Analysis of variance
APS	Ammonium persulfate
ARE	Antioxidant response element
AST	Aspartate transaminase
ATG7	Autophagy related 7
ATP	Adenosine triphosphate
β	Beta
Bcl-2	B-cell lymphoma 2
BSA	Bovine serum albumin

BSEP	Bile salt export pump
BTB	Broad complex Tramtrack and Bric-a-brac
bZIP	Basic-region leucine zipper
C	Cysteine
ºC	Degree celsius
CAR	Constitutive androstane receptor
CAT	Catalase
CDK1	Cyclin-dependent kinase 1
CDK2	Cyclin-dependent kinase 2
cDNA	Complement DNA templet
CO_2	Carbon dioxide
COX-2	Cyclooxygenase-2
C_t	Cycle threshold
Cul3	Cullin3
CYP45	Cytochrome P450
DCFH-DA	2′,7′-Dichlorofluorescin diacetate
DMEM	Dulbecco's Modified Eagle's Medium
DMSO	Dimethyl sulphoxide
DMU	De Montfort University
DNA	Deoxyribonucleic acid
DNPH	Dinitrophenyl hydrazone
dNTPs	Deoxribonucleoside triphosphates
dsDNA	Double strand DNA
dsRNA	Double strand RNA
EBV-EA	Epstein-Barr virus early antigen
ECACC	European Collection of Animal Cell Cultures
EDTA	Ethylenediaminetetraacetic acid
EH	Epoxide hydrolase
EPHX2	Epoxide hydrolase 2
ERK	Extracellular-signal-regulated kinase

ex	Fluorescence excitation wavelengths
em	Fluorescence emission wavelengths
EtOH	Ethanol
F4/80	EGF-like module-containing mucin-like hormone receptor-like 1
FAD	Flavin adenine dinucleotide
FBS	Fetal bovine serum
Fe	Iron
FISH	Fluorescent *in situ* hybridization
FOXM1	Forkhead Box M1
G	Guanine
g	Gram
GADD153	Growth arrest and DNA damage 153
GC/ MS	Gas Chromatography/Mass Spectrometry
GCL	Glutamate cysteine ligase
GLUT1	Glucose transporter 1
GPX	Glutathione peroxidase
GR	Glutathione reductase
GSH	Glutathione
GST	Glutathione s-transferase
H_2O_2	Hydrogen peroxide
HCl	Hydrochloric acid
$HO^{\bullet}_2$	Hydroperoxyl radical
HO-1	Hemoxygenase-1
HPLC	High Performance Liquid Chromatography
HRM	High resolution melt
HSP60	Heat shock protein 60
IARC	International Agency for Research on Cancer
IC_{50}	The half maximal inhibitory concentration
IL-10	Interleukin 10
iNOS	Inducible nitric oxide synthase

IVR	Intervening region
JNK	Jun N-terminal kinases
kDa	Kilodalton.
Keap1	Kelch-like ECH-associated protein 1
KOH	Potassium hydroxide,
L•	Lipid radical
LAR	Luciferase Assay Reagent
LC/ MS	Liquid Chromatography/Mass Spectrometry
LDH	Lactate dehydrogenase
LH	Polyunsaturated fatty acid
LL	Lipid dimer
LO_2•	Lipid peroxyl radical
LOOH	Lipid hydroperoxide
LOX	Lysyl oxidase
LPO	Lipid peroxidation
M_1dA	Malondialdehyde-deoxyadenosine
M_1dC	Malondialdehyde-deoxycytidine
M_1dG	Malondialdehyde-deoxyguanosine
MAPK	Mitogen-activated protein kinase
MCP	Monocyte chemoattractant protein
MDA	Malondialdehyde
Mef	Small musculoaponeurotic fibrosarcoma
MEM	Minimum Essential Medium
METC	Mitochondrial electron transport chain
Mg	Magnesium
ml	Millilitre
mm	Millimetre
mM	Millimolar
MMP	Matrix metalloproteinase
mRNA	Messenger RNA

MRP	Multidrug resistance protein
mtDNA	Mitochondrial DNA
mTOR	Mammalian target of rapamycin
MTT	Thiazolyl blue tetrazolium bromide
MW	Microwave
Myt1	Myelin Transcription Factor 1
NaCl	Sodium chloride
NAD	Nicotinamide adenine dinucleotide
NADPH	Nicotinamide adenine dinucleotide phosphate
NaOH	Sodium hydroxide
NEAA	Non-essential amino acid
NF-κB	Nuclear factor kappa-light-chain-enhancer of activated B cells
NMOR1	NADH-menadione reductase
NO	Nitrogen oxide
NOX	Nicotinamide adenine dinucleotide phosphate oxidase
NQO1	NAD(P)H: quinone oxidoreductase 1
Nrf2	The Nuclear factor-erythroid 2 p45 subunit-related factor 2
O_2	Dioxygen
$O_2^{\bullet-}$	Superoxide radical
O_3	Ozone
OD	Optical density
$P21^{WAF1}$	Cyclin-dependent kinase inhibitor 1
$P27^{KIP1}$	Cyclin-dependent kinase inhibitor 1B
PARP	Poly-ADP ribose polymerase
PBS	Phosphate buffered saline
PBS-T	Phosphate buffered saline- Tween 20
PCR	Polymerase Chain Reaction
PDBe	Protein Data Bank in Europe
PGH_2	Prostaglandin H_2
PL	Prestained protein Ladder

P-p38	Phospho-p38
PPAR	Peroxisome proliferator-activated receptor
PRX	Peroxiredoxin
PUFA	Polyunsaturated fatty acid
PVDF	Polyvinylidene difluoride
px	Pixel
PXR	Pregnane X receptor
qPCR	Quantitative Polymerase Chain Reaction
RCHO	Aldehydes
RIPA	Radio-immunoprecipitation assay
RISC	RNA-induced silencing complex
RLB	Reporter Lysis Buffer
RNA	Ribonucleic acid
RNAi	RNA interference
RNS	Reactive nitrogen species
$RO^{\bullet}$	Alkoxyl radicals
$RO_2^{\bullet}$	Organic peroxyl radicals
ROOH	Organic hydroperoxides
ROS	Reactive oxygen species
rpm	Revolutions per minute
RT	Reverse transcriptase
s	Second
SDS	Sodium dodecyl sulfate
SDS-PAGE	Sodium dodecyl sulfate polyacrylamide gel electrophoresis
siRNA	Small interfering RNA
SKP-2	S-phase kinase-associated protein 2
SOD	Superoxide dismutase
SV40	Simian virus 40
T	Thymine
TBA	2-Thiobarbituric acid

TBAR	Thiobarbituric Acid Reactive
***t*-BHQ**	*Tert*-Butylhydroquinone
TEMED	*N,N,N,N*- Tetramethylethylenediamine
TMP	1,1,3,3-Tetramethoxypropane
Tris	Trizma base
TRX	Thioredoxin
U	Uracil
UGT	Uridyl glucuronosyl transferase
UGT1A1	UDP-glucuronosyltransferase 1A1
UV	Ultraviolet
V	Voltage
x g	X Gravity

Chapter 1 **Introduction**

1.1 Cancer

Cancer is increasingly recognised as a serious worldwide public health concern. A report by the WHO (2018) shows that approximately 9.6 million deaths worldwide occurred by cancer in 2018, and they list that the most common cancers were lung, breast, colorectal, prostate, skin and stomach. Moreover, they show that lung cancer was the most common type of cancer that leads to death (Figure **1.1**). Cancer may also develop due to a variety of different risk factors such as lifestyle, infections, exposure to occupational pollutants, and genetics factors (Knowles and Selby, 2005). Katzke *et al.* (2015) listed smoking cigarette, alcohol consumption, obesity, diet, non-physical activity and hormonal factors as the main features of lifestyle that can induce cancer. Moreover, it has been reported that smoking cigarettes are the highest leading cause of cancer (Cancer Research UK, 2019).

Cancer has been defined as unusual cell growth and prevalence under uncontrolled conditions (WHO, 2018), and is assumed not to be a single disease as there are a variety of different categories, depending on the cell, tissue and organ that cancer emerges in. For example, cancers that originate from epithelial transforming cells are called "carcinoma", such as colon, skin, prostate, breast, pancreas, stomach and lung. Cancers that originate from the fibroblasts of mesenchymal tissues are called "sarcoma" such as muscle and bone tumours. In addition, myelomas, leukaemias, and lymphomas are related to hematopoietic organs, finally, the tumour of neural cells called "neuroectodermal" and that sub-categorise into neurofibrosarcoma, neuroblastoma, neuroma, melanoma and glioblastoma (Robert, 2015).

A

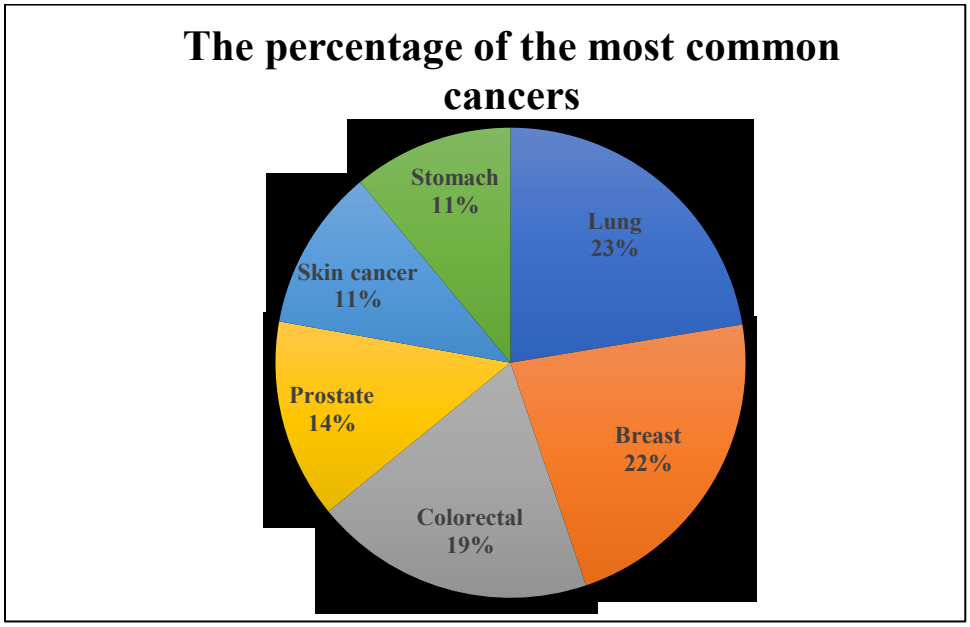

B

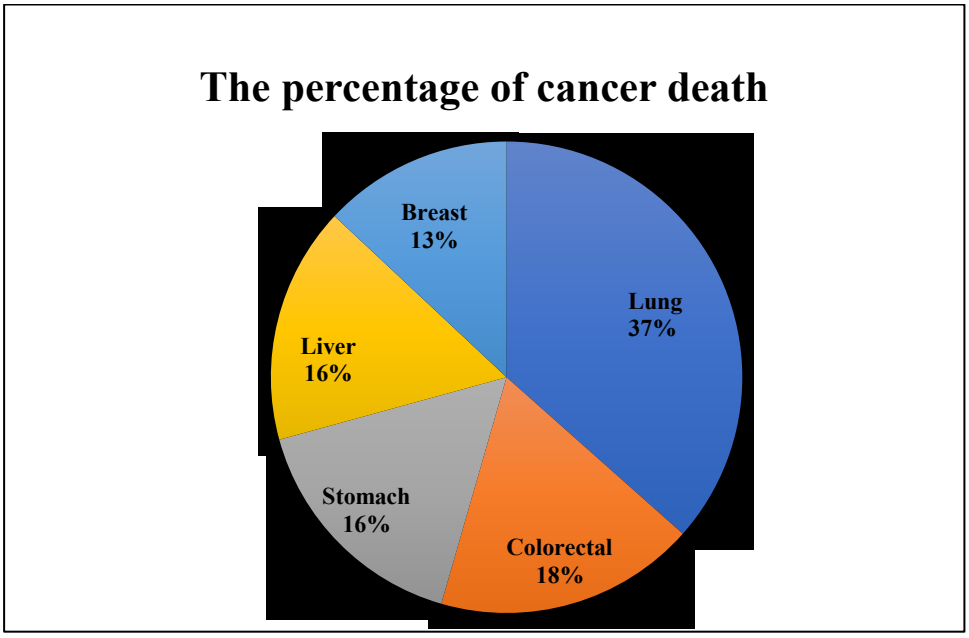

Figure 1.1 Shows the percentage of (A) the most common cancer and (B) cancer mortality in 2018 worldwide (WHO, 2018).

It is assumed that a number of cancers arise through a proliferation of one single aberrant cell by several stages. The processes to transform a normal cell to cancer has three stages (Figure **1.2**):

a- Initiation stage

The first stage might be induced by carcinogenic agents such as chemicals, viruses, radiation, UV light and replication errors inducing deoxyribonucleic acid (DNA) mutations, due to destroy specific gene in the stem cell of relating tissue (Franks, 1997; Tung *et al.*, 2019). The initiation stage occurs when the proliferating cell has a short period to repair DNA damage (Oliveira *et al.*, 2007). This stage features genotoxic, mutation, non-reversible and DNA modification, but is not sufficient to produce cancer (Klaassen and Watkins, 2015).

b- Promotion stage

In this stage, the initiated cells are encouraged to divide by interfering with cell differentiation (Tung *et al.*, 2019). In addition, a cell proliferation agent will accelerate cell proliferation in vulnerable tissues, helping repair gene variation, promote modification of gene expression and bring about alteration in growth control of the cell (Oliveira *et al.*, 2007). Additionally, promoters have no direct DNA modification capacity, can cause multiple cell divisions, decrease apoptosis and are reversible (Klaassen and Watkins, 2015).

c- Progression stage

In this stage, the tumour cells gain further multiple mutations, which affect critical pathways, for example, the tumour suppressor p53 is mutated in 50% of cancers at this point and will lead to mutant the cells by ruling the population of the tumour. This process is named “clonal selection” because the mutant cells can raise some properties such as growth rate, survival, invasion and metastasis (Cooper and Hausman, 2009). At this stage, DNA is modified by genotoxic agents, mutation, disarrangement of chromosomes, irreversible and the pre-neoplastic cell will be transformed to a malignant cell (Oliveira *et al.*, 2007; Klaassen and Watkins, 2015).

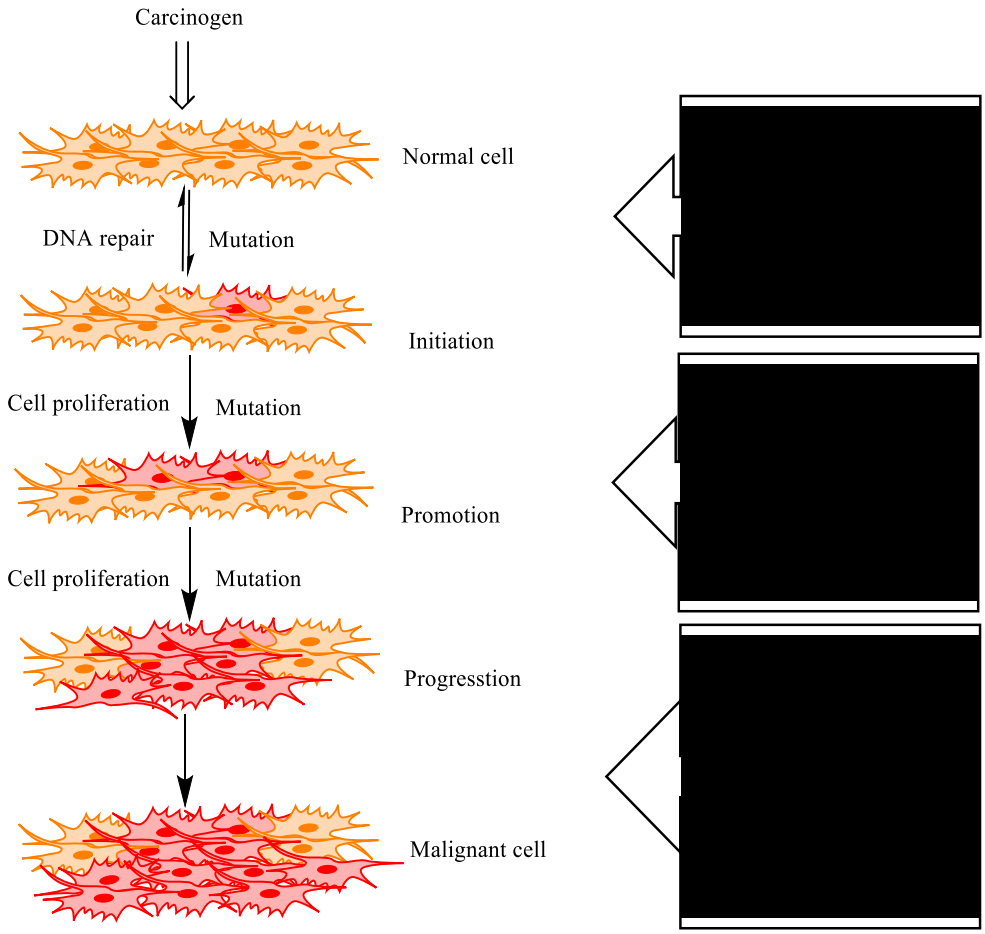

Figure 1.2 The processes of transforming a normal cell to cancer, which induced by carcinogens, including three stages: initiation, promotion and progression

1.1.1 Lung cancer

Lung cancer is the most common cancer worldwide with 23% with the highest mortality rate (37%) (Figure **1.1**). The American Cancer Society has reported that lung, bronchus and trachea cancer were the highest leading death in men (1.2 million) and the second leading death in women (576,100) in 2018. Factors that cause lung cancer include cigarette smoking, exposure to radon gas, air pollution, diesel exhaust, chemicals, metals and radiation. From all of that, tobacco smoking causes the highest number of lung cancer deaths worldwide with approximately 75% of deaths in men and 50% in women in 2018 (American Cancer Society, 2018).

The lung is in direct contact to the external air, because of this the respiratory tract can get injured during inhalation of contaminated air composed of materials such as cigarette smoke, metals, asbestos, or non-materials such as pesticides, gases, biological agents and volatile organic. Inhaled substances can remain for a lifetime in the lung owing to the damage in the clearance system, which leads to lung injury such as fibrosis, chronic obstructive pulmonary disease and cancer (Gupta, 2019). In addition, lung cancer is classified into small cell carcinoma (20%) derived from epithelial cell or non-small carcinoma such as adenocarcinoma (glandular, 30%), large cell carcinoma (25%), and squamous cell carcinoma (25%) derived from stem cell (Oie and Gazdar, 2000; King and Robins, 2006).

Exposure to pollutants can induce variations in the apoptosis pathway such as Tp53, $p16^{INK}$, Bcl2, Rb, ras, myc and telomerase. Additionally, it is thought that tobacco substances induce *Tp53* mutation in the lungs that include transition mutation such as G:C to A:T , A:T to G:C, deletions, insertions or other types of mutation (King and Robins, 2006; Best and Sutherland, 2018).

1.2 Lifestyle

There is epidemiological evidence to indicate that lifestyle factors play an important role in causing cancer. It is thought that 90% of cancer incidents are associated with lifestyle and environment. Lifestyle factors including smoking, diet and alcohol consumption can cause cancer (Figure **1.3**), as well as pollution, UV, obesity, infections and stress (Anand *et al.*, 2008; Parkin *et al.*, 2011).

1.1.1.1. **Smoking**

Cigarette smoking is reported as an extensive risk factor of cancer. It caused 33% of cancer worldwide (Cancer Research UK, 2019). This is due to cigarettes containing many carcinogenic chemicals, for instance, polycyclic aromatic hydrocarbons, aromatic amines, nitrosamines, acrylonitrile, acrylamide, benzene and nicotine (IARC, 2004; Ritchie *et al.*, 2007). A consequence of tobacco use is the occurrence of many types of cancer such as mouth, pharynx, oesophagus and lung cancer (Ames and Gold 1998). Exposure to tobacco smoke leads to oxidation of membrane phospholipids inducing lipid peroxidation (LPO), increasing free radical species, which is superoxide radical ($O_2^{\bullet}$) and hydroxyl radical ($^{\bullet}OH$), consequently increasing malondialdehyde (MDA) and 4-hydroxy-2-nonenal (4-HNE) (Figure **1.3**) (Rahman and Adcock, 2006; Miao *et al.*, 2019).

1.1.1.2. **Diet**

Diet has been a critical cause related to the occurrence of cancers. In addition, an imbalance of food intake, for example, a large amount of fat or red meat, and low portion of vegetables, fruit and fibres may lead to the incidence of some cancers, for instance, colorectal, endometrial, breast and prostate (Irigaray *et al.*, 2007; Parkin *et al.*, 2011). It is assumed diet that contains ω-6 polyunsaturated fatty acids (PUFA) can induce cancer,

due to increasing cellular oxidative stress and LPO. Thus can form MDA and 4-HNE that might induce free radical mutagen, activate protein kinases, changing the transcription factor, and subsequently inducing damage in DNA and proteins (Figure **1.3**) (Bartsch *et al.*, 1999). However, vegetables intake such as cabbage, broccoli, kale, spinach, carrots, tomato, cucumber, leek, turnip, lettuce and cauliflower is thought to have an anticancer effect as they contain high amounts of minerals, vitamins, fibres and phytochemicals such as terpenes, allyl sulfur, phenols, polyphenols, indoles, isothiocyanates and phytoestrogens that have antioxidant properties (Davis and Ross, 2019).

1.1.1.3. **Alcohol consumption**

It is known that drinking alcohol is also another risk factor for causing cancer. It is responsible for 12.5% of cancer mortality (WHO, 2014), and there is a positive relationship between alcohol consumption and different types of cancers as alcohol consumption increases the incidence of cancers in the mouth, pharynx, esophagus, larynx, breast, colorectal, and liver. It is believed that many of the aforementioned factors result in an increase of processes such as oxidative stress and LPO, leading to the production of toxic compounds like MDA, 4-HNE and acrolein that may be mutagenic and carcinogenic (American Cancer Society, 2018; Ali *et al.*, 2019).

Oxidative metabolism of alcohol produces acetaldehyde and acetate, the latter can bind to microtubules, microsomal proteins, and enzymes. In addition, alcohol impacts on the mitochondria and decreases adenosine triphosphate (ATP) level, rate of respiration, increases reactive nitrogen species (RNS) and reactive oxygen species (ROS), affects xanthine oxidase, cytosolic enzymes, α-ketoglutarate dehydrogenase and aldehyde oxidases cytochrome P450 (CYP450) by increasing $O^{\bullet}_2$ and hydrogen peroxide (H_2O_2). It has been demonstrated that a high intake of alcohol results in damage to proteins, lipids

and DNA through the generation of ROS, acetaldehyde and acetate (Figure **1.3**) (Davis and Ross, 2019).

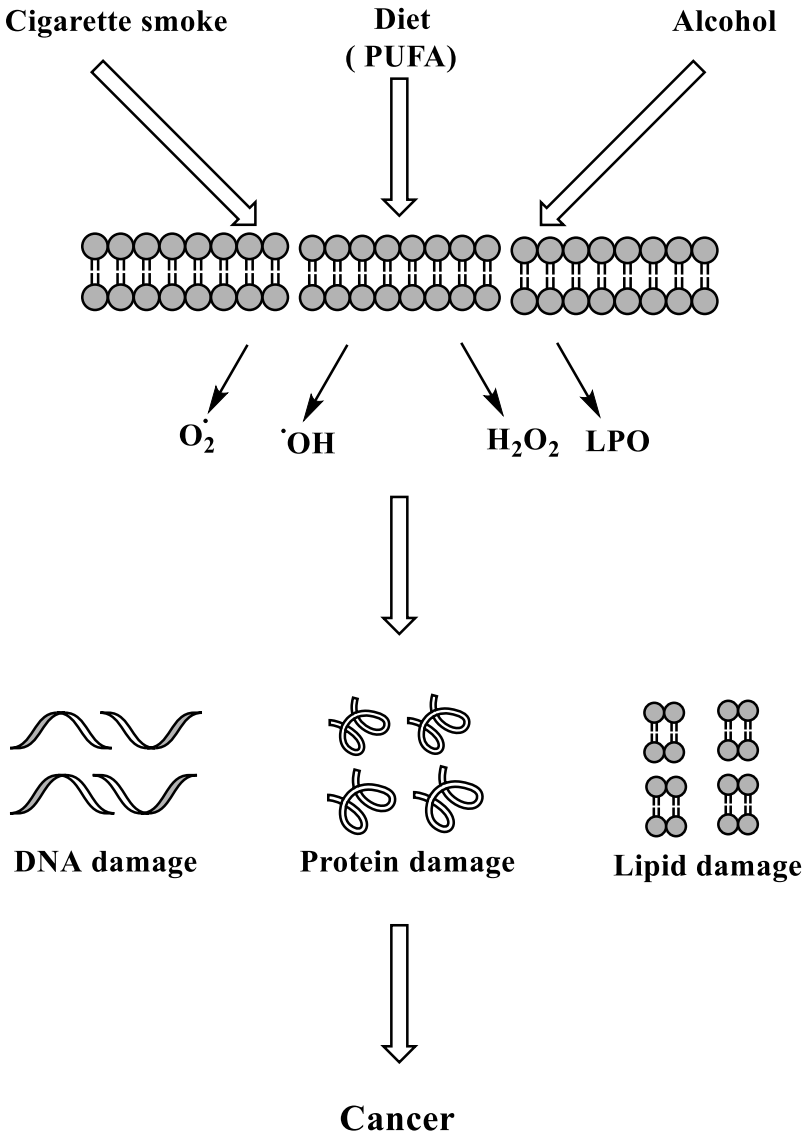

Figure 1.3 The pathway for inducing cancer by smoking, diet and alcohol.

1.3 Oxidative stress

Oxidative stress is a result of an increase in oxidising molecular species and a decrease in antioxidants (Boelsterli, 2007). Additionally, it can occur through energy transfer or electron transfer reactions (Ahmad, 1995). Oxidative stress occurs in the pathogenesis of several diseases, for example, cancer, liver, pancreatic, lung, kidney, cardiovascular diseases and ageing (Rahman *et al.*, 2012). Principally, oxidative stress may happen when the production of free-radicals overtakes the ability of the body to neutralise them (Ad, 2015). Oxidative stress may have an effect on lipids by inducing lipid peroxidation and subsequently forms MDA, 4-HNE and other reaction products, also effect on proteins and DNA by producing DNA adducts that may lead to DNA damage, mutations and induce cancer (Boelsterli, 2007; Ma *et al.*, 2013; Menezo *et al.*, 2016).

According to Rahman *et al.* (2012), oxidative stress can produce the initiation of toxic ROS, where they exceed the average range of free radicals attack in a normal cell which is about 1 x 10^4 –2 x 10^4 radical/ day (Gupte and Mumper, 2009). It is thought that ROS involves: H_2O_2, $O_2^{\bullet-}$, $^{\bullet}OH$, singlet oxygen ($^1O_2$), hydroperoxyl radicals ($HO_2^{\bullet}$), alkoxyl radicals ($RO^{\bullet}$) and organic hydroperoxides (ROOH) that promote DNA oxidation, and may also play an important role in causing cytotoxicity, mutation and DNA damage (De Bont and van Larebeke, 2004; Townsend and Tew, 2014). Electron transfer reactions can generate reactive species such as:

- Superoxide radical ($O_2^{\bullet-}$): it is produced by the transfer of one electron to dioxygen (O_2) (Reaction 1), it performs as a weak base that readily forms a $HO_2^{\bullet}$ (Reaction 2) (Ahmad, 1995):

$$O_2 + e^- \rightarrow O_2^{\bullet-} \text{ ……..(1)}$$

$$O_2^{\bullet-} + H^+ \rightarrow HO_2^{\bullet} \text{ ……..(2)}$$

- Hydrogen peroxide (H_2O_2): it is a non-radical compound, generated by reaction $O_2^{\bullet-}$ with H^+ (Reaction 3) (Ahmad, 1995):

$$2O_2^{\bullet-} + 2H^+ \rightarrow H_2O_2 + O_2 \text{ …….(3)}$$

- Hydroxyl radical ($^{\bullet}OH$): it is a very reactive radical that can induce lipid peroxidation in cell membranes, it is generated by either Haber-Weiss reaction through react $O_2^{\bullet-}$ with H_2O_2 in the presence of a metal catalyse Fe or Cu (Reaction 4) or Fenton type reaction through conjugate Fe^{2+} with H_2O_2 (Reaction 5) (Ahmad, 1995; Smart and Hodgson, 2008).

$$O_2^{\bullet-} + H_2O_2 \xrightarrow{Fe/Cu} O_2 + HO^- + HO^{\bullet} \text{…….....(4)}$$

$$Fe^{2+} + H_2O_2 \rightarrow Fe^{3+} + HO^- + HO^{\bullet} \text{……..(5)}$$

- Peroxyl radicals ($RO_2^{\bullet}$): It is generated by reacting O_2 with carbon centred polymer radicals ($R^{\bullet}$) (Reaction 6) (Marnett, 1991; Ahmad, 1995):

$$R^{\bullet} + O_2 \rightarrow RO_2^{\bullet} \text{ ……..…… (6)}$$

- Hydroperoxides (ROOH): they are generated via the reaction between peroxyl radicals and PUFA (LH) (Reaction 7) (Han *et al.*, 2018):

$$RO_2^{\bullet} + LH \rightarrow ROOH + L^{\bullet} \text{ ……. (7)}$$

It has been determined that ROS may be generated through different sources. The mitochondrial source is the main source of ROS owing to the production of O_2 during the activity of mitochondrial electron transport chain (METC) that consists of several redox catalysts such as cytochromes, flavoproteins, ubiquinone, pyridine nucleotides and iron-sulfur proteins. It is thought that in METC, O_2 undergoes one electron reduction and forming $O_2^{\bullet-}$ and subsequently can convert to H_2O_2. It has been demonstrated that the level of $O_2^{\bullet-}$ and H_2O_2 are elevated in cancer cells compared with normal cells, and that

might occur due to inducing mutation in METC complex and also in mitochondrial DNA (mtDNA). This leads to increase ROS and consequently changes the cell characteristics such as cell proliferation, differentiation, genome variation and cancer progression (Townsend and Tew, 2014).

Nicotinamide adenine dinucleotide phosphate (NADPH) oxidases (NOXs) are another source of ROS. It is believed that the family of NOX enzymes play an important role via forming $O_2^{\bullet-}$ and H_2O_2 by transferring electrons from NADPH to O_2, also they can transduce and mediate reduction–oxidation reaction signals pathway. Moreover, CYP45, peroxisomal metabolism, lysyl oxidase (LOX) and inflammatory reactions that are also associated with elevated production of $O_2^{\bullet-}$ and H_2O_2 (Townsend and Tew, 2014), and consequently increase mutagenic compounds. For example, damaging proteins lead to produce carbonyl group that may interfere with 2,4-dinitrophenylhydrazine and form dinitrophenyl hydrazone (DNPH) (Dalle-Donne *et al.*, 2003), in addition to *N*-terminal valine adducts such as 2-hydroxyethyl-valine and 2-cyanoethyl-valine. Moreover, damaging lipids can generate 4-HNE and MDA, and damaging DNA leads to produce 8-oxo-7,8-dihydro-2′-deoxyguanosine (8-oxodG) and thymidine glycol (Farmer, 2004). Furthermore, MDA may react with DNA and produce DNA adducts such as 3-(2-deoxy-*β*-d-erythro-pentofuranosyl)pyrimido[1,2-α]purin-10(3H)-one (Malondialdehyde-deoxyguanosine (M_1dG)), and 3-(2-deoxy-*β*- d -erythropentofuranosyl)-pyrimido[1,2-f]purine-6,10(3H,5H)-dione (6-oxo-M_1dG) (Figure **1.4**) (Blair, 2008; Wauchope *et al.*, 2018).

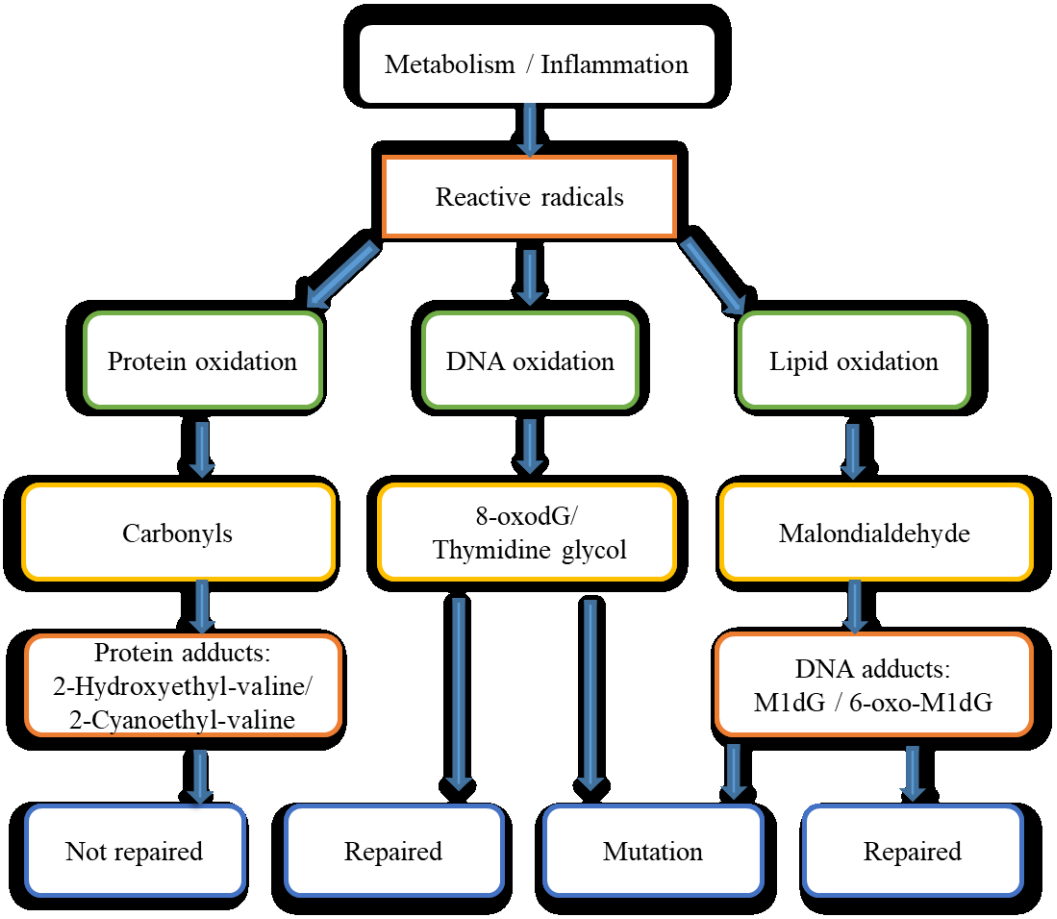

Figure 1.4 The use of damaging lipids, proteins or DNA as biomarkers of oxidative stress and genotoxicity, adopted from Farmer (2004).

Cellular defence against such toxicity may occur by both nonenzymatic and enzymatic antioxidant defence systems, including molecules such as ascorbic acid (vitamin C), α-tocopherol (vitamin E), urate, carotenoids, glutathione (GSH), glutathione S-transferase (GST), superoxide dismutase (SOD), catalase (CAT) and cascade that can terminate the cycle of lipid peroxidation (Ahmad, 1995). Thus, they can regulate intracellular and extracellular redox levels by protecting the cell from oxidative stress that occurs by ROS. It is believed that the steady-state of oxidative metabolism can regulate the gene expression and transduction via transcription factors, phosphatase and redox-sensitive kinases. However, the flux of ROS is increased in cancer cells, because the oxidative

metabolism pathways are disrupted, which leads to upregulate ROS by reductive antioxidant pathways (Townsend and Tew, 2014).

Several studies have examined the correlation between oxidative stress and inducing DNA damage. DNA damage might occur by an increase in the level of ROS that is induced by many factors including arsenic, which is a co-carcinogen (Zhou, 2019), by benzo(a)pyrene and polycyclic aromatic hydrocarbons like retene (Peixoto *et al.*, 2019; Velali *et al.*, 2019). Moreover, oxidative stress has been found to induce DNA damage in agricultural workers due to use of pesticides (Kisby *et al.*, 2009), in benzene-exposed workers (Liu *et al.*, 1996), in lead-exposed workers (Fracasso *et al.*, 2002) and in cigarette smokers (Piperakis *et al.*, 1998; Hininger *et al.*, 2004). Moreover, oxidative stress has been found to increase in pancreatic cancer cells (Zhang *et al.*, 2008; Wason, 2013), lung cancer patients (Misthos *et al.*, 2005), in prostate and bladder cancer patients (Chiou *et al.*, 2003). Meanwhile, ROS have been used as a growth inhibitor and chemopreventive agent due to their ability to induce transcription factors such as Nrf2 and NF-κB (Klaunig *et al.*, 2010) as well as stimulate *Tp53* expression that induces apoptosis (Liu and Xu, 2011). For that reason, many researchers have either inhibited ROS as a chemoprotection of normal cells or induced ROS as inhibitor growth of cancer cells (Ka *et al.*, 2003; Wu, 2005; Zhang *et al.*, 2014).

1.4 Lipid peroxidation

Lipids are one of the biological targets of oxidative stress, and the overall product of the oxidative stress impact on lipids is called “lipid peroxidation”, which results from oxidation of the phospholipids in membrane lipids via free radicals like $^{\bullet}OH$. Besides, hydroperoxyl ($HO^{\bullet}_2$) species, which is a strong oxidant can promote polyunsaturated phospholipids oxidation. This can peroxidise carbon-carbon double bond lipids such as PUFA (Ayala *et al.*, 2014; Angel and Mario, 2017). Membrane lipid peroxidation impacts on membrane features such as nutrient transport, fluidity and permeability of the membrane, lipid-protein, lipid-lipid interaction, pathways of cellular transduction and signalling (Angel and Mario, 2017). According to Ahmad (1995) and Ayala *et al.* (2014), lipid peroxidation has three stages, which are:

1.4.1 Initiation

In this stage, PUFA (LH) donates allylic hydrogen to a hydroxyl radical forming $L^{\bullet}$ at a carbon centre (Reaction 8) (Scheme 1).

$$LH + {}^{\bullet}OH \quad \rightarrow \quad L^{\bullet} + H_2O \ldots\ldots\ldots\ldots (8)$$

1.4.2 Propagation

In this stage, the $L^{\bullet}$ reacts with O_2 forming a lipid peroxyl radical ($LO_2^{\bullet}$) (Reaction 9). The latter may receive a hydrogen atom from a new lipid molecule producing lipid hydroperoxide (LOOH) and another lipid radical (Reaction 10) (Scheme 1). Unless the lipid peroxyl radical is cyclized to generate an intermediate free radical (cyclic peroxide) then produce bicycle endoperoxides. Thereafter, bicycle endoperoxides can generate aldehydes (RCHO) such as MDA and 4-HNE in a present of two molecules of oxygen and metal ions (Fe^{+2}) (Reaction 11).

$$L^{\bullet} + O_2 \rightarrow LO_2^{\bullet} \quad \ldots\ldots\ldots\ldots (9)$$

$$LH + LO_2^{\bullet} \rightarrow L^{\bullet} + LOOH \quad \ldots\ldots\ldots\ldots (10)$$

$$LO_2^{\bullet} + O_2 \rightarrow RCHO \quad \ldots\ldots\ldots\ldots (11)$$

1.4.3 Termination

In this phase, the $L^{\bullet}$ can terminate the process by self-reaction forming a lipid dimer (LL) conjunction (Reaction 12), or it might continue the reaction (Reaction 9). Therefore in this stage antioxidants such as *α*-tocopherol (*α*T-OH) can donate hydrogen to lipid peroxyl radical forming LOOH and an α-tocopherol radical (*α*T-$O^{\bullet}$) (Reaction 13), which can then react with one more $LO_2^{\bullet}$ to form non-radical products (Reaction 14) (Scheme 1).

$$L^{\bullet} + L^{\bullet} \rightarrow L\text{-}L \quad \ldots\ldots\ldots\ldots (12)$$

$$\alpha T\text{-}OH + LO_2^{\bullet} \rightarrow \alpha T\text{-}O^{\bullet} + LOOH \quad \ldots\ldots\ldots\ldots (13)$$

$$\alpha T\text{-}O^{\bullet} + LO_2^{\bullet} \rightarrow \alpha T\text{-}O\text{-}LO_2 \quad \ldots\ldots\ldots\ldots (14)$$

Generally, lipid peroxidation has primary products like lipid hydroperoxides and secondary products, which form during lipid peroxidation process. Thirty-two aldehydes have been found as lipid peroxidation products such propanal, acrolien, MDA, decanal, hexanal, butanal and octanal, as saturated aldehydes; undecenal, decenal, nonenal, octenal and hexenal as 2,3-*trans*-unsaturated-aldehydes and a chain of 4-hydroxylated,2,3-*trans*-unsaturated aldehydes like 4-HNE and 4-hydroxyundecenal. It has reported that MDA, acrolien and 4-HNE are the more important products of lipid peroxidation. These can react with cellular thiols and free amino groups of proteins, and consequently effect on cell signalling proteins, enzymes such as hexokinase, glyceraldehyde-3-phosphate

dehydrogenase, lactate dehydrogenase, aldolase, glucose-6-phosphatase, 5′-nucleotidase and DNA polymerases and also on metabolic pathways such as calcium pumps, glycolysis, mitochondrial functions, protein synthesis, cell differentiation, proliferation, apoptosis, ribonucleic acid (RNA) and DNA (Salvayre *et al.*, 2002; Repetto *et al.*, 2012). It is assumed that MDA has a high mutagenic effect, while 4-HNE has a high toxicant effect, however, acrolien has more effects on proteins (Ayala *et al.*, 2014; Taso *et al.*, 2019).

Several studies have used MDA and 4-HNE as biomarkers of lipid peroxidation. León *et al.* (2019) have examined the effect of lifestyle, occupation, dietary and sociodemographic in adipose tissue by measuring MDA level as a biomarker of lipid peroxidation. Another researcher has used MDA as a biomarker of the effect of ozone (O_3) on cardiovascular diseases (Day, 2017). Moreover, MDA and 4-HNE have been measured to determine liver injury induced by alcohol (Sampey *et al.*, 2003), as well as a loss of body weight induced by cigarette smoke (Ardite *et al.*, 2006). Moreover, acrolein has been measured to determine the biological effect of lifestyle agents like cigarette smoke and heated oils on a human cholesterol regulator apolipoprotein E (Tamamizu-Kato *et al.*, 2007).

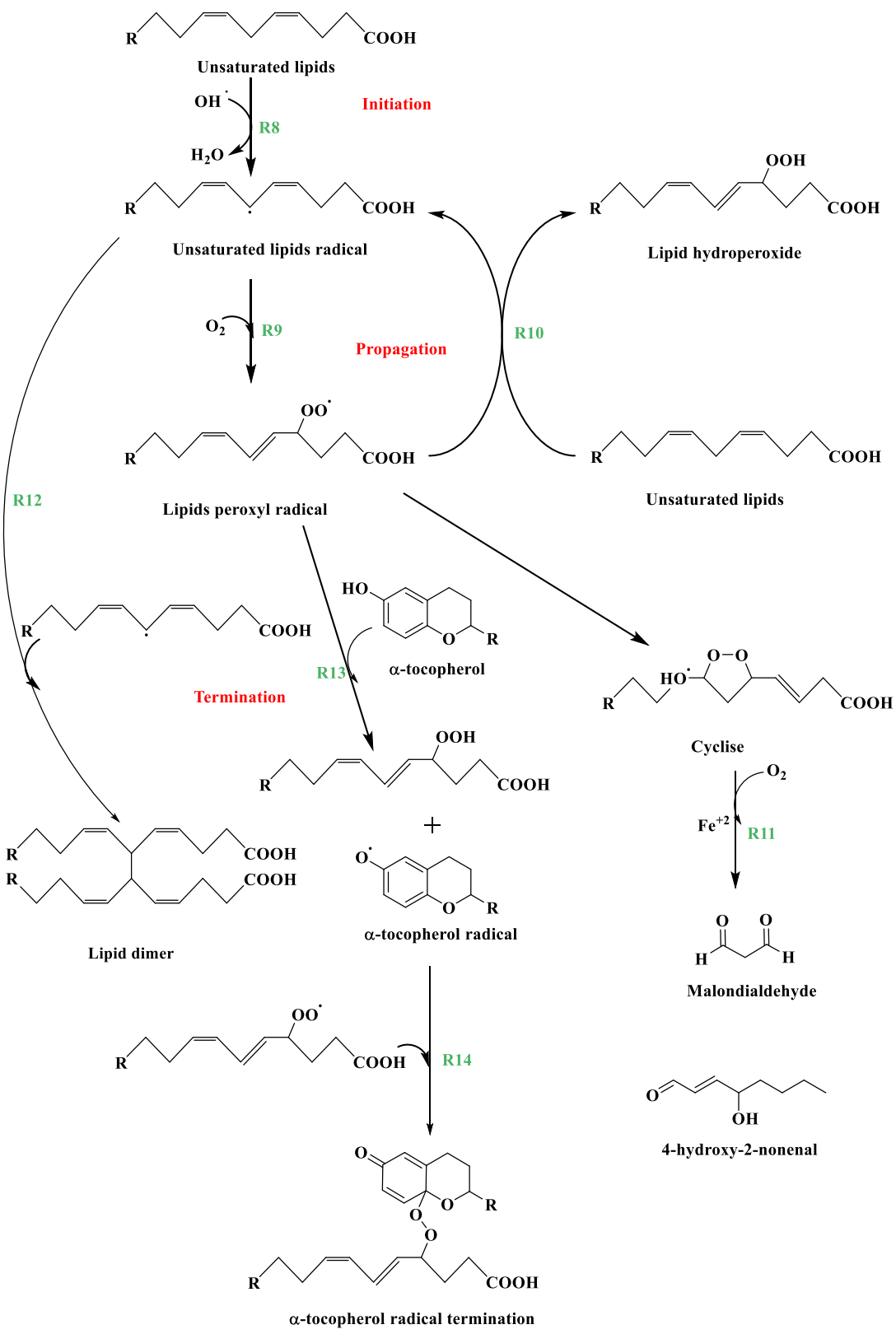

Scheme 1 The process of generating lipid peroxidation

1.5 Malondialdehyde

MDA is the end decomposition product of lipid peroxidation, generated by peroxidation of membrane PUFA (arachidonic acid) through cyclised the lipid peroxyl radical, then producing different bicyclic endoperoxides as intermediate compounds (Scheme 2). Moreover, it is the most common index for lipid peroxidation used as a biomarker of oxidative stress *in vitro* and *in vivo,* as well as in several disease such as cancer, diabetes, hypertension and heart (Gönenç *et al.*, 2001; Fay *et al.*, 2010) (Onyango and Baba, 2010) (Jadoon and Malik, 2017). It may produce by several lifestyle factors including cigarette smoking (Yao *et al.*, 2019), high fat diet and alcohol consumption (Saini *et al.*, 2019) and consequently inducing several cancers such as oral cavity, lung, oropharyngeal, prostate, breast, bladder, renal and colorectal (Jelic *et al.*, 2019).

Chemically, MDA is a 1,3-propanedial ($C_3H_4O_2$) features as soluble in ethanol, methanol and water and insoluble in diethyl ether, a weakly acidic, the responsibility for its activity owing to a carbonyl functional group. It is easy to polymerise and can react with nucleophiles of different molecules such as proteins, amino acids and DNA. It is classified into two groups; either through the interaction of the two aldehyde groups with nucleophiles or with methylene H atoms by CH-acidity (Tsikas, 2017; Taso *et al.*, 2019).

It has been reported that MDA can be generated by enzymatic or nonenzymatic processes (Figure **1.5**). In enzymatic processes, it assumed that MDA is created by prostaglandin H_2 (PGH_2) that is produced by cyclooxygenases actions through the metabolism of arachidonic acid. On the other hand, in nonenzymatic processes, PUFA might be converted to a lipid peroxide radicals (Scheme 1) that then generates MDA. As soon as it is produced, MDA might be metabolised enzymatically through mitochondria by aldehyde dehydrogenase then decarboxylation to generate acetaldehyde.

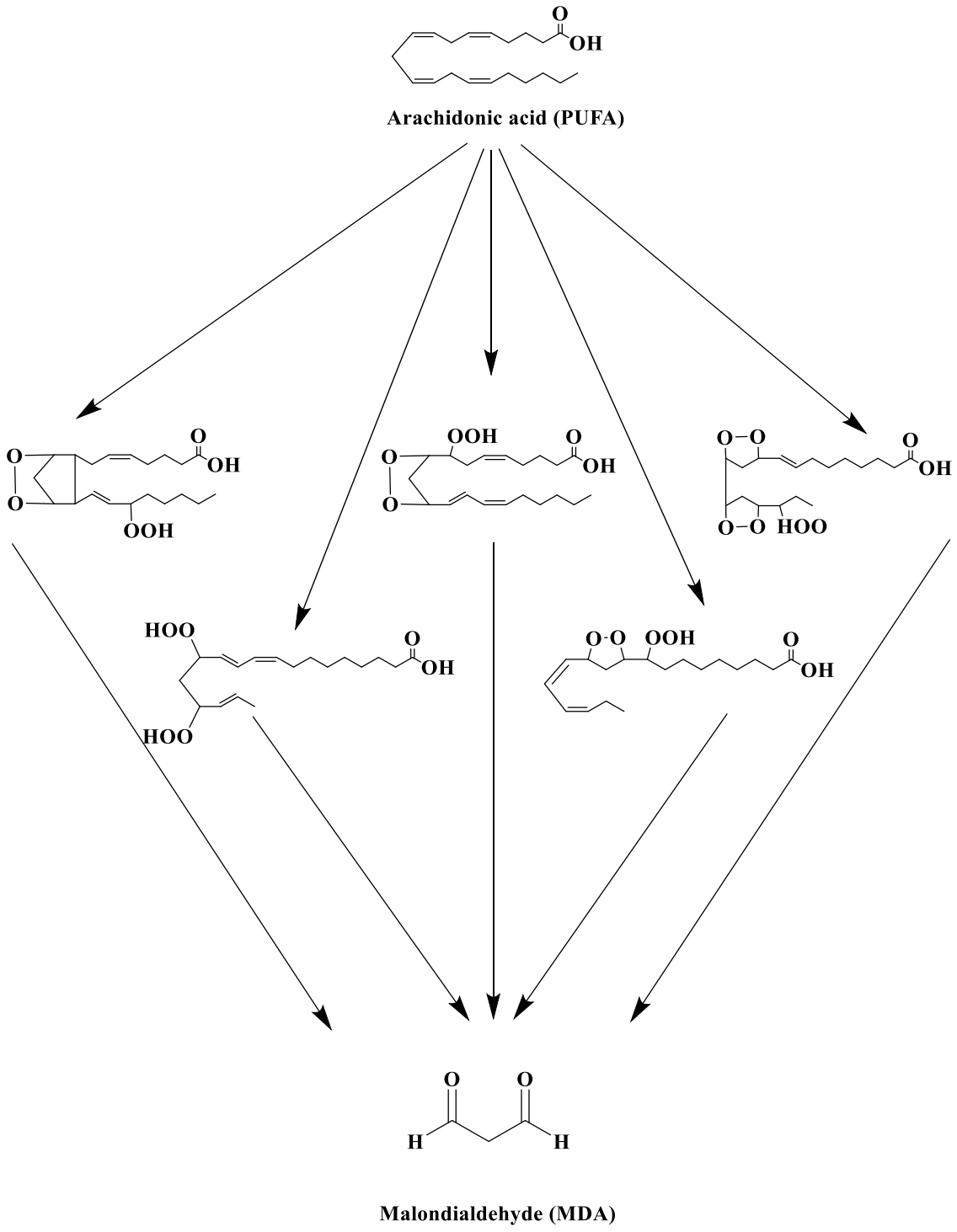

Scheme 2 Pathways for PUFA peroxidation and the formation of MDA, adapted from Onyango and Baba (2010)

Thereafter, MDA is oxidised by aldehyde dehydrogenase to produce acetate then acetyl CoA and finally generates CO_2 and H_2O. Otherwise, it may metabolise in the cytoplasm to methylglyoxal by phosphoglucose isomerase then to D-lactate by GSH enzyme (Ayala *et al.*, 2014), or by CYP45 enzymes in the presence of NADPH and O_2 (Ahmed Laskar and Younus, 2019; Rodríguez-Zavala *et al.*, 2019). However, if MDA is not metabolised, it might induce biomolecular damage by forming protein adducts due to modify proteins of cytoskeletal, carrier, antioxidant and mitochondrial, as well as inducing DNA adducts that initiate DNA damage due to inducing mutations, strand breaks, cell cycle arrest and generate cell death program (Ayala *et al.*, 2014; Ito *et al.*, 2019).

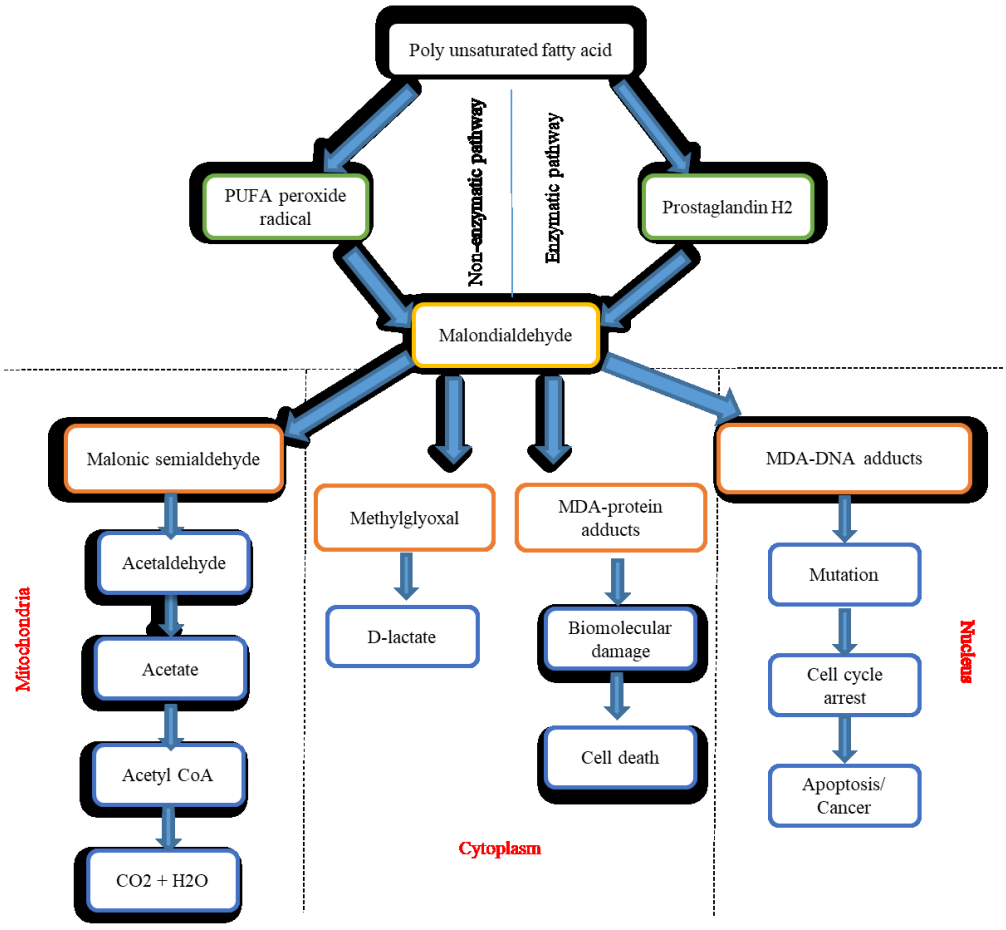

Figure 1.5 Generating and metabolise MDA by enzymatic and non-enzymatic processes

It has been found that MDA has mutagenic and carcinogenic effects caused by reacting with DNA producing DNA adducts, such as M_1dG, which is the most crucial MDA-DNA adducts result of reacting MDA with positions N^1 and N^2 of guanine, as well as reacting MDA with cytosine produce N^4-(3-oxopropenyl)-2′-deoxycytidine (Malondialdehyde-deoxycytidine (M_1dC)) and with adenine N^6-(3-oxopropenyl)-2′-deoxyadenosine (Malondialdehyde-deoxyadenosine (M_1dA)) (Leuratti *et al.*, 1998; Roede *et al.*, 2010; Hwa Yun *et al.*, 2018). It has been reported that M_1dG can oxidise to the 6-oxo-M_1dG, which is more stable and mutagenic than M_1dG adducts (Scheme 3) (Wauchope *et al.*, 2015).

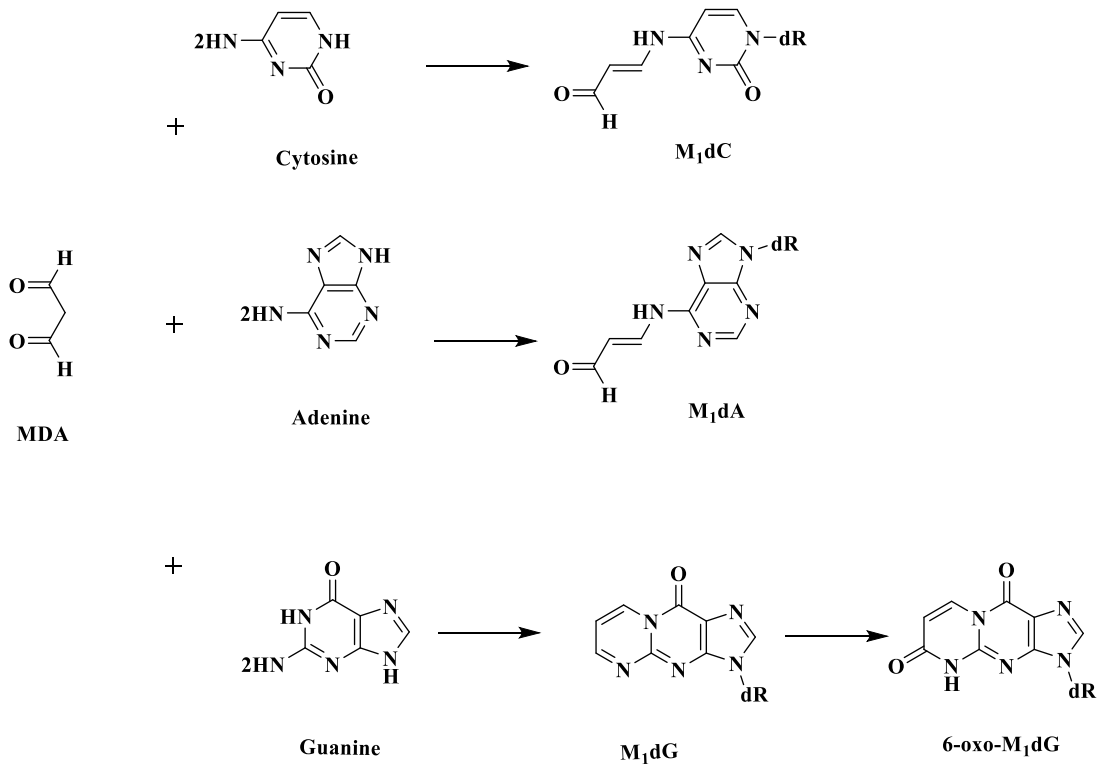

Scheme 3 MDA-DNA adducts

MDA has been found in different diseases such as cancer, cardiovascular, diabetes, liver, Parkinson's and Alzheimer's disease (Onyango and Baba, 2010). Several studies have examined the correlation between smoking cigarette and MDA level, the level of serum MDA was found higher in the smokers than non-smokers (Isik *et al.*, 2007; Kashinakunti *et al.*, 2011; Thorat *et al.*, 2019). In addition, Sakaguchi *et al.* (2019) have reported the urine MDA level was higher in smokers than non-smokers. Moreover, in the study of lung cancer patients, the level of MDA was found to be higher in smokers than non-smokers (Petruzzelli *et al.*, 1990).

In regard to the genotoxicity effect of MDA, researchers have indicated that lipid peroxidation has the ability to generate M_1dG adducts, 8-oxodG and DNA strand breaks in HepG2 cells (Beddowes *et al.*, 2003). Furthermore, the potential effect of MDA to generate DNA adducts like M_1dG has been examined in lung cancer patients, and it was found that the M_1dG adducts was higher in larynx and bronchi of cigarette smoker cancer patients (Munnia *et al.*, 2004; Munnia, 2006).

Yates *et al.* (2019) have found that MDA can induce more mutations in *Tp53* in MRC-5 lung normal cell line than the transformed cells MRC-5 SV2. Also, Fahn *et al.* (1998) reported that the frequency of mtDNA mutation and the level of MDA were found higher in cigarette smokers than non-smokers by using blood and lung tissue samples. Moreover, another group have found that MDA can induce mutation for more than 15 fold in the reporter gene *supF* (Niedernhofer *et al.*, 2003).

1.6 Genetic Material

An important macromolecules, carrying genetic genetic information through a long sequence of DNA and is made up of purine bases such as adenine (A) and guanine (G), pyrimidine bases such as thymine (T) and cytosine (C), in addition to pentose sugar and phosphate units. The genome contains genes, each gene carries a DNA sequence that codes for RNA, which contains A, G, C and uracil (U), in addition to producing proteins as a final product (Plopper *et al.*, 2015; Lesk, 2017).

DNA can be duplicated by replication, an accurate process but is also prone to error. The Cell has two pathways to ensure the accuracy of DNA sequences through the proofreading of replication and monitoring DNA damage and fixing it using repaired systems. One of the functions of DNA is to act as a template for RNA synthesis through RNA polymerase (transcription), thereafter the RNA functions as a template for protein synthesis through ribosomes (translation). Moreover, the process to translate RNA to DNA is called reverse transcription (Figure **1.6**) (Plopper *et al.*, 2015).

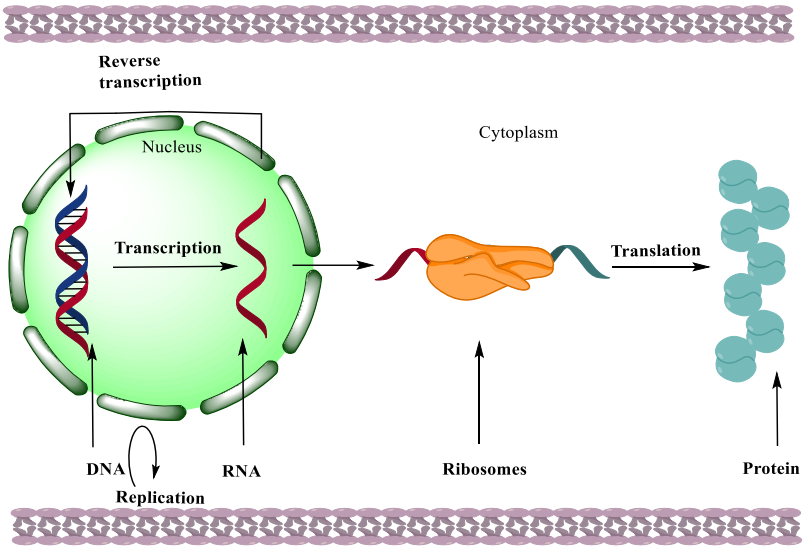

Figure 1.6 Gene expression by transcription the RNA from DNA then translation to protein

1.6.1 DNA damage

DNA damage is the first crucial step induced by a mutagen to cause cancer. It may occur throughout replication as well as errors in proofreading, these include many steps such as insertion, deletion or modification of bases or a segment of DNA or a chromosome (Plopper *et al.*, 2015). Inducing DNA damage may occur by exogenous agents such as chemical substance, ionizing radiation and UV and/or by endogenous agents such as hydrolysis and ROS. The exogenous agents like chemicals from tobacco, diet or alcohol can induce DNA damage either by insertion of the chemical between bases (Indirect) or DNA-reactive (Direct) (Klaassen and Watkins, 2015). The DNA damage are categorise to following factors:

1- **Alkylating**: which is one of chemical effect on DNA by adding ethyl, methyl or any alkyl group to the oxygen or nitrogen atoms in the nucleotide, such as methylation guanine forming methyl-guanine (Figure **1.7**) (Plopper *et al.*, 2015).

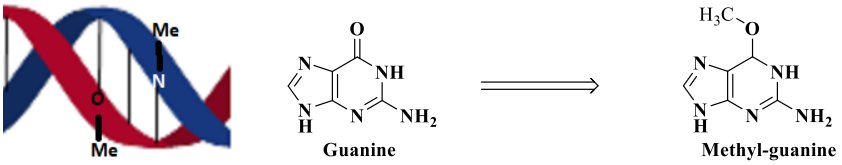

Figure 1.7 DNA alkylation

2- **Oxidation**, the nucleotides are oxidising as a result of adding an oxygen atom to the bases like guanine, which will lead to producing 8-oxoguanine adducts (Figure **1.8**) (Plopper *et al.*, 2015).

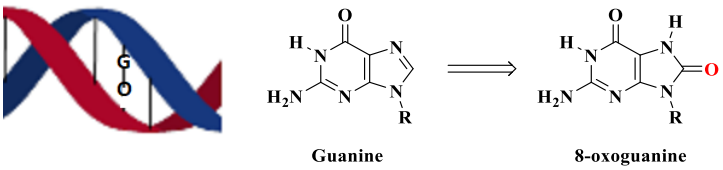

Figure 1.8 DNA oxidation

3- **Deamination**: it can occur by removing amine group from adenine, guanine and cytosine forming hypoxanthine, xanthine and uracil respectively, the deamination of cytosine is the most common than the others (Figure **1.9**) (Plopper *et al.*, 2015; Krebs *et al.*, 2018).

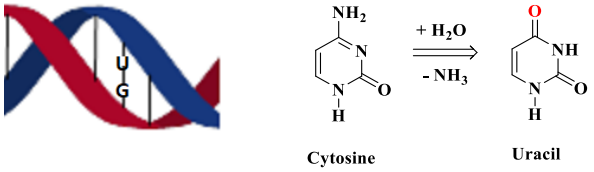

Figure 1.9 DNA deamination

4- **Mismatched:** in case there is an error in replication such as insertion cytosine instead of adenine or vice versa that will lead to mismatched base pairs (Figure **1.10**) (Krebs *et al*., 2018).

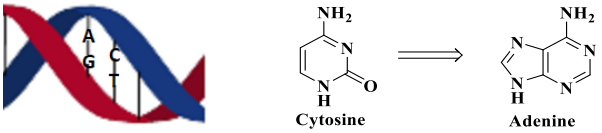

Figure 1.10 DNA mismatched

5- **Depurination:** occurs in the event of disconnecting between the bonds of purine bases and the sugar molecular in N-glycosyl bond through hydrolysis (Figure **1.11**) (Plopper *et al.*, 2015).

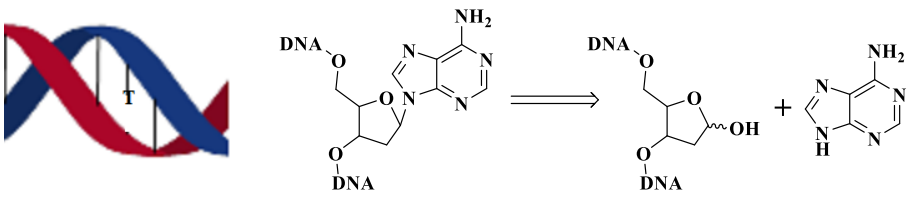

Figure 1.11 DNA depurination

6- **Pyridine dimer:** may occur by a covalent link between two pyridine bases site in one strand producing a dimer such as thymine (Figure **1.12**) (Krebs *et al.*, 2018).

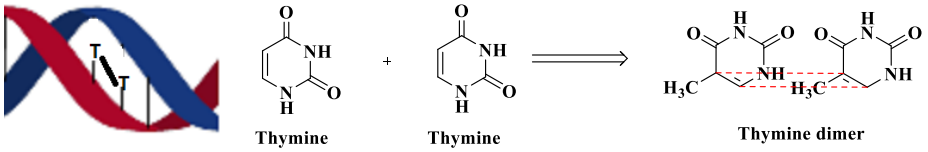

Figure 1.12 Pyridine dimer

7- **Peroxidation:** may occur by reacting MDA with DNA inducing DNA adducts such as M_1dG, M_1dA and M_1dC (Figure **1.13**) (Singh *et al.*, 2014).

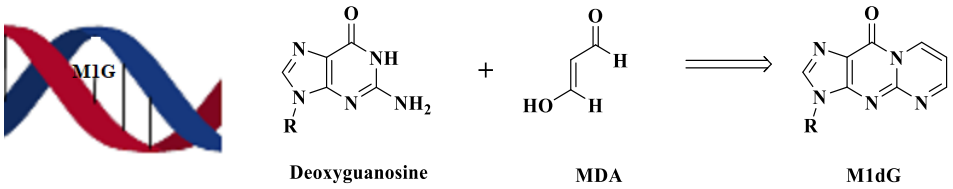

Figure 1.13 DNA peroxidation

8- **Cross-links**: it occurs in the event of the covalent link between two bases in two strands in the presence of an alkylation agent such as nitrogen mustard gas or cisplatin (Figure **1.14**) (Plopper *et al.*, 2015).

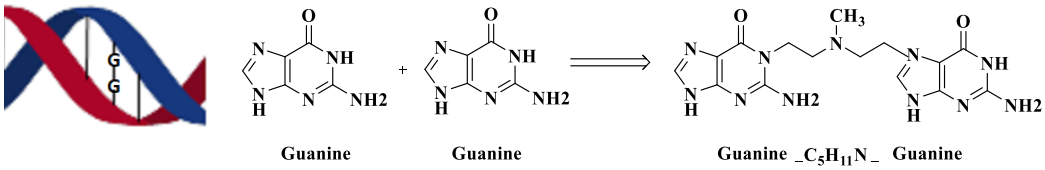

Figure 1.14 Cross –links

9- **Single and double strand breaks:** occur due to the deletion of a nucleotide in one or both strands, which creates a groove or break in the DNA helix and that will bring about loss of DNA information (Figure **1.15**) (Krebs *et al.*, 2018).

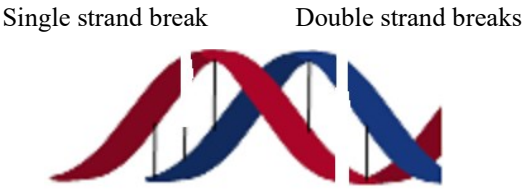

Figure 1.15 Single and double strand breaks

From all of this, DNA adduct formation is the most damaging if not repaired (Krebs *et al.*, 2018). In addition, hydroxyl radicals that are induced by ROS can induce more than 80 different types of DNA damage such an 8-oxoguanine by oxidation, which can be pairing with adenine and cytosine, forming 8-oxoguanine:A and 8-oxoguanine:C. Indeed the base pairing between 8-oxoguanine:C can translate to G:C, however, 8-oxoguanine:A can translate to T:A (Plopper *et al.*, 2015).

In regards to inducing DNA damage by MDA, MDA can generate DNA adducts such as M_1dG, M_1dA and M_1dC. Moreover, the most detected adduct was M_1dG, which are formed as a result of peroxidation by carbonyl equivalent reaction between MDA and DNA through losing two water molecules. It has been found that increased MDA concentration leads to an increase in mutations as well as an increase in M_1dG adducts. Moreover, diets with the high polyunsaturated fatty acid content increase in M_1dG levels (about 20 fold) (Marnett, 1999).

After DNA damage, cells may be recognised at the G_1/S, S, or G_2/M checkpoints of damage where cell repair or apoptosis mechanisms will be initiated to induce cell cycle arrest (Higdon and Frei, 2004; Ayala *et al.* 2014). In case of DNA damage, the cell can produce a transcription regulation of p53 protein to arrest the cell on G_1 phase that can give the cell more time to repair the DNA damage before completing the replicate process, however, if the damage is not repaired, p53 can lead to apoptosis. Nevertheless, it has been found that most of the human cancers have a mutation in *TP53* gene (Alberts *et al.*, 2019) and also they have reported that MDA is one of *TP53* mutagenic inducer (Yates *et al.*, 2019). It is known that living systems are based on the metabolism of O_2, although, ROS can form by $O_2^{\bullet-}$ through reduction of O_2. It is thought the reactive species products can escape the antioxidant pathway causing DNA damage and that induces cancer (Townsend and Tew, 2014).

Several studies have examined the mutagenic effect of MDA, for example, the study by Fahn *et al.* (1998) reported that mtDNA mutation was increased in smokers' lung tissues. Furthermore, it has been found that MDA can generate single base change such as GC base pairs mutation as well as DNA cross-links in human fibroblasts cells (Niedernhofer *et al.*, 2003). Moreover, Collado *et al.* (2014) have found that MDA can induce cytogenetic abnormalities in chromosomes position 11q22-23, 13q14 and 17p13 in chronic lymphocytic leukaemia patients.

1.7 Cancer treatment

In regard of increasing cancer incidences, health care system have been using different treatment modalities to remove or reduce cancer incidences such as systemic treatment, like chemotherapy, immunotherapy and hormonal therapy as well as radiation therapy, and surgery (Miller *et al*., 2019).

1.7.1 Chemotherapy

It is the first step of cancer treatment, deliver as a palliative, adjuvant or curative. Also, it is classified depending on the target of cell mechanism of actions such as cell cycle inhibition, cell metabolic activity like cell mobility, proteins, DNA and RNA synthesis, also mitotic catastrophe like anti-proliferative mechanism. Moreover, it is referred to the agent either natural from plant like vincristine and paclitaxel (taxol), from marine like halichondrion B (eribulin) and trabectedin (yondelis) that can induce DNA damage then apoptosis and or semisynthetic like docetaxel as mitotic catastrophe (Da Rocha *et al.*, 2001; Kleinsmith, 2006; Palmieri *et al.*, 2013; Yildizhan *et al.*, 2018). However, the side effect of chemotherapy may increase cell proliferation in normal cells such as skin, bone marrow and gastrointestinal tract, also induce toxicity in whole organ system such as effect on blood, heart, nerves and fertility (Palmieri *et al.*, 2013; Yildizhan *et al.*, 2018).

1.7.2 Hormone Therapy

Hormones transmit through blood stream to the target organs, and generally regulate cell development and differentiation. For this reason, they are used to treat targeting cancer cells especially hormone depending tissues such as endometrial, kidney, breast, ovarian and prostate, to control the cancer cell growth. Drugs like tamoxifen, which can block estrogen and cell surface receptor interactions and abemaciclib (verzenio), which can

inhibit the cell proliferation, are already been in use as a hormonal therapy to treat cancer (Lohr, 2018; Yildizhan *et al.*, 2018).

1.7.3 Immunotherapy

Our immune system is programmed as a cell defence mechanism by preventing the cells from various types of foreign bodies. The system also identifies, reduces or blocks the cancer cells by recognising particular surface protein like antigens via protein-protein interaction. Despite of the presence of checkpoints in the immune system responsible for cell-protection, the cancer cells can escape from these checkpoints leading to tumours formation. Immunotherapy is classified into immune cells genetic modifications, adoptive cell transfer therapy, and cellular therapy. Many drugs being in use as immunotherapy such as avastin, bexxar, campath, erbitux, herceptin, myolotarg, rituxan, vectibix and zevalin (Yildizhan *et al*., 2018; Tanoue and Detterbeck, 2019). However, the side effects of immunotherapy may induce allergic reactions (Schuster *et al*., 2006), unresponsiveness and can be life threatening as an extreme effect (Yu *et al*., 2019). Moreover the cost of the treatment is also high (Blons, 2019).

1.7.4 Radiotherapy

It is the most efficient non-surgical treatment for tumours. It includes use of gamma rays, x-ray, photons, protons or electron beams that can produce by a direct accelerator targeting malignant cells due to induced cell apoptosis through increase oxidative stress that leads to DNA damage (Palmieri *et al.*, 2013; Yildizhan *et al.*, 2018). It is used to treat cancer and also to control and reduce the tumour size (Yildizhan *et al.*, 2018). The side effects of radiotherapy include DNA damage of normal cells either temporarily, when the cell can repair the damage or permanently, when the cell cannot repair itself (Palmieri *et al*., 2013).

1.7.5 Surgery

This type of treatment stratifies locally by removing the tumour as a part or whole organ. It is applied in different types of metastatic diseases such as lung, bladder, kidney, breast and prostate (Palmieri *et al.*, 2013). It can bring about to a cure for the patient living with cancer for a long time. However, sometimes the cancer cells may spread from original tissue to others, which make the surgery unsuccessful (Yildizhan *et al.*, 2018). The side effect of surgery are related to change the quality of patient life like suffering from psychological and physiological effect. For example, woman with breast cancer may increase anxiety, depression, and effect on body image and may be on the fertility (Salonen *et al*., 2011).

1.8 Lung cancer treatment

Treatments of lung cancer are depend on the type of cells such as non-small cells or small cell, also cancer molecular features and stage (American Cancer Society, 2018), it can apply in different methods such as:

1.8.1 Lung chemotherapy

Chemotherapy is used to treat the small and non-small lung cancer cells either alone or combined with radiotherapy (McCready, 2006; American Cancer Society, 2018). There are several drugs are in use as lung chemotherapy such as doxorubicin, epirubicin, and daunorubicin as lung topoisomerase II inhibitors; docetaxel, paclitaxel, vinblastine and vinorelbine as lung microtubule inhibitors; cisplatin and carboplatin as lung DNA replication and RNA transcription inhibitors; as well as iressa can effect on lung epidermal growth factor receptor (Kleinsmith, 2006; Palmieri *et al.*, 2013; Tanoue and Detterbeck, 2019). It has reported that crizotinob, erlotinib and gefitinib compounds have approval from Food and Drug Administration (FDA) and used to treat non-small lung

cancer cells as epidermal growth factor receptor inhibitors (Workman and Collins, 2014). Moreover, small lung cancer cells can be treated by using etoposide and/or cisplatin, as well as platinum combined with irinotecan or etoposide (Parikh *et al.*, 2018).

1.8.2 Lung immunotherapy

Recently, immunotherapy might use to treat non-small lung cancer cells. To minimise lung cancer there are two clinical target pathways, which are the suppressor receptor PD-1 and anticytotoxic T-lymphocyte antigen 4 pathways. There are different immune drugs have used to treat non-small lung cancer cells such as pembrolizumab, Nivolumab, Atezolizumab are used against PD-1 and ipilimumab and tremelimumab as anticytotoxic T-lymphocyte antigen 4 (Tanoue and Detterbeck, 2019).

1.8.3 Lung radiotherapy

It is used to treat the small cells and early stage of non-small cells lung cancer, for the cases that cannot go through surgery, also it is used as palliative and curative. Sometimes, it is used in combination with chemotherapy or after surgery (Hunt *et al.*, 2009; Corso *et al.*, 2015; Yu *et al.*, 2015; American Cancer Society, 2018). Nevertheless, it has found that lung radiotherapy is more toxic and leads to an increase in the rate of mortality compared with surgery (Yu *et al.*, 2015). Moreover, radiotherapy has applied onto the non-small cells lung cancer a patient in N0, N1 and N2 nodal stages, and it found the radiotherapy can increase survival in a patient with N2 but not in N0 or N1 (Lally *et al.*, 2006).

1.8.4 Lung surgery

In the cases of lung cancer, surgery is used to remove a part (segmentectomy), lob (lobectomy) or all the lung (pneumonectomy), as well as the associated lymphatic related to it. The principle of lung surgery is including confirm the tumour area, tumour resection

and evaluating the lymph nodes related to it (McCready, 2006; Tanoue and Detterbeck, 2019). The non-small cells lung cancer in stages I and II are treated by surgery for a patient who can tolerate it (Tanoue and Detterbeck, 2019). However, it less uses in small cell lung cancer due to quickly spread in the body (Kleinsmith, 2006).

Finally, most lung cancer treatments are unsatisfying because they may not usually give the patient long life because of the side effect. Also statically depending on cancer research UK between 2014- 2016 there were 47,235 lung cancer cases and consequently in 2015-2017 there were 35,349 deaths, however there were 79% preventable cases (Cancer Research UK, 2019). Moreover, worldwide the survival rate of the lung cancer patient is approximately 18% with a 5-year lifetime (American Cancer Society, 2018). For that reason prevention lung cancer is more effective than treatment, due to prevention can decrease the mortality of lung cancer (Hunt *et al.*, 2009).

1.9 Cancer prevention

It is known cancers might take time to develop from the mutant of a normal cell in the initiation stage to malignant cells in the progression stage. For instance, lung, pancreas, colorectal, prostate, breast and ovary cancers have a long latent period, for about ≤ 20 years. This long period, it can provide a possibility to reduce cancer incidence by change the lifestyle via increase physical activity and smoking cessation as well as employ a chemopreventive drug for repairing or blocking abnormal cells (Pop *et al.*, 2019; Soto-Perez-de-Celis and Hurria, 2020).

1.9.1 Chemoprevention

Chemoprevention can be defined as the utilisation of pharmacological, natural or synthetic products to eliminate or minimise the initial phase of carcinogenesis or the development of neoplastic cells to cancer (Mokhtari, 2010; Steward and Brown, 2013).

Chemicals from plants, are termed ‘phytochemicals’ and may harbour the potential to act as cancer chemopreventive compounds. Cancer chemopreventive compounds may act by several mechanisms to reduce cancer incidence, including prophylactically to prevent cancer incidence, to prevent the progression of existing cancers and to prevent the relapse of patients who have already been treated successfully (Li, 2004; William *et al.*, 2009; Steward and Brown, 2013).

Chemopreventive agents can be categorised into blocking agents, which obstruct the initiation stages of tumour development blocking the DNA mutation that occur from carcinogens, also it could induce detoxifying and antioxidant enzymes. In addition, suppressing agents that suppress the progression and promotion stages, through modification of gene expression (Figure **1.16**) (Chen and Kong, 2004; Chen and Kong, 2005; Steward and Brown, 2013).

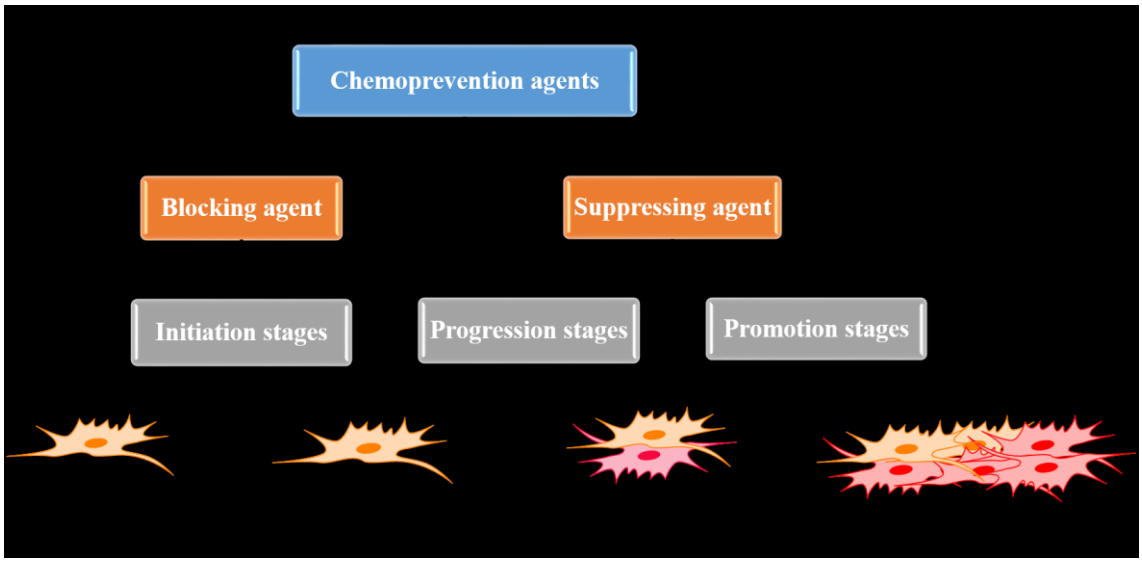

Figure 1.16 Chemopreventive agents classification: blocking agents, which effect on initiation stage after transform normal cell to mutant cell, and suppressing agent, which impact on promotion and progression stage to inhibit transform mutant cell to a malignant tumour, adapted from Chen and Kong (2004)

Cancer chemopreventive agents have been classified depending on the compound type, this compound could be natural or synthetic, which divided into diverse groups such as polyphenols, flavonoids, alkaloids, carotenoids, vitamins and other groups (Mehta *et al.*, 2010). Surh (2003) has reviewed phytochemicals such as curcumin **(1),** capsaicin **(2),** caffeic acid phenethyl ester **(3),** [6]-gingerol, diallyl sulphide **(4),** resveratrol **(5),** sulphoraphane **(6),** epigallocatechin-3-gallate **(7),** indole-3-carbinol **(8),** genistein **(9)** and lycopene **(10)** have chemopreventive activity through inducing xenobiotic enzymes.

1.10 Cellular defence genes

1.10.1 The Nuclear factor-erythroid 2 p45 subunit-related factor 2 (Nrf2)

Nrf2 (PDB ID: 2lz1) or called NFE2L2; HEBP1 and IMDDHH as well, is a monomer (~100 kDa) human enzyme has six functional domains and 605 amino acids (Figure **1.17**). These domains are include Neh1 (binding with DNA and small musculoaponeurotic fibrosarcoma (Maf)), Neh2 (negative regulatory domain), Neh3 (promoting antioxidant response element (ARE) genes), Neh4 and Neh5 (transactivation domain), Neh6 (regulate Nrf2 negatively by Keap1) and Neh7 (inhibits Nrf2-ARE signaling). It is monitoring by *NRF2* gene that is located on human chromosome 2q31.2 (Gene ID: 4780), in position 177,260 – 177,230, it has a 45 Kbp length including six exons (Figure **1.18**). Moreover, it links with ARE promoter, which regulates the expression for more than 200 genes encoding the enzymes of chemopreventive and detoxify (Niture and Jaiswal, 2010; Baird and Dinkova-Kostova, 2011; Townsend and Tew, 2014; NCBI, 2019). The half-life of *NRF2* is approximately 15 minutes in normal condition, and 30 min under the stress condition (Nguyen *et al.*, 2009).

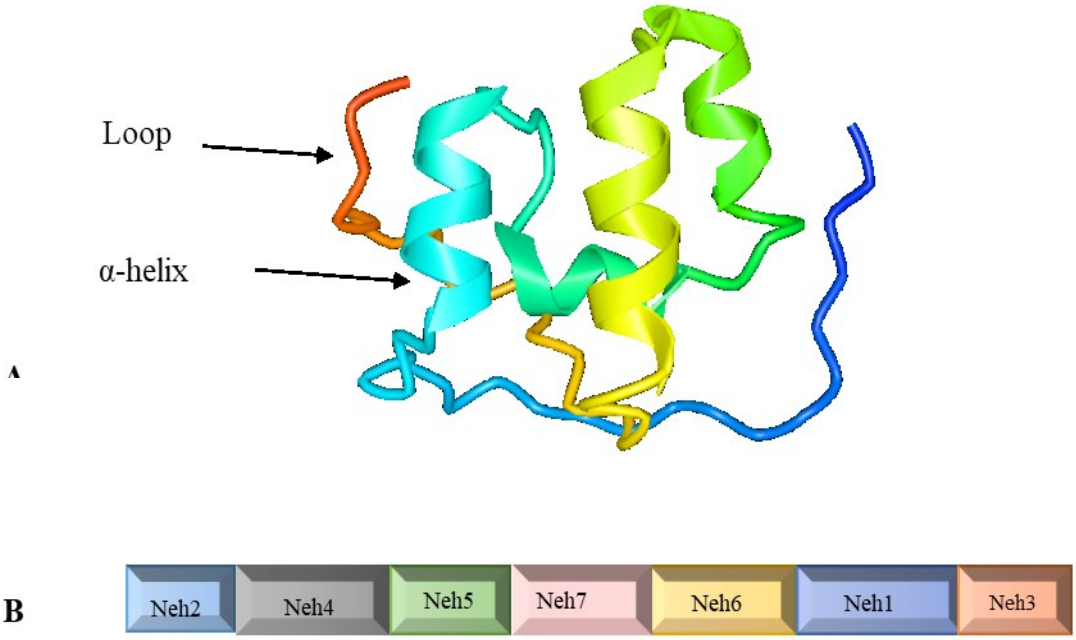

Figure 1.17 (A) Core domain of Nrf2. (B) Functional domains Neh1-7 of Nrf2.

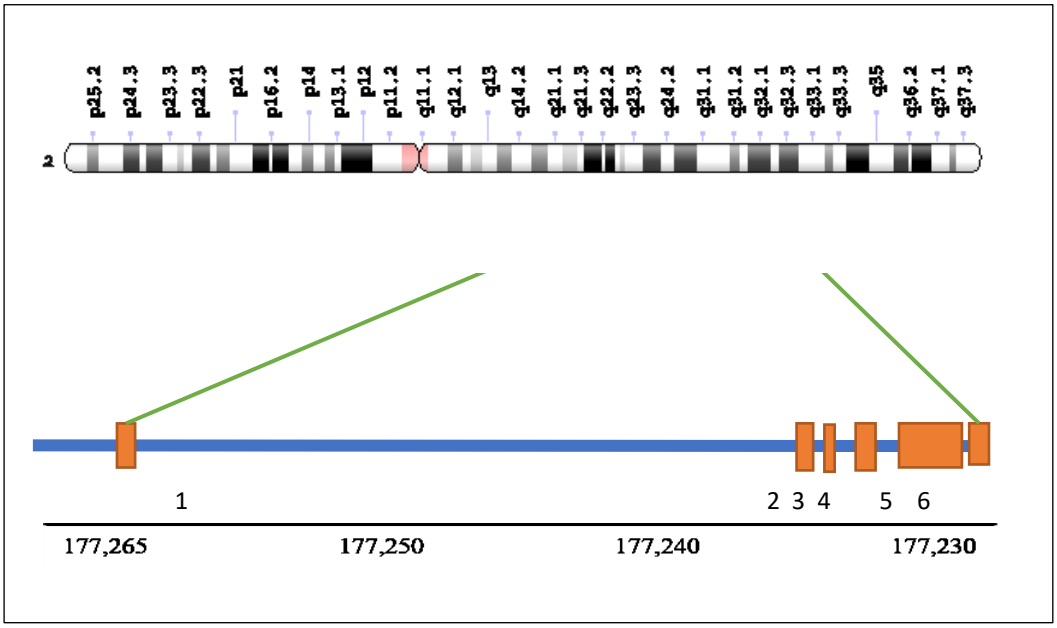

Figure 1.18 Location of *NRF2* gene on chromosome 2

The Nrf2 (Figure **1.19** A) is a transcription factor related to the basic-region leucine zipper (bZIP) family, which controls the antioxidant enzymes and the battery expression of drug-metabolising all of which have an ARE in their gene promoter which allows the binding of the Nrf2 transcription factor (Higgins, 2008; Barrera-Rodríguez, 2018). The Nrf2 pathway is an essential pathway that balances cellular reduction and oxidation (Kumar *et al.*, 2013). This pathway has many stages, under basal conditions, Nrf2 is maintained in the cytoplasm by homodimerisation of Kelch-like ECH-associated protein 1(Keap1), which is a cysteine-rich protein has five zones: NH_2 (N-terminal), the Broad complex Tramtrack and Bric-a-brac (BTB) domain, Intervening region (IVR), Kelch repeat domain and COOH (C-terminal) (Figure **1.19** B). Moreover, this Keap1 binding by cullin3 (Cul3) for Nrf2 ubiquitination (Figure **1.19** C). Upon oxidative stress, Nrf2 dissociates from Keap1 and translocates to the nucleus (Goldring *et al.*, 2006; Lau *et al.*, 2008; Kansanen *et al.*, 2013; Wu *et al.*, 2014; Nishimoto *et al.*, 2016). Thirdly, it is thought that in the nucleus, Nrf2 must connect with Mef proteins (~18 kDa) to become a heterodimer (Ma, 2013). Following that, the heterodimer binds with ARE, to induce the cell expression of cell defence genes such as *GST*, glutamate-cysteine ligase (*GCL*), hemoxygenase-1 (*HO-1*), peroxiredoxin (*PRX*), and xenobiotic metabolizing enzyme (*NQO1*) (Figure **1.19** D) (Thurston, 2007; Bryan *et al.*, 2013; Zhang *et al.*, 2016; Ding *et al.,* 2017; Hopkins *et al.,* 2018).

Kinnula (2005) has reported several antioxidant defence enzyme such as HO-1, GCL, GST, GPX, GSH, GAT, SODs, PRX, glutathione reductase (GR), thioredoxin (TRX) and multidrug resistance protein (MRP) in human lung that monitoring by Nrf2 as shown in (Figure **1.20**).

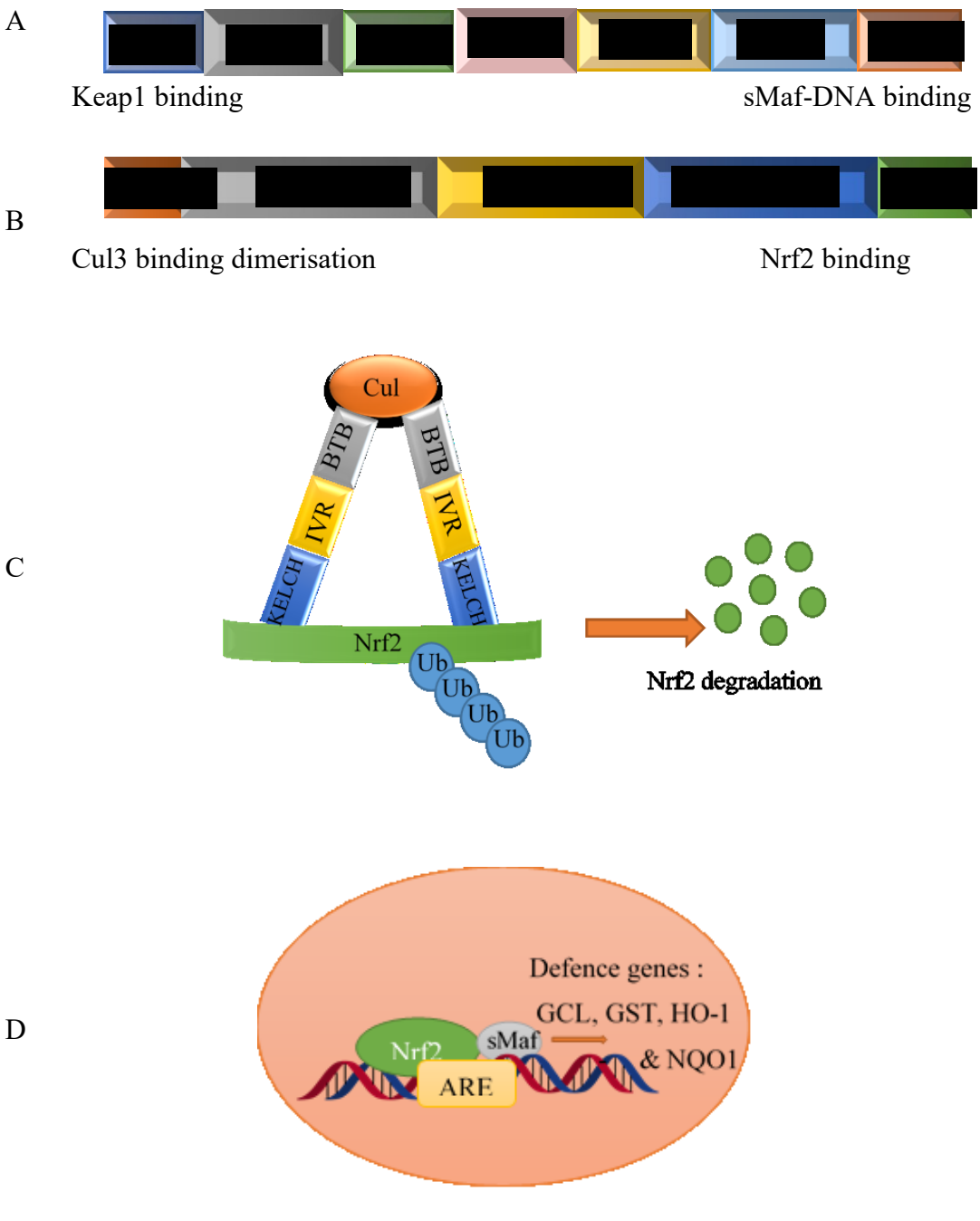

Figure 1.19 (A) Nrf2 domains (Neh 1-7), (B) Keap1 involves a number of functional domains including N-terminal region, the Broad complex, Tramtrack and Bric-a-brac (BTB), Intervening linker domain (IVR), double glycine/Kelch repeats and the C-terminal region. (C) Keap1-Nrf2 complex under basal condition cause ubiquitination and degradation Nrf2. (D) GCL, GST, HO-1 and NQO1 defence genes into nucleus induced by Nrf2-Maf-ARE complex.

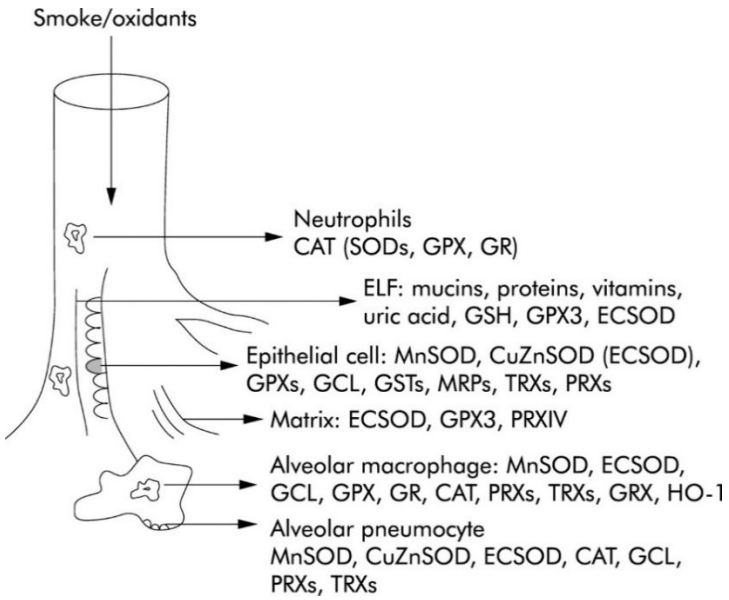

Figure 1.20 show several enzymatic and non-enzymatic antioxidant defence system in lung, adopted from Kinnula (2005)

Researchers have examined a variety of phytochemical compounds either natural or synthetic to induce Nrf2 and related cell defence genes as a cytoprotective or chemopreventive against carcinogenesis. Surh (2003) has reviewed phytochemical compounds such as sulphoraphane **(6)** can increase the expression of *GST* and *NQO1*, as well as caffeic acid phenethyl ester **(3)** and curcumin **(1)** can increase *HO-1* gene expression. The study by Liu *et al.* (2017) reported laminarin **(11),** a polysaccharide extracted from brown algae, could induce *NRF2* gene and subsequently induce cell defence gene including *NQO1*, *HO-1* and *GCL*, thus could protect the cell from H_2O_2 effect. Sohretoglu and Huang (2018) have reviewed the extract of *Ganoderma lucidum* polysaccharides can induce NQO1, GST, CAT, GPX and SOD by the switch on Nrf2 signalling pathway *in vivo* and *in vitro*. Additionally, researchers have found gastrodigenin **(12),** acerogenin A **(13),** α-Iso -cubebenol **(14)** and mangiferin **(15)** have chemopreventive features against H_2O_2 through induced *NRF2, NQO1, GSH, GCL and HO-1* gene expressions (Tavakkoli *et al.*, 2019). Moreover, another group have used

Houttuynia cordata, a traditional Chinese medicinal herb, as chemoprevantive for lung cancer against benzo(a)pyrene, and they found that this herb can induce NQO1 and HO-1 by activating the expression of *NRF2* pathway (Lou *et al.*, 2019). Two more recent studies showed that physalin A **(16)** isolated from *Physalis alkekengi,* and cymopol **(17),** isolated from green alga *Cymopolia barbata* can stimulate Nrf2 in HepG2 (Shin *et al.*, 2019; Bousquet *et al.*, 2019).

1.10.2 NAD(P)H:quinone oxidoreductase 1

NQO1 (PDB ID: 1QBG), or called NAD(P)H dehydrogenase, quinone 1, DT-diaphorase and NADH-menadione reductase (NMOR1) as well, is a homodimer (61.7 kDa) human cytosolic enzyme which has two active sites that bind to a co-factor flavin adenine dinucleotide (FAD) (Figure **1.21**) and is under the control of the ARE. NQO1 is considered to be the archetypal gene that denotes Nrf2 activation (Dinkova-Kostova and Talalay, 2010).

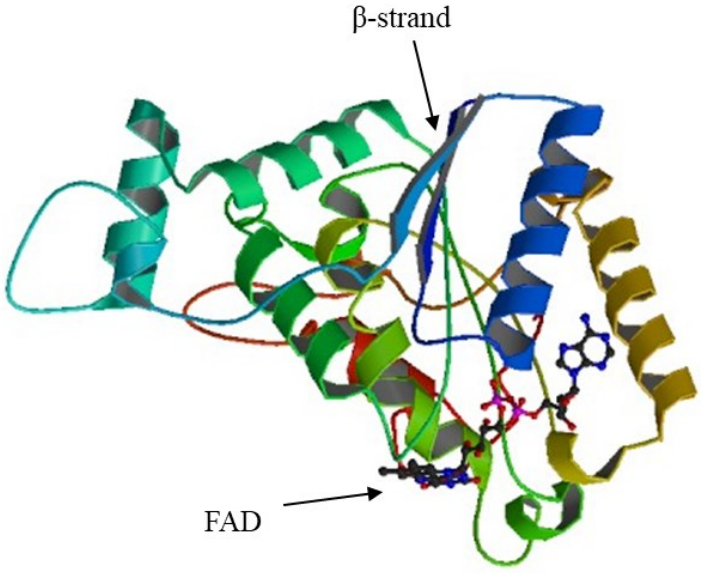

Figure 1.21 The crystal structure of NQO1 protein (PDBe, 2019)

It is monitoring by *NQO1* gene that is locate on human chromosome 16q22.1 (Gene ID: 1728), in position 69,709,401 - 69,726,668, it has a 21kbp length including five introns and six exons (Figure 1.22) (Ross *et al.,* 2000; Niture and Jaiswal, 2010; Pidugu *et al*., 2016).

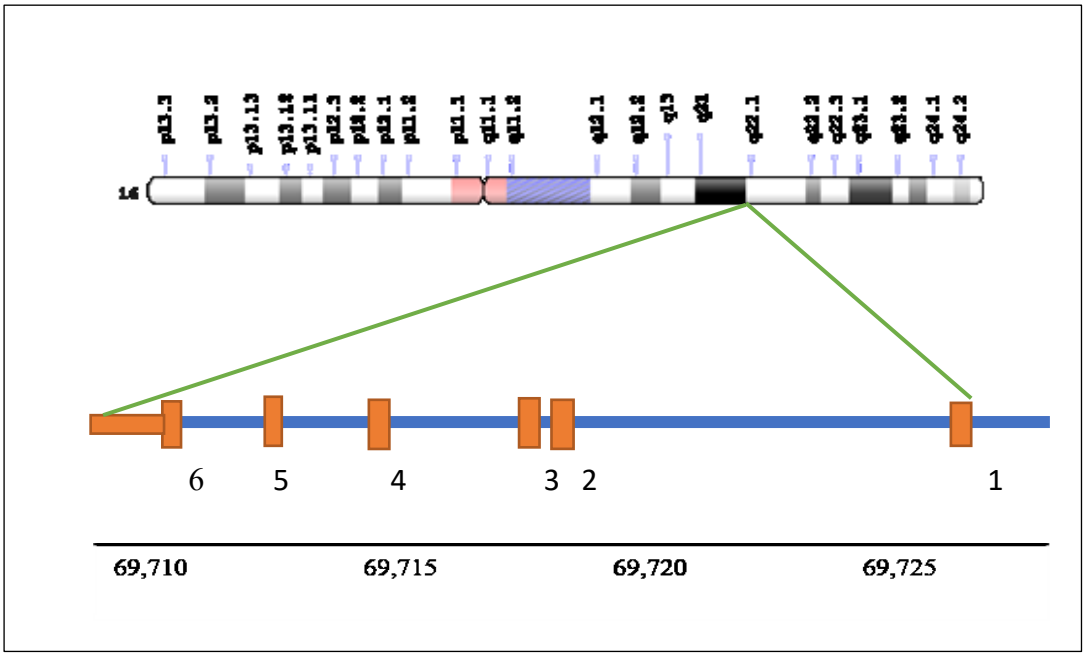

Figure 1.22 Activation position of NQO1 in chromosome 16, in addition to exons and introns sites

NQO1 has been used as a biomarker of chemoprevention due to its role in protecting cells from exogenous and endogenous oxidative stress generated by cytotoxic, mutagenic and carcinogenic factors, and it has the potential to catalyse the two electron reduction of quinones to form hydroquinones (quinol) in the presence of NADPH and $NADP^+$ co-factors (Scheme 4). It is a fundamental enzyme in the antioxidant defence system, involved in chemoprotection, antitumor bioactivation, detoxification, in addition to maintenance of tumour suppressors gene such as *p33, Tp53* and *Tp73* (Ross *et al.*, 2000; Lienhart *et al.*, 2014; Pidugu *et al.*, 2016; Ezzat *et al.*, 2018; Siegel, 2018; Pey *et al.*, 2019; PDBe, 2019).

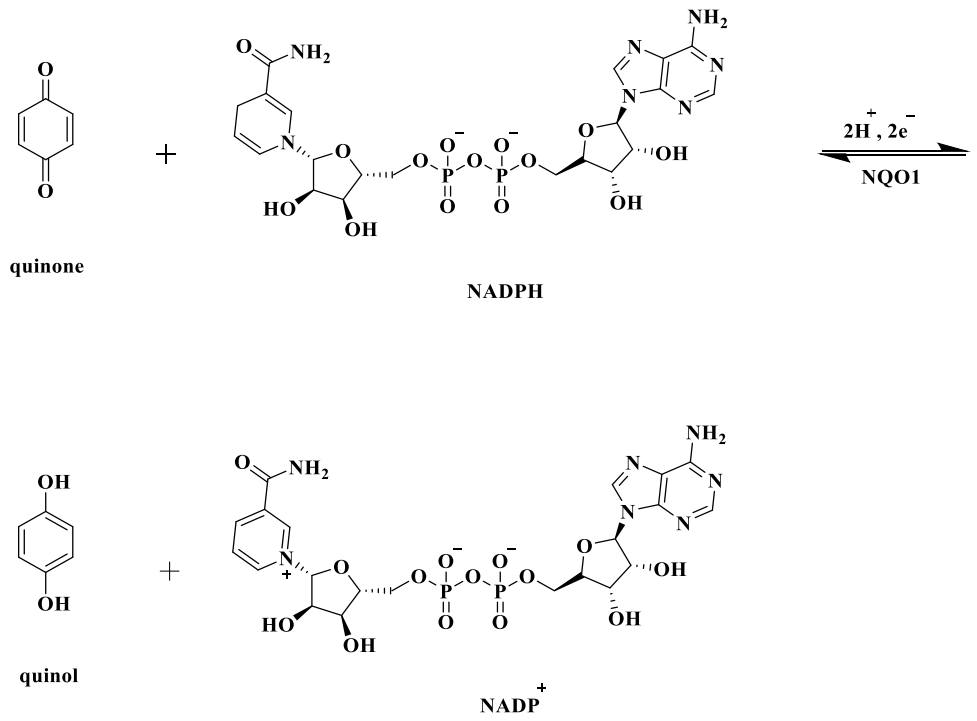

Scheme 4 Catalytic activity of NQO1 by modification quinones to hydroquinones

The activity of NQO1 might elevate due to the presence of mutagenic and carcinogenic compounds, and may also be found in cancer cells such as colon and lung (Skelly *et al.*, 1999) due to increase cell metabolism initiating free radicals (Pey *et al.*, 2019). Nevertheless, the mutation in *NQO1* has found reduce the defiance activity in some human carcinomas like lung and colon (Jaiswal, 2000).

The NQO1 enzyme has several metabolic and nonmetabolic roles in the cell, a metabolic function such as a detoxification enzyme through (i) reduction of vitamin K3 (menadione); (ii) it can remove the hydrogen groups from quinone; (iii) the benzene-derived metabolite 1,4-benzoquinone that induces DNA adducts are detoxified through release two electron by NQO1. The second role of NQO1, as an antioxidant enzyme, NQO1 can (i) prevent oxidative damage of cellular membranes through quinones reduction, (ii) maintain the level of α-tocopherol, (iii) it has found in several tissues that

involve in a high antioxidant protection (Ross *et al.*, 2000; Ross and Siegel, 2017), (iv) it has the ability to scavenge superoxide (Dinkova-Kostova and Talalay, 2010).

A nonmetabolic role, as a (i) RNA binding, NQO1 can bind with mRNA through amino acids and derivatives pathway in the present of co-factor dinucleotide (Castello, 2012), (ii) protein binding, NQO1 can interact with p53 protein, preventing proteasomal degradation (Ross and Siegel, 2017), (iii) Importantly however in some evidence has also been found of a positive correlation between NQO1 and cancer cell growth (Pidugu *et al.*, 2016).

Several studies have investigated the potential effect of chalcones to induce NQO1, and report increased *NQO1* expression in the Hepa 1c1c7 cell line after treatment with chalcones xanthoangelol **(18)**, 4-hydroxyderricin **(19)** and isobavachalcone **(20)** extracted from *Angelica keiskei* (Luo *et al.*, 2012), and chalcone 3,4,2′,4′-tetrahydroxychalcone-4′-*O*-*β*-D-glucopyranoside **(21)** extracted from *Coreopsis tinctoria* (Li *et al.*, 2015). In addition, a synthetic chalcone (*E*)-1-(2-methoxyphenyl)-3-(2-(trifluoromethyl)phenyl)prop-2-en-1-one **(22)** has elevated NQO1 induction in normal human lung epithelial cells (Beas-2B) (Kumar *et al.*, 2011).

Structure activity relationships have previously shown electrophilic compounds such as chalcones, which have an *α,β*-unsaturated moiety, as well as undergoing Michael reactions can induce chemoprotective enzyme such as NQO1 (Talalay *et al.*, 1988; Dinkova-Kostova *et al.*, 1998; Dinkova-Kostova and Talalay, 2010). Moreover, chalcones lophirones B **(23)** and C **(24)** induce NQO1 in rat liver, in addition to preventing lipid peroxidation, protein oxidation, and DNA damage (Ajiboye *et al.*, 2014).

1.11 Chalcones

They are a group of intermediate compounds related to the flavonoid family (Rosa *et al.*, 2019). In nature, chalcones play an important role in the ecology, biochemistry, and physiology of plants. They have diverse roles in plant physiology including insect attraction and defence against UV light and pathogens. Moreover, they have pharmacological activity as recent researches have also begun to reveal their effects on human biology as their use as antineoplastic and antimicrobial agents has been investigated, in addition to their potential use as antioxidants and chemopreventive agents (Gutierrez *et al.*, 2015; Raghavan *et al.*, 2015; Zhou and Xing, 2015).

Chemically, chalcone is a common chemical scaffold of 1,3 diaryl-2-propen-1-one **(25)**, an open-chain having two aromatic rings, connected via three fragments of carbon bearing *α* and *β*-unsaturated carbonyl motif, which is found in a wide range of natural products related to flavonoid group (Figure **1.23**) (Xue *et al*., 2010; Liu *et al*., 2015). For example, they are found in *Humulus, Artocarpus, Glycyrrhiza, Angelica, Sophora, Morus Ficus, Dorstenia, Scutellaria*, citrus fruits and vegetables like shallots, tomatoes, potatoes and bean sprouts (Orlikova *et al.*, 2011; Kulkarni *et al.*, 2016).

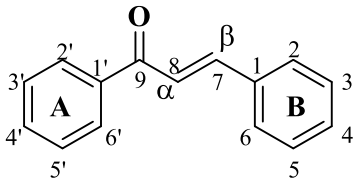

Figure 1.23 Structure of chalcone

Chalcone might extract from natural sources or synthesis artificially. They have been synthesised since the 1800s due to their relative ease of production and their convenience as a template for medicinal chemistry, also because it takes a long time to isolate from natural sources as well as using toxic organic solvents and by-product wastes, for that reason many researchers have been attracted to develop the synthetic of chalcones (Gupta

et al., 2010; Sun *et al.*, 2015). Several studies illustrate that chalcone may be of use in pharmacological studies, for instance, anticancer, antitumor, anti-inflammatory, antidiabetic, cancer chemopreventive, antioxidant and radical-scavenger (Suwito *et al.*, 2014; Raghavan *et al.*, 2015; Zhou and Xing, 2015). On account of the side effects and unsatisfactory cancer treatments, researchers are trying to find chemopreventive non-toxic dietary compound(s) consumption alone or as a co-treatment, therefore chalcones are a prototype of substance that uses as (for) chemoprevention reagents, because they can suppress cancer in different stage from early-stage (initiation) to late-stage that cause metastasis (Orlikova *et al.*, 2011). Furthermore, they have the ability to interfere with the signal transduction pathways, the mitotic phase of the cell cycle and interfere with mitochondria (Gutierrez *et al.,* 2015).

It is reported that the biological activity of chalcones may be related to *α,β*-unsaturated keton, which can activate nuclear factor- κB (NF-κB) and Keap1/Nrf2 pathways by reacting with thiol group in cysteines residues under Michael reaction, Thes feature provide chalcones the opportunity to use as antioxidant, chemopreventive or cytotoxic agents (De Freitas Silva *et al.*, 2018; Lepetsos *et al.*, 2019). Chalcones have been using clinically such as hesperidin methyl chalcone (*E*)-1-[4-[[6-O-(6-Deoxy-α-L-mannopyranosyl)-β-D-glucopyranosyl]oxy]-2-hydroxy-6-methoxyphenyl]-3-(3-hydroxy-4-methoxyphenyl)-2-propen-1-one) **(26)**, which extract from citrus, is using in dietary supplement, pharmaceutical, and cosmetic products as UV and vascular protective (Yosef *et al.*, 2016; Ye, 2017), metachalcone (1-(2,4-Dimethoxyphenyl)-3-(4-methoxyphenyl)-2-propen-1-one) **(27)** is used in choleretic drug and sofalcone (2′-carboxymethoxy-4,4′-bis(3-methyl-2-butenyloxy)chalcone) (**28**), which is a synthetic chalcone, is use as antiulcer and gastric mucosa protective drug due to switch on Nrf2 pathway (**Figure 1.24**) (Aksöz and Ertan, 2011; Zhuang *et al.*, 2017; Kim *et al.*, 2019).

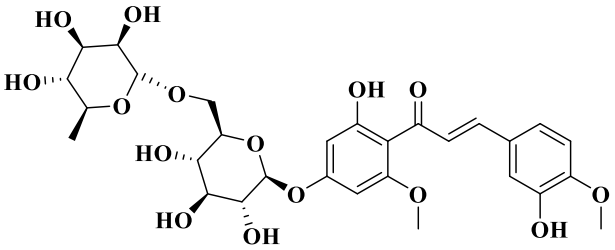

Hesperidin methylchalcone

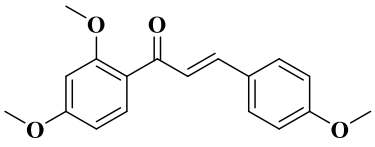

Metachalcone

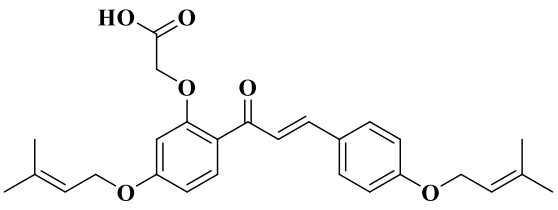

Sofalcone

Figure 1.24 Chalcones hesperidin mrthylchalcone, metachalcone and sofalconen are using as drugs in clinical

1.11.1 Chalcone synthesis

Chalcones are considered privileged structures in medicinal chemistry due to the relative ease with which they may be produced and modified, reflecting the similar ease with which they are produced in nature. From as early as the nineteenth century, many researchers have consequently developed synthetic chalcones, with Kostanecki and Tambor being credited as the first to successfully prepare synthetic chalcones (Kostanecki and Tambor, 1899; Mahapatra *et al.*, 2015). Current synthetic chalcone synthesis is based upon the use of an aromatic ketone and aldehyde base under Claisen-Schmidt methods with a variety of catalytic system being used to couple the A and B rings such as:

1- NaOH and alcoholic solvent under microwave irradiation (Scheme 5) (Kumar *et al.*, 2012; Cazarolli *et al.*, 2013).

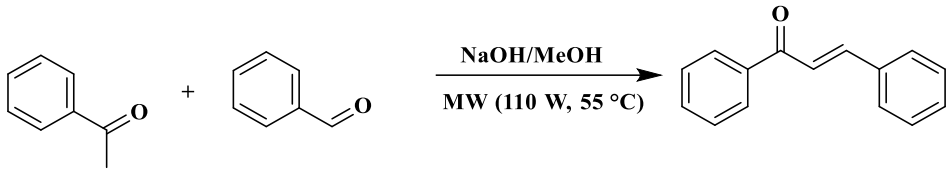

Scheme 5 Chalcones synthesized using NaOH/MeOH

2- $SOCl_2$ and alcoholic solvent at room temperature (Scheme 6) (Petrov *et al.*, 2008; Cazarolli *et al.*, 2013).

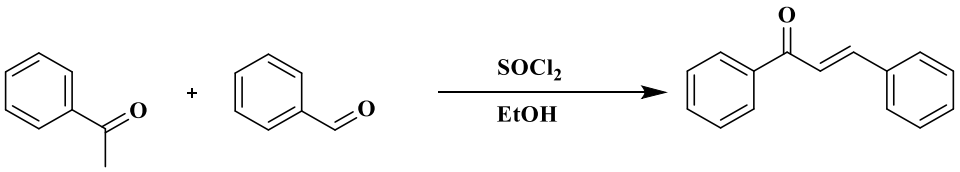

Scheme 6 Chalcones synthesized using $SOCl_2$/EtOH

3- Lithium nitrate ($LiNO_3$) and natural phosphate (NP) catalytic system at room temperature (Scheme 7) (Sebti *et al.*, 2002; Cazarolli *et al.*, 2013).

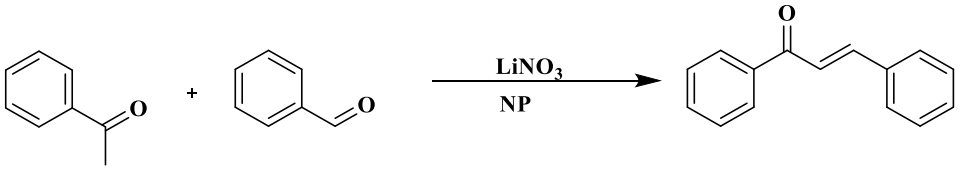

Scheme 7 Chalcones synthesized using $LiNO_3$/NP

4- Zeolite under ultrasound irradiation (Scheme 8) (Watson, 2017).

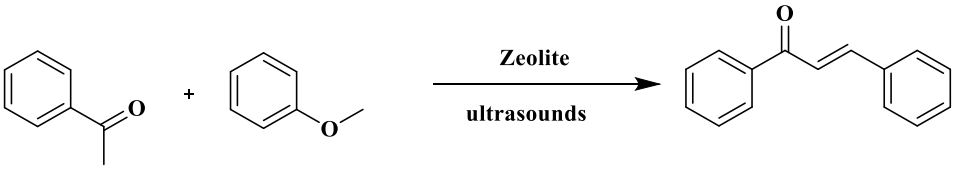

Scheme 8 Chalcones synthesized using zeolite

1.11.1.1 DMU-synthetic chalcone

A group of De Montfort University (DMU) researchers have prepared a novel library of synthetic chalcones (Table 1) in 43-94% yields at room temperature, by Claisen-Schmidt methods using acetophenone and benzaldehyde with (ten equivalents) collection of aqueous sodium hydroxide solution in methanol (Ruparelia *et al.*, 2018).

Table 1 A library of DMU-synthetic chalcones

DMU No	Chemical name	Ring A	Ring B
DMU-102	(*E*)-3-(4-methoxyphenyl)-1-(3,4,5-trimethoxyphenyl)-prop-2-en-1-one	3′,4′,5′-$(CH_3O)_3C_6H_2$	4-$CH_3OC_6H_4$
DMU-104	(*E*)-3-(3,4-dimethoxyphenyl) - 1-(3,4,5-trimethoxyphenyl)-prop-2-en-1-one(	3′,4′,5′-$(CH_3O)_3C_6H_2$	3,4-$(CH_3O)_2C_6H_3$
DMU-105	(*E*)-3-(4-Methoxyphenyl)-1-phenylprop-2-en-1-one	C_6H_5	4-$CH_3OC_6H_4$
DMU-120	(*E*)-1-(3, 5-dimethoxyphenyl)-3-(4-methoxyphenyl)-prop-2-en-1-one	3′,5′-$(CH_3O)_2C_6H_3$	4-$CH_3OC_6H_4$
DMU-121	(*E*)-3-(4-methoxyphenyl)-1-(2,3,4-trimethoxyphenyl)-prop-2-en-1-one	2′,3′,4′-$(CH_3O)_3C_6H_2$	4-$CH_3OC_6H_4$
DMU-132	(*E*)-3-(2,4-dimethoxyphenyl)-1-(3,4,5-trimethoxyphenyl)-prop-2-en-1-one	3′,4′,5′-$(CH_3O)_3C_6H_2$	2,4-$(CH_3O)_2C_6H_3$
DMU-133	(*E*)-1-(2,4-Dimethoxyphenyl)-3-(4-methoxyphenyl)prop-2-en-1-one	2′,4′-$(CH_3O)_2C_6H_3$	4-$CH_3OC_6H_4$
DMU-135	(*E*)-3-(3,4-Methylenedioxyphenyl)-1-(3,4,5-trimethoxy-phenyl)-prop-2-en-1-one	3′,4′,5′-$(CH_3O)_3C_6H_2$	3,4-OCH_2O-C_6H_3

DMU No	Chemical name	Ring A	Ring B
DMU-160	(*E*)-1-(3,4-Dimethoxyphenyl)-3-(3,4-methylenedioxyphenyl)-prop-2-en-1-one	3′,4′-$(CH_3O)_2C_6H_3$	3,4-OCH_2O-C_6H_3
DMU-191	(*E*)-3-(4-propoxyphenyl)-1-(3,4,5-trimethoxyphenyl)-prop-2-en-1-one	3′,4′,5′-$(CH_3O)_3C_6H_2$	4-$PrOC_6H_4$
DMU-192	(*E*)-3-(4-butoxyphenyl)-1-(3,4,5-trimethoxyphenyl)-prop-2- en-1-one	3′,4′,5′-$(CH_3O)_3C_6H_2$	4-$BuOC_6H_4$
DMU-403	(*E*)-1-(3,5-Dimethoxyphenyl)-3-(3,4-methylenedioxyphenyl)-prop-2-en-1-one	3′,5′-$(CH_3O)_2C_6H_3$	3,4-OCH_2O-C_6H_3
DMU-407	(*E*)-1-(2,4-Dimethoxyphenyl)-3-(3,4-methylenedioxyphenyl)-prop-2-en-1-one	2′,4′-$(CH_3O)_2C_6H_3$	3,4-OCH_2O-C_6H_3
DMU-408	(*E*)-1-(2,4-Dimethoxyphenyl)-3-(4-propoxyphenyl)-prop-2-en-1-one	2′,4′-$(CH_3O)_2C_6H_3$	4-$PrOC_6H_4$
DMU-411	(*E*)-3-(3,4-Methylenedioxyphenyl)-1-phenylprop-2-en-1-one	C_6H_5	3,4-OCH_2O-C_6H_3
DMU-416	(*E*)-1-(3-methoxyphenyl)-3-(3,4-methylenedioxyphenyl)-prop-2- en-1-one	3′-$CH_3OC_6H_4$	3,4-OCH_2O-C_6H_3
DMU-419	(*E*)-3-(3,4-Methylenedioxyphenyl)-1-(2,3,4-trimethoxy-phenyl)-prop-2-en-1-one	2′,3′,4′-$(CH_3O)_3C_6H_2$	3,4-OCH_2O-C_6H_3
DMU-423	(*E*)-1-(2,5-Dimethoxyphenyl)-3-(3,4-methylenedioxyphenyl)-prop-2- en-1-one	2′,5′-$(CH_3O)_2C_6H_3$	3,4-OCH_2O-C_6H_3
DMU-427	(*E*)-1-(2,5-Dimethoxylphenyl)-3-(4-methoxyphenyl)-prop-2-en-1-one	2′,5′-$(CH_3O)_2C_6H_3$	4-$CH_3OC_6H_4$
DMU-470	(*E*)-1-(4-methoxylphenyl)-3-(2-methoxyphenyl)-prop-2-en-1-one	2′-$CH_3OC_6H_4$	4-$CH_3OC_6H_4$
DMU-1103	(*E*)-3-(2,4-Dimethoxyphenyl)-1-(3,4-methylenedioxyphenyl)-prop-2-en-1-one	3′,4′-OCH_2O-C_6H_3	2,4-$(CH_3O)_2C_6H_3$
DMU-1112	(*E*)-1-(3,4-methylenedioxyphenyl)-3-(2,3,4-trimethoxy-phenyl)prop-2-en-1-one	3′,4′-OCH_2O-C_6H_3	2,3,4-$(CH_3O)_3C_6H_2$

DMU No	Chemical name	Ring A	Ring B
DMU-1113	(*E*)-1-(4-methoxyphenyl)-3-(3,4,5-trimethoxyphenyl)-prop-2-en-1-one	4′-$CH_3OC_6H_4$	3,4,5-$(CH_3O)_3C_6H_2$
DMU-1119	(*E*)-1-(4-methoxyphenyl)-3-(phenyl) prop-2-en-1-one	4′-$CH_3OC_6H_4$	C_6H_5
DMU-1122	(*E*)-1-(2,4-dimethoxyphenyl)-3-(4-ethoxyphenyl)-prop-2-en-1-one	2′,4′-$(CH_3O)_2C_6H_3$	4-$EtOC_6H_4$
DMU-1133	(*E*)-1-(2,4-Dimethoxyphenyl)-3-(3,4-ethylenedioxyphenyl)-prop-2-en-1-one	2′,4′-$(CH_3O)_2C_6H_3$	3,4-$O(CH_2)_2O$-C_6H_3
DMU-1144	(*E*)-3-(2,5-Dimethoxyphenyl)-1-(3,4-methylenedioxyphenyl)-prop-2-en-1-one	3′,4′-OCH_2O-C_6H_3	2,5-$(CH_3O)_2C_6H_3$
DMU-2201	(*E*)-1-(2,4-Dimethoxyphenyl)-3-(3,4-dimethoxyphenyl)-prop-2-en-1-one	2′,4′-$(CH_3O)_2C_6H_3$	3,4-$(CH_3O)_2C_6H_3$
DMU-2207	(*E*)-1-(2,4-Dimethoxyphenyl)-3-(2,4-dimethoxyphenyl)-prop-2-en-1-one	2′,4′-$(CH_3O)_2C_6H_3$	2,4-$(CH_3O)_2C_6H_3$
DMU-2210	(*E*)-1-(3,4-dimethoxyphenyl)-3-(3, 4-dimethoxyphenyl)-prop-2-en-1-one	3′,4′-$(CH_3O)_2C_6H_3$	3,4-$(CH_3O)_2C_6H_3$
DMU-2219	(*E*)-1-(2-Chlorophenyl)-3-(3,4-methylenedioxyphenyl)-prop-2-en-1-one	2′-ClC_6H_4	3,4-OCH_2O-C_6H_3
DMU-2263	(*E*)-1-(2,4-Dichlororyphenyl)-3-(3,4-methylenedioxyphenyl)-prop-2-en-1-one	2′,4′-$Cl_2C_6H_3$	3,4-OCH_2O-C_6H_3
DMU-2265	(*E*)-1-(2-Methoxyphenyl)-3-(3,4-methylenedioxyphenyl)-prop-2-en-1-one	2′-$CH_3OC_6H_4$	3,4-OCH_2O-C_6H_3
DMU-2267	(*E*)-1-(4-Methoxyphenyl)-3-(3,4-methylenedioxyphenyl)-prop-2-en-1-one	4′-$CH_3OC_6H_4$	3,4-OCH_2O-C_6H_3
DMU-5505	(*E*)-3-(4-ethoxyphenyl)-1-(3,4,5-trimethoxyphenyl)-prop-2-en-1-one	3′,4′,5′-$(CH_3O)_3C_6H_2$	4-$EtOC_6H_4$

1.12 Biological mechanisms of chalcone action

1.12.1 Activation of NRF2 and cellular defence genes

In recent years, there has been an increasing amount of literature detailing the relationships between chalcones and Nrf2, with a number of studies reporting the ability of chalcones to induce Nrf2. Ajiboye *et al.* (2014) report that natural chalcones lophirone B **(23)** and C **(24)** (Table 2) have the ability to induce Nrf2. In addition, the natural chalcone, 3,4,2′,4′-tetrahydroxychalcone 4′-*O*-*β*-D-glucopyranoside **(21)**, has been noted to increase the level of NQO1 in Hepa 1c1c7 cells (Li *et al.*, 2015). Martinez *et al.* (2017) reported that *trans*-chalcone **(25)** has the ability to increase GSH, HO-1, and Nrf2 by the switch on the Nrf2 pathway (Figure **1.25**). Furthermore, other researchers found 2-chloro-4′,6′-dimethoxy-2′-hydroxychalcone **(29)** has the potential to increase GSH levels (Kachadourian *et al.*, 2012), while isobavachalcone **(20)** (Gao *et al.*, 2019) and ligustrazine-chalcone **(30)** (Li *et al.*, 2019) have been found to activate Nrf2 signalling. Moreover, chalcone 2′,4′-dihydroxy-6′-methoxy-3′,5′-dimethylchalcone **(31)** that extract from *Cleistocalyx operculatus* can induce Nrf2 level as well as increase defend genes related to Nrf2 like *HO-1* (Tran *et al.*, 2019). Moreover, flavokawain A **(32)** has chemopreventive features through the switch on Nrf2 pathway and consequently induced HO-1 and NQO1, also reduce ROS level in A7r5 (rat aortic muscle) cell line (Hseu *et al.*, 2019).

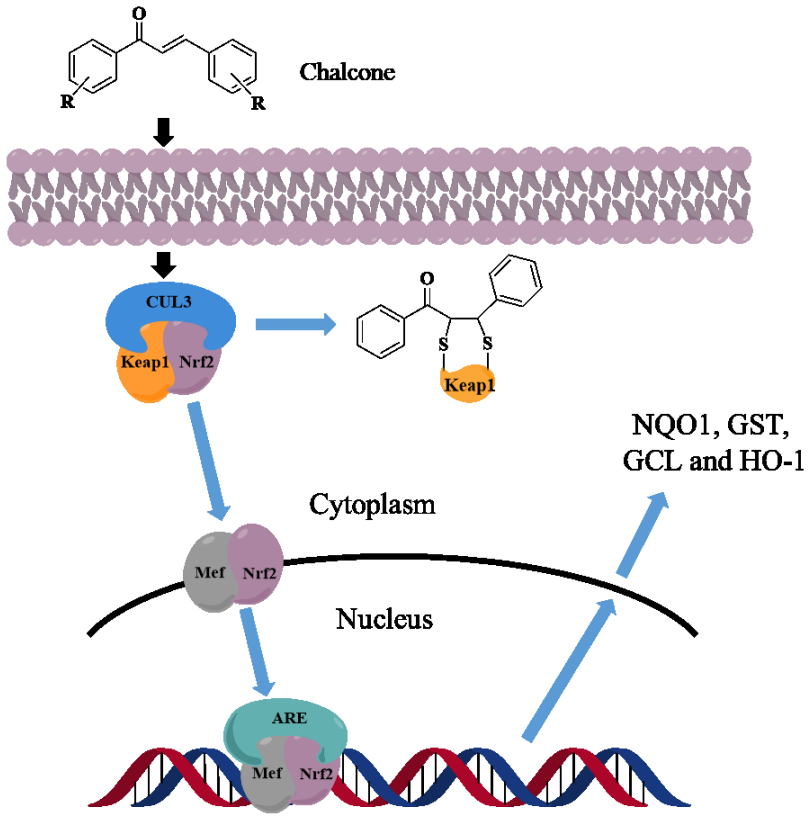

Figure 1.25 Mechanisms of chalcone to switch on Nrf2 pathway and consequently, induce cell defence enzymes like NQO1, GST, GCL and HO-1. Under Michael reaction, chalcone can bind with thiol group in the Keap1-Nrf2 complex. Then Nrf2 is dissociation of the complex and binding with Mef. Thereafter, Nrf2-Mef are binding with a driven gene ARE following by inducing antioxidant defence genes.

1.12.2 Chalcones as anticancer agents

Several studies have investigated the bioactivity of chalcones against cancer and have found that both natural (Table 2) and synthetic chalcones may act as anticancer agents either through the induction of tumour cell death or as chemopreventive agents. Research groups who are interested in the cytotoxicity of chalcones such as Sumiyoshi *et al.* (2015) reported that two chalcone derivatives, xanthoangelol **(18)** and 4-hydroxyderricin **(19)**, isolated from *Angelica keiskei* roots have the ability to inhibit metastasis and tumour growth. In addition, flavokawain B **(33)** was isolated from *Alpinia pricei* and examined

by Hseu *et al.* (2019) who reported that the ability of this chalcone to induce cell death in A549 cell line. Moreover, Abbas *et al.* (2019) synthesised a library of quinoline-chalcone derivatives, and they found chalcones N'-((*Z*)-1-(4-Aminophenyl)-3-(4-chlorophenyl)allylidene)-2-(4-methoxphenyl)quinoline-4-carbohydrazide **(34)** and *N*'-((*Z*)-1-(4-aminophenyl)-3-(4-chlorophenyl)allylidene)-2-(4-methylphenyl)quinoline-4-carbohydrazide **(35)** have anticancer activity against K562 and A549 cells by suppressing the pathway of PI3K/Akt/mTOR. Sakagami *et al.* (2017) reported that fifteen synthetic chalcones (Figure **1.26**), have the ability to act as selective anticancer agents in several human oral squamous cancer cell lines such as HSC-2, HSC-3, HSC-4 and Ca9-22.

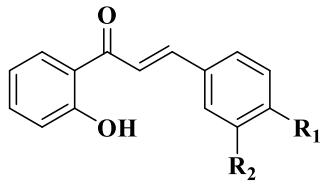

Chalcone **36-42**

36- R_1= H, R_2=H
37- R_1=H, R_2=OH
38- R_1=H, R_2=OCH_3
39- R_1=OCH_3, R_2=OCH_3
40- R_1=H, R_2=F
41- R_1=H, R_2=Cl
42- R_1=H, R_2=Br

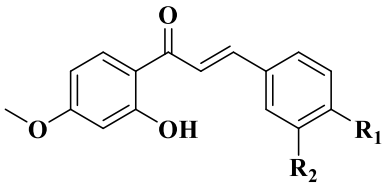

Chalcone **43-47**

43- R_1= H, R_2= OH
44- R_1= H, R_2= H
45- R_1= H, R_2= OCH_3
46- R_1= OCH_3, R_2= OCH_3
47- R_1= H, R_2= Br

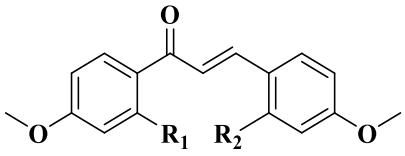

Chalcone **48-50**

48- R_1= H, R_2 = H
49- R_1= H, R_2= OCH_3
50- R_1= OCH_3, R_2= H

Figure 1.26 Synthetic chalcones investigated as anticancer agents by Sakagami *et al.* (2017)

A number of studies have also examined the mechanism of action of chalcones by inducing apoptosis or acting as chemopreventive agents (Table 2), Yang *et al.* (2013) have treated lung cancer cell lines such as H322M, H460, H358, H1792 and H157 with a novel chalcone, 2'-hydroxy-4',5'-dimethoxychalcone **(51)** that was isolated from *S. hainanensis,* and demonstrated this chalcone could increase the level of cellular ROS and induced cell apoptosis. Ramirez-Tagle *et al.* (2016) have used 31-bromo-3,4-dimethoxy-chalcone **(52)** and 2,3,41-trimethoxy-21-hydroxy-chalcone **(53),** on mouse hepatocytes (HepM) and human hepatoma cells (HepG2 and Huh-7), and report that both chalcones lead to cellular apoptosis and an increase ROS levels. Synthetic chalcone (*E*)-1-(2-hydroxyphenyl)-3-(4-methyl-phenyl)-prop-2-en-1-one) **(54)** has also been examined as a chemopreventive agent with the results indicating this chalcone can decrease DNA damage (Da Silva Lima *et al.*, 2017).

Table 2. Properties of representative chalcones from natural sources and its bioactivity

Chalcone	Chemical structures	Plant		Bioactivity	Model	References
Lophirone B **(23)**	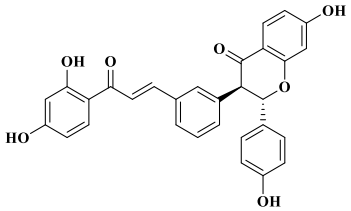	*Lophira alata*	Chemopreventive	↑ Nrf2, NAD, SOD, CAT, GPX and GSH ↓ Keap1, NQO1, GST, EH and UGT	Rat	Ajiboye *et al.* (2014)
Lophirone C **(24)**	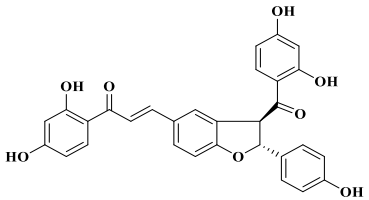					
3,4,2′,4′-tetrahydroxychalcone-4′-*O*-*β*-D-glucopyranoside **(21)**	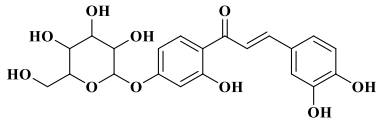	*Coreopsis tinctoria*		↑ NQO1	Hepa 1c1c7	Li *et al.* (2015)
Echinatin **(55)**	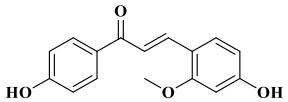	*Glycyrrhyz inflata*		↑ Nrf2 ↓ ALT, AST and LDH	HepG2 cells and mice	Lin *et al.* (2017)

Chalcone	Chemical structures	Plant		Bioactivity	Model	References
Isoliquiritigenin **(56)**	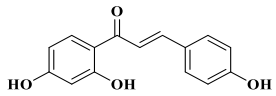	*Glycyrrhiza radix*	Chemopreventive	↑ Nrf2 ↓*UGT1A1, GCL, MRP2, and BSEP*	HepG2 cells and mice	Gong *et al.* (2015)
Xanthoangelol I **(57)**	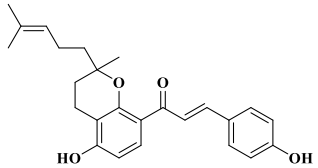	*Angelica keiskei*		┤NO and EBV-EA	Raji cells (Burkitt's lymphoma) and mice	Akihisa *et al.* (2006)
Xanthoangelol J **(58)**	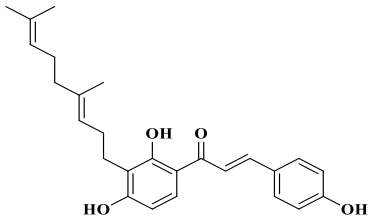					
Deoxydihydroxanthoangelol H **(59)**	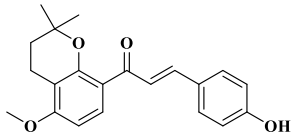					

Chalcone	Chemical structures	Plant		Bioactivity	Model	References
Licochalcone C **(60)**	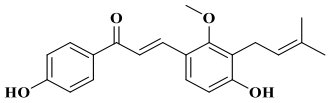	*Glycyrrhiza glabra*	Chemopreventive	↓ iNOS, SOD, ROS and NF-kB ↑ CAT and GP	THP-1 cells (human myelomonocytic leukaemia)	Franceschelli *et al.* (2011)
Isosalipurposide **(61)**	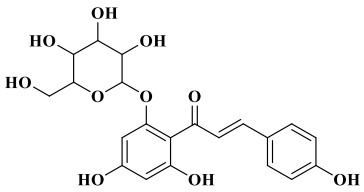	*Corylopsis coreana*		↑ ERK, AMPK, GCL and HO-1 → Nrf2	HepG2 cells	Han *et al.* (2015)
Naringenin chalcone **(62)**	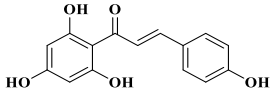	*Helichrysum maracandicum*	Cytotoxic	↓ MAPK , COX-2, proliferative ┤p38	Mice	Yagura *et al.* (2008)

Chalcone	Chemical structures	Plant		Bioactivity	Model	References
Lonchocarpin **(63)**	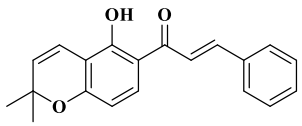	*Pongamia pinnata*	Cytotoxic	┤Bcl-2, tumuor ↓ Cell proliferation, ↑ Bax, caspase-9 and caspase-3 →Apoptosis	Mice and H292 Human lung cancer cells	Chen *et al.* (2017)
Isobavachalcone **(20)**	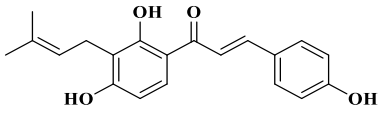	*Psoralea corylifolia*		↓ Bcl-2, (MMP)-2 and MMP-9 ↑ Bax, caspase-3 ┤Proliferation, migration and invasion → Apoptosis	Tca8113 cells (tongue squamous cell carcinoma)	Shi *et al.* (2017)
Flavokawain A **(32)**	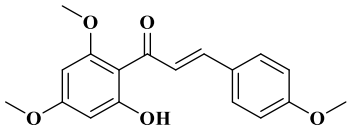	*Piper methysticum*		↑ $p21^{WAF1}$, $p27^{KIP1}$,CDK1, cyclin B1, G1 and G2-M arrest ↓ SKP-2, Myt1 and Wee1 ┤CDK2	T24, UMUC3, TCCSUP, 5637, HT1376, and HT1197 (bladder cancer cell lines)	Tang *et al.* (2008)

Chalcone	Chemical structures	Plant		Bioactivity	Model	References
Flavokawain B **(33)**	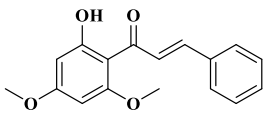	*Piper methysticum*	Cytotoxic	┤Cell proliferation, migration and invasion ↓ NF-kB and COX-2, $GLUT_1$, $FOXM_1$ ↑JNK, c-Jun and HSP60 → G_2/M arrest and apoptosis	MCF-7 and MDA-MB231 (breast cancer cell lines)	Abu *et al.* (2016)
		Alpinia pricei		↓ Bcl-2 ↑ ROS, Bim, GADD153, p-P38 → Apoptosis	HCT116 (colon cell line)	Kuo *et al.* (2010)
				┤Cell proliferation, ROS ↑ ATG7, caspase-9, caspase-3, PARP ↓ cell viability, mTOR → autophagy and apoptosis	A549 (Human non-small cell lung cancer)	Hseu *et al.* (2019)

Chalcone	Chemical structures	Plant		Bioactivity	Model	References
Xanthoangelol **(18)**	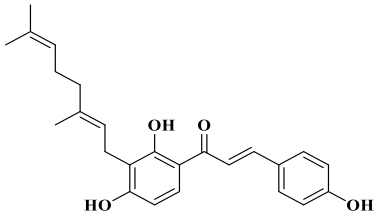	*Angelica keiskei*	Cytotoxic	↓ Cell viability and F4/80 ┤ IL-10, MCP, tumuor and metastasis	LM8 osteosarcoma cells, THP-1 human monocyte and Mice	Sumiyoshi *et al.* (2015)
4-Hydroxyderricin **(19)**	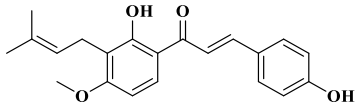					

┤ Inhibition, ↑ increase, ↓ decrease, → induce, Nrf2 (nuclear factor erythroid 2-related factor 2), NAD (nicotinamide adenine dinucleotide), SOD (superoxide dismutase), CAT (catalase), GP (glutathione peroxidase), GSH (glutathione reductase), Keap1 (Kelch Like ECH Associated Protein 1), NQO1 (reduced quinone oxidoreductase-1), GST (glutathione-S-transferase), EH (epoxide hydrolase), UGT (uridyl glucuronosyl transferase), ALT (alanine aminotransferase), AST (aspartate transaminase), LDH (lactate dehydrogenase), UGT1A1 (UDP-glucuronosyltransferase 1A1), GCL (glutamate cysteine ligase), MRP2 (multidrug resistance protein 2), BSEP (bile salt export pump), NO (nitrogen oxide), EBV-EA (Epstein-Barr virus early antigen), iNOS (inducible nitric oxide synthase), ROS (reactive oxygen species), NF-kB (nuclear factor kappa-light-chain-enhancer of activated B cells), ERK (extracellular-signal-regulated kinase), AMPK (AMP-activated protein kinase), HO-1 (heme oxygenase-1), MAPK (mitogen-activated protein kinase), COX-2 (cyclooxygenase-2), Bcl-2 (B-cell lymphoma 2), MMP (matrix metalloproteinase), $p21^{WAF1}$ (cyclin-dependent kinase inhibitor 1), $p27^{KIP1}$ (cyclin-dependent kinase inhibitor 1B), CDK1 (cyclin-dependent kinase 1), SKP-2 (S-phase kinase-associated protein 2), Myt1 (myelin transcription factor 1), Wee1 (nuclear kinase), CDK2 (cyclin-dependent kinase 2), GLUT1 (glucose transporter 1), FOXM1 (forkhead Box M1), JNK (c-Jun N-terminal kinases), HSP60 (heat shock protein 60), GADD153 (growth arrest and DNA damage 153), P-p38 (phospho-p38), ATG7 (autophagy related 7), PARP (poly-ADP ribose polymerase), mTOR (mammalian target of rapamycin), F4/80 (EGF-like module-containing mucin-like hormone receptor-like 1), IL-10 (Interleukin 10), MCP (monocyte chemoattractant protein).

1.13 Aims and objectives

Despite the health care system are using different types of treatment to reduce or cure cancer incident, cancer remain the main problems leading to death worldwide specially lung cancer, which is the highest common cancer. Moreover, it might be the cause of that are related to smoking cigarette that can generate MDA, which is one of the main carcinogenic products leading to induce mutation and consequently lung cancer. For that reason many researchers are offered to find natural or synthetic compound to prevent or reduce cancer incidents through switch on Nrf2 pathway, which is responsible for inducing several defence genes.

Indeed, natural compounds like chalcones are a well-known compounds have been isolated from several plants and also used as cancer chemopreventive and cytotoxic agents, therefore researcher are seeking to prepare synthetic chalcones, which are easy to prepare as well as consuming time and cost, to induce defence genes that can reduce the toxicity effect of MDA.

The aims of this project were to investigate the potential of a library of novel synthetic chalcones to prevent DNA damage via activation of the transcription factor Nrf2.

This aim contained the following objectives:

- To screen the novel library of synthetic chalcones for their ability to activate Nrf2 in the AREc32 reporter cell line (chapter 3).
- To investigate if synthetic chalcones activate Nrf2 in MRC-5 and MRC-5 SV2 cell lines (chapter 4).
- To determine the capacity of chalcones to prevent MDA toxicity in MRC-5 and MRC-5 SV2 cell lines (chapter 5).

- To investigate if the synthetic chalcones, identified in the previous objectives, have the ability to modulate DNA damage induced by MDA in MRC-5 cell lines (chapter 6).
- To investigate the molecular mechanisms responsible for the prevention of DNA damage and/or cell death by selected chalcones (chapter 7).

1.13.1 An overview of the project plan

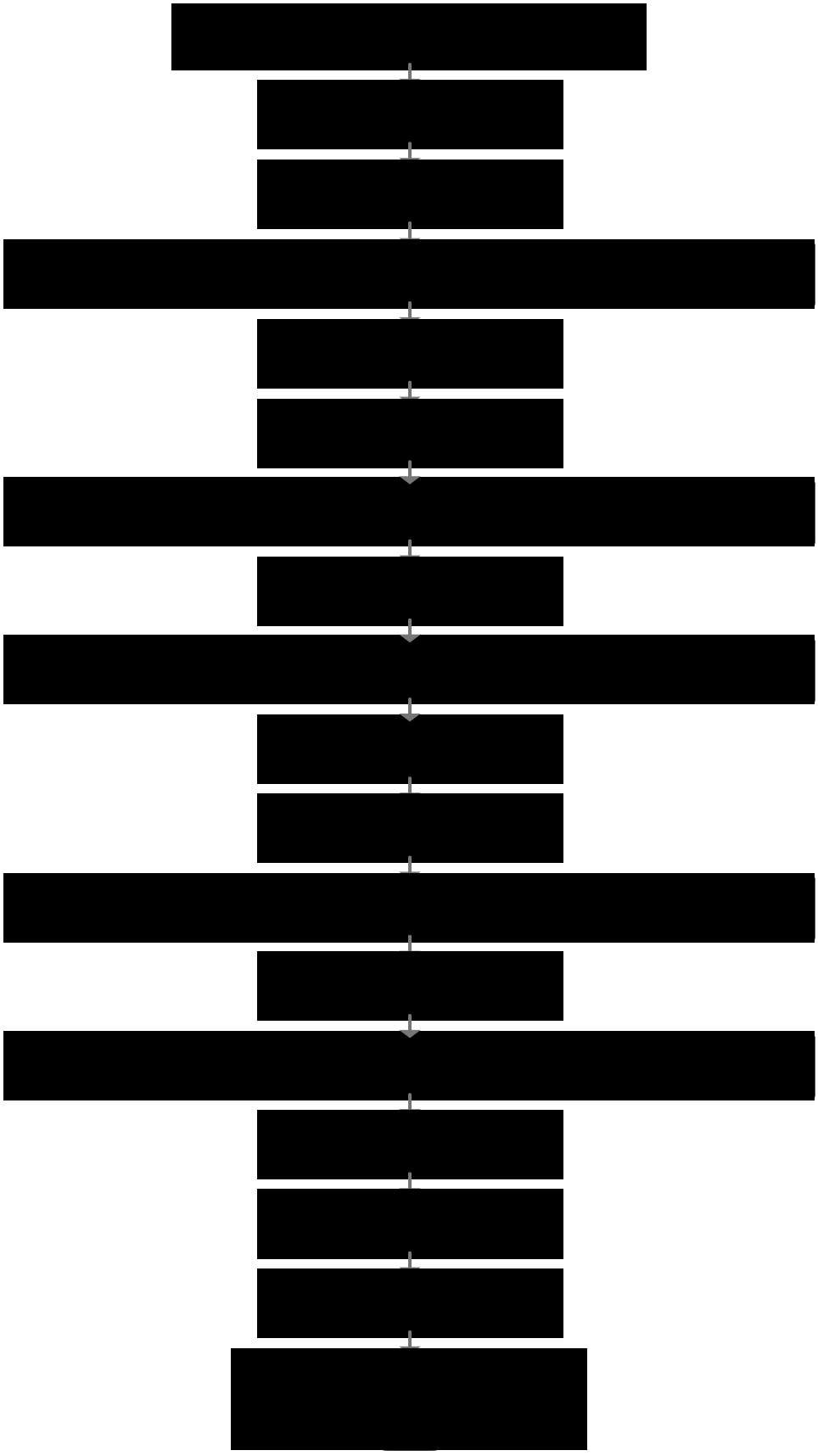

Scheme 9 The project plan

Chapter 2 **Materials and Methods**

2.1 Materials

2.1.1 Reagents

The used materials, origin and suppliers are shown in fallowing Table 3:

Table 3 Materials have used, the origin and the suppliers

No	Materials	Origin	Supplier
1	1,1,3,3-Tetramethoxypropane (TMP)	China	Sigma-Aldrich
2	2′,7′-Dichlorofluorescin diacetate (DCFH-DA)	UK	Sigma-Aldrich
3	2-Thiobarbitiric acid from (TBA)	Germany	Sigma-Aldrich
4	4X Laemmli sample buffer	USA	Bio-rad
5	5x siRNA buffer	UK	Dharmacon
6	Acrylamide/bis-Acrylamide 30%	Germany	Sigma-Aldrich
7	Amersham Hybond P0.45 polyvinylidene difluoride (PVDF)	Germany	GE Healthcare
8	Ammonium persulfate (APS)	Canada	Sigma-Aldrich
9	Anti-rabbit IgG	USA	Abcam
10	β-mercaptoethanol	UK	Thermo-Fisher
11	beta-actin (NM_001101.3) primer	Germany	QIAGEN
12	beta-actin antibody	USA	Abcam
13	Blotting Membrane	Germany	GE Healthcare
14	Bovine Serum Albumin (BSA)	UK	Thermo-Fisher

No	Materials	Origin	Supplier
15	Bradford Reagent	UK	Sigma-Aldrich
16	Comet assay Kit (STA-351)	UK	Biolabs
17	DharmaFECT 1 (transfection reagent)	UK	Dharmacon
18	Dimethyl sulphoxide (DMSO)	UK	Sigma-Aldrich
19	Dried skimmed milk	UK	Marvel
20	Dulbecco's Modified Eagle's medium (DMEM) High Glucose	UK	Sigma-Aldrich
21	Enhanced chemiluminescence (ECL) Prime western blotting detection	UK	GE Healthcare
22	Ethanol	UK	Thermo-Fisher
23	Fetal bovine serum (FBS)	UK	Gibco
24	Gentamicin (G418)	UK	Sigma-Aldrich
25	Glycine	UK	Thermo-Fisher
26	Human ON-TARGETplus SMARTpool siRNA NFE2L2: 5'UAAAGUGGUGCUCAGAAU, GAGUUACAGUGUCUUAAUA, UGGAGUAAGUCGAGAAGUA CACCUUAUAUCUCGAAGUU,	UK	Dharmacon
27	Hydrochloric acid (HCl)	France	VWR chemicals
28	Hydrogen peroxide (H_2O_2)	Belgium	Thermo-Fisher
29	L-glutamine	UK	Sigma-Aldrich

No	Materials	Origin	Supplier
30	Luciferase assay kit reagent	USA	Promega
31	Methanol	Belgium	Thermo-Fisher
32	Minimum Essential Medium (MEM)	UK	Gibco
33	NFE2L2 (NM_006164.4) primer	Germany	QIAGEN
34	Non-essential amino acid (NEAA)	UK	Gibco
35	NQO1 (NM_000903.2) primer	Germany	QIAGEN
36	NQO1 antibody	USA	Abcam
37	Nuclease-Free water	UK	GE Healthcare
38	ON-TARGETplus Non-targeting Control siRNA #1 UGGUUUACAUGUCGACUAA	UK	Dharmacon
39	ON-TARGETplus Non-targeting Pool UGGUUUACAUGUCGACUAA, UGGUUUACAUGUUGUGUGA, UGGUUUACAUGUUUUCUGA, UGGUUUACAUGUUUUCCUA	UK	Dharmacon
40	Penicillin(10^4 U/ml)	UK	Sigma-Aldrich
41	Phosphate buffered saline (PBS)	UK	Sigma-Aldrich
42	Potassium hydroxide (KOH)	USA	Sigma-Aldrich
43	Precision DNase Kit	UK	Primer Design
44	Prestained protein Ladder (PL)	Lithuania	Thermo-Fisher
45	Protease inhibitor cocktail tablets	UK	Sigma-Aldrich

No	Materials	Origin	Supplier
46	QuantiNova Reverse Transcription Kit	Germany	QIAGEN
47	QuantiTect SYBR® Green PCR Kit	Germany	QIAGEN
48	RNaseZap	Lithuania	Thermo-Fisher
49	RNeasy Mini Kit	Germany	QIAGEN
50	Sodium chloride (NaCl)	USA	Sigma-Aldrich
51	Sodium Dodecyl Sulfate (SDS)	UK	Thermo-Fisher
52	Sodium hydroxide (NaOH)	India	Sigma-Aldrich
53	Streptomycin (10mg/ml)	UK	Sigma-Aldrich
54	TEMED	China	Sigma-Aldrich
55	Tert-Butylhydroquinone (tBHQ)	UK	Sigma-Aldrich
56	Thiazolyl blue tetrazolium bromide (MTT, 97.5%)	USA	Sigma-Aldrich
57	Trizma base (Tris)	USA	Sigma-Aldrich
58	Trypan blue solution (0.4% w/v)	UK	Sigma-Aldrich
59	Trypsin/EDTA solution (0.25%)	UK	Sigma-Aldrich
60	Tween 20	UK	BDH
61	Whitman gel blot filter	Germany	GE Healthcare

2.1.2 Cell lines

The AREc32 cell line is a stable and adherent cell line developed from human breast cancer (MCF7) cells that have been genetically modified to contain a luciferase gene construct under the control of the ARE allowing the quantification of ARE induction (via Nrf2 activation), this cell was obtained kindly from Professor Roland Wolf, University of Dundee. In addition, MRC-5 cell lines was a human normal lung fibroblast generated from 14 weeks gestation male. MRC-5 SV2 cell line were a human foetal lung fibroblast derived from MRC-5 by transformation with the SV40 virus. Both cells are characteristic as adherent cells purchased from the European Collection of Animal Cell Cultures (ECACC).

2.1.3 Chalcones

Thirty-one synthetic chalcones were prepared by Dr Ketan Ruparelia as reported in (Ruparelia *et al.*, 2018), and supplied generously by Prof. Randolph Arroo from De Montfort University (DMU). Chalcone numbering was used as provided by the supplier.

Generally, based on compound structure, the number and the position of alkoxy and methylene-dioxy groups, thirty-one chalcones were classified into two main categories: group **1**, all compounds had alkoxy groups, that was divided into two subgroups depending on the alkyl substituent. Group **1a** (Table 4) had only methyl substituents, and group **1b** had methyl group(s) on ring A with ethyl, propyl or butyl groups on ring B (Table 5). The second group, which presented in Table 6, have increased the number of ring group, also it contained alkoxy groups and methylene-dioxy groups. All categories were divided into two sub-groups depend on ring A or ring B.

Table 4. Structures of group **1a** chalcones have vary numbers and positions of methoxy substituents on both the A and B rings.

	Ring A + 3 Methoxy		Ring A + 2 Methoxy		Ring A+ 1 Methoxy
DMU-121	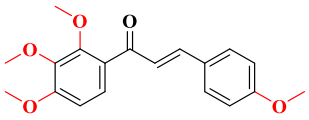	**DMU-120**	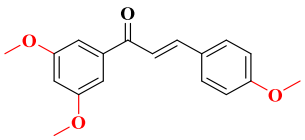	**DMU-1119**	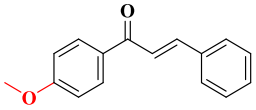
DMU-102	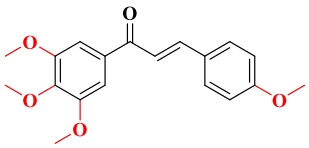	**DMU-427**	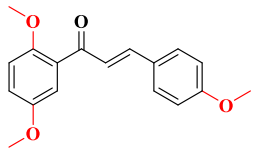	**DMU-470**	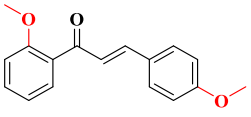
DMU-104	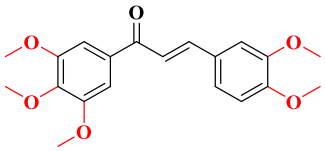	**DMU-2210**	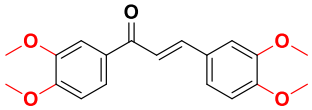	**DMU-1113**	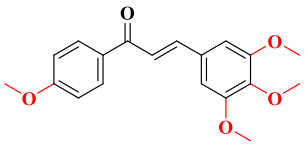
DMU-132	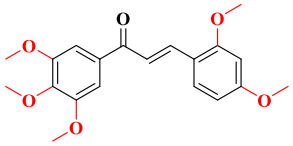	**DMU-2201**	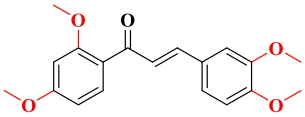		
		DMU-2207	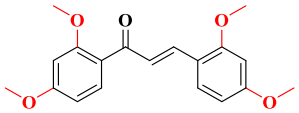		

Table 5. Structures of group **1b** chalcones, which have longer-chain alkoxyl groups on the B ring and varying numbers and positions of methoxy substituents on A ring.

Ethyl-Methyl		Propyl , Butyl - Methyl	
DMU-1122	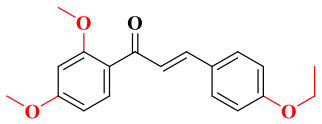	**DMU-408**	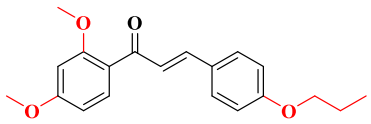
DMU-5505	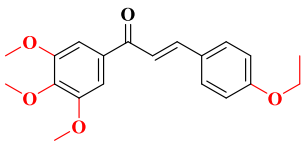	**DMU-191**	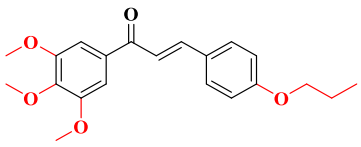
		DMU-192	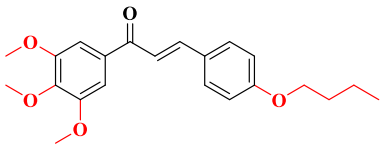

Table 6. Structures of group 2 chalcones, which have methoxy, methylene-dioxy substituents on both the A or B rings or dioxin.

Ring B		Ring A	
DMU-411	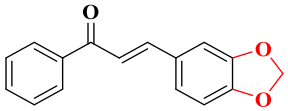	**DMU-1112**	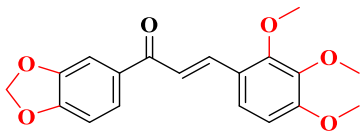
DMU-2219	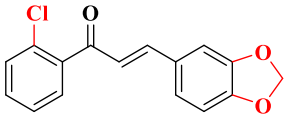	**DMU-1103**	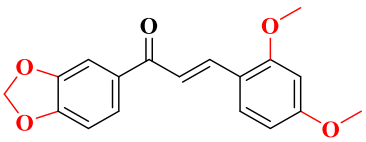
DMU-2267	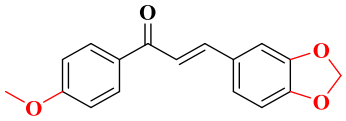	**DMU-1144**	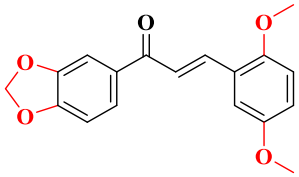

Ring B		Ring A	
DMU-403	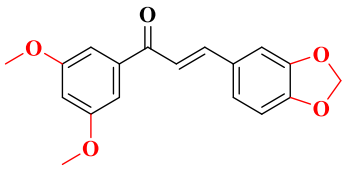		
DMU-423	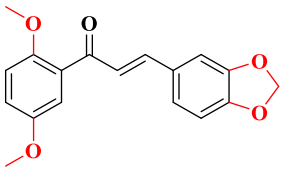		
DMU-135	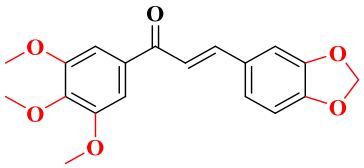		
DMU-419	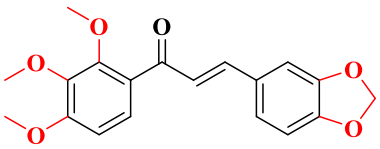		
DMU-416	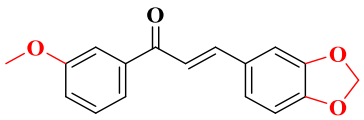		
DMU-160	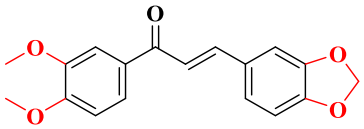		
DMU-2265	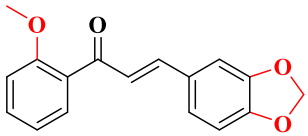		
DMU-1133	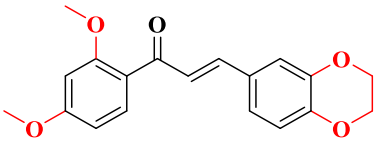		

2.2 Methods

2.2.1 Cell line maintenance and plating

AREc32 cells were maintained in Dulbecco's Modified Eagle's medium (DMEM) supplemented with 10% foetal bovine serum, 0.8% G418, 1% L-glutamine and 1% penicillin/streptomycin. MRC-5 and MRC-5 SV2 were grown in Minimum Essential Medium (MEM) supplemented with 10% foetal bovine serum (FBS), 1% non-essential amino acid (NEAA), 1% L-glutamine, 1% penicillin/streptomycin.

First of all, cells were defrosted around 2 min and then cultured in T-75 tissue culture flask containing 15 ml medium, and incubated in 37 °C until reach a 70-80% confluent. Thereafter, the medium was removed and the monolayers washed twice via 5 ml (1X) PBS to remove any residual FBS that could inhibit trypsin activity. In addition, to detach the monolayers from the primary culture vessel surface, 3-4 ml trypsin-EDTA was added into the flask and settled for two minutes, then removed and incubated at 37 °C for about 5 minutes. A 10 ml of complete medium was added to stop trypsinisation activity, in this stage cells-suspension were ready for counting. Cells were counted by mixing 50 µl from cell suspension with 50 µl trypan blue after 5 minutes cell was counted in 10 squares in a haemocytometer, viable cells have a round shape and colourless, while the dead cells appeared as a dark blue stain. To define cells per millimetre calculated by:

$$*\text{Cell/ml} = \text{average count per square} \times 2 \times 10^4$$

*Note: 2 was dilution factor. 10^4 was the volume correction factor for haemocytometer that was 1x1x0.1 mm.

Cells were suspended in media and either was subcultured into a new flask T-25 or T-75 at ratio 1:3 or 1:5 depending on the cell growth rate otherwise seeded into 96-well, 24-well, 12-well or 6-well plates for experimental purposes. Depending on the assay incubation time or a type of well plates, those were seeded at 1 - 1.2 x 10^4 cells/ well of a 96 well plate (for MTT assay, luciferase assay and ROS), 16 x 10^4/well of 12 well plate (for qPCR) or 36 x 10^4 cells/ well of 6 well plate (for western blotting and comet assay) in a working volume of 180 µl/well, 900 µl/well or 1800 µl/well respectively. Both flask and plate were labelled with subculture date and passage number, then incubated under growth conditions of the optimal temperature 37 °C, humidity 5% carbon dioxide (CO_2) and 95% air.

2.2.2 Freezing the cells

All cell lines were grown and passaged as normal. Cells were counted and centrifuged at 1200 rpm/ 5 minutes. The medium was removed, then the pellet was suspended in a cryoprotective medium (70% MEM, 20% FBS and 10% DMSO) to avoid the freezing lethal effect, and divided in cryo-tubes (each tube has 1 x10^6 cell). Then they were placed in the cryo-box (filled by isopropanol) and stored at -80 ºC overnight or short-term storage. Later, vials were stored in liquid nitrogen at -196 ºC for long-term storage.

2.2.3 Compound dilution and treatment

All chalcones were dissolved in DMSO to make a 100 mM stock solution. The stock solution was then diluted, firstly to 1 mM in DMSO then to 0. 005-10 µM in a fresh cell-culture medium. Secondly, chalcones on 100 mM, stock solution was diluted in DMSO to make 10 mM and then to 10-100 µM in the cell culture medium. Finally, chalcones on 100 mM were prepared on higher concentrations 20 mM in DMSO then to 100-200 µM

in the cell culture medium, from stock solution (the highest percentage of DMSO for all dilutions not exceeding 0.1%). After 24 h of cells seeding, the plate was treated by adding 20 µl from each chalcone dilution (0.005 – 200 µM), 20 µl from DMSO 0.1% (negative control) and 20 µl from DMSO 100% (positive control) as a final solution. Moreover, in case of treated with MDA, MDA was prepared with different concentrations which were 10 µM - 400 µM depending on Yates (2015) results, The plate was incubated at 37 °C for 24 h.

2.2.4 Cell viability assays

Cell viability was determined using MTT assay. MTT reagent was dissolved in warm PBS to a concentration of 5 mg/ml and then filtered and protected from light. Cells were plated at 1-1.2 x 10^4 cells/well to determine the cell viability following treatment with a range of dilutions of chalcones and/or MDA. Following treatment, a 180 µl new medium and 20 µl of MTT solution were added to each well. The plate was then incubated at 37 °C for 3 h. Thereafter, the medium removed from wells and 100 µl DMSO (100%) was added to each well, plates mixed by shaker for 5-10 minutes, then placed in the plate reader (CLARIO Star Microplate reader, BMG Labtech, UK), and measured at OD_{570} nm. The MTT process shown in (Figure **2.1**). The mean % cell viability was calculated as follows:

$$\text{Mean \% Cell Viability} = \frac{\text{Sample Mean Absorbance – Blank (medium without cells)}}{\text{Control Mean Absorbance – Blank}} * 100$$

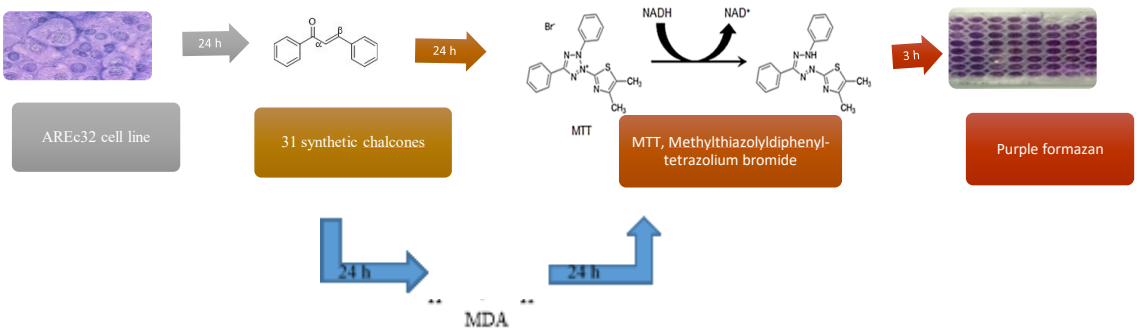

Figure 2.1 Process of MTT assay, including seeding cell, treatment and collect the results

2.2.5 Production of MDA

2.2.5.1 Synthesis of MDA:

MDA was synthesis by acid hydrolysis of TMP as shown in Scheme 10, depending on Yates (2015) procedure, a mixture of 165 µl TMP with 4690 µl HCl (0.1 M), incubated at room temperature for 40 minutes. The solution was then neutralised by adding 4690 µl KOH (0.1 M), next a volume made up to 10 ml by adding 455 µl water to prepare a 100 mM stock solution of MDA.

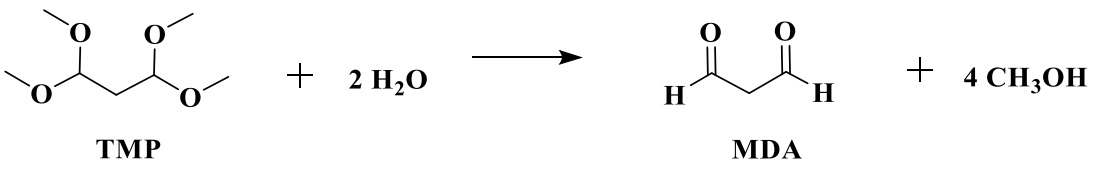

Scheme 10 Forming MDA by TMP hydrolysing

2.2.5.2 Analysis of MDA standards by TBARS

A 100 mM MDA stock solution was diluted with water produced standards in the range 0-1000 µM MDA. Besides, a TBARS reagent was prepared by dissolving 0.375 g TBA in 100 ml HCl (0.25 M) and stirred for 1-2 hours to dissolve. Later, a 100 µl aliquot of each MDA standard was added to 1 ml of TBARS reagent and incubated at 95 °C for 5 minutes, followed by cooling on ice to room temperature. The samples were centrifuged at 2000 x g for 10 minutes. Then 50 µl from supernatant transferred to a 96 well plate and read at OD_{532} nm.

2.2.6 Luciferase assay for measurement of luciferase induction

Luciferase activity in treated cells was determined using the Luciferase Assay System according to the manufacturer instructions (Promega). The process of luciferase assay has shown in Figure **2.2**.

2.2.6.1 Reagent preparation

1X Reporter Lysis Buffer (RLB) was prepared by adding 1 volume of 5X RLB to 4 volumes of distilled water and mixed well. Luciferase Assay Reagent (LAR) was prepared by adding 10 ml of Luciferase assay buffer to the Lyophilised, then mixed and used directly.

2.2.6.2 Cells preparation

AREc32 cells were plated at 1.2 x 10^4 cells/well for 24 h in 96 wells plate then treated in triplicate with 31 synthetic chalcones at non-toxic concentration assessed by MTT assay. 20 µl from each chalcone dilution was added to each well including 180 µl medium.

Negative and positive controls were also included (DMSO 0.1% as negative control and *t*-BHQ in 25 µM as positive control). It was then incubated for 24 h at 37 ºC.

2.2.6.3 Cell lysis

After 24 h, the culture medium was removed, and cells were washed twice by 1X PBS, and then 20 µl from RLB was added to each well. RLB required a single freeze-thaw cycle to complete cell lysis. For that reason, the plates were frozen directly at -20 ºC until the following step.

2.2.6.4 Luciferase measurement

The 20 µl of cell lysate was defrosted and transferred from clear 96 wells plate to a white opaque 96 well plates, followed by adding 100 µl from freshly prepared LAR, the photon emission was measured for a period of less than 1 minute in plate reader (ClarioStar microplate reader, BMG Labtech, UK) and calculated by luminometres units. The luciferase activity level was expressed comparative to the level of luciferase activity in control (DMSO 0.1%) and presented as a fold increase (relative to control).

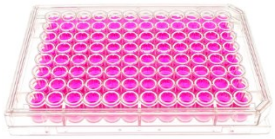

- Plating AREc32 cell line
- 1.2 x 10^4 cell /well

24 h

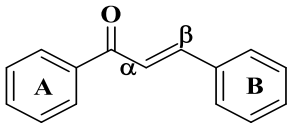

- Treated cell with selective concentration of chalcones

24 h

- Washing cells by PBS
- Adding 20 µL from PLB
- Freezing the plate

24 h

- Transfer lysis cell to white 96 well plate.
- Prepare LAR by adding Luciferase buffer to Lyophilized.

10 s

- Adding 100 µL LAR.
- Reading the emission light.

Figure 2.2 The process of luciferase assay

2.2.7 Western blot for measurement of protein level

2.2.7.1 Sample preparation

MRC-5 and MRC-5 SV2 cells were seeded at concentration 36 x 10^4 cells/well in 6 wells plate, incubated for 24 h cells then treated with chalcones, DMSO (negative control) and tBHQ (positive control). Cells were harvested at 0, 3, 6, 12 and 24 h.

2.2.7.2 Radioimmunoprecipitation assay (RIPA) buffer preparation

A 100 ml of RIPA buffer was prepared by added 3 ml NaCl (5 M), 1 ml EDTA (0.5M), 5 ml Nonidet P-40 (20%), 5 ml SDS (10%), 0.5 g sodium deoxycholate and 5 ml Tris (1M, pH 7.4), which was then made up to 100 ml with water. Also, one tablet of protease inhibitor cocktail was added to 10 ml RIPA buffer, just before used.

2.2.7.3 Cell harvest

The medium was removed and cells washed three times by cold PBS, then 150 µl of cold RIPA buffer was added to each well for 30 minutes. Cells were scrubbed and transferred to Eppendorf tubes then sonicated three times for 10 seconds after that centrifuged at 14000 rpm for 20 minutes, then the supernatant was aliquot in Eppendorf and frozen at -20 ºC.

2.2.7.4 Bradford assay

The amount of protein was determined by Bradford assay. Using a microplate micro-assay, a dilution of bovine serum albumin as protein standard curve was prepared in a range of 0 - 20 µg/ml as showing in Table 7, while, cell lysate samples were diluted on 100X and 1000X by distilled water. A 100 µl of each sample was added on 96 wells plate

in addition to 100 µl Bradford reagent, then incubated for 5 minute at room temperature and the plate was read on OD_{595} nm.

Table 7. A BSA Standard protein curve prepared using micro-assay dilutions

Tube	Standard Volume (µl)	Source of standard	Diluent Volume (µl)	Final [Protein] (µg/ml)
1	10	2 mg/ml stock	990	20
2	500	Tube 1	500	10
3	500	Tube 2	500	5
4	500	Tube 3	500	2.5
5	500	Tube 4	500	1.25
6	-	-	500	0

2.2.7.5 SDS-polyacrylamide gel electrophoresis preparation

A resolving gel (12%) was prepared by adding 1.6 ml double distilled water, 2 ml of acrylamide mix (30%), 1.3 ml of Tris (1.5 M, pH 8.8), 0.05 ml SDS (10%), 0.05 ml of APS (10%) and 0.002 ml of TEMED. Then immediately 5 ml of the prepared gel was poured in between two glass plates, the remaining space being filled with double distilled water to remove air bubbles. The gel was then allowed to polymerise for 30-40 minutes.

To prepare the stacking gel, 0.68 ml double distilled water, 0.17 ml of acrylamide (30%), 0.13 ml of Tris (1.0 M, pH 6.8), 0.01 ml of SDS (10%), 0.01 ml of APS (10%) and 0.001 ml of TEMED were mixed together. The stacking gel mix was then added on top of the resolving gel to fill the space, followed by inserting of the appropriate combs. Then it was left to set for 30-40 minutes for polymerising.

2.2.7.6 Loading and running the gel

a) **Running buffer:** 10 x SDS-page running buffer was prepared by adding 30 g Tris, 144 g glycine and 10 g SDS to 800 ml double distilled water, made up to 1000 ml with water. The 10 x buffer was diluted to 1 x with double distilled water, for running the gel.

b) **SDS-page sample:** 100 µl of samples were prepared by adding protein sample, volume dependent on protein concentration, 25 µl sample buffer (0.9 ml laemmli + 0.1 ml β-mercaptoethanol) and then completed to 100 µl with RIPA buffer. The sample mixture was then incubated at 95 °C for 5 minutes, then cooling on ice.

c) **SDS-Page electrophoresis:** An aliquot of 10 µl from prepared samples were then added to each well in addition to a protein ladder (Figure **2.3**). The electrophoresis has set on 180 V for 55 minutes.

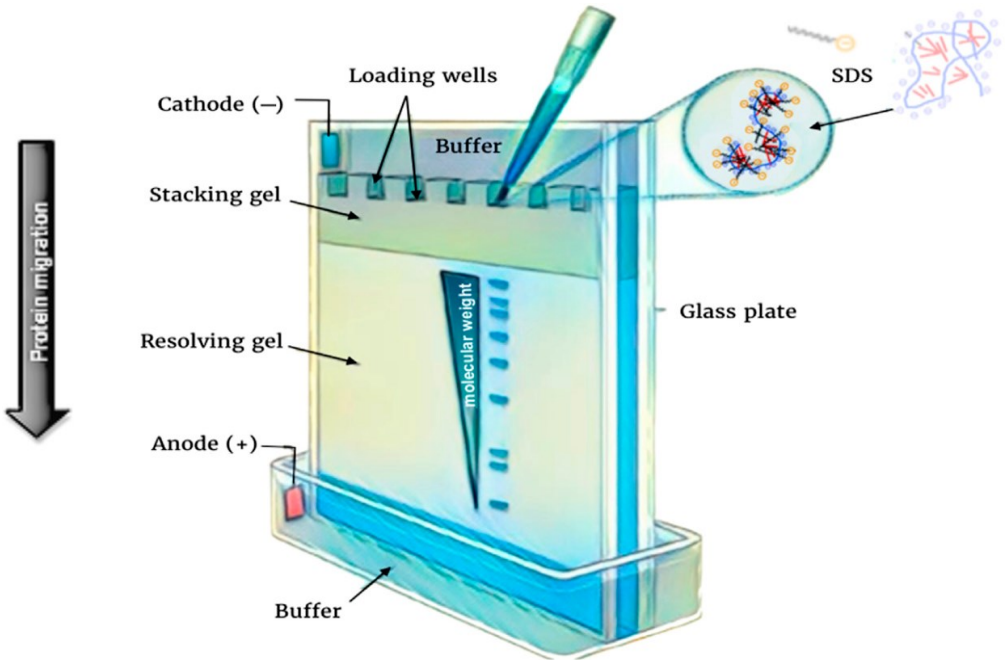

Figure 2.3 SDS-Page electrophoresis using polyacrylamide gel that includes resolving and stacking gel. Protein samples were inserted into wells on upper of the gel. Based on the molecular weight, electrophoreses causes proteins separation by forcing the proteins to migrate in the direction of the anode (+), adapted from Gwozdz and Dorey (2017)

2.2.7.7 Transferring the protein from the gel to the membrane

a) **Transfer buffers:** A 10X transfer buffer was prepared by dissolving 29.3 g glycine, 58.1 g Tris and 3,75 g SDS on 800 ml double distilled water, then the mix made up to 1000 ml. A 1X transfer buffer was prepared by mixing 100 ml (10X transfer buffer) and 200 ml methanol with 700 ml double distilled water.

b) **Blotting:** Proteins were transferred from the gel to PVDF membrane by blotting for 30 minutes at 1 A and 25 V in Bio-Rad Trans-Blot Turbo System (Figure **2.4**).

2.2.7.8 Blocking

After protein transferring from the gel to the membrane, the membrane was marked and proteins were blocked by blocking buffer (5% milk in PBS-T), which was prepared by adding 5 g of skim milk in 100 ml PBS-T (1 ml of Tween 20 mixed with 999 ml of 1X PBS). Afterwards, the membrane was incubated at room temperature for one hour on the shaker.

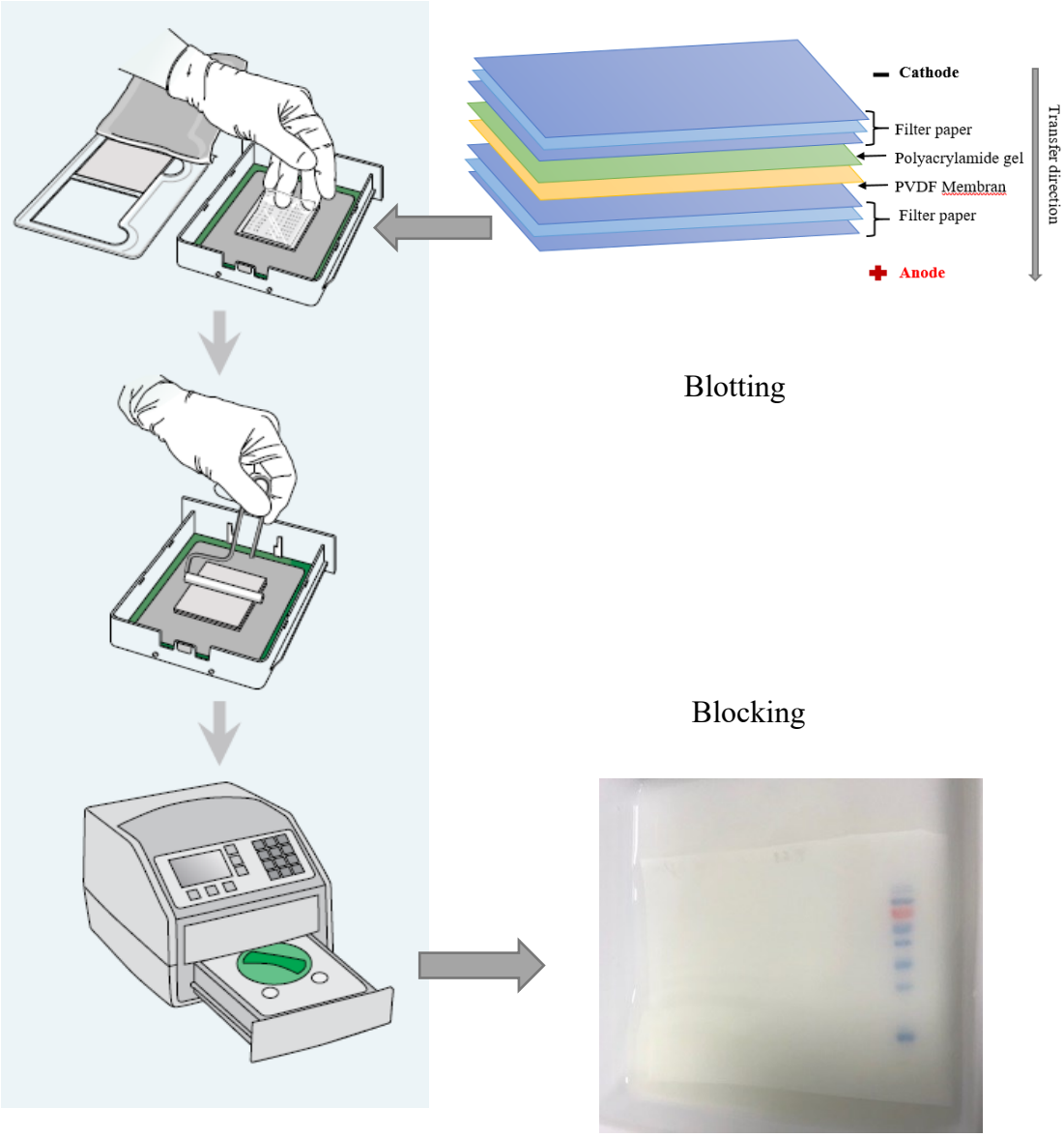

Figure 2.4 The process of blotting and blocking the membrane

2.2.7.9 Immunodetection

2.2.7.9.1 Antibody incubation

a) **Primary antibody:** 10 µl from primary antibody NQO1 (protein of interest) or beta-actin (reference protein) was diluted in 10 ml blocking buffer, then added to the membrane, and incubated overnight at 4 °C on the shaker. At the end of the

incubation period of the membrane (not exceeding 16 h), membrane washed three times by PBS-T for 5 minutes each.

b) **Secondary antibody:** 10 µl secondary antibody IgG was diluted in 10 ml blocking buffer, then added to the membrane and incubated for 1 h at room temperature, then the membrane washed three times by PBS-T for 5 minutes each.

2.2.7.9.2 Chemiluminescent detection

Equal amount from each ECL reagent A (Luminol solution) and B (Peroxide solution) was mixed together and added to the membrane for 1 minute. Then the membrane carefully removed from the detection reagent and positioned between plastic layers, the reaction shows in Figure **2.5**. The protein blot has imaged by Bio-Rad ChemiDoc MP Imaging Machine.

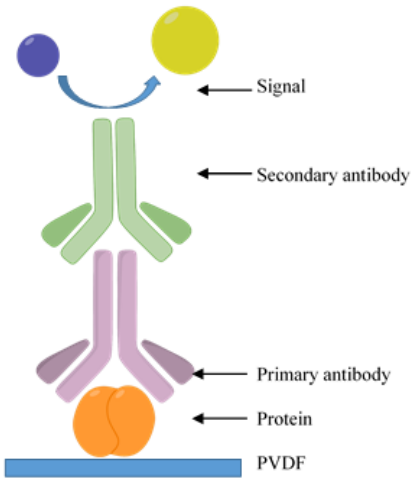

Figure 2.5 The conjunction between proteins, primary and secondary antibody and the detector

2.2.7.10 Stripping

a) **Stripping buffer:** To detect another protein, primary and secondary antibodies should be removed by stripping buffer to incubate the membrane with an additional antibody. Preparing 1X stripping buffer (pH 2.2) was required, it was prepared by dissolving 14 g glycine, 1 g SDS and 10 ml Tween-20 in 800 ml double distilled water, and then the solution made up to 1000 ml.

b) **Stripping membrane:** After NQO1 protein detection, a beta-actin was used as housekeeping (references protein). Membrane was stripped by incubation in stripping buffer twice for 7 minutes each, followed by washing with 1X PBS twice for 10 minutes. Thereafter, the membrane was washed by PBS-T twice for 5 minutes, finally, it was incubated in blocking buffer for 1 h after that membrane was ready for another antibody detection. The process of adding a new antibody was repeated as before (section 2.2.7.9).

2.2.8 ROS assay

A 2′,7′-dichlorofluorescin diacetate (DCFH-DA) has used to detect the ROS in MRC-5. A 4.87 mg was dissolved in 1 ml ethanol to prepare 10 mM stock solution. Cells were seeded at concentration 1.2 $x10^4$ cell/well in 96 wells plate and incubated for 24 h. afterwards, cells were treated with chalcones DMU-1122, 2210 and 1103 for 24 h. The next day medium was removed and 10 µM was prepared in warm PBS, then added to each well for 40 minutes., after that the dye was removed and the wells were washed twice by warm PBS, later, treated the cell with MDA at 10-400 µM as well as with 100 µM H_2O_2 as a positive control. The plate was incubated for 5 h, and then placed in the plate reader (CLARIO Star Microplate reader) and read at λ_{exc}=492 nm and λ_{em}525.

2.2.9 Comet assay

The comet assay was performed in accordance with the kit instruction OxiSelect™ Comet Assay Kit (Cell Biolabs), The following solutions were prepared for use with the kit: TE buffer (10 mM Tris (pH 7.5) with 1 mM EDTA), 1 x Vista Green DNA dye was diluted in ratio 1:10000 in TE buffer. Moreover, a 100 ml of 1X lysis buffer has prepared by dissolving 14.6 g NaCl, 20 ml EDTA, 10 ml from 10 x lysis solution and the volume completed with double distilled water then adjust to pH 10 with 10 N NaOH. The prepared solution was chilled at 4 °C until used.

Additionally, an alkaline solution was prepared by dissolving 1.2 g NaOH and 0.2 ml EDTA in 80 ml double distilled water and the volume adjusted to 100 ml then chilled at 4 °C. Moreover, alkaline electrophoresis solution has prepared by dissolving 12 g NaOH and 2 ml EDTA solution in 800 ml double distilled water and the volume adjust to 1 L, (stored at 4 °C).

2.2.9.1 Preparing cell samples

Cells were plated at 36 x 10^4 cell/well in 6 wells plate for 24 h, then pre-treated with DMU-1122 (20 µM), DMU-2210 (10 µM) and DMU-1103 (10 µM) for 24 h, afterwards, cells were treated with MDA (100 and 400 µM) for 24 h. After 24 h treatment with MDA and one hour with 100 µM H_2O_2 as a positive control, the medium was removed and the cells were washed once by ice-cold PBS than 200 µl/ well of trypsin added for 5 minutes. The complete medium was added to stop the trypsinisation and the cells transferred to vials. Then cells were then centrifuged at 700 x g for 5 minutes and the supernatant discarded. Cells were then washed with ice-cold PBS and centrifuged again and the supernatant discarded. Finally, 1 x 10^5 cells were re-suspended in cold PBS.

2.2.9.2 Preparing slides

To prepare the slide, 75 µl of melted agarose was added to each well. Thereafter, a 10 µl of cell suspension was added to 90 µl of agarose, 75 µl of this sample-agarose mixed was then spread on each well on top of agarose base layer. The slide was maintained horizontally and chilled at 4 °C for 15 minutes in the dark.

After 15 minutes slide was immersed in pre-chilled lysis buffer and incubated for 60 minutes at 4 °C in the dark. After one hour, the lysis buffer was aspirated and immersed in chilled alkaline solution at 4 °C in the dark for 30 minutes.

2.2.9.3 Electrophoresis

Following a 30 minutes incubation in alkaline solution, slides were maintained horizontally in electrophoresis chamber. Approximately 500 ml of pre-chilled alkaline electrophoresis solution was then added to the electrophoresis chamber and applied to 15 V, 0.32 Am for 25 minutes.

2.2.9.4 Staining

The slide was then immersed twice in cold double distilled water at intervals of 2 minutes. Then the water was removed and replaced with 70% cold ethanol for 5 minutes. Thereafter, the slide was removed from ethanol and dried (5-10 minutes). After drying, 100 µl/well from diluted vista green DNA dye was added and incubated in room temperature to dry for 15 minutes. After that, the slide was scanned using a Leica Fluorescence Microscope (DMI6000B).

2.2.9.5 Data analysis

A total of 100 comets were selected randomly, on each well to be analysed using Tri-Tek comet score software (2.0.0.38). The program can measure the pixel (px) and percentage of several parameters such as the area and DNA intensity of the head and tail as well as comet probability, tail moment and Olive moment (Figure **2.6**), which calculate by:

$$Tail\ DNA\% = \frac{100\ *\ Tail\ DNA\ intensity}{Cell\ DNA\ intensity}$$

$$Head\ DNA\% = 100 - Tail\ DNA\ \%$$

$$Extent\ Tail\ Moment = Tail\ DNA\ \% * Length\ of\ Tail$$

$$Olive\ Tail\ Moment = Tail\ DNA\ \% * Tail\ Moment\ Length$$

- Tail DNA intensity means the sum of all tail point.
- Cell DNA intensity means the sum of all point of the head and the tail intensities.

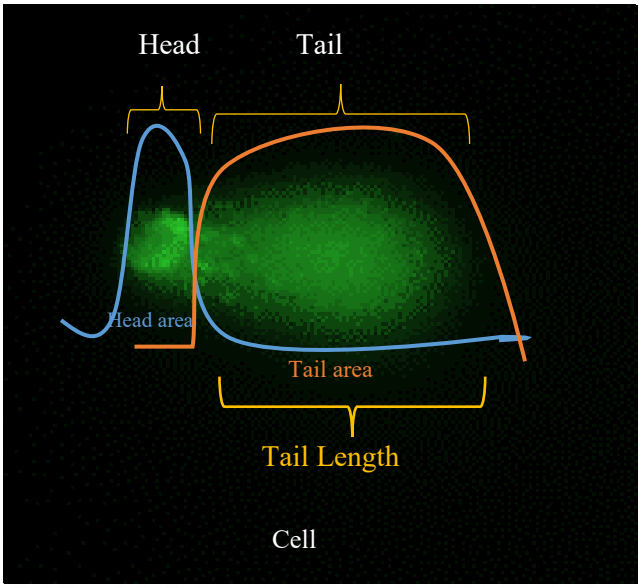

Figure 2.6 Comet assay parameters

2.2.10 Determine gene expression of *NRF2* and *NQO1* using reverse transcription quantitative polymerase chain reaction

RNA mini kit was used to extract RNA, and the following solutions were required: RNA lysis buffer was prepared by adding 10 µl β-mercaptoethanol to 1 ml RLT buffer. In addition, RPE buffer was prepared by adding 44 ml from 100% ethanol to RPE buffer.

2.2.10.1 Cell preparation

Cells were seeded on 12 well plates at concentration 16 x10^4 cell/well. After 24 h cells were treated with chalcones DMU-1122, 2210 and 1103 for post time (0, 3, 6, 12 and 24 h). Then the cells were then washed 3 times with PBS. Later, cells were harvest by adding 300 µl RNA lysis buffer for 5 minutes, than cell lysate was frozen at -80 °C.

2.2.10.2 mRNA extraction

Cells were thawed and 300 µl from 70% ethanol was added and mixed well. Soon after cell lysate-ethanol mix transferred to the column, and centrifuged in high speed 14000 rpm for 15 seconds. The liquid then removed from the tube bottom and 700 µl of RW1 was added to the column and centrifuged at 14000 rpm, for 15 seconds. Afterwards the filtered liquid was discarded and cell lysate washed by adding 500 µl of RPE and centrifuged at 14000 rpm for 15 seconds. Later, another 500 µl was added in the column and centrifuged at 14000 rpm for 2 minutes. The tube was then changed to a new one and centrifuged again for 1 min and 16000 x g. In this stage, the RNeasy spin column transferred to new 1.5 ml qPCR tube. Afterwards, 50 µl from RNase free water was added directly to the span membrane and centrifuged for 1 min at 8000 x g. Moreover, the same water was reused again and centrifuged at 8000 x g for 1 minute.

2.2.10.3 mRNA concentration:

Nanodrop 2000 spectrophotometer was used to determine the purity and concentration of mRNA, Samples were measured at $OD_{260/280}$ nm.

2.2.10.4 Quantification of genes by RT-qPCR

To remove any DNA, a 5 µl from DNase buffer and 0.5 µl DNase enzyme were added to the samples. Samples were incubated for 10 minutes at 30 °C and then incubated on ice. To make ensure each sample contained the same concentration of mRNA, each sample was diluted with RNase-free water to prepare a volume of 13 µl.

A reverse transcription master mix was prepared by mixing 2 µl gDNA, 1 µl Reverse transcriptase (RT enzyme) and 4 µl RT reaction mix. The reaction mix was added to 13 µl prepared sample to make 20 µl RT reaction sample. At the same time, Non-RT sample was prepared in the same process but the RT enzyme was replaced by RNase-free water instead. A cDNA was synthesized in a thermal cycler, according to Table 8. Afterwards, the cDNA was diluted in ratio 1:10 by adding 180 µl RNase-free water to 20 µl sample. The sample was stored on ice for immediate use, or at -20 °C for later use. Each sample was prepared in triplicate. Additionally, each sample was prepared with RT and Non-RT.

Table 8. A thermal cycler for synthesised cDNA

Step	Temperature °C	Time (min)
Annealing	25	3
Reverse transcriptase	45	10
Inactivation of reaction	85	5

An RT-PCR reaction mix was prepared by adding 10 µl SYBR® Green, 6 µl RNase-free water, 2 µl primer and 2 µl cDNA sample to make 20 µl qPCR sample reaction. The sample was added in 0.1 ml strip tube then closed by cap and incubate in Rotor-Gene Q, that was previously programmed with SYBR Green as the detection dye. The cycling conditions are shown in Table 9.

Table 9. A thermal cycling conditions of RT-PCR using Rotor-Gene Q

Step		Temperature °C	Time	Cycles number
Hold		95	15 min	1
Cycling	**Denaturation**	94	15 s	40
	Annealing	55	30 s	
	Extension	72	30 s	
Melt		72-95	90 s (first step)	1
			5 s (each step)	

The expression of the target genes (NRF2 and NQO1) were relative to the reference gene (*beta-actin*) using a cycle threshold (C_T) comparative quantification ($\Delta\Delta C_T$) method through normalisation of the ΔC_T for gene of interest with the ΔC_T for internal reference gene (house-keeping gene) (Schmittgen and Livak, 2008) as shown in following equation (Livak and Schmittgen, 2001):

$$\Delta C_T = C_T,\text{Target} - C_T,\text{reference}$$

$$\Delta\Delta C_T = (C_T,\text{Target} - C_T,\text{reference})\text{Time x} - (C_T,\text{Target} - C_T,\text{reference})\text{ Time 0}$$

Time *x* is any time point and Time 0 represents the 1x expression of the target gene normalise to housekeeping gene.

Each sample was prepared in duplicate, using RT sample with the gene of interest and the reference, as well as using Non-RT sample just with the reference gene. In addition to used SYBR® Green master mix with RNase-free water instead of the sample.

2.2.11 NRF2 gene transfection

Cells were plated in a 96 well plate (1.2 x 10^4 cell/well) for MTT assay, 12 well plate (16 x 10^4 cell/well) for qPCR assay, and 6 well plate (36 x 10^4 cell/well) for Western blotting assay, in MEM (antibiotic free, 10% FBS, 1% NEAA), and incubated overnight.

2.2.11.1 siRNA resuspension

The *NRF2* gene silencing was investigated using A ON-TARGETplus SMARTpool siRNA *NRF2*, ON-TARGETplus Non-targeting Pool and ON-TARGETplus Non-targeting Control siRNA #1. In addition to a DharmaFECT 1 as a transfection reagent.

A 20 µM stock solutions of siRNA were prepared by adding 1 ml from 1X siRNA buffer (Dharmacon) (1 ml 5X siRNA buffer with 4 ml RNase free water) to the 20 nmol siRNA. Thereafter, the vial placed on an orbital mixer for 30 min, at room temperature. The siRNA tube was then centrifuged briefly. Next, the siRNA concentration was verified by nanodrop 2000 spectrophotometer at $OD_{260/280}$ nm (1 µM was equal to 13.3 ng/ µl). The solution was divided into aliquots and frozen at -20 °C. These were further diluted by 1X siRNA buffer forming a volume of 5 µM working solution. The 5 µM was diluted in serum free medium to make 50 nM as a final concentration of siRNA, with the amount dependent on the type of experiment, which is shown in Table 10.

Table 10. Volumes/well for transfecting siRNA at 50 nM final concentration

Well plate	Tube 1: dilution siRNA target or nontarget (ul/well)		Tube 2: dilution DharmaFECT (ul/well)		Complete medium (µl /well)	Total transfection volume (µl /well)
	Volume of 5 uM siRNA (µl)	Serum free medium	Volume of DharmaFECT reagent (µl)	Serum free medium		
96	1	9	0.1	9.9	80	100
12	10	90	1	99	800	1000
6	20	180	2	198	1600	2000

Tube 1 and tube 2 solutions were incubated for 5 minutes, thereafter, the two solutions were mixed together gently and incubated for 20 minutes to form siRNA-Dharmafect complexes. The medium removed from the well and the siRNA-Dharmafect solution was added to the well and incubated at 37 °C at intervals of 24 h, followed by a normal treatment with chalcone or/and MDA using the antibiotic free complete medium. The MTT, Western blotting and qPCR experiments were done the same as previous methods. Each experiment was done in duplicate, Moreover, each siRNA experiment including negative control (DMSO 0.1%), 20 µM DMU-1122, 10 µM DMU-2210 and 10 µM DMU-1103 alone or with MDA at concentration 10-400 µM for MTT assay and 100 µM for Western blotting and qPCR. As well as the same samples were examined with non-target gene as a control.

2.3 Statistical analysis

All experimental results were carried out in triplicate and the data were expressed as mean ± SD. Depending on the experiment a *t*-test or one-way analysis of variance (ANOVA) were used to determine whether there are any statistically significant differences between treatments by *P*-values less than 0.05 ($p<0.05$). The data were statistically analysed by Graph Prism 7.0 software.

Chapter 3 **Screening of chalcones for induction of luciferase activity in the AREc32 cell line**

3.1 Introduction

The Nrf2, a transcription factor that regulates several defence genes, contain ARE-driven gene in their promoters, and determine the potential of chemopreventive compounds to induce the expression of ARE-driven gene. Researchers used luciferase enzyme as indicator of switch on Nrf2/ARE pathway, which is reporter gene assay and is commonly used in biochemistry, biomedical, biomolecular and pharmaceutical research (Wang *et al.*, 2006; Allard and Kopish, 2008).

The Nrf2 induction has been determined by using different assays such as luciferase complementation imaging assay by measuring luciferin enzyme concentration in HEK293T cells and flanks of nu/nu CD-1 nude mice (Ramkumar *et al.*, 2013), fluorescence correlation spectroscopy in HepG2 cells (Yoshizaki *et al.*, 2017), HRP-conjugated secondary antibody (ELISA kit) in mice (Aliyu *et al.*, 2018) and in HCC (primary human cells), THLE5B (immortalized human hepatocyte cell), Huh7 and WRL68 (Human hepatoma cell) lines (Czauderna *et al.*, 2018). Moreover, it has measured by Western blotting and qPCR in HepG2, Hepa-1c1c7, MCF-7 and MDA-MB-231 cell lines (Dong *et al.*, 2019; Shin *et al.*, 2019) as well as by luciferase assay in AREc32 and HepG2 reporter Cell lines (Rubio-Navarro *et al.*, 2019; Shan *et al.*, 2019).

Furthermore, to develop a simple, robust and beneficial assay to determined Nrf2 induction, researchers have used luciferase gene transfected into different cell lines, for example, Boerboom *et al.* (2006) have transfected Hepa-1c1c7 and HepG2 cells with vector pTI(mGST-Ya-EpRE)Luc+ (mouse) or pTI(hNQO1-EpRE)Luc+ (human), and they found transfected HepG2 with mouse vector pTI(mGST-Ya-EpRE)Luc+ showed higher luciferase activity than others. Moreover, another group directed by Prof Roland Wolf from the University of Dundee have transfected CHO, Hepa1c1c7, HepG2 and MCF7 cell lines with ARE-luciferase reporter plasmids. The upstream gene of firefly

luciferase contain several copies of *pGL-nxARE*, which present in rat as *GSTA2* and in mouse as *gsta1* gene promoters. Prof. Wolf's team found that MCF7 cell line has the highest induction of ARE transcription and are more stable than others. They called the MCF7 transfected cell as AREc32 cell line and the later are using to determine the induction of ARE-driven gene expression by chemoprevation drugs (Wang *et al*., 2006).

Initially, measurement of cell viability was an essential step in cell culture and drug discovery due to assistance to determine the drug toxicity as well as the number of healthy cells. Various cell viability assays such as trypan blue dye, MTT (3-(4,5-dimethylthiazol-2-yl)-2,5-diphenyltetrazolium bromide), XTT (sodium3'-[1-(phenylaminocarbonyl)-3,4-tetrazolium)-bis-(4-methoxy-6-nitro) benzene sulphonic acid hydrate), MTS (3-(4,5-dimethylthiazol-2-yl)-5-(3-carboxymethoxyphenyl)-2-(4-sulphophenyl)-2H-tetrazolium), alamar blue, ATP (adenosine triphosphate), confocal imaging for live/dead staining, LDH (lactate dehydrogenase), caspase activity, apoptosis, necrosis, xCELLigence system for label-free and real-time monitoring, sulforhodamine B and clonogenic assays and RAMAN microscopy, are commonly used experimental methods. These methods are range from simplest like trypan blue dye to the complex like RAMAN micro-spectroscopy. In addition to complexity, the speed, cost, limitations and equipment required are playing an important role to choose the type of using assay (Stoddart, 2011).

In this project, to determine the potential of chalcones to induce Nrf2 activity, the AREc32 luciferase reporter cell line containing Nrf2 binding site linked to the luciferase gene was used. This reporter assay therefore allows the quantification of ARE induction by various classes of chemicals.Before screening for luciferase activity induction it was necessary to determine the highest concentration of chalcones that cells can tolerate prior to exhibiting the previously defined acceptable level of toxicity, and to investigate that the cell viability assay was used.

3.1.1 The MTT assay

Cytotoxic and cell viability assays are used widely to determine chemical drug toxicity. In contrast of other assays that might be sensitive to the environment, interfering with several factors, limitation of cell number or suitable for selective cells, the MTT assay is a one of common assay for screening anticancer and pharmaceuticals drugs, because it can metabolise by several cell types and very robust (Stoddart, 2011).

The MTT assay depends on the reduction of the dye 3-(4,5-dimethylthiazol-2-yl)-2,5-diphenyltetrazolium bromide by NADH resulting in the formation of the formazan product with an intense purple colour which absorbs light at OD_{570} nm. This reaction takes place in viable cells only. It is thought that this process occurs in the cytoplasm, mitochondria and cell membrane (Scherlieb, 2011; Stoddart, 2011; Riss *et al.*, 2016).

3.1.2 Luciferase assay

The luciferase reporter assay is commonly used to quantify the ability of compounds to switch on the expression of ARE promoter gene that responsible for activating transcription factor Nrf2. The principal of the assay depend upon generating light by the luciferase enzyme. In addition, that can be carried out using AREc32 reporter cell line.

The principle of the assay relies on the production of light by the luciferin enzyme. The reaction involves the substrate luciferin ((*S*)-2-(6-hydroxybenzo[d]thiazol-2-yl)-4,5-dihydrothiazole-4-carboxylic acid) which is also known as dehydroluciferin, reacting with ATP (Kheradvar *et al.*, 2015) in the presence of Mg^{2+} and the enzyme 'luciferase'. The product of this reaction is luciferin adenylate (LH_2-AMP), is then oxidised to form oxyluciferin and hence generate light emission (Scheme 11) (DeLuca and McElroy, 1974; Bai *et al.*, 2015).

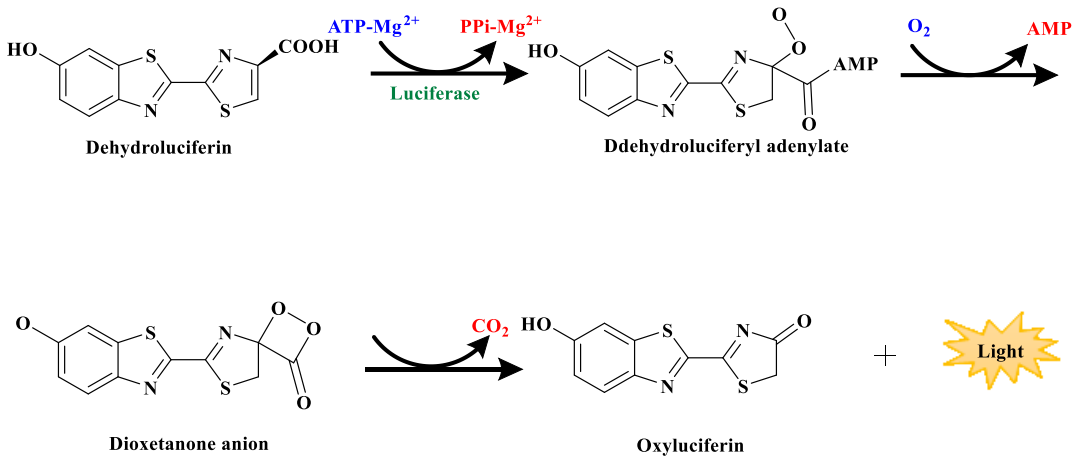

Scheme 11 The mechanism of luminescence

3.1.3 The aims and objectives of this chapter

Nrf2 is a transcription factor that regulates the expression of more than 250 antioxidant defence genes. It has been used for the development of several pharmacological drugs due to its electrophilicity, which can bind with thiol group like cysteines residues in Keap1-Nrf2 complex that lead to separation Nrf2 from Keap1, and then induce a number of defence genes (Robledinos-Antón *et al.*, 2019). To determine the induction of Nrf2, researchers had developed reporter cell line like AREc32, which has luciferase in there promoter as an indicator of Nrf2 induction (Wang *et al.*, 2006). Moreover, chalcones are a well-known natural product used as chemopreventive and anticancer drugs, having *α,β*-unsaturated carbonyl feature as electrophilic compound that can react with thiol group. It is reported that chalcones can react with thiol group in Keap1, dissociation Nrf2 than increase the expression of defence genes (Maydt *et al.*, 2013). Taking into account all theafore mentioned evidences, this chapter has been aimed to identify the non-toxic concentration of chalcones, and to investigate whether chalcone can activate Nrf2 or not by comparing with control (non-treated cells). These aims have been investigated by following objectives:

1- Determine the non-toxic concentration of thirty-one novel DMU-chalcones on AREc32 cell line using MTT assay.

2- Assess the induction of Nrf2 that induced by non-toxic concentration of chalcones on AREc32 cell line using luciferase assay.

3.2 Results and Discussion

3.2.1 Toxicity screening of the chalcone library

The following results are grouped according to chemical similarities in the structure of the compounds, which have different substituents on the ring. It has been reported that the activity of chalcones against cancer depends on the positions and the number of methoxy groups in ring A and B (Champelovier *et al.*, 2011). The novel DMU-chalcones tested in this study were grouped according to the same classification as shown in Table 4 - Table 6 (Section 2.1.3).

Initially, all chalcones have assessed on AREc32 cell line, with rang of different concentrations depending on the toxicity from low concentration and high toxicity to high concentration and low toxicity that were applied by diluting chalcones from 0.0005-1 µM, chalcones that non-toxic up to 1 µM were diluted in higher concentration, which were1-10 µM, then chalcones that non-toxic up to 10 µM diluted in higher concentration, which were 10-20 µM.

AREc32 cells are time and dose dependent, because the aim of this chapter to indicate the fold induction of luciferase, which can increase two folds by 1 µM *t*-BHQ (luciferase inducer) in 24 h (Wang *et al.*, 2006), therefore, the toxicity of chalcones were determine by the MTT assay for 24 h incubation as well.

3.2.1.1 *trans*-Chalcone

To determine the toxicity effect of alkoxy, methylene-dioxy and dioxin groups in these synthetic compounds, the results were compared to *trans*-chalcone as a natural product which has no substituents on both rings. The results showed that *trans*-chalcone is non-toxic up to 25 µM concentration and toxic in high concentrations (Figure **3.1**).

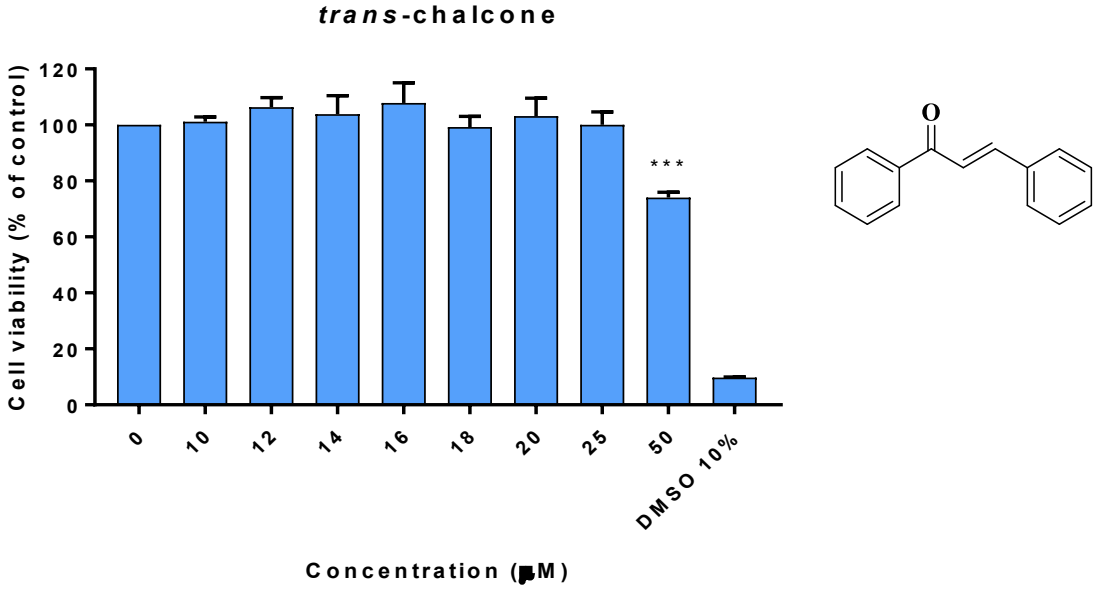

Figure 3.1 AREc32 were exposed to *trans*-chalcones for 24 h after which cell viability was determined using the MTT assay. Data are presented mean ± SD. (n=3), *** for $p<0.001$ significant compared to control (0.1% DMSO)

3.2.1.2 DMU-chalcones group 1a

3.2.1.2.1. Three methoxy groups on ring A

The first sub-group (first column of Table 4) (Section 2.1.3.) is those chalcones where the alkoxy groups are methoxy only (three methoxy in ring A and one or two methoxy in ring B) Figure **3.2** and Figure **3.3** show that the compounds in the first column of Table 4, DMU-121 and 104 were non-toxic up to 0.5 μM, while DMU-102 was non-toxic up to 0.1 μM and DMU-132 was non-toxic up to 0.05 μM. Chalcone DMU-121 has 2',3',4'-OMe on ring A, whereas based on ring B it has a methoxy group in positions C-4 only. However, DMU-102, 104 and 132 have 3',4',5'-OMe on ring A. Whereas based on ring B, the three chalcones all have a methoxy group on the position C-4 but DMU-104 and 132 have an additional methoxy in position C-3 and C-2 respectively. DMU-104 was not only different from DMU-102 and DMU-132 in a number and position of methoxy groups which is 3,4-OMe in DMU 104, 4-OMe in DMU-102 and 2,4-OMe in DMU-132, but also it was less toxic than them. It might be that the 3-OMe in ring B reduces the toxicity of DMU-104 compared with DMU-102 and 132, which do not have a methoxy group on position C-3.

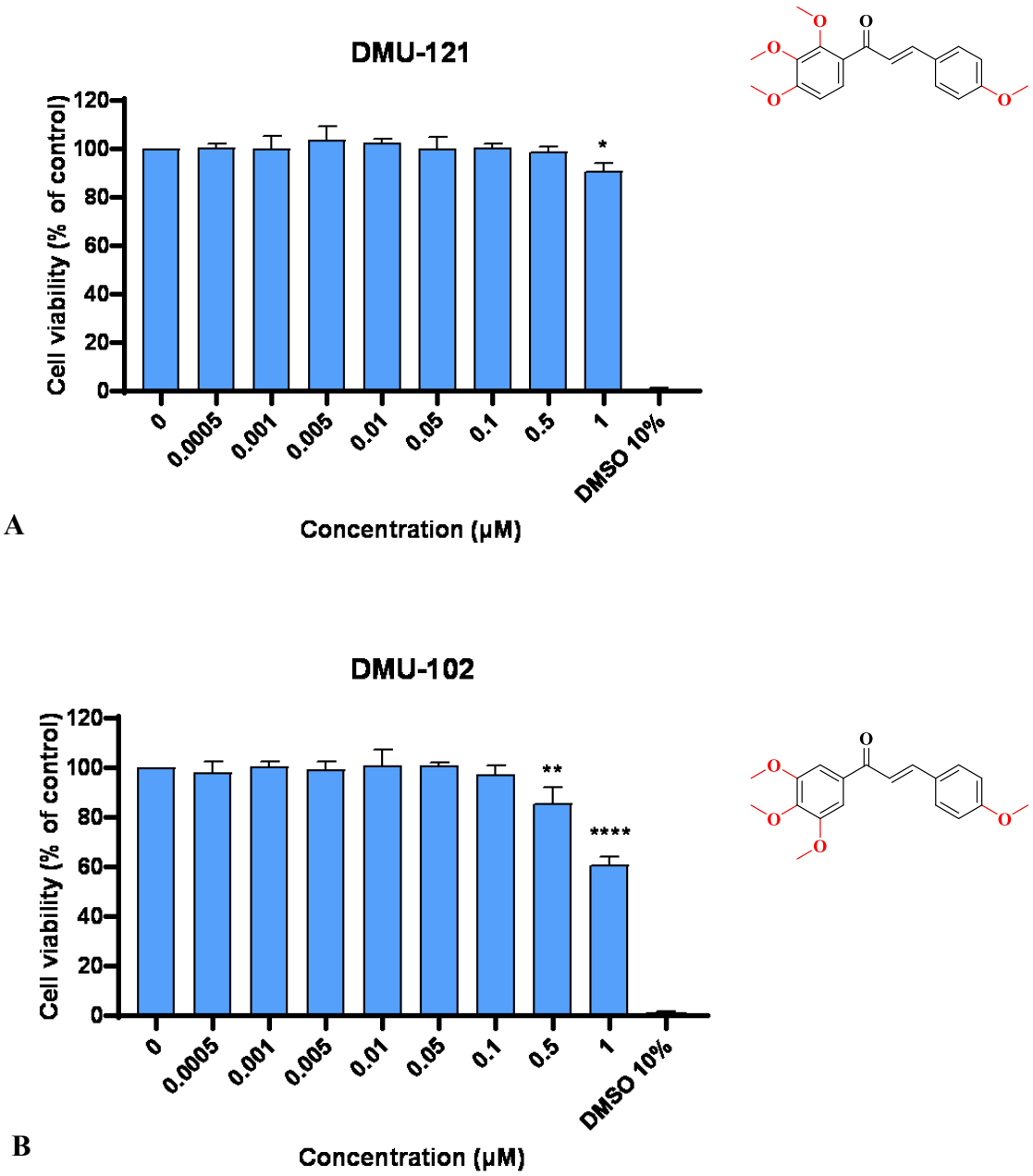

Figure 3.2 AREc32 were exposed to chalcones (A) DMU-121 and (B) DMU-102 for 24 h after which cell viability was determined using the MTT assay. Data are presented mean ± SD. (n=3), * for $p<0.05$, ** for $p<0.01$ and **** for $p<0.0001$ significant compared to control (0.1% DMSO)

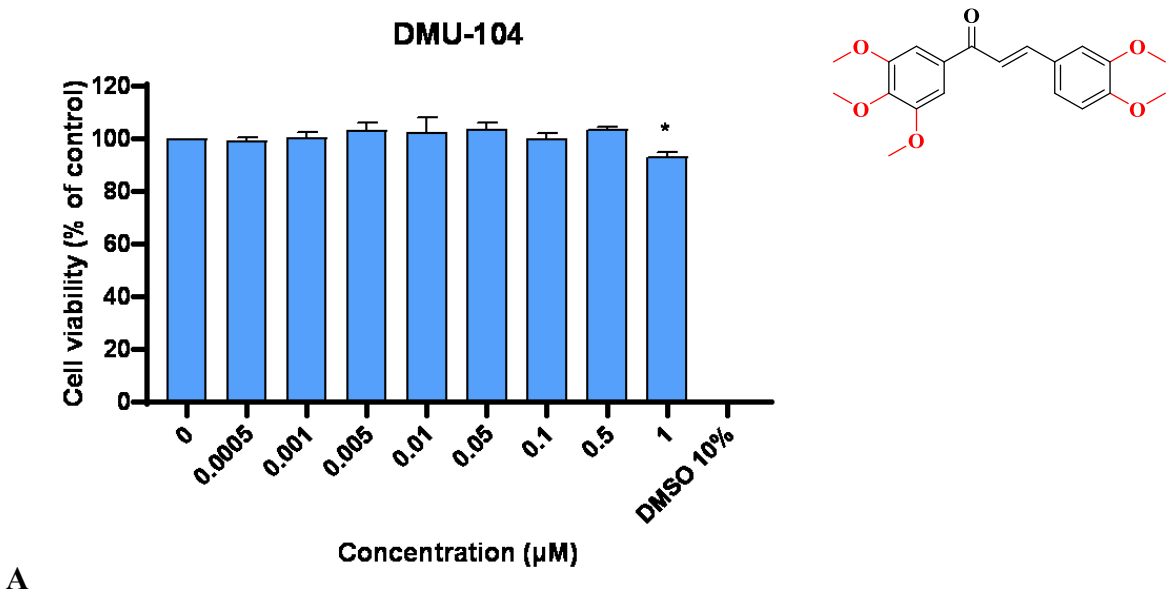

A

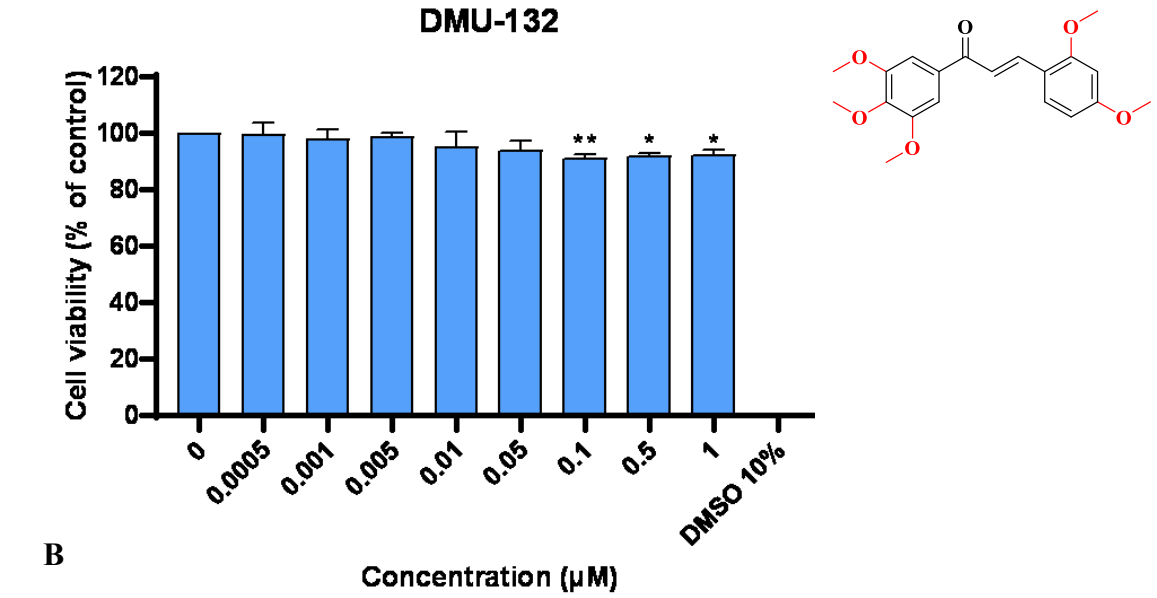

B

Figure 3.3 AREc32 were exposed to chalcones (A) DMU-104 and (B) DMU-132 for 24 h after which cell viability was determined using the MTT assay. Data are presented mean ± SD (n=3), * for $p<0.05$ and ** for $p<0.01$, significant compared to control (0.1% DMSO)

The toxicity of these compounds has been examined by Ducki *et al.* (2009) through K562 human leukaemia cell line, they found the half-maximal inhibitory concentration (IC_{50}) for the same four chalcones at 0.2-0.3 μM. It is thought that the more methoxy groups linked with acetophenone (ring A), the higher the toxicity of the compounds. This aspect will be examined in subsequent sections. Moreover, these chalcones had been reported by Ruparelia *et al.* (2018) through MCF-7, MDA-468 and MCF-10A and they found that the IC_{50} were between 0.06 – 4.2 μM. For that reason changing trimethoxy group from C- 3',4',5' to C-2',3',4' on ring A made DMU-121 less toxic than DMU-102 (Ruparelia *et al.*, 2018), also changing dimethoxy group on ring B from C-2,4 in DMU-132 to C-3,4 in DMU-104 reduced the chalcone toxicity. Comparing with *trans*-chalcone (non-toxic up to 25 μM), adding three methoxy groups to the A ring and one or two on the B ring leads to far higher toxicity (0.05-0.5 μM).

3.2.1.2.2. Two methoxy groups on ring A

The next sub-group from group 1a (the middle column of Table 4) (Section 2.1.3.), which has two methoxy in ring A and one or two methoxy in ring B are shown in Figure 3.4 and Figure 3.5, which illustrates that the viability of cells decreased with compounds tested. Comparing with control (0.1% DMSO), DMU-2210 and DMU-2207 (Figure 3.5 A and C) were non-toxic up to 7.5 μM. However, DMU-2201 (Figure 3.5 B) showed an initial statistical difference at 2.5 μM, while DMU-120 and DMU-427 (Figure 3.4 A and B) presented initial statistical difference compared to control at 0.5 μM. This sub-group, DMU-120, 427, 2210, 2201 and 2207 have two methoxy groups on ring A. Meanwhile, DMU-120 and 427 both have one methoxy group on ring B. While, DMU-2210, 2201 and 2207 have two methoxy groups on ring B.

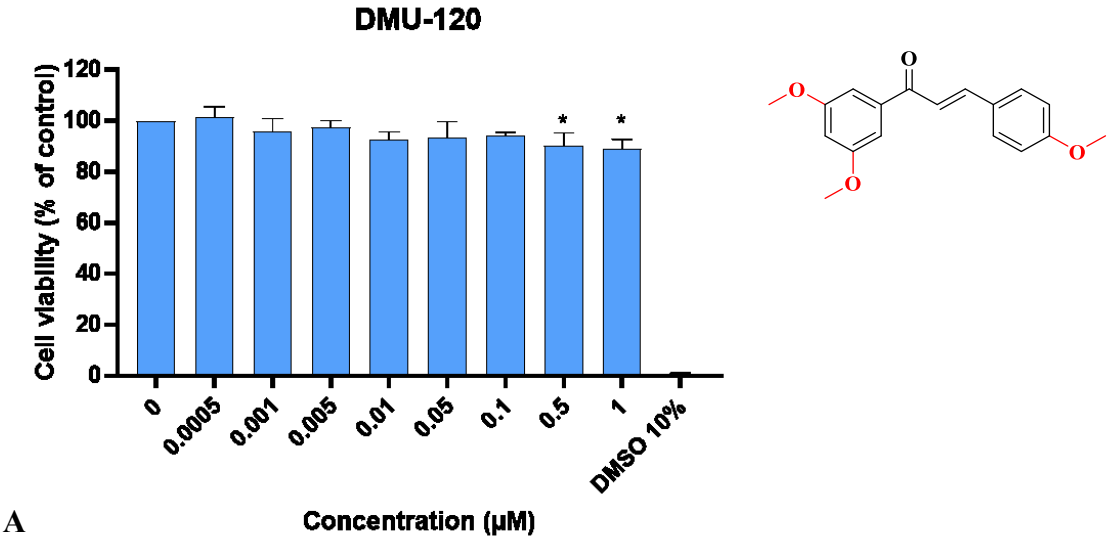

A

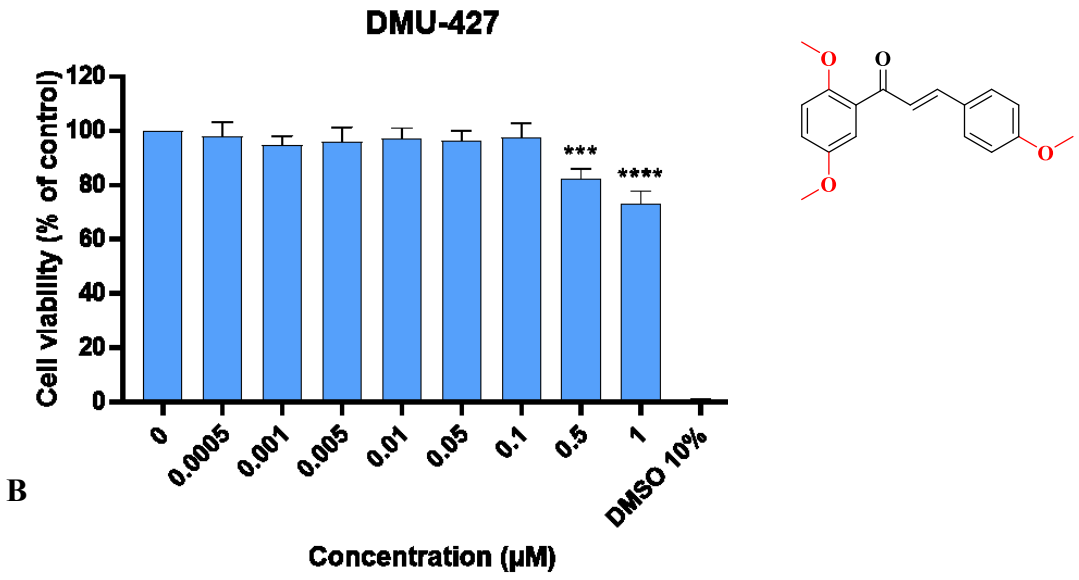

B

Figure 3.4 AREc32 were exposed to chalcones (A) DMU-120 and (B) DMU-427 for 24 h after which cell viability was determined using the MTT assay. Data are presented mean ± SD (n=3), * for $p<0.05$, *** for $p<0.001$ and **** for $p<0.0001$ significant compared to control (0.1% DMSO)

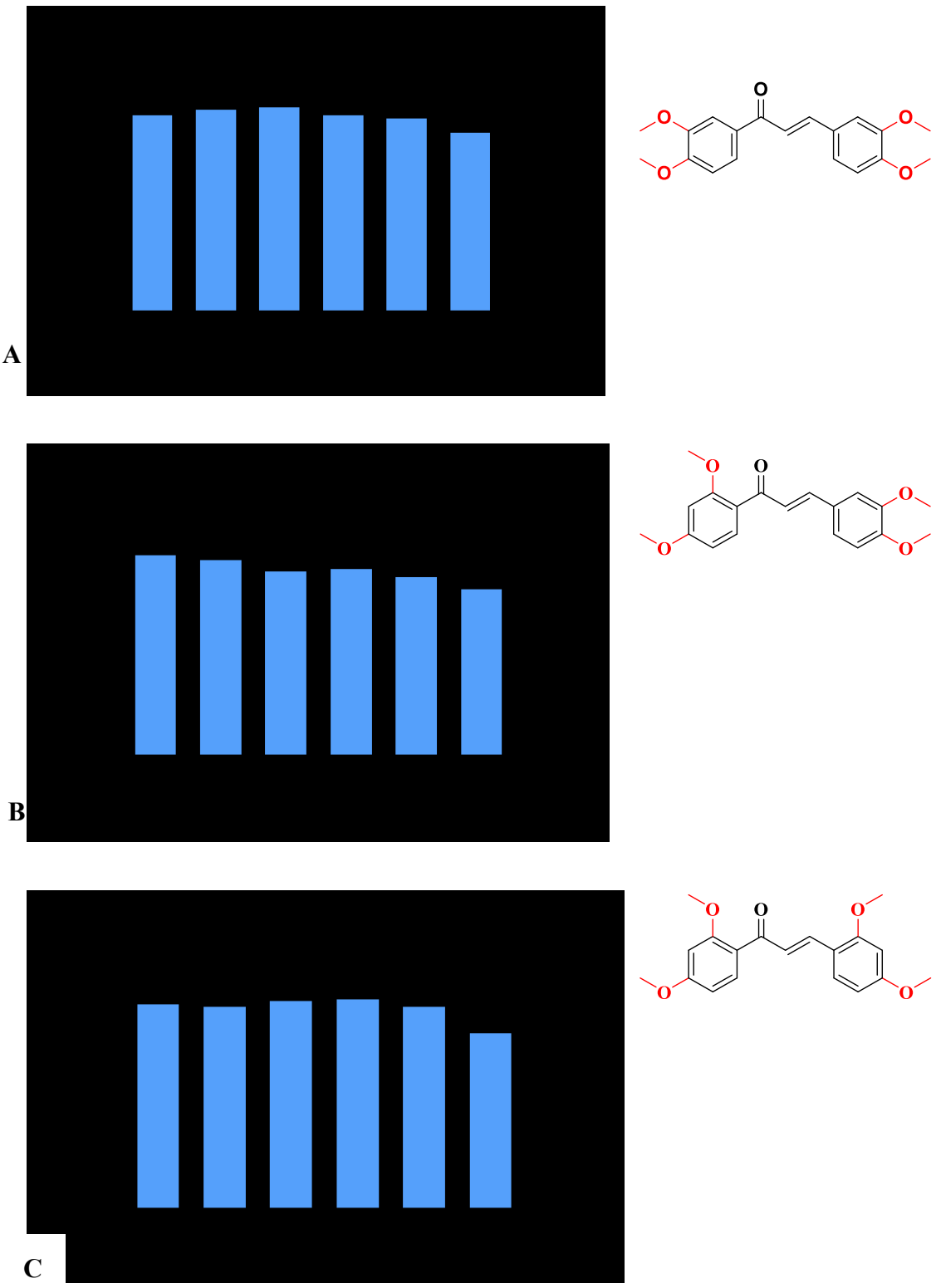

Figure 3.5 AREc32 were exposed to chalcones (A) DMU-2210, (B) DMU-2201 and (C) DMU-2207 for 24 h after which cell viability was determined using the MTT assay. Data are presented mean ± SD. (n=3), * for $p<0.05$, ** for $p<0.01$ and *** for $p<0.001$ significant compared to control (0.1% DMSO)

Comparing with Juvale *et al.* (2012) results, DMU-2210 was less toxic on AREc32 cell line, which was 10 μM, than in MCF-7 MX and MDCK BCRP cell lines, which were 3.3 and 3.8 μM, respectively. However, chalcone DMU-2201 showed toxicity on MDCK BCRP and MCF-7 MX cell line with IC_{50} 1 and 2.2 μM, respectively, and that is consistent with current results, this compound was toxic up to 2.5 μM whereas DMU-2210 was less toxic. Moreover, another group have found that the IC_{50} of DMU-2210 and DMU-2207 were 9.5 and 17 μM on MCF-7, which is closer to present results as these chalcones were less toxic than the other compounds in the same group. Also, they found DMU-120 and DMU-427 were more toxic with IC_{50} of 0.32 and 0.13 μM (Ruparelia *et al.*, 2018) and the results showed that both chalcones were non-toxic up to 0.1 μM.

Depending on structure activity relationships, chalcones DMU-2210 and 2207 were not toxic up to 7.5 μM possibly because the distance and the position between the methoxy groups were the same in both rings. For example, DMU-2210 has 3,4-OMe in both ring, and DMU-2207 has 2,4-OMe in both rings. Meanwhile, DMU-2201 has two methoxy groups in both rings, but in different positions, they were 2',4'-OMe on ring A, which are the same positions as DMU-2207 and 3,4-OMe on ring B, which are in the same positions as DMU-2210, but it was more toxic than both of the other chalcones. Moreover, DMU-120 and 427 have a single methoxy group on C-4 position in ring B while, in ring A, there were two methoxy groups in position C-3',5' in DMU-120 and C-2',5' in DMU-427, and that made the chalcones more toxic. Furthermore, DMU-120 and 427 may be more toxic than the others due to the absence of a methoxy group on the C-4' position on ring A.

3.2.1.2.3. One methoxy group on ring A

The final sub-group in Table 4 (last column), which has one methoxy group on ring A, while ring B had no methoxy group in DMU-1119, one methoxy group in DMU-470 or three methoxy groups in DMU-1113. Thus chalcones were examined and the MTT assay results illustrate that DMU-1119 was non-toxic up to 10 µM (Figure **3.6**), DMU-470 showed the initial statistical difference at 1 µM (Figure **3.7** A). Moreover, DMU-1113 showed non-toxicity at 5 µM (Figure **3.7** B).

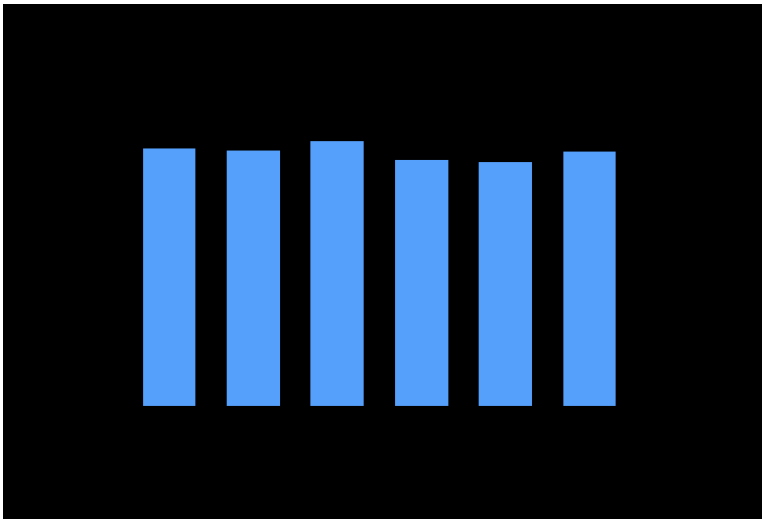

Figure 3.6 AREc32 were exposed to chalcone DMU-1119 and for 24 h after which cell viability was determined using the MTT assay. Data are presented mean ± SD. (n=3), compared to control (0.1% DMSO)

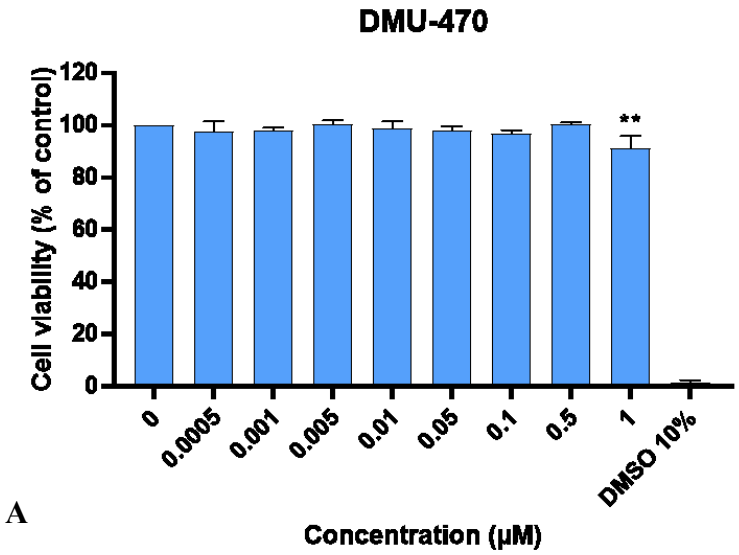

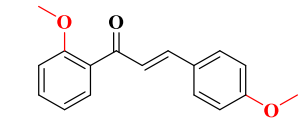

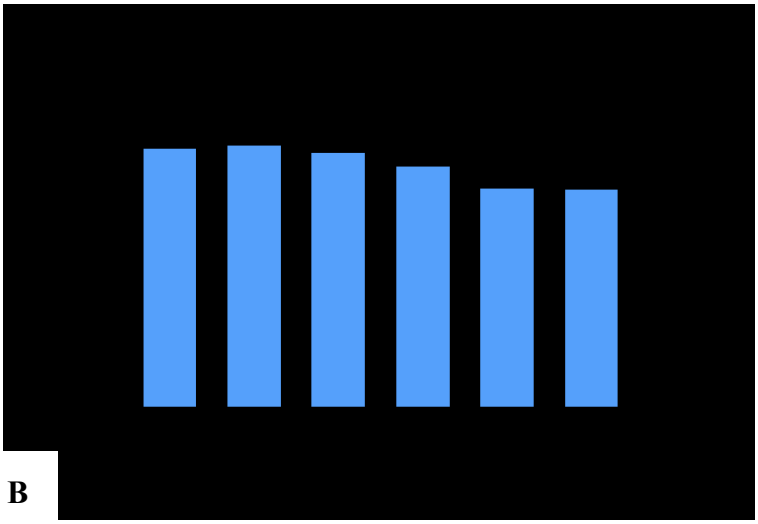

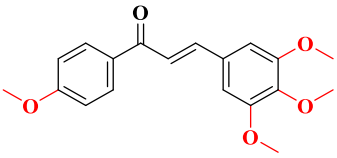

Figure 3.7 AREc32 were exposed to chalcones (A) DMU-470 and (B) DMU-1113 for 24 h after which cell viability was determined using the MTT assay. Data are presented mean ± SD. (n=3), ** for $p<0.01$ significant compared to control (0.1% DMSO)

DMU-1119 was examined by Harmastuti *et al.* (2012) on HeLa cell line, and the results showed the IC_{50} were 47.8 μM which is consistent with non-toxicity being shown under the conditions tested here. Moreover, DMU-1113 reported by Ducki *et al.* (2009) and showed the IC_{50} was 4.5 μM on K562 cell line, however, it shows non-toxicity on AREc32 at 10 μM. In addition, Ruparelia *et al.* (2018) have reported that the IC_{50} of DMU-1119 and DMU-1113 at 20 and 6 μM respectively on MCF-7 also, DMU-470 has IC_{50} 0.74 on MCF-10A. It is thought that presence of methoxy group on C-4' position on ring A made the compound less toxic because the presence of the methoxy group on the C-2' site on DMU-470 made it more toxic than others in the same group.

A possible explanation for these results may be due to the number and the position of methoxy group. There is some evidence from Wermuth (2008) who suggested that if the compound has at least one methyl group that will increase the lipophilicity. Increasing the latter could be modifying the drug bioavailability. Additionally, comparing with *trans*-chalcone, which does not have any methoxy groups and shows less toxicity than chalcones with a single methoxy group on the A ring.

Table 11. The non-toxic concentration (μM) of group **1a** chalcones that have determined by MTT assay

DMU No.	Ring A	Ring B	Non-toxic concentration(μM)
DMU-1119	4′-$CH_3OC_6H_4$	C_6H_5	10
DMU-2210	3′,4′-$(CH_3O)_2C_6H_3$	3,4-$(CH_3O)_2C_6H_3$	7.5
DMU-2207	2′,4′-$(CH_3O)_2C_6H_3$	2,4-$(CH_3O)_2C_6H_3$	7.5
DMU-1113	4′-$CH_3OC_6H_4$	3,4,5-$(CH_3O)_3C_6H_2$	5
DMU-2201	2′,4′-$(CH_3O)_2C_6H_3$	3,4-$(CH_3O)_2C_6H_3$	1
DMU-121	2′,3′,4′-$(CH_3O)_3C_6H_2$	4-$CH_3OC_6H_4$	0.5
DMU-104	3′,4′,5′-$(CH_3O)_3C_6H_2$	3,4-$(CH_3O)_2C_6H_3$	0.5
DMU-470	2′-$CH_3OC_6H_4$	4-$CH_3OC_6H_4$	0.5
DMU-102	3′,4′,5′-$(CH_3O)_3C_6H_2$	4-$CH_3OC_6H_4$	0.1
DMU-120	3′,5′-$(CH_3O)_2C_6H_3$	4-$CH_3OC_6H_4$	0.1
DMU-427	2′,5′-$(CH_3O)_2C_6H_3$	4-$CH_3OC_6H_4$	0.1
DMU-132	3′,4′,5′-$(CH_3O)_3C_6H_2$	2,4-$(CH_3O)_2C_6H_3$	0.05

3.2.1.3 DMU-chalcones group 1 b

3.2.1.3.1 Methoxy with longer chain alkoxy groups on ring B

Longer chain alkoxy group based on ring B (Table 5) were split into ethyl groups or longer chain alkoxy substituents. For instance, chalcone DMU-1122 and 5505 all contain ethoxy substituents on C-4 position on ring B and two or three methoxy group on ring A. The results show that DMU-1122 (Figure 3.9 A) was non-toxic up to 18 μM, while, DMU-5505 (Figure 3.9 B) was non-toxic up to 1 μM, both chalcones were the same on ring B, however, there were methoxy groups on C-2',4' positions on DMU-1122, while DMU-5505 had methoxy group on C-3',4',5' positions. For the longer chain alkoxy, in ring A there were 2',4'-OMe in DMU-408, while 3',4',5'-OMe in DMU-191 and 192. However, in ring B DMU-408 (Figure **3.9** A) and DMU-191 (Figure **3.9** B) have a propyl group on C-4, and DMU-192 (Figure **3.9** C) has a butyl group on C-4. The results showed that DMU-191 and 408 were non-toxic up to 7.5 μM, while, DMU-192 was non-toxic up to 10 μM.

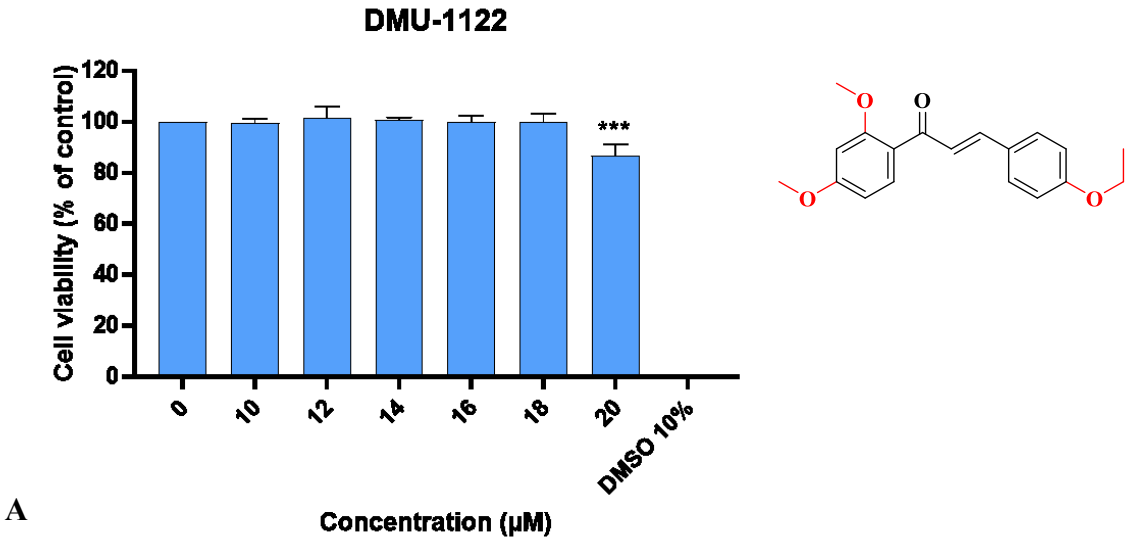

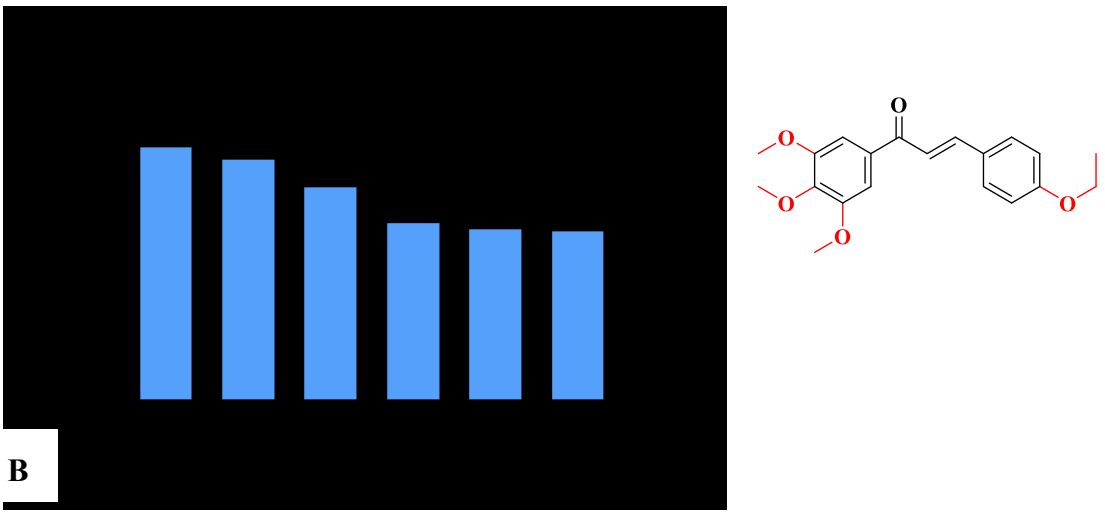

Figure 3.8 AREc32 were exposed to chalcones (A) DMU-1122 and (B) DMU-5505 for 24 h after which cell viability was determined using the MTT assay. Data are presented mean ± SD. (n=3), * for $p<0.05$, ** for $p<0.01$ and *** for $p<0.001$ significant compared to control (0.1% DMSO)

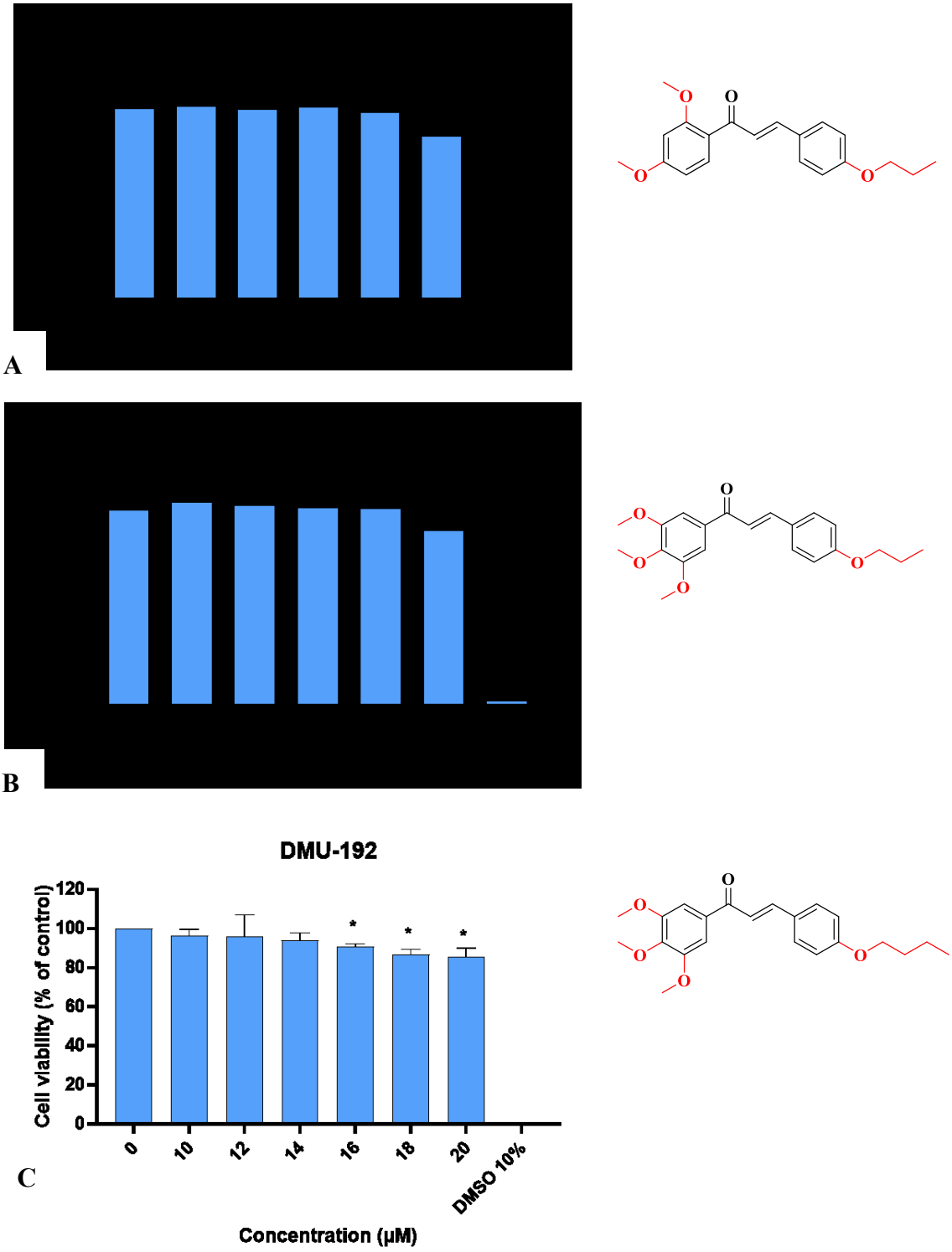

Figure 3.9 AREc32 were exposed to chalcones (A) DMU-408, (B) DMU-191 and (C) DMU-192 for 24 h after which cell viability was determined using the MTT assay. Data are presented mean ± SD. (n=3), * for $p<0.05$, ** for $p<0.01$ and *** for $p<0.001$ significant compared to control (0.1% DMSO)

The result of DMU-1122 (Figure 3.9 A) shows non-toxicity at 18 μM, and DMU-5505 shows non-toxicity at 1 μM, both chalcones have ethoxy group on C-4. However, DMU-5505 was more toxic than DMU-1122. It is assumed that the presence of methoxy group on C-2' position could reduce the cytotoxicity of DMU-1122. Otherwise, the C-3' or/and C-5' on DMU-5505 increase the toxicity. Furthermore, the results are consistent with more methoxy groups on ring A causing higher toxicity as seen in previous sections. Ruparelia *et al.* (2018) have found the IC_{50} for both chalcones DMU-1122 and 5505 were 40 μM and 10 μM respectively on MCF-7. In addition, DMU-5505 has the same number and position of methoxy group on A ring with DMU-102 (Figure **3.2**), however, DMU-5505 less toxic then DMU-102 owing to the change from methoxy group to ethoxy group on C-4 position on ring B showing the effect of additional carbon in the alkoxy group.

The results presented here show that there is a decreased toxicity as the length of the alkoxy group increases i.e. DMU-102 was non-toxic up to 0.1 μM, DMU-5505 at 1 μM, DMU-191 at 7.5 μM and DMU-192 at 10 μM. These compounds all have a 3',4',5'-OMe substituted A ring but the C-4 substituted B ring increases from methoxy to butoxy across the series. A similar pattern was seen in the C-2',4' substituted A ring series of DMU-1122 and 408 but a more extensive comparison with other compounds was not possible.

The IC_{50} of DMU-408, 191 and 192 on MCF-7 showed 10, 30 and more than 100 μM respectively (Ruparelia *et al.*, 2018). All of group **1b** had two or three methoxy group on ring A. Interestingly; four out of five of the long-chain alkoxy chalcones categories were non-toxic up to 7.5 μM or more. It is probable the longer alkoxy chain, the less toxicity due to the lipophilicity as shown in current results.

Silverman and Holladay (2015) illustrated that the lengthening of saturated carbon chain from methyl group to ethyl, propyl and butyl lead to reduced potency and molecular lipophilicity, and that could increase the pharmacological characteristics, of compounds. In addition, the long alkyl chain might be interfering with receptors.

Table 12. The non-toxic concentration (μM) of group **1b** chalcones that have determined by MTT assay

DMU No.	Ring A	Ring B	Non-toxic concentration(μM)
DMU-1122	2′,4′-$(CH_3O)_2C_6H_3$	4-$EtOC_6H_4$	18
DMU-192	3′,4′,5′-$(CH_3O)_3C_6H_2$	4-$BuOC_6H_4$	10
DMU-191	3′,4′,5′-$(CH_3O)_3C_6H_2$	4-$PrOC_6H_4$	7.5
DMU-408	2′,4′-$(CH_3O)_2C_6H_3$	4-$PrOC_6H_4$	7.5
DMU-5505	3′,4′,5′-$(CH_3O)_3C_6H_2$	4-$EtOC_6H_4$	1

3.2.1.4 Increase the number of the ring group

Based on compound structure, compounds with a methylene-dioxy or ethylene-dioxy group (group 2, Table 6) were split into two sub-groups depending on increasing the number of rings on ring A or B. The MTT assay results for DMU-chalcones that contain a methylene-dioxy on ring B, comparing with the control (0.1% DMSO), the order of toxicity showed that DMU-2267 (4'-OMe) (Figure **3.10** C) and DMU-2265 (2'-OMe) (Figure **3.13** A) were not toxic up to 16 and 10 μM, respectively. Next, DMU-411

((Figure **3.10** A) and DMU-2219 (2'-Cl) ((Figure **3.10** B) showed that no statistical difference at 7.5 µM. Following that DMU-403 (3',5'-OMe) (Figure **3.11** A) was not toxic up to 2.5 µM, then DMU-423 (2',5'-OMe) (Figure **3.11** B) and DMU-135 (3',4',5'-OMe) (Figure **3.11** C) were non-toxic up to 0.5 µM. Moreover, the compounds DMU-419 (2',3',4'-OMe) (Figure **3.12** A), 416 (3'-OMe) (Figure **3.12** B), and 160 (3',4'-OMe) (Figure **3.12** C) showed no significant toxicity at 0.1, 0.01 and 0.005 µM respectively. Finally, chalcones that have ethylene-dioxy on ring B such as DMU-1133 (2',4'-OMe) (Figure **3.13** B) was not toxic up to 0.05 µM.

In contrast, chalcones DMU-1112, 1103 and 1144 have methylene-dioxy group in ring A whereas, ring B has two or three methoxy groups. The MTT assay result showed that DMU-1112 (2,3,4-OMe) (Figure **3.14** A) and DMU-1103 (2,4-OMe) (Figure **3.14** B) were non-toxic up to 7.5 µM. However, DMU-1144 (2,5-OMe) (Figure **3.14** C) was toxic up to 0.01 µM.

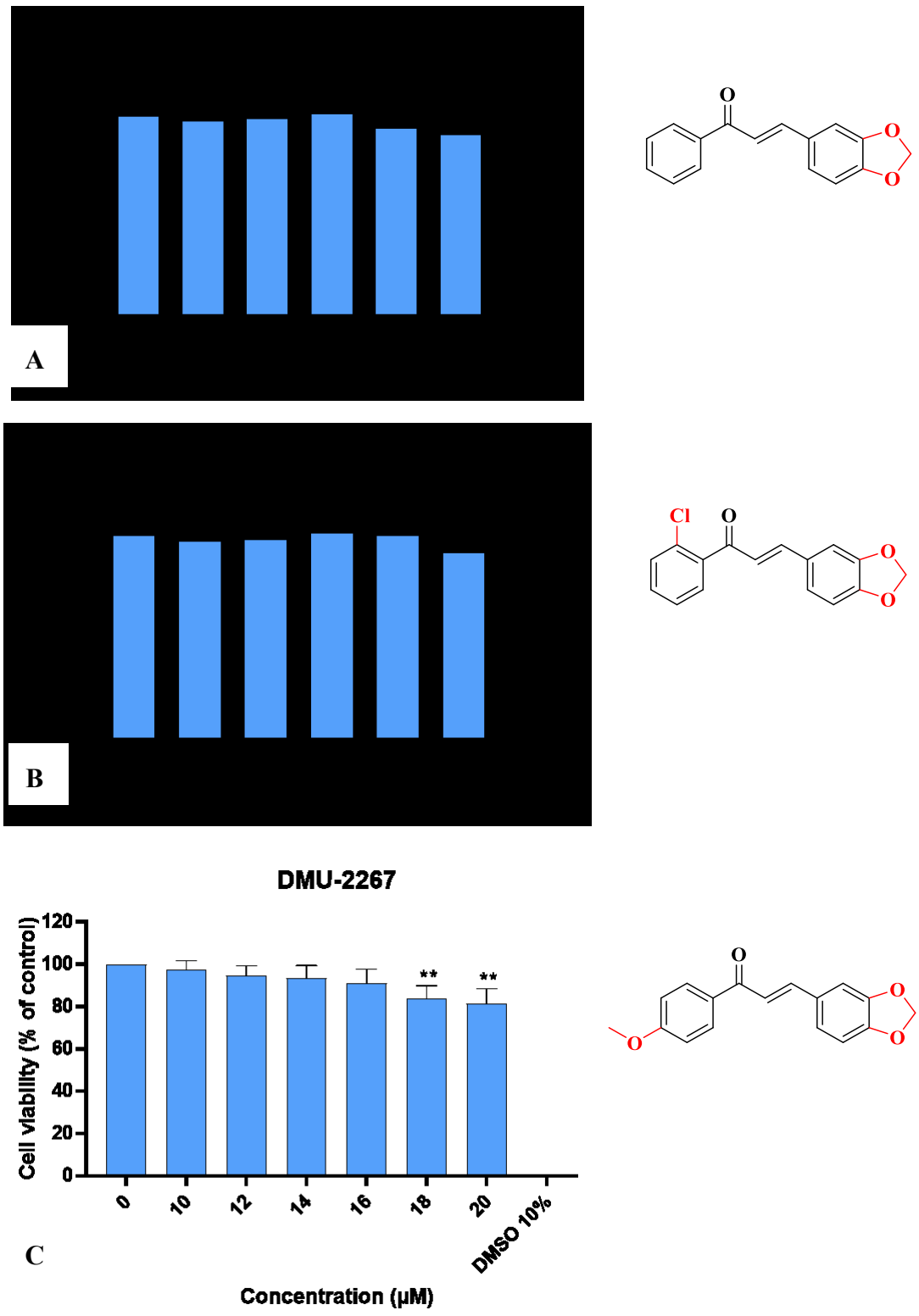

Figure 3.10 AREc32 were exposed to chalcones (A) DMU-411 and (B) DMU-2219 and (C) DMU-2267 for 24 h after which cell viability was determined using the MTT assay. Data are presented mean ± SD. (n=3), * for $p<0.05$, ** for $p<0.01$ and **** for $p<0.0001$ significant compared to control (0.1% DMSO)

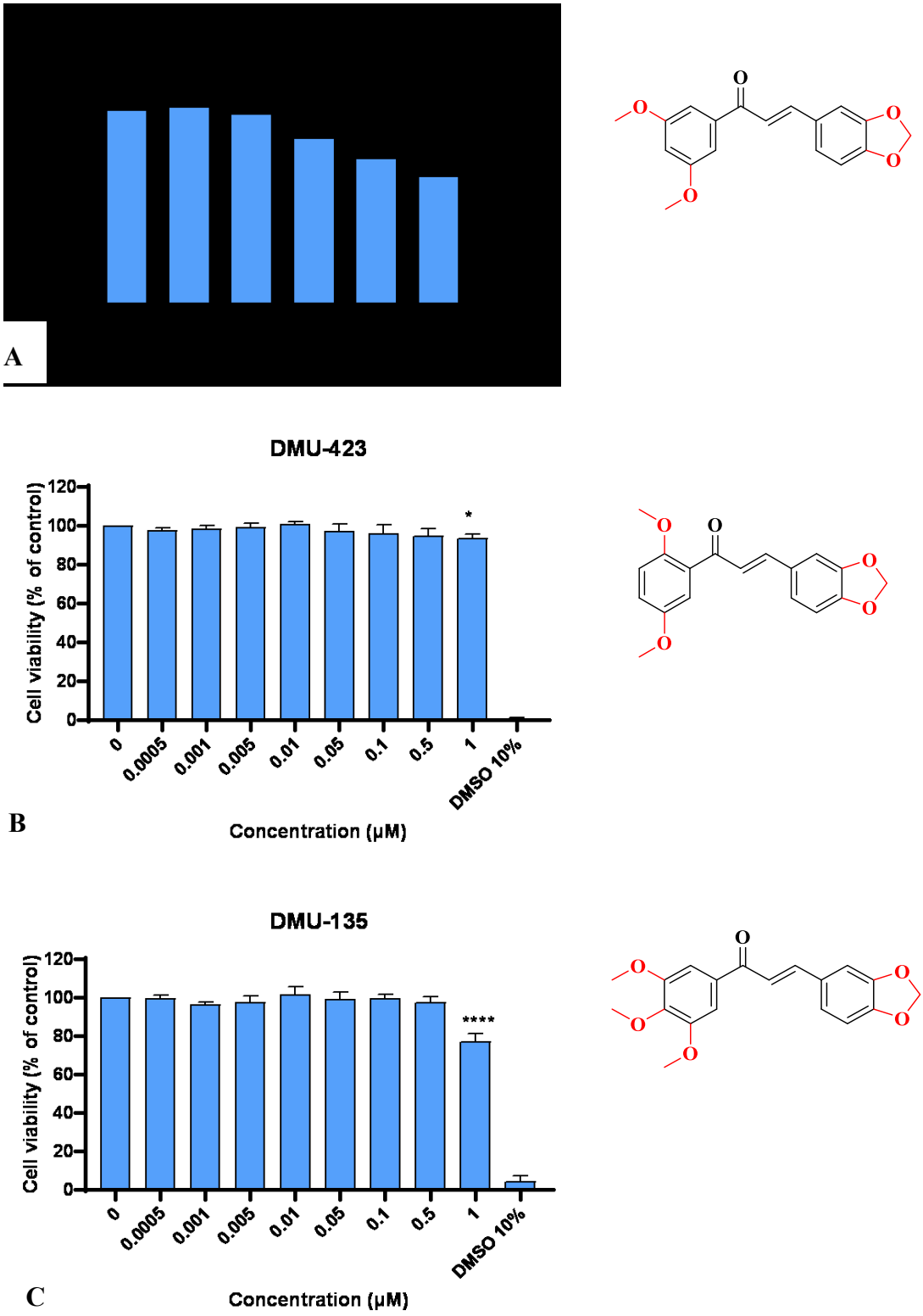

Figure 3.11 AREc32 were exposed to chalcones (A) DMU-403, (B) DMU-423 and (C) DMU-135 for 24 h after which cell viability was determined using the MTT assay. Data are presented mean ± SD. (n=3), * for $p<0.05$, ** for $p<0.01$, *** for $p<0.001$ and **** for $p<0.0001$ significant compared to control (0.1% DMSO)

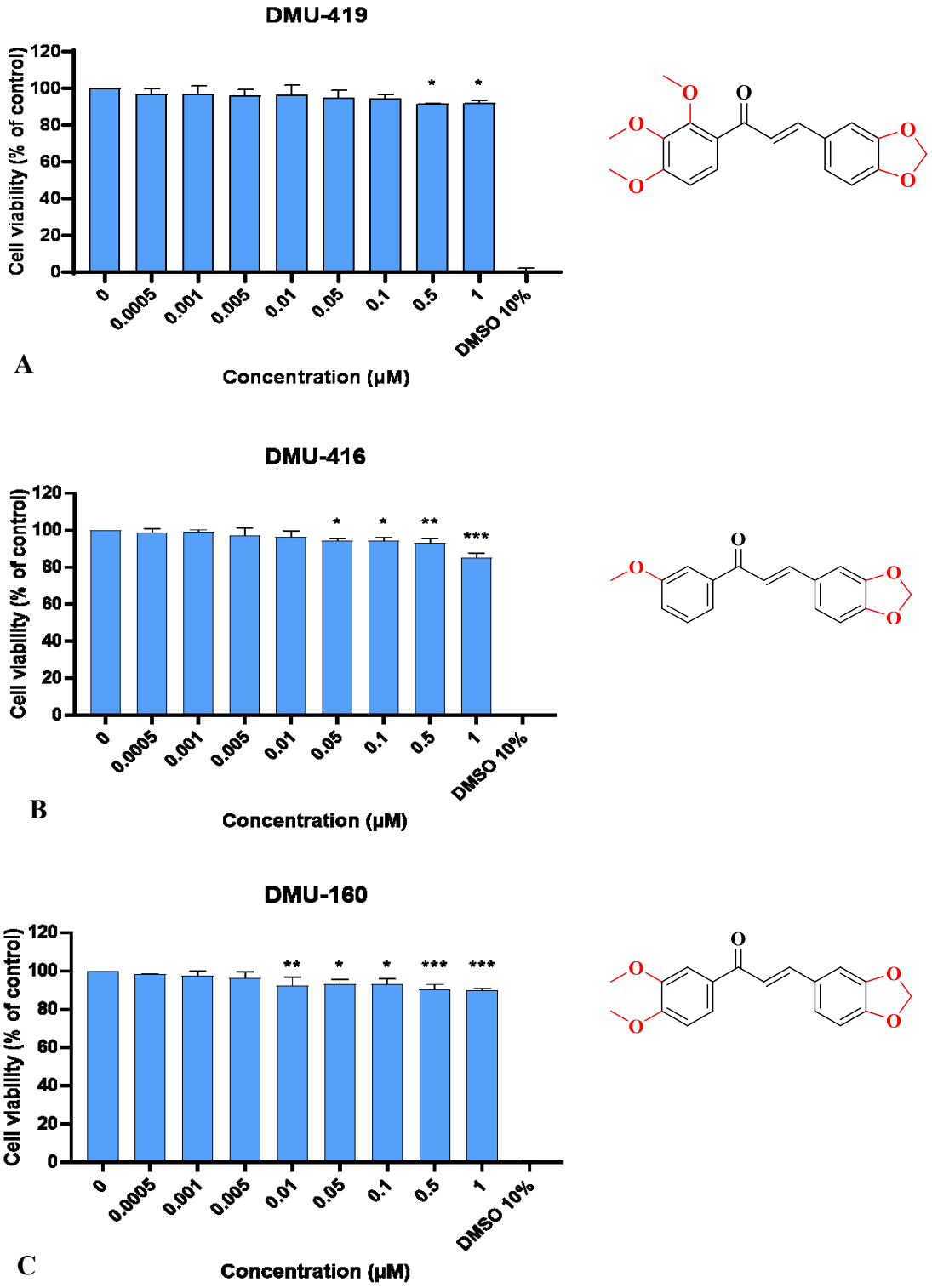

Figure 3.12 AREc32 were exposed to chalcones (A) DMU-419, (B) DMU-416 and (C) DMU-160 for 24 h after which cell viability was determined using the MTT assay. Data are presented mean ± SD. (n=3), * for $p<0.05$, ** for $p<0.01$ and *** for $p<0.001$ significant compared to control (0.1% DMSO)

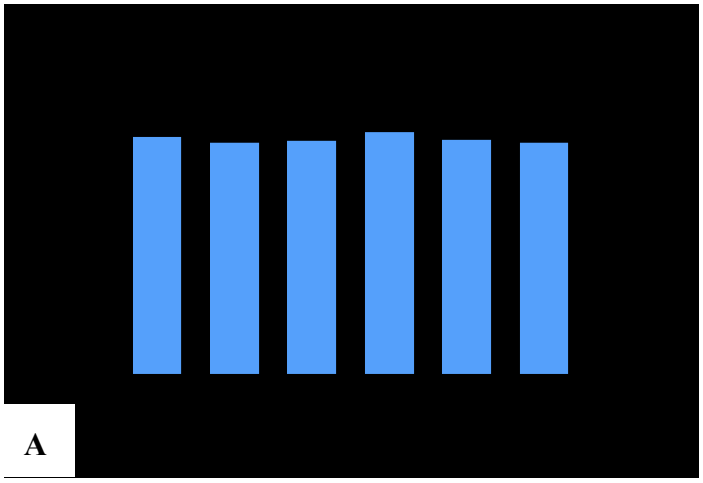

A

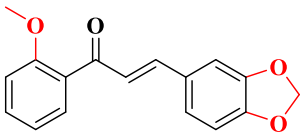

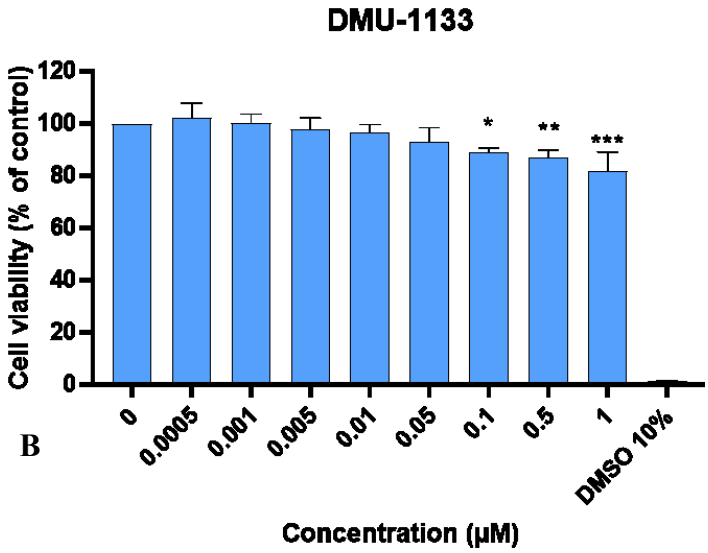

B

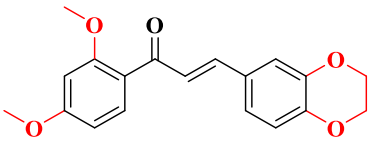

Figure 3.13 AREc32 were exposed to chalcones (A) DMU-2265 and (B) DMU-1133 for 24 h after which cell viability was determined using the MTT assay. Data are presented mean ± SD. (n=3), * for $p<0.05$, ** for $p<0.01$ and *** for $p<0.001$ significant compared to control (0.1% DMSO)

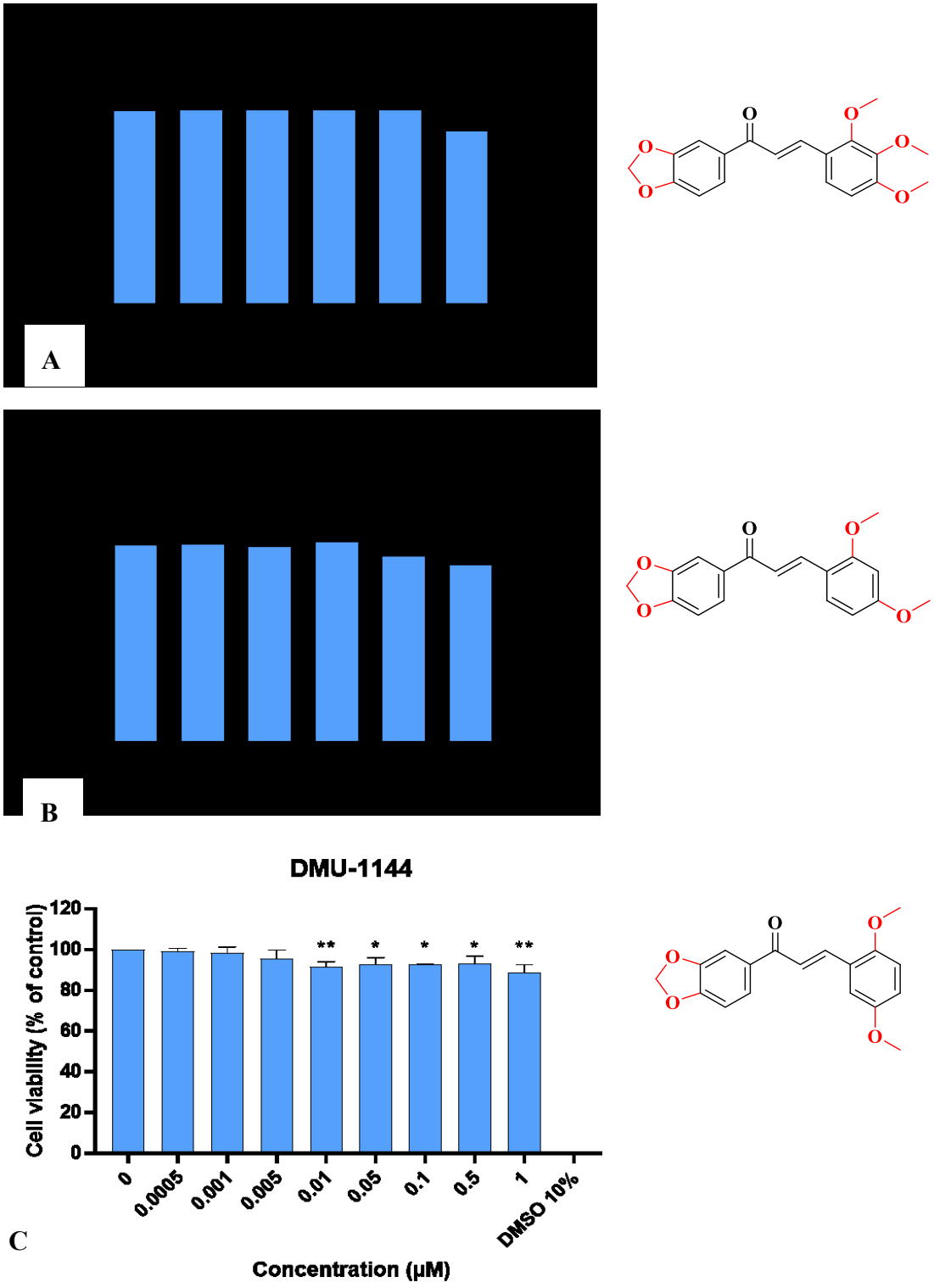

Figure 3.14 AREc32 were exposed to chalcones (A) DMU-1112, (B) DMU-1103 and (C) DMU-1144 for 24 h after which cell viability was determined using the MTT assay. Data are presented mean ± SD. (n=3), * for $p<0.05$, ** for $p<0.01$, *** for $p<0.001$ and **** for $p<0.0001$ significant compared to control (0.1% DMSO)

All compounds in Figure **3.10** - Figure **3.13** have a methylene-dioxy group in ring B, but the difference between them depends on ring A (Table 6). Considering ring A structure, chalcone DMU-2267 and 2265 were less toxic than the others, and both chalcones have one methoxy group. It is thought that a single methoxy group alone are weaker than several groups which make the compound less toxic (Clayden, 2002). Surprisingly, DMU-411 has no substituents and slightly higher toxicity than 2267 and 2265. Comparing with *trans*-chalcone, which was not toxic up to 25 μM, DMU-411 was the same structure of *trans*-chalcone but has methylene-dioxy substituents in ring B, and it is thought that the methylene-dioxy group increases the compound toxicity. Moreover, DMU-2219 has the same structure and non-toxic concentration as DMU-411, but it has a halogen group (chlorine) in C-2' position on ring A. A possible explanation for these results may be the presence of Cl on DMU-2219 has no cytotoxicity effect. Meanwhile, comparing these chalcones with DMU-2267 and 2265, which have one methoxy group, showed less toxicity then DMU-411 and 2219.

DMU-416 illustrated high toxicity, although, it has methylene-dioxy group in ring B and one methoxy group in ring A similar to DMU-2267 and 2265. It seems possible that these results are due to the presence of methoxy group in C-3' position which increases the toxicity of DMU-416. However, whether DMU-416 compared with DMU-403, the latter has methoxy groups in C-3',5' position on ring A, but it was showed less toxicity then DMU-416. This result may be explained by the fact that the presence of methoxy group in both C-3',5' position decreases the toxicity. Furthermore, chalcone DMU-423 and 160 have two methoxy groups in position C-3',5' and C-3',4' respectively. Additionally, DMU-135 and 419 both have methoxy groups in positions C- 3', 4', while they have C-5' and C-2' respectively, all these compounds showed high toxicity. According to Chauhan *et al.* (2014), who demonstrated that the presence of methoxy groups in position 3, 4 or 3, 4, 5

increased thetoxicity. The findings of the current study are consistent with those of Ruparelia *et al.* (2018) who found that the IC_{50} of DMU-2265 was 100 µM, which was less toxic than the others. Followed by DMU-2267 and 2219, which were the IC_{50} 30 and 22 µM respectively, and the remaining chalcones were more toxic than these three with IC_{50} between 3.5 – 13.9 µM on MCF-7.

The last compound in this group is DMU-1133 (Figure **3.13** B), this chalcone has 3',4'-OMe on ring A, and ethylene-dioxy group in ring B, also it was showing toxicity on 0.1 µM. Comparing with *trans*-chalcone, the toxicity of DMU-1133 may be the presence of methoxy group in ring A or/and the presence of ethylene-dioxy group in ring B, which was not in *trans*-chalcone structure. There are, however, other possible explanations, comparing with DMU-408, which has 2',4'-OMe as well, but was non-toxic up to 7.5 µM. The difference between both chalcones was in ring B, where DMU-408 has a butyl group and DMU-1133 has ethylene-dioxy group, it seems possible that these results are due to the present of ethylene-dioxy group.

In accordance with the present results, previous studies by (Ruparelia *et al.*, 2018) have demonstrated that both chalcones DMU-1112 and 1103 have IC_{50} at 25 µM on MCF-7 cell line. This consistency may be due to the presence of methoxy group in C-2,4 positions in both compounds. However, DMU-1144 has methoxy group in C-2,5, and it was toxic up to 0.01 µM, this rather contradictory result may be due to the absence of methoxy group in C-4 position, comparing with DMU-1112 and 1103. In addition, recent research by Altıntop *et al.* (2017) have suggested that benzodioxole group has perfect bioavailability and least toxicity, and also it was found in many antitumor compounds, for instance, steganacin, podophyllotoxin, and combretastatin.

Table 13. The non-toxic concentration (μM) of group **2** chalcones that have determined by MTT assay

DMU No.	Ring A	Ring B	Non-toxic concentration(μM)
DMU-2267	4′-$CH_3OC_6H_4$	3,4-OCH_2O-C_6H_3	16
DMU-2265	2′-$CH_3OC_6H_4$	3,4-OCH_2O-C_6H_3	10
DMU-411	C_6H_5	3,4-OCH_2O-C_6H_3	7.5
DMU-2219	2′-ClC_6H_4	3,4-OCH_2O-C_6H_3	7.5
DMU-1112	3′,4′-OCH_2O-C_6H_3	2,3,4-$(CH_3O)_3C_6H_2$	7.5
DMU-1103	3′,4′-OCH_2O-C_6H_3	2,4-$(CH_3O)_2C_6H_3$	7.5
DMU-403	3′,5′-$(CH_3O)_2C_6H_3$	3,4-OCH_2O-C_6H_3	2.5
DMU-423	2′,5′-$(CH_3O)_2C_6H_3$	3,4-OCH_2O-C_6H_3	0.5
DMU-135	3′,4′,5′-$(CH_3O)_3C_6H_2$	3,4-OCH_2O-C_6H_3	0.5
DMU-419	2′,3′,4′-$(CH_3O)_3C_6H_2$	3,4-OCH_2O-C_6H_3	0.1
DMU-1133	2′,4′-$(CH_3O)_2C_6H_3$	3,4-$O(CH_2)_2O$-C_6H_3	0.05
DMU-416	3′-$CH_3OC_6H_4$	3,4-OCH_2O-C_6H_3	0.01
DMU-160	3′,4′-$(CH_3O)_2C_6H_3$	3,4-OCH_2O-C_6H_3	0.005
DMU-1144	3′,4′-OCH_2O-C_6H_3	2,5-$(CH_3O)_2C_6H_3$	0.005

3.2.2 Screening of the chalcone library for Nrf2 activity using the luciferase reporter assay

Using the previously determined non-toxic concentrations, each chalcone in the library was then investigated for its ability to induce Nrf2 transcriptional activity as indicated by the luciferase reporter assay. Compared with control (0.1% DMSO), and related to chalcones structures, the results showed that group **1a**, which has vary methoxy group in both rings, such as DMU-2210 (3,4,3′,4′-OMe) at 7.5 μM (Figure **3.16** B) has the highest luciferase fold induction, which was 15.9 fold, followed by DMU-1119 (4′-OMe) at 10μM, DMU-1113 (3,4,5,4′-OMe) (5μM) (Figure **3.16** A) and DMU-2207 (2,4,2′,4′-OMe) (10μM) (Figure **3.16** B) that showed 9.4, 2.7 and 2.4 fold induction respectively. Moreover, group 1b, which has different methoxy group in ring A and long-chain alkoxyl group on ring B such as DMU-1122 (2′,4′-OMe,4-EtO) (18 μM) induce luciferase up to 7 fold then DMU-192 (3′,4′,5′-OMe, 4-BuO) (10 μM) to 1.9 fold induction (Figure **3.16** A). However, the remaining chalcones DMU-2201, 5505 (Figure **3.16** A), 102, 104 and 121 (Figure **3.17** A) failed to induce Nrf2 activity.

On the other hand, group 2 of DMU chalcones illustrated that chalcones with dioxin group in ring B and different methoxy group in ring A such as DMU-2267 (4′-OMe) (16 μM) (Figure **3.16** A) has induced luciferase up to 9 fold induction, followed by DMU-2265 (2′-OMe) (10 μM) (Figure **3.16** A), DMU-411 (7.5 μM) and DMU-2219 (2′-Cl) (7.5 μM) (Figure **3.16** B) that showed 3.3, 2.5 and 2.3 fold induction respectively. Moreover, chalcones with dioxin group in ring A and different methoxy group in ring B such as DMU-1103 (2,4-OMe) (7.5 μM) and DMU-1112 (2,3,4-OMe) (7.5 μM) (Figure **3.16** B) have induce luciferase up to 8.5 and 4 fold induction respectively. However, the remaining chalcones DMU-1133, 419, 135 (Figure **3.17** A), 1144, 160,416, 403 (Figure **3.17** B) failed to induce Nrf2 activity.

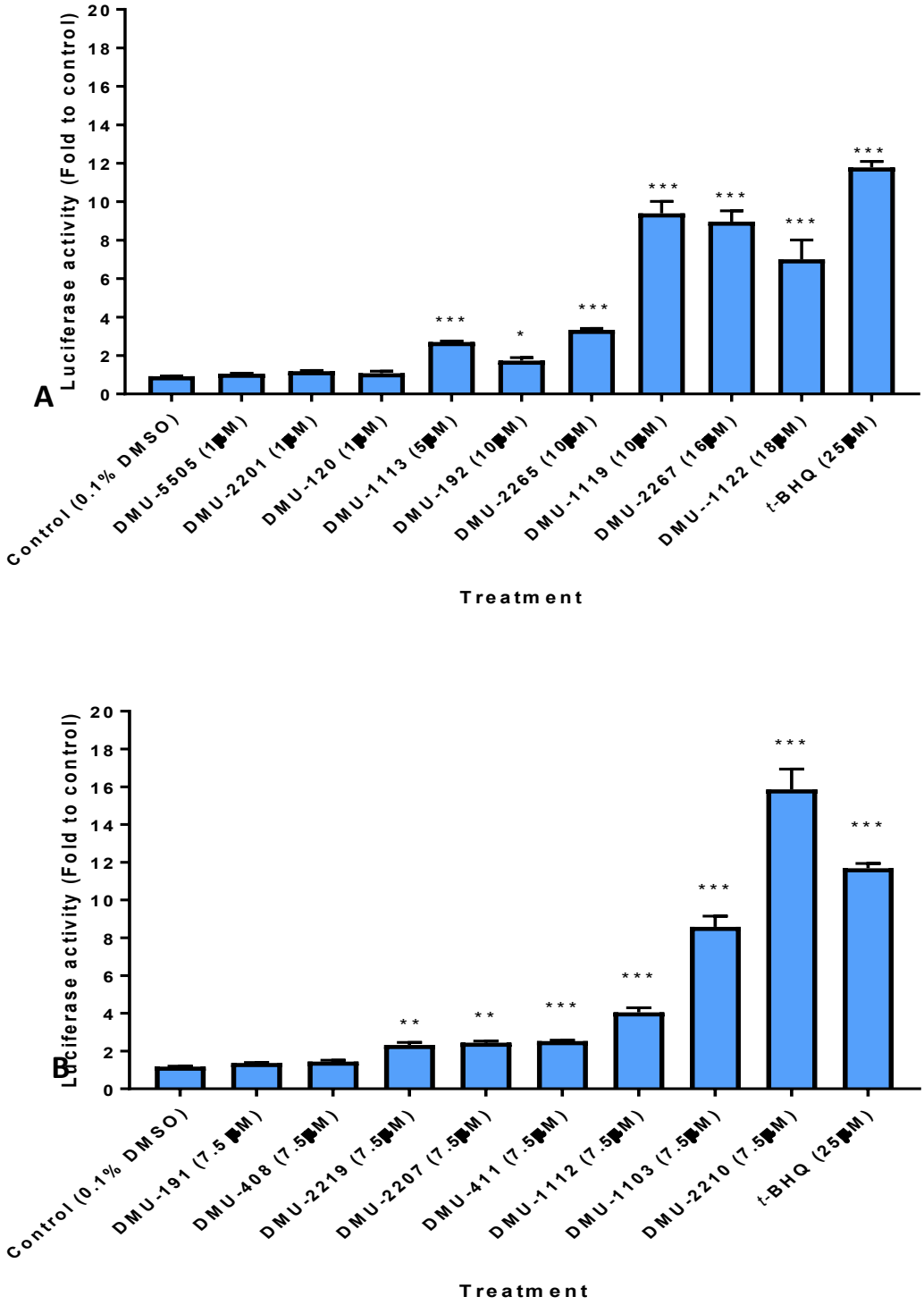

Figure 3.15 AREc32 were exposed to chalcones, 0 (negative control DMSO 0.1%), *t*-BHQ (Positive control). A: DMU-5505, 2201, 120, 1133, 192, 2265, 1119, 2267, 1122. And B: DMU-191, 408, 2219, 2207, 411, 1112, 1103, 2210 for 24 h after which cell viability was determined using the Luciferase assay. Data are presented mean ± SD. (n=3), * for $p<0.05$, ** for $p<0.01$ and *** for $p<0.001$ significant compared to control

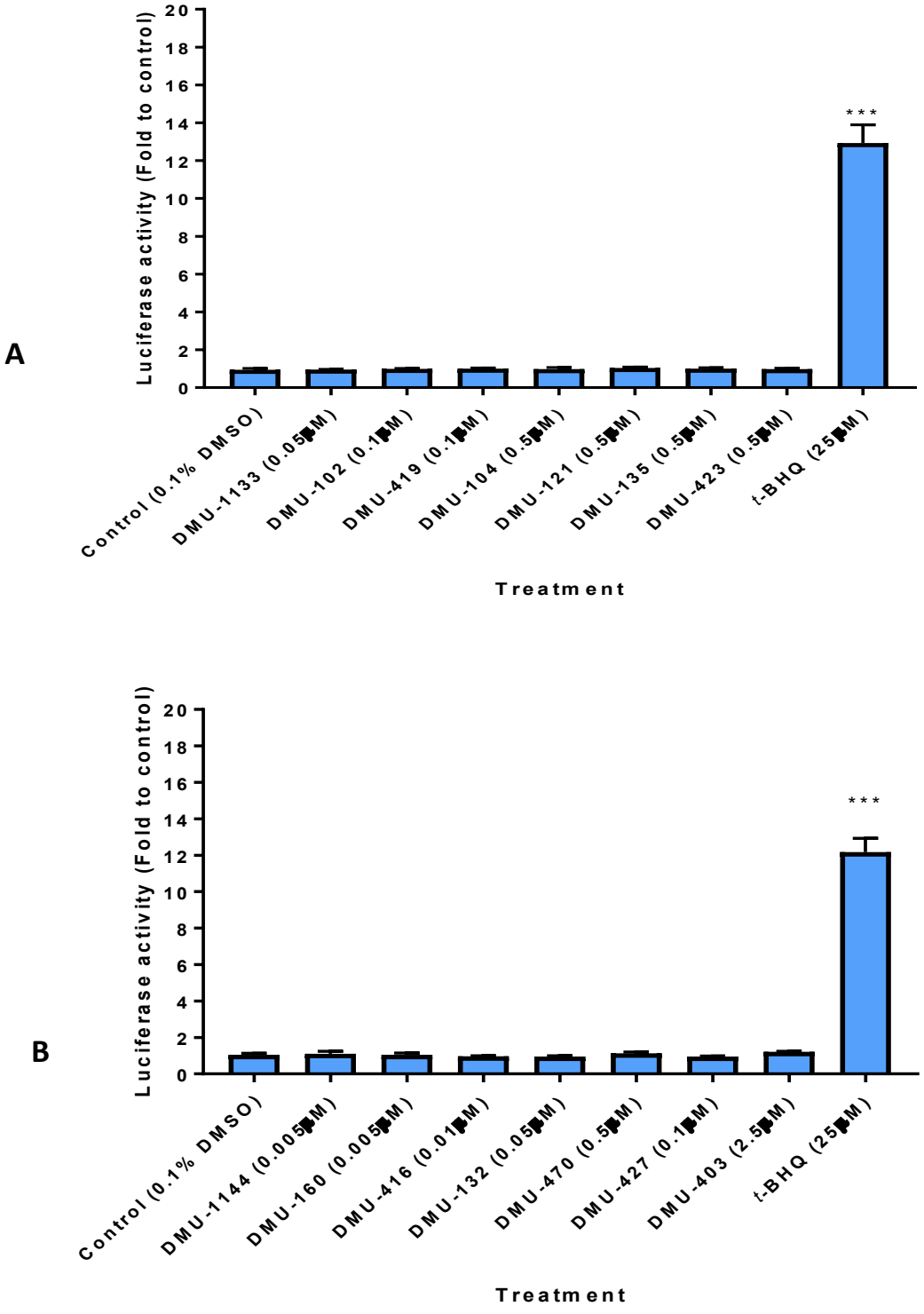

Figure 3.16 AREc32 were exposed to chalcones, 0 (negative control DMSO 0.1%), *t*-BHQ (Positive control). A: DMU-1133, 102, 419, 104, 121, 135, 423 and B: DMU-1144, 160, 416, 132, 470, 427, 403 for 24 h after which cell viability was determined using the Luciferase assay. Data are presented mean ± SD. (n=3), * for $p<0.05$, ** for $p<0.01$ and *** for $p<0.001$ significant compared to control

These results conclusively demonstrated that several of the chalcones investigated in this novel library could switch on Nrf2. Further analysis also indicated that chalcones containing a methoxy group on the C-4' position on ring A induce luciferase maximally. DMU-2210 (Figure **3.15**) with two methoxy groups at C-3',4' positions on ring A and at C- 3,4 on ring B has shown the best induction of luciferase about 16 fold. In addition, chalcones with methylene-dioxy group on ring B with or without a methoxy group on ring A, such as DMU-2219, DMU-411, DMU-2265 and DMU-2267 (Figure **3.15**), also can induce luciferase activity. Similarly, chalcones with a methylene-dioxy group on ring A with two or three methoxy groups on ring B such as DMU-1112 and DMU-1103 (Figure **3.15**) also have the ability to induce luciferase.

A previous study which also utilised the AREc32 cell line, reported similar results with chalcone (*E*)-3-(2-chlorophenyl)-1-(2-hydroxy-4,6-dimethoxyphenyl)prop-2-en-1-one) **(64)** (Figure **3.17**). This also has a 4'-OMe substituent on the A ring and has the ability to induce Nrf2 (Kachadourian *et al.*, 2012).

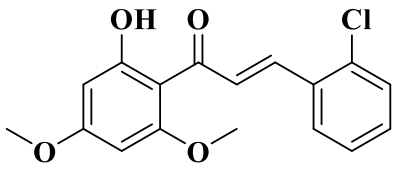

Figure 3.17 Chalcone (*E*)-3-(2-chlorophenyl)-1-(2-hydroxy-4,6-dimethoxyphenyl)prop-2-en-1-one) **(64)** (Kachadourian *et al.*, 2012)

Further researchers also utilised the AREc32 cell line to investigate chalcones, which were α-X-substituted 2′,3,4,4′-tetramethoxychalcones and report significant (200-300 fold) induction (Figure **3.18**) (Rucker *et al.*, 2015). The structures are similar to those found in this study that had a high fold induction in the luciferase assay.

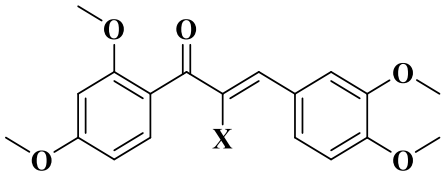

65- X= α-CF_3-TMC

66- X= α-Br-TMC

67- X= α-Cl-TMC

Figure 3.18 α-X-substituted 2′,3,4,4′-tetramethoxychalcones by (Rucker *et al.*, 2015).

Moreover, Zhao *et al.* (2017) have quantified Nrf2 activation in A549 cells, following transfection with a luciferase reporter plasmid and report that five indolyl-chalcones (phenyl- (3-methyl-1H-indol-2-yl)-prop-2-en-1-one) (Figure **3.19**) have the ability to increase Nrf2 after 24 h treatment.

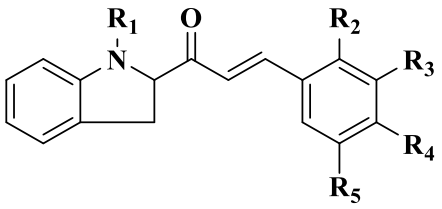

68- R_1= H, R_2= OCH_3

69- R_1=H, R_4= Cl

70- R_1=H, R_2= Cl, R_3=Cl

71- R_1= $C_{10}H_{10}O$

72- R_1=CH_3, R_2= OH, R_5=OH

Figure 3.19 A library of indolyl-chalcones inducing Nrf2

In conclusion, of the research reported here it is notable that twelve chalcones have been found to possess the capacity to switch on Nrf2. With the highest luciferase induction being produced by DMU-2210, which has two methoxy groups in both rings in the same position C-3,4.

Despite the medicinal features of chalcones and the advantage of using MTT and luciferase assay and the reporter AREc32 cell line, there are some limitations as mentioned below:

1- MTT assay, if there is over confluence in cells then it may reduce the rate of metabolism and will eventually decrease the number of cells. Also, the rate of cells metabolism could change by the treatment. In addition, removal of cell culture medium after the treatment and after the addition of MTT solution may result in losing cell during the process.
2- Luciferase assay, may induce by another factor other than the transcriptional factor being examined. Also, because it must be measured within less than 1 minute reduce the compassion between two compounds, unless they can measure in the same time.
3- AREc32 cell line, which was a reporter cell line, originally from cancer cells, therefore the chalcone toxicity that determine by MTT assay may relate to cytotoxicity features and could be not toxic to the normal cells.
4- Chalcones are known as a lipophilic compounds and this characteristic made an solubility issue during the dilution by having crestlasation when they were mixed with cell culture medium, therefore, some chalcones could not dilute more than 10 μM with 0.1% DMSO and some at 20 μM.

Chapter 4 Nrf2 induction in MRC-5 and MRC-5 SV2 cell lines

4.1 Introduction:

The previously reported findings (Chapter 3) detected twelve chalcones with the ability to induce Nrf2 as indicated by the ability to induce luciferase activity. Functional Nrf2 activity in non-genetically modified cells is however indicated by the induction of prototypical ARE-associated genes such as NADP(H) quinine oxidoreductase I (NQO1).

Epidemiologically, lung cancer is the highest causing cancer worldwide. Smoking cigarette and related factors like MDA have most crucial influence in lung cancer induction (Rahman and Adcock, 2006; Cancer Research UK, 2019). Depending on the fact the current chapter is designed to determine the chamopreventive effect of chalcones through inducing NQO1 as well as reduce MDA toxicity in lung cells. The cell lines chosen for the study were the human lung fibroblast MRC-5, which is provided from a 14 week male embryonic diploid (Jacobs *et al.*, 1970; Freshney, 2016). Genetically, it is stable until senescence (Doyle and Griffiths, 1998). In addition to MRC-5 SV2 cell lines, which is prepared by transfection of MRC-5 with virus SV40, it can be passaged 650 times, without senesce or the slowing of growth (Huschtscha and Holliday, 1983; Pipas, 2009). Both cells have been previously used in several studies to determine protein induction following Nrf2 induction using Western blotting (Elhalem *et al.*, 2014). Ho *et al.* (2017) have examined the chemopreventive effect of diallyl sulphide in MRC-5 cells using HO-1 protein induction as an indicator of Nrf2 activity.

4.2 Immunoblotting

Proteins are a translate product from RNA. They have an important role by suppressing biological activity such as forming enzymes and some hormones that can use as indicator of causing or preventing cancer (Whitford, 2005; Plopper *et al.*, 2015). Several methods are used to determine the protein level, for example, protein quantification using Lowry

or Bradford methods, as well as flow cytometry, HPLC, mass spectrometry, ELISA or electrophoreses like immunoblotting using SDS polyacrylamide gel (Walker, 2002).

Immunoblotting is the most common protocol used to detect the presence of specific proteins in complex samples. This technique includes the fractionation of proteins by electrophoresis, cathode (-) to anode (+) through sodium dodecyl sulfate polyacrylamide gel electrophoresis (SDS-PAGE) and then transfer proteins to a blotting membrane, which known as protein blotting (Western blotting) and finally protein detection by specific antibodies (Kurien and Scofield, 2009; Najafov, 2017; Schwartz and Bochkariov, 2017; Sajjad *et al.*, 2018).

4.2.1 The aims and objectives of this chapter

The ability of the twelve selected chalcones to induce NQO1 protein production was consequently investigated in lung cells *in vitro* consistent with the previous chapter, an initial study was thus conducted to determine the maximal concentration of each chalcone that could be used before significant toxicity occurred. For that reason, the aims of this chapter are finding the non-toxic concentration of chalcones in MRC-5 and MRC-5SV2 cells and investigating if chalcone can increase the level of NQO1 protein comparing with control (non-treated cells). These aims can be investigated by the following objectives:

1- To determine the non-toxic concentration of 12 chalcones on MRC-5 and MRC-5 SV2 cell lines using MTT assay.

2- To assess the induction of NQO1 protein induced by the non-toxic concentration of chalcones using Western blotting assay.

4.3 Results and discussion

4.3.1 Assessment of chalcone toxicity in MRC-5 and MRC-5 SV2 cell lines

The results, as shown in (Figure **4.1**-Figure **4.12**), indicate that DMU-1122 was non-toxic up to 20 μM on both MRC-5 and MRC-5 SV2 cell lines (Figure **4.1**). Also, DMU-2267 was non-toxic to MRC-5 cells at 20 μM, while it was not-toxic to MRC-5 SV2 at 10 μM (Figure **4.2**). Chalcones DMU-192 (Figure **4.3**), DMU-1112 (Figure **4.4**), DMU-1113 (Figure **4.5**), DMU-1119 (Figure **4.6**), and DMU-2265 (Figure **4.7**) did not show any differential toxicity between both the cell lines at 10 μM concentration. In addition, DMU-1103 (Figure **4.8**), DMU-2210 (Figure **4.9**), DMU-2219 (Figure **4.10**) and DMU-411 (Figure **4.11**) were not toxic up to 10 μM to MRC-5, but interestingly they were toxic to the MRC-5 SV2 cells. DMU-1103 was found to be non-toxic up to 8 μM. Similar differential toxicity was also noted for DMU-2210 and DMU-2219, which were not toxic up to 7 μM in MRC-5 SV2 cells. DMU-411 was also found to be non-toxic up to 1 μM to MRC-5 SV2 cells. DMU-2207 (Figure **4.12**) was equally toxic to both cell lines (5 μM). The non-toxic concentrations are summarised in Table 14.

1- DMU-1122

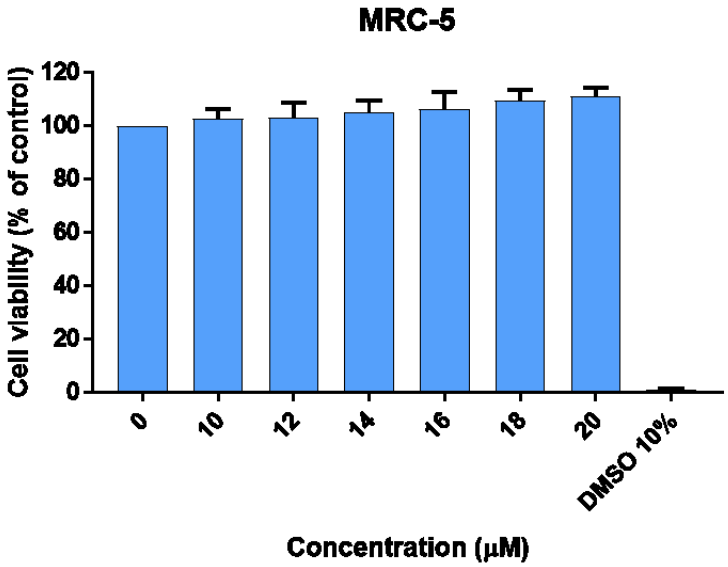

A

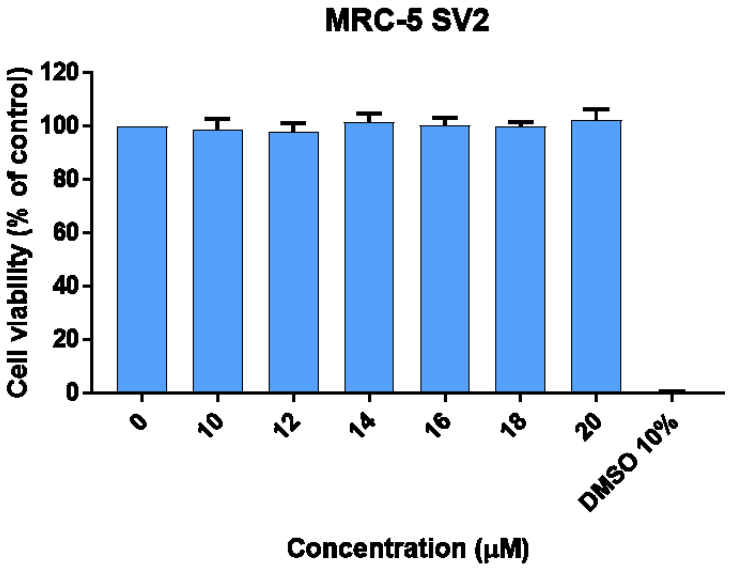

B

Figure 4.1 Effects of DMU-1122 on cell viability of (A) MRC-5 and (B) MRC-5 SV2. Cells were exposed to chalcones at the indicated concentrations for 24 h. Cellular toxicity was then assessed using the MTT assay. Data are presented mean ± SD. (n=3), compared to control (0.1% DMSO)

2- DMU-2267

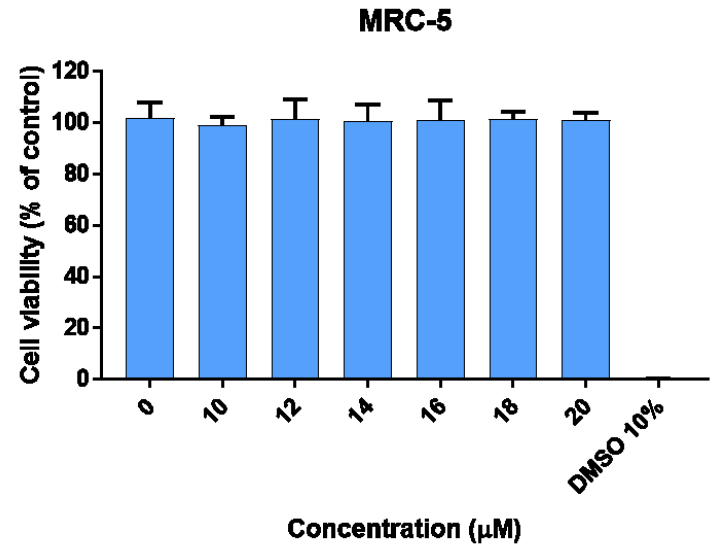

A

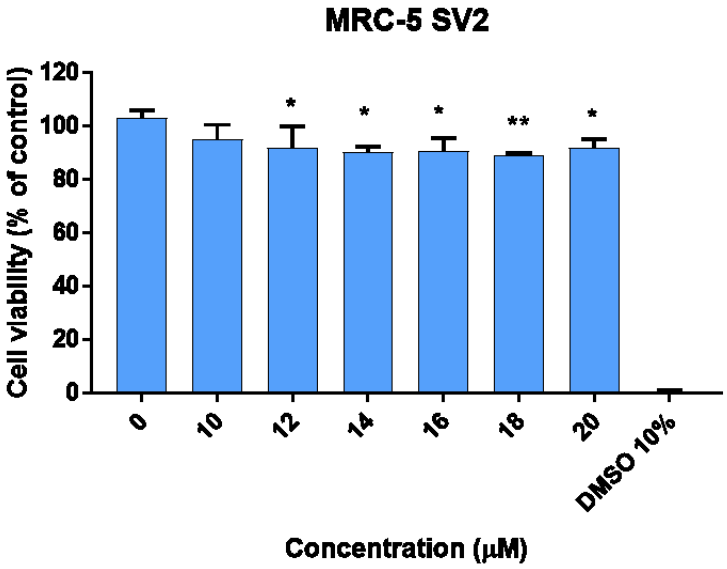

B

Figure 4.2 Effects of DMU-2267 on cell viability of (A) MRC-5 and (B) MRC-5 SV2. Cells were exposed to chalcones at the indicated concentrations for 24 h. Cellular toxicity was then assessed using the MTT assay. Data are presented mean ± SD. (n=3), * for $p<0.05$ and ** for $p<0.01$ significant compared to control (0.1% DMSO)

3- DMU-192

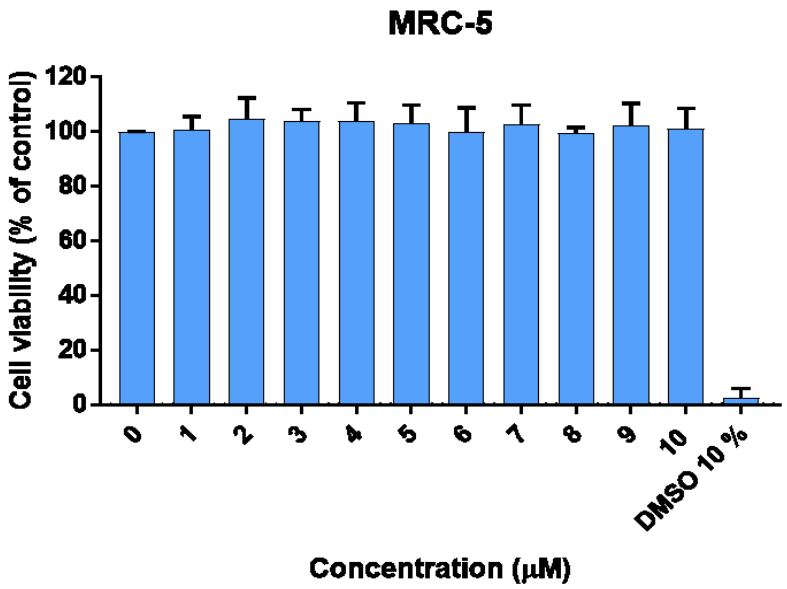

A

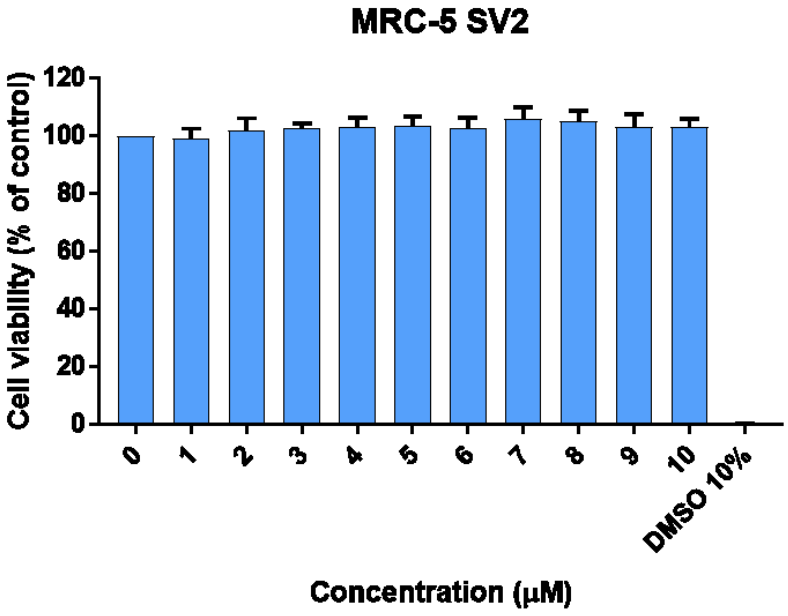

B

Figure 4.3 Effects of DMU-192 on cell viability of (A) MRC-5 and (B) MRC-5 SV2. Cells were exposed to chalcones at the indicated concentrations for 24 h. Cellular toxicity was then assessed using the MTT assay. Data are presented mean ± SD. (n=3), compared to control (0.1% DMSO)

4- DMU-1112

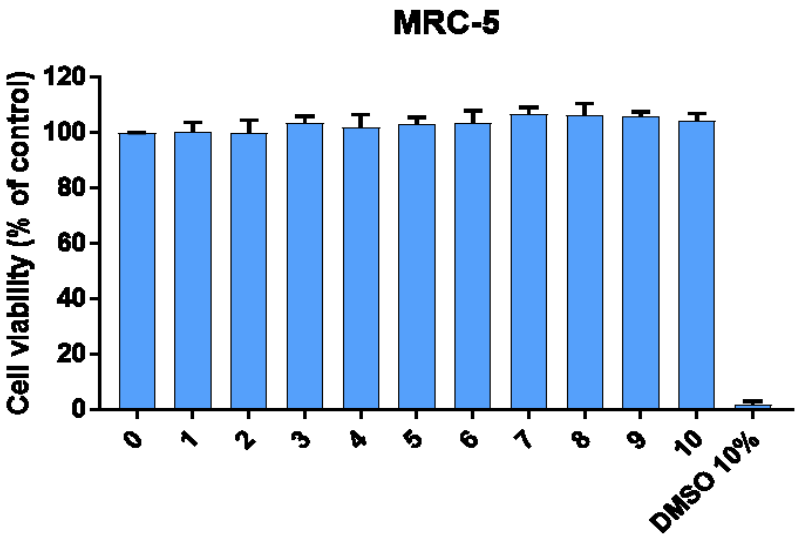

A

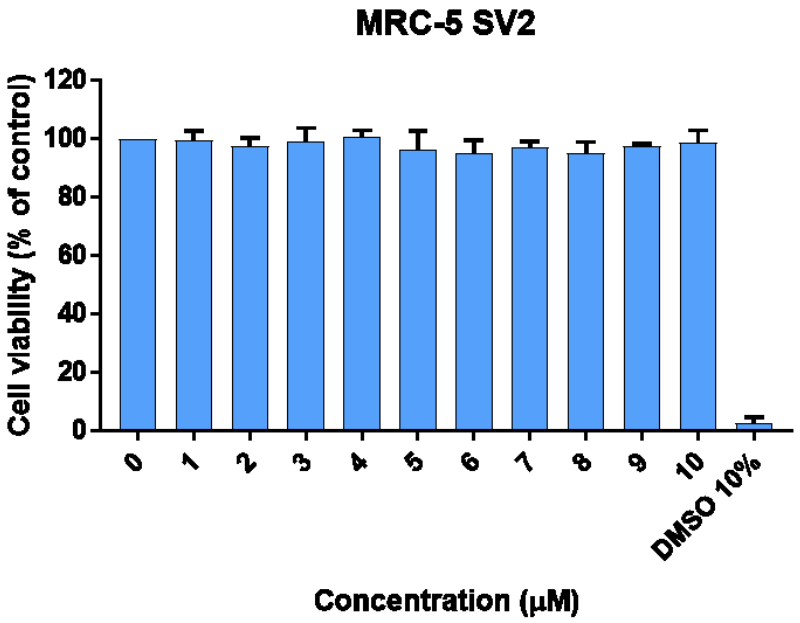

B

Figure 4.4 Effects of DMU-1112 on cell viability of (A) MRC-5 and (B) MRC-5 SV2. Cells were exposed to chalcones at the indicated concentrations for 24 h. Cellular toxicity was then assessed using the MTT assay. Data are presented mean ± SD. (n=3), compared to control (0.1% DMSO)

5- DMU-1113

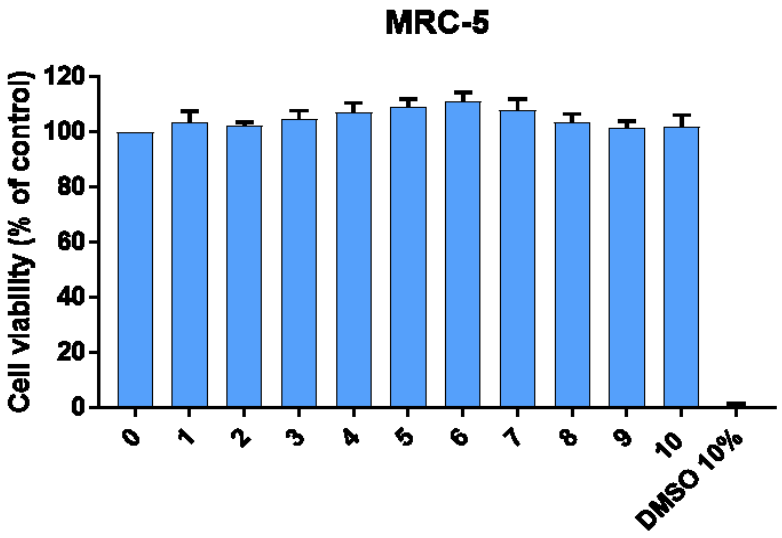

A

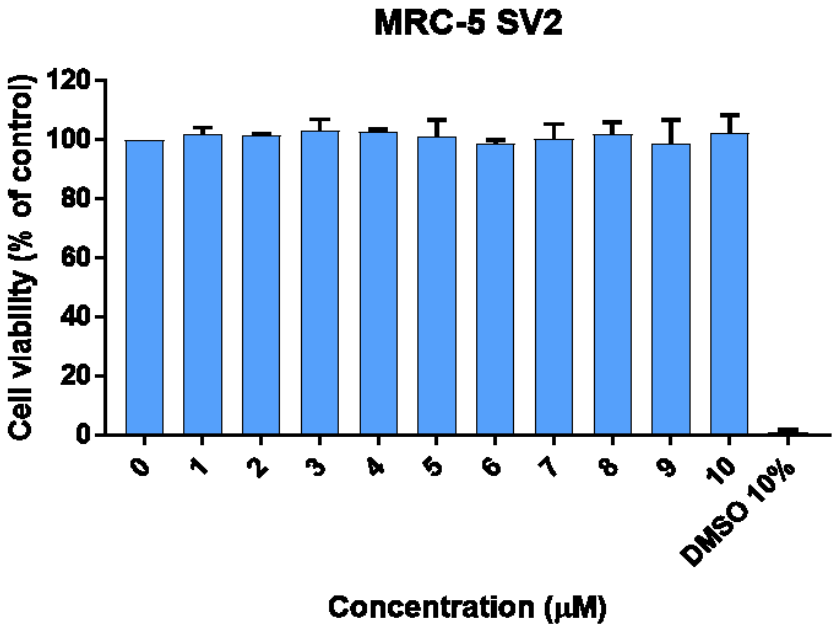

B

Figure 4.5 Effects of DMU-1113 on cell viability of (A) MRC-5 and (B) MRC-5 SV2. Cells were exposed to chalcones at the indicated concentrations for 24 h. Cellular toxicity was then assessed using the MTT assay. Data are presented mean ± SD. (n=3), compared to control (0.1% DMSO)

6- DMU-1119

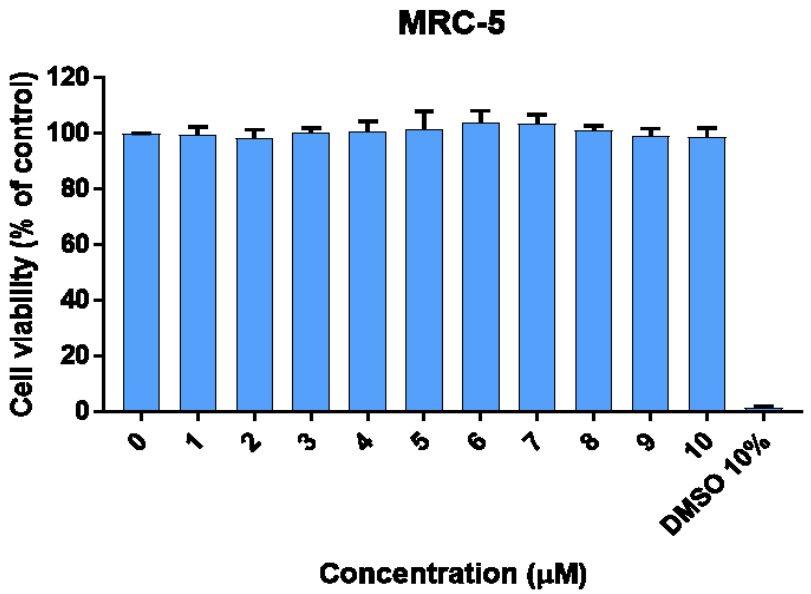

A

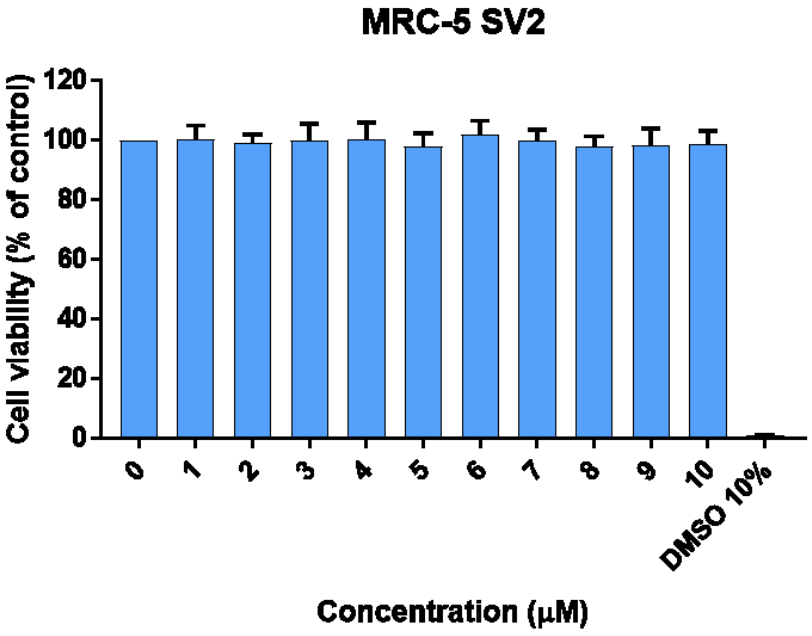

B

Figure 4.6 Effects of DMU-1119 on cell viability of (A) MRC-5 and (B) MRC-5 SV2. Cells were exposed to chalcones at the indicated concentrations for 24 h. Cellular toxicity was then assessed using the MTT assay. Data are presented mean ± SD. (n=3), compared to control (0.1% DMSO)

7- DMU-2265

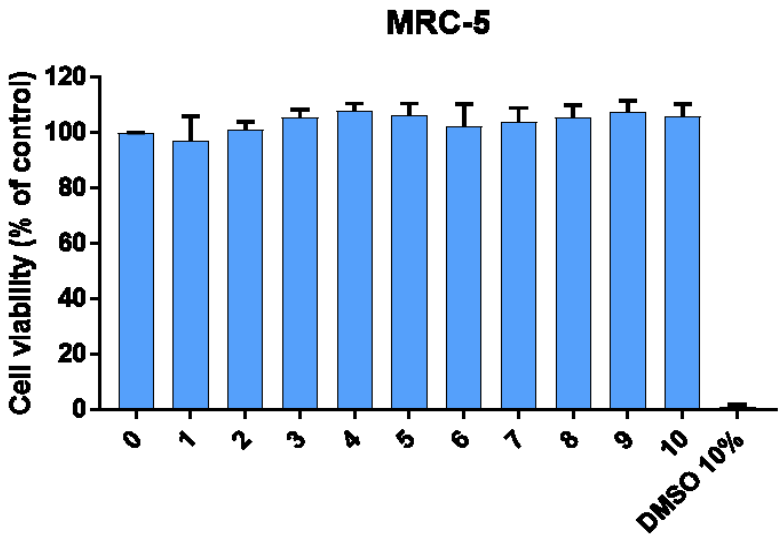

A

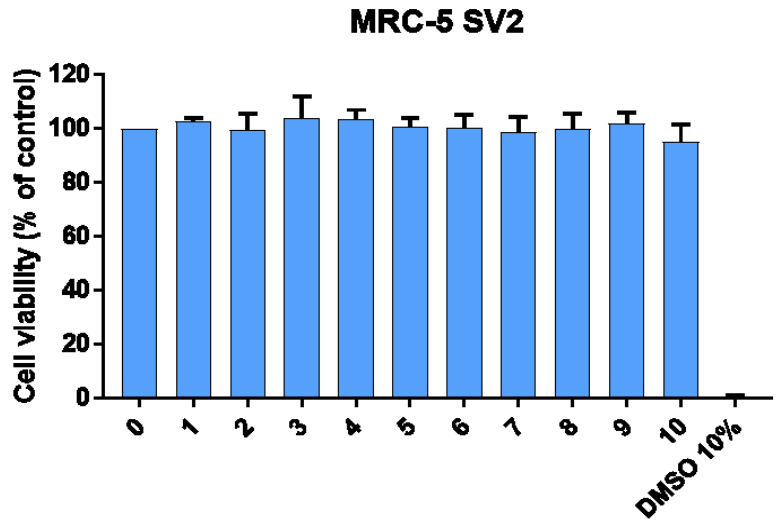

B

Figure 4.7 Effects of DMU-2265 on cell viability of (A) MRC-5 and (B) MRC-5 SV2. Cells were exposed to chalcones at the indicated concentrations for 24 h. Cellular toxicity was then assessed using the MTT assay. Data are presented mean ± SD. (n=3), compared to control (0.1% DMSO)

8- DMU-1103

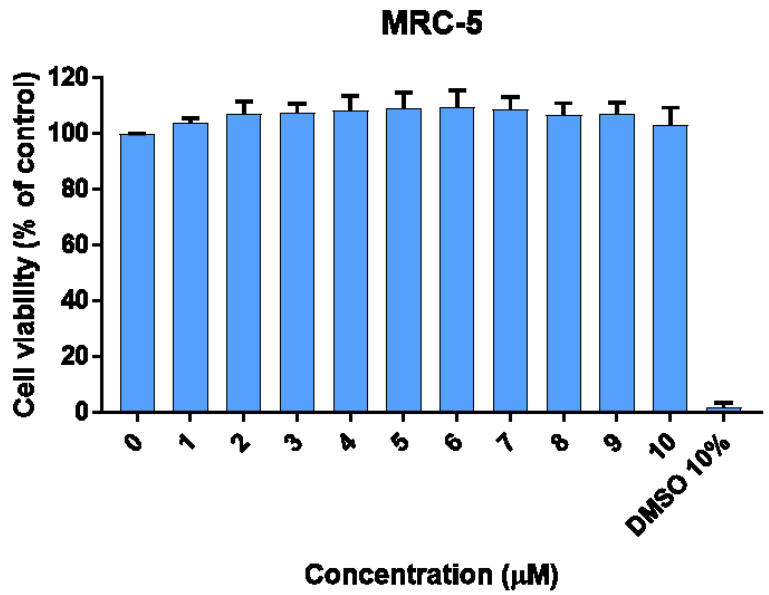

A

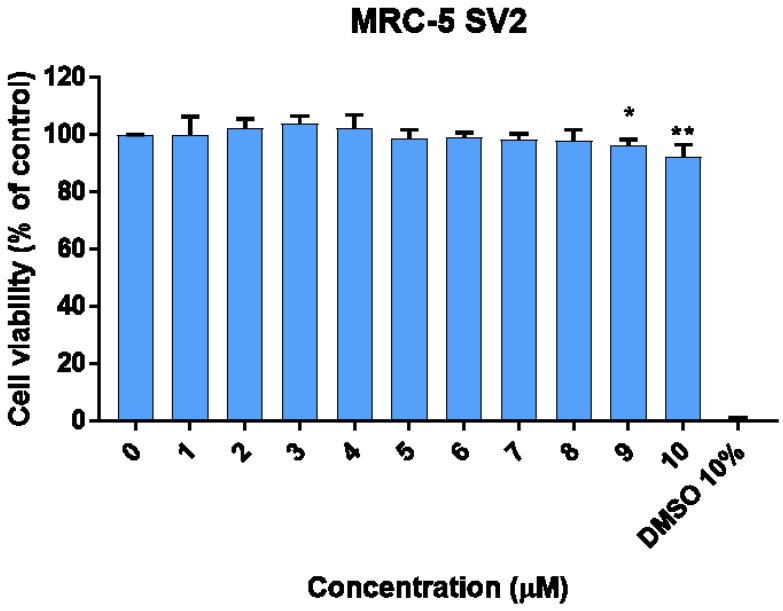

B

Figure 4.8 Effects of DMU-1103 on cell viability of (A) MRC-5 and (B) MRC-5 SV2. Cells were exposed to chalcones at the indicated concentrations for 24 h. Cellular toxicity was then assessed using the MTT assay. Data are presented mean ± SD. (n=3), * for $p<0.05$ and ** for $p<0.01$ compared to control (0.1% DMSO)

9- DMU-2210

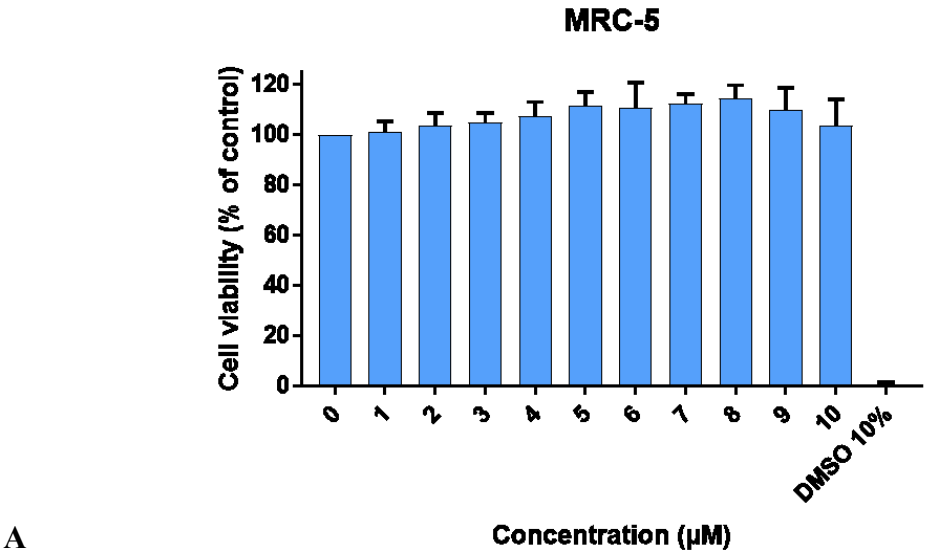

A

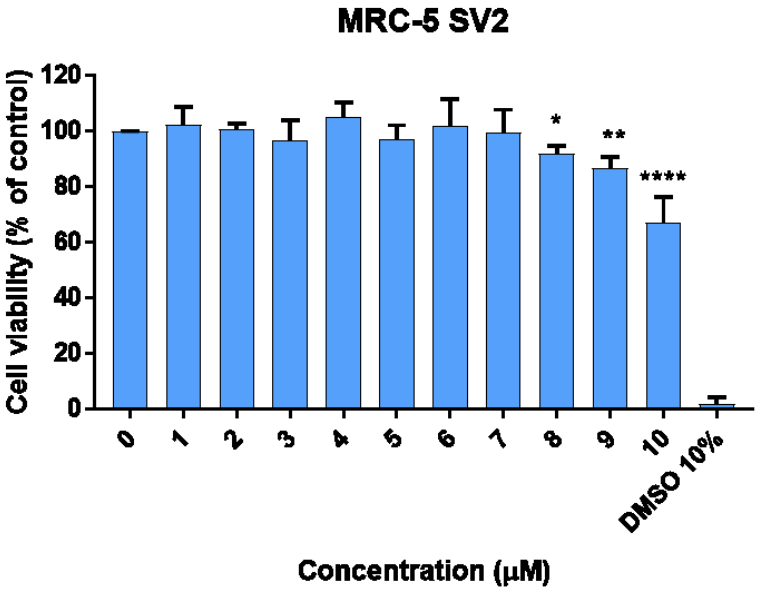

B

Figure 4.9 Effects of DMU-2210 on cell viability of (A) MRC-5 and (B) MRC-5 SV2. Cells were exposed to chalcones at the indicated concentrations for 24 h. Cellular toxicity was then assessed using the MTT assay. Data are presented mean ± SD. (n=3), * for $p<0.05$, ** for $p<0.01$ and **** for $p<0.0001$ significant compared to control (0.1% DMSO)

10- DMU-2219

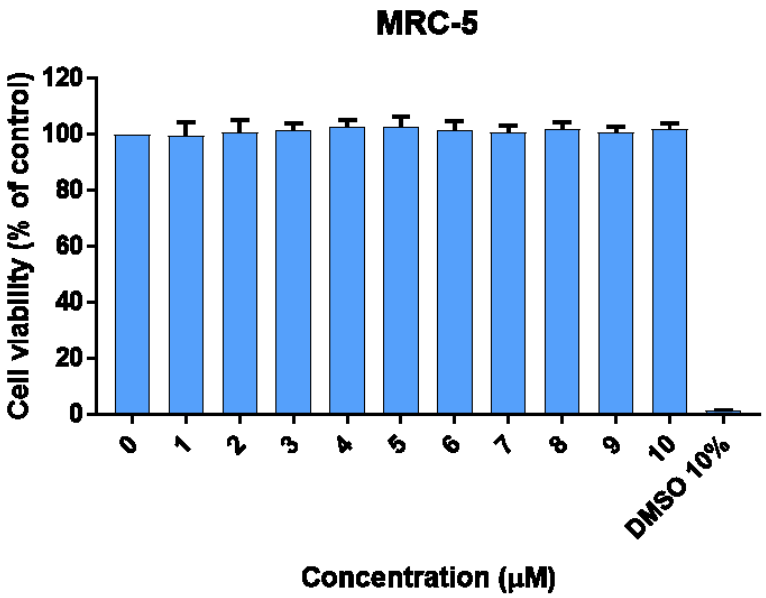

A

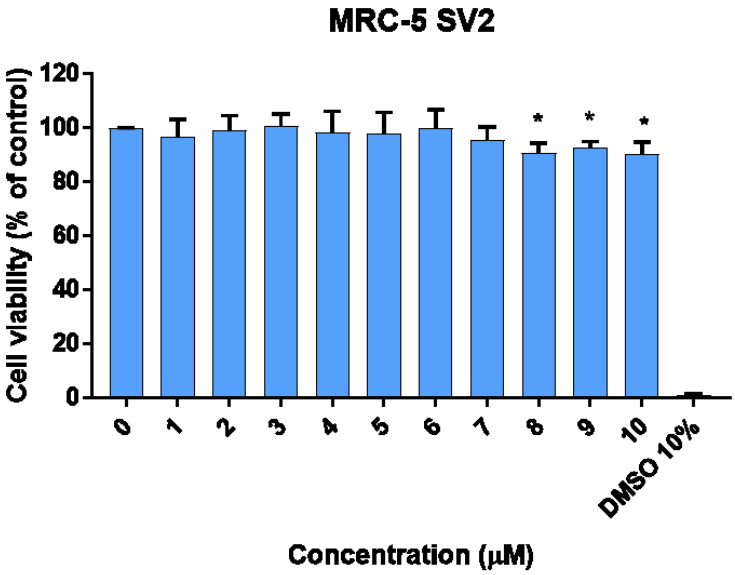

B

Figure 4.10 Effects of DMU-2219 on cell viability of (A) MRC-5 and (B) MRC-5 SV2. Cells were exposed to chalcones at the indicated concentrations for 24 h. Cellular toxicity was then assessed using the MTT assay. Data are presented mean ± SD. (n=3), * for $p<0.05$ significant compared to control (0.1% DMSO)

11- DMU-411

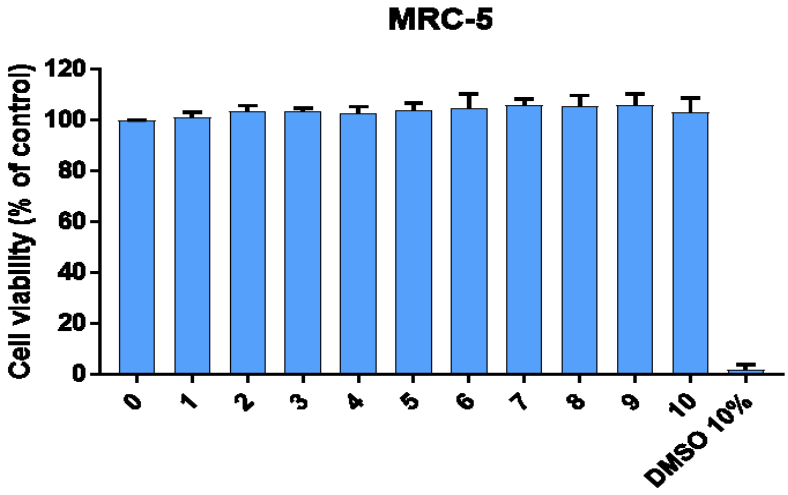

A

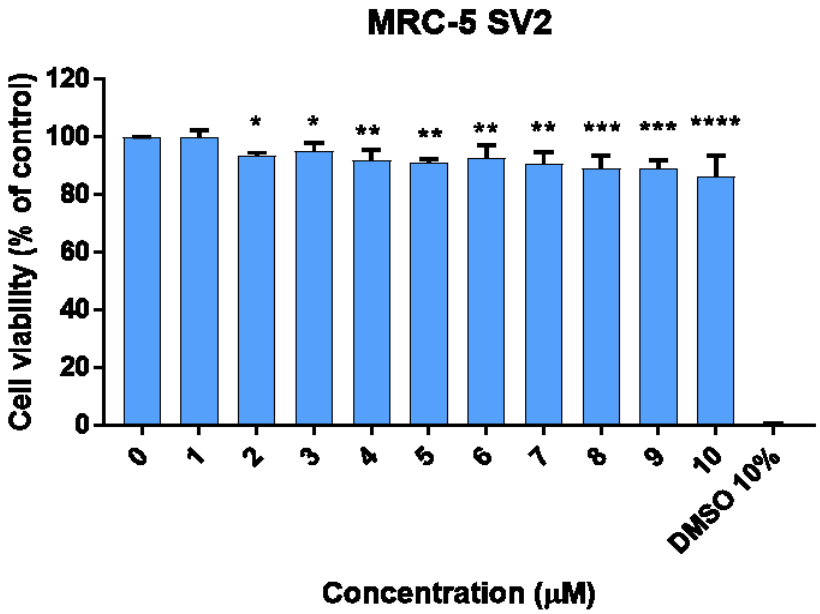

B

Figure 4.11 Effects of DMU-411 on cell viability of (A) MRC-5 and (B) MRC-5 SV2. Cells were exposed to chalcones at the indicated concentrations for 24 h. Cellular toxicity was then assessed using the MTT assay. Data are presented mean ± SD. (n=3), * for $p<0.05$, ** for $p<0.01$, *** for $p<0.001$ and *** for $p<0.001$ significant compared to control (0.1% DMSO)

12- DMU-2207

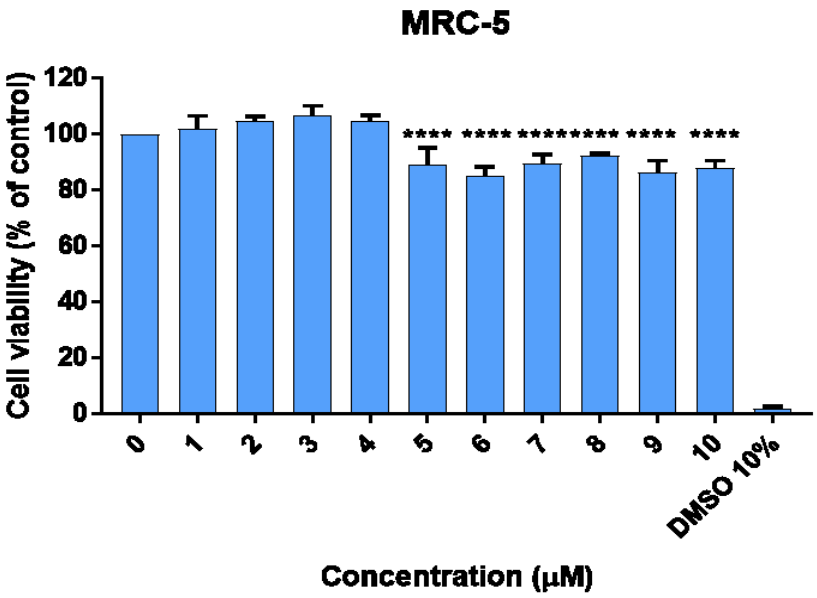

A

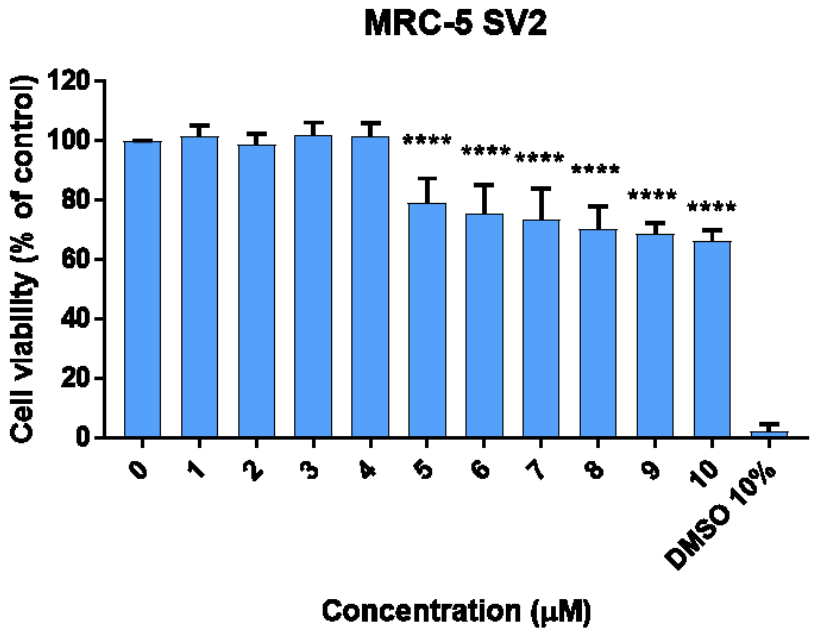

B

Figure 4.12 Effects of DMU-2207 on cell viability of (A) MRC-5 and (B) MRC-5 SV2. Cells were exposed to chalcones at the indicated concentrations for 24 h. Cellular toxicity was then assessed using the MTT assay. Data are presented mean ± SD. (n=3), **** for $p<0.0001$ significant compared to control (0.1% DMSO)

Table 14. Non-toxic concentrations of chalcones on MRC-5 and MRC-5 SV2 cell lines

Chalcone	MRC-5 Concentration (µM)	MRC-5 SV2 Concentration (µM)
DMU-1122	20	20
DMU-2267	20	10
DMU-192	10	10
DMU-1112	10	10
DMU-1113	10	10
DMU-1119	10	10
DMU-2265	10	10
DMU-1103	10	8
DMU-2210	10	7
DMU-2219	10	7
DMU-411	10	1
DMU-2207	4	4

It is apparent from Table 14 that DMU-1122 showed less toxicity on both cells. In addition, it is interesting to note that chalcones DMU-2267, 2210, 1103, 411 and 2219 have been found to be of equivalent toxicity in both MRC-5 SV2 cells (lung carcinoma) and AREc32 cells (MCF-7 cells – breast carcinoma) whilst being non-toxic, at the same concentrations to the MRC-5 cell line (untransformed).

Some of these results are in agreement with those obtained by (Ruparelia *et al.*, 2018), who found that DMU-2267, 2210, 1103 and 411 were more toxic to MCF-7 cells than MCF-10A cells (untransformed). Additionally, they also report that DMU-192, 2265 and 1112 have equivalent toxicity in both cancer and normal cells. However, they also report that DMU-1113 was more toxic to cancer cell than normal cells, and DMU-2219 was more toxic to normal cells than cancer cells. Moreover, it also reported by these same researchers that DMU-1119 displays differential toxicity to different types of cancer cells.

4.3.2 Western blotting

Using the previously determined non-toxic concentrations of chalcones, the ability of these twelve chalcones to induce the Nrf2 as indicated by NQO1 protein induction was investigated by Western blotting in both MRC-5 and MRC-5 SV2 cell lines. The results were compared with control (no treatment) as well as with beta-actin as a reference protein.

From the data presented in Figure **4.13** - Figure **4.18**, it is apparent that DMU-2210 (Figure **4.13**) can induce NQO1 protein level at 12 and 24 h in MRC-5 and at 24 h in MRC-5 SV2 cells. In addition, DMU-1122 (Figure **4.13**), 1103 and 2265 (Figure **4.14**) can induce NQO1 protein level at 24 h in MRC-5 and MRC-5 SV2 cells. However, in contrast, DMU-1112 (Figure **4.15**) induced NQO1 protein level only in MRC-5 SV2 cells at 12 and 24 h, a finding which is also found to be replicated by DMU-411 (Figure **4.15**) and 2207 (Figure **4.16**) at 24 h. DMU-2267 (Figure **4.16**), DMU-1119, DMU-1113 (Figure **4.17**), DMU-2219 and DMU-192 (Figure **4.18**) all failed to induce NQO1 protein level (relative to control), all results have shown in Table 15.

1- DMU-2210

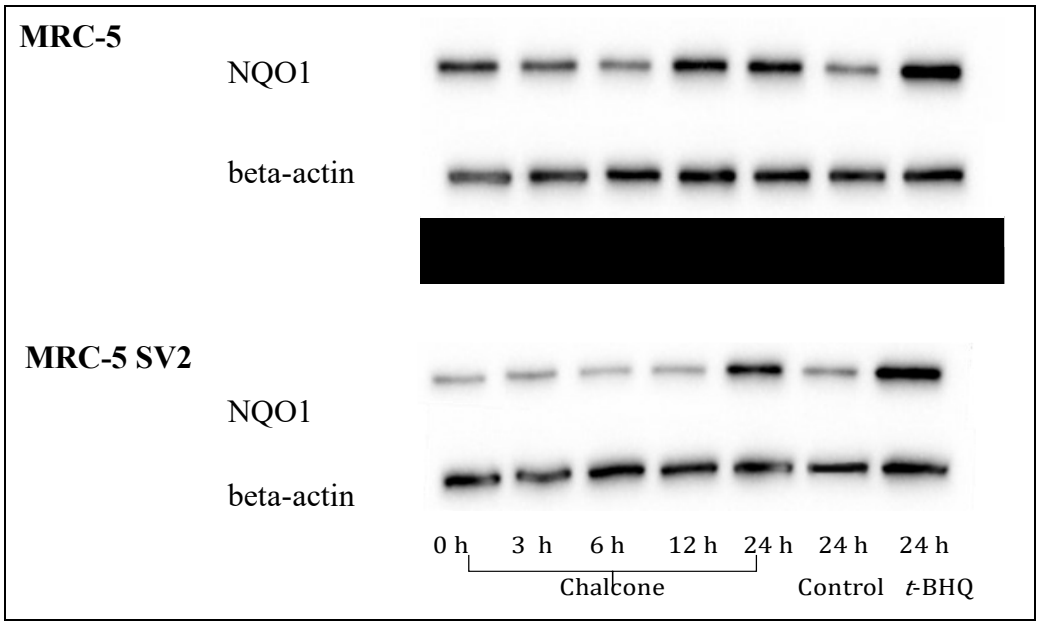

2- DMU-1122

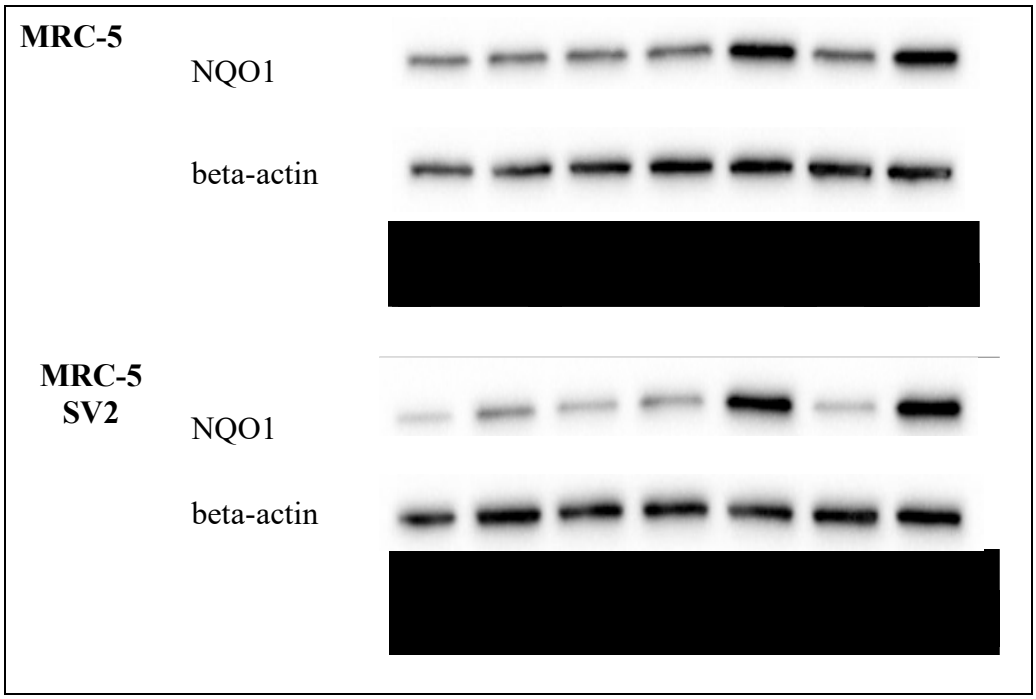

Figure 4.13 Time course of NQO1 protein level following chalcone (1) DMU-2210 and (2) DMU-1122 treatment. MRC5 and MRC5-SV2 cells were incubated with the indicated chalcones up to a maximum of 24 h before being harvested and then subjected to Western blotting (as detailed in methods section 2.2.7). Vehicle control (Control) (0.1% DMSO at 24 hours), *t*-BHQ (25 μM) was included as a positive control (24 h incubation)

3- DMU-1103

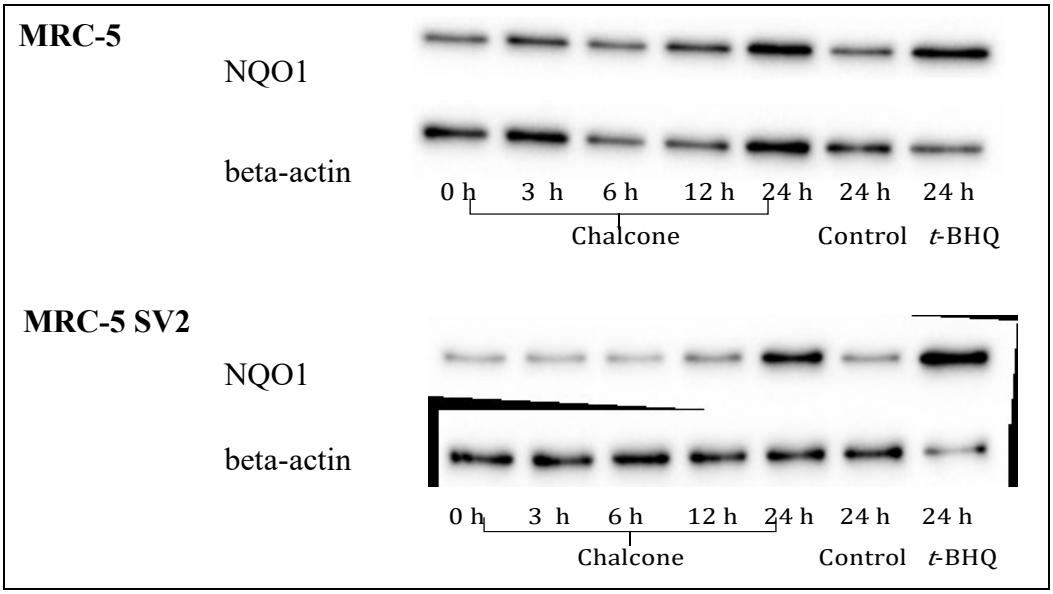

4- DMU-2265

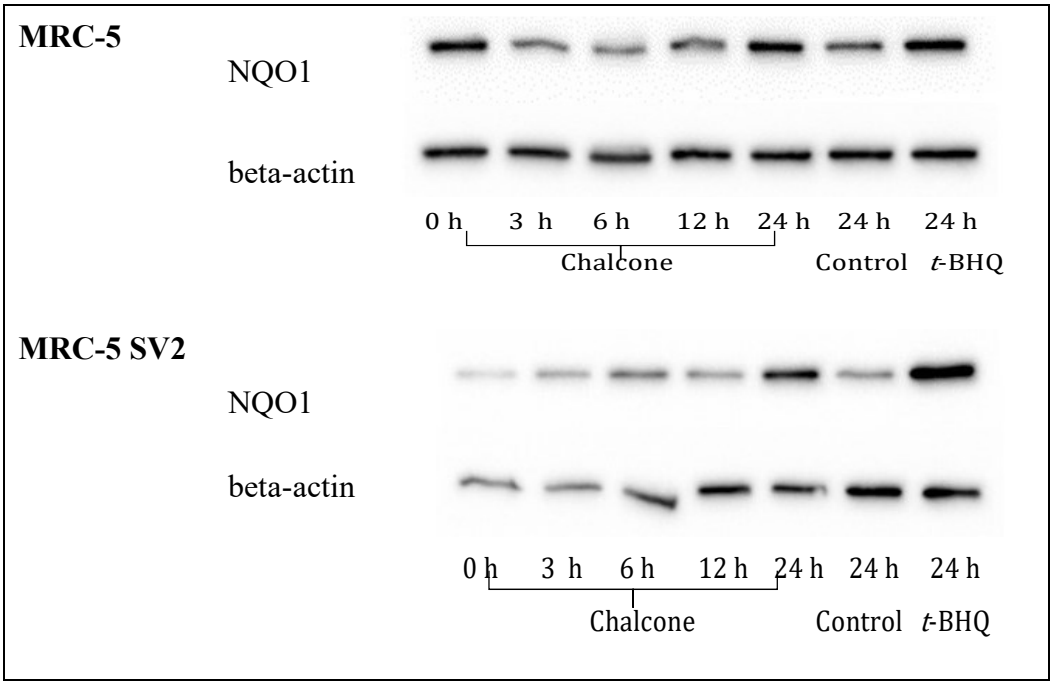

Figure 4.14 Time course of NQO1 protein level following chalcone (3) DMU-1103 and (4) DMU-2265 treatment. MRC5 and MRC5-SV2 cells were incubated with the indicated chalcones up to a maximum of 24 h before being harvested and then subjected to Western blotting (as detailed in methods section 2.2.7). Vehicle control (Control) (0.1% DMSO at 24 hours), *t*-BHQ (25 μM) was included as a positive control (24 h incubation)

5- DMU-1112

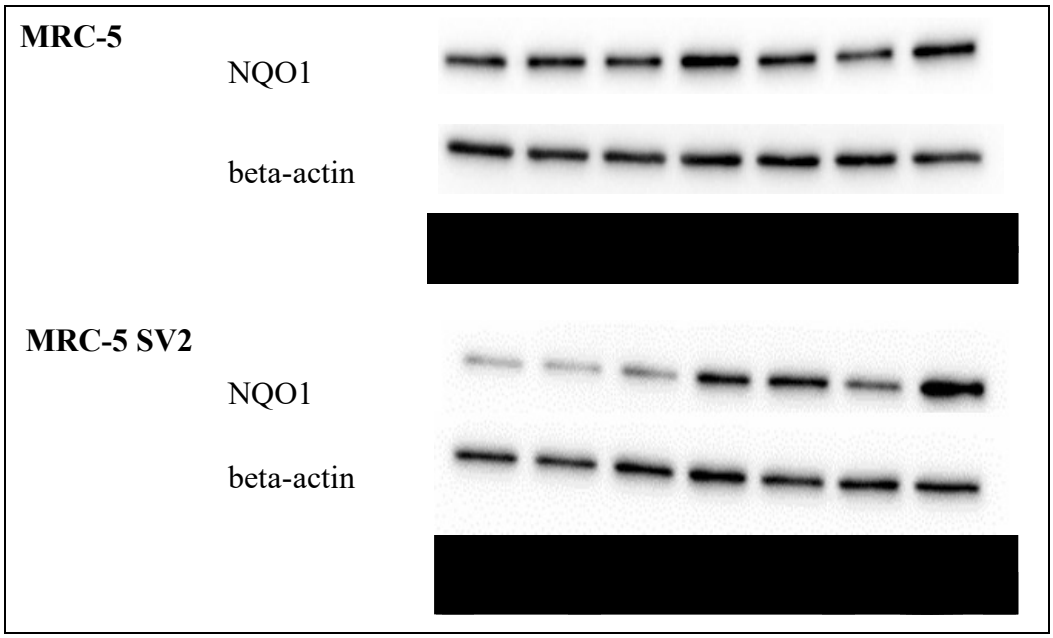

6- DMU-411

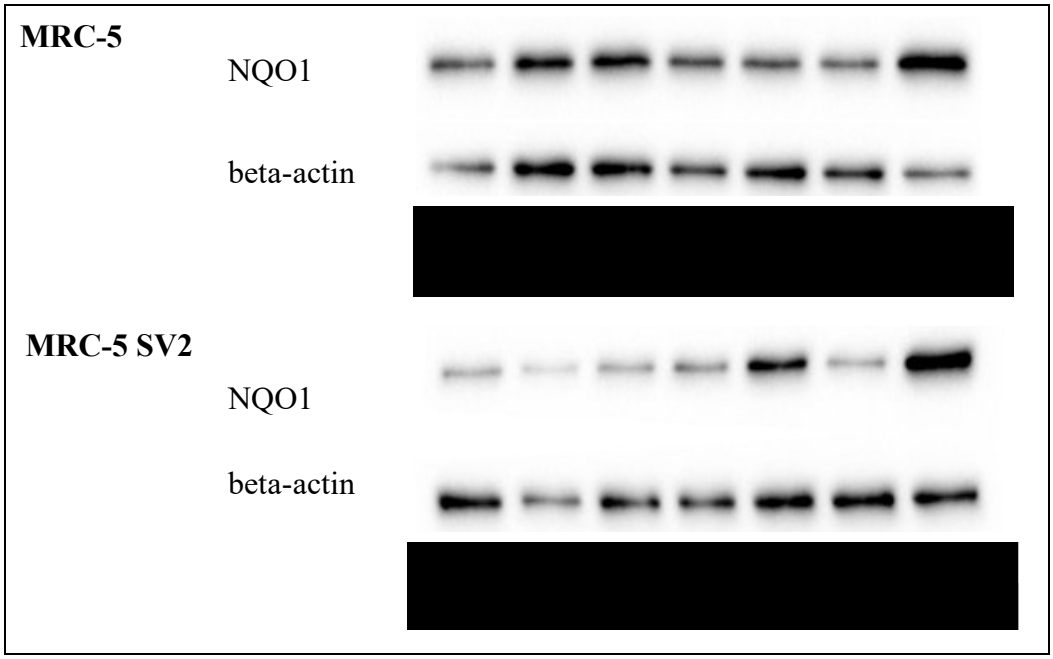

Figure 4.15 Time course of NQO1 protein level following chalcone (5) DMU-1112 and (6) DMU-411 treatment. MRC5 and MRC5-SV2 cells were incubated with the indicated chalcones up to a maximum of 24 h before being harvested and then subjected to Western blotting (as detailed in methods section 2.2.7). Vehicle control (Control) (0.1% DMSO at 24 h), *t*-BHQ (25 μM) was included as a positive control (24 h incubation)

7- DMU-2207

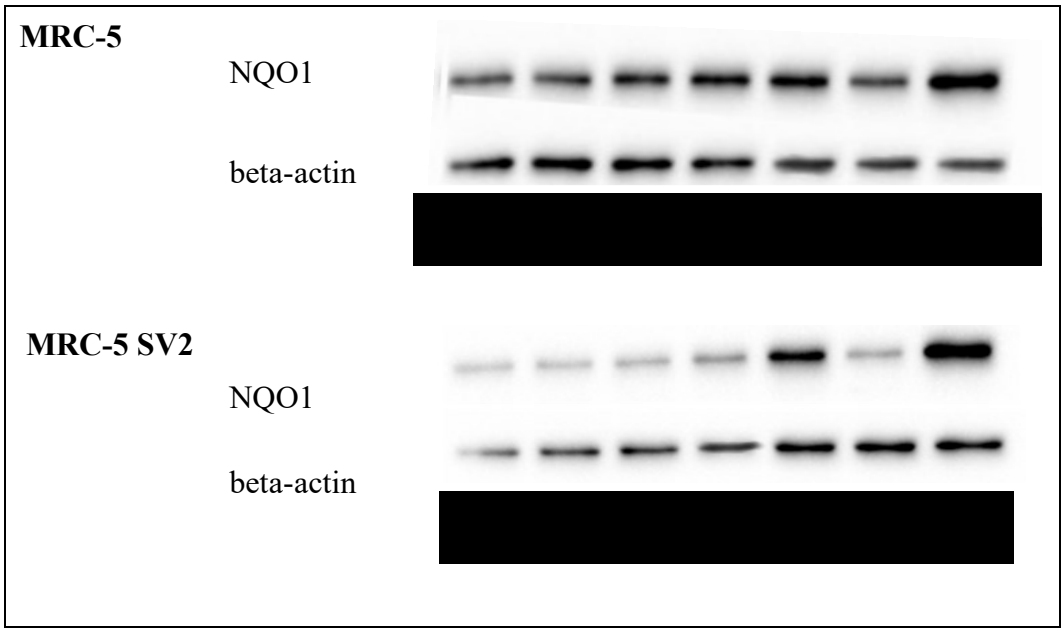

8- DMU-2267

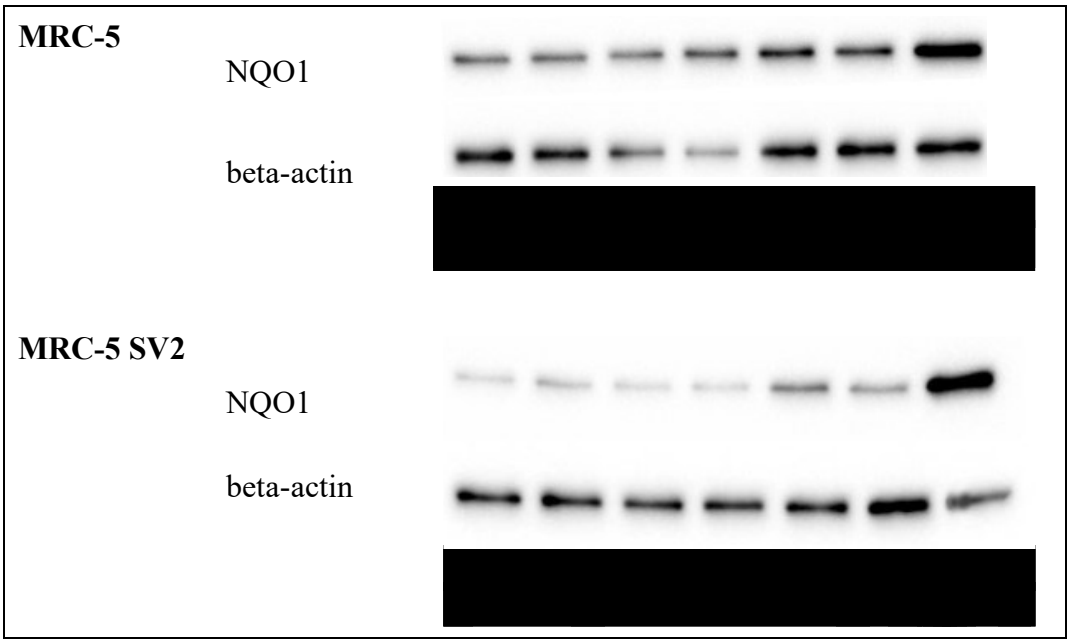

Figure 4.16 Time course of NQO1 protein level following chalcone (7) DMU-2207 and (8) DMU-2267 treatment. MRC5 and MRC5-SV2 cells were incubated with the indicated chalcones up to a maximum of 24 h before being harvested and then subjected to Western blotting (as detailed in methods section 2.2.7). Vehicle control (Control) (0.1% DMSO at 24 hours), *t*-BHQ (25 μM) was included as a positive control (24 h incubation)

9- DMU-1119

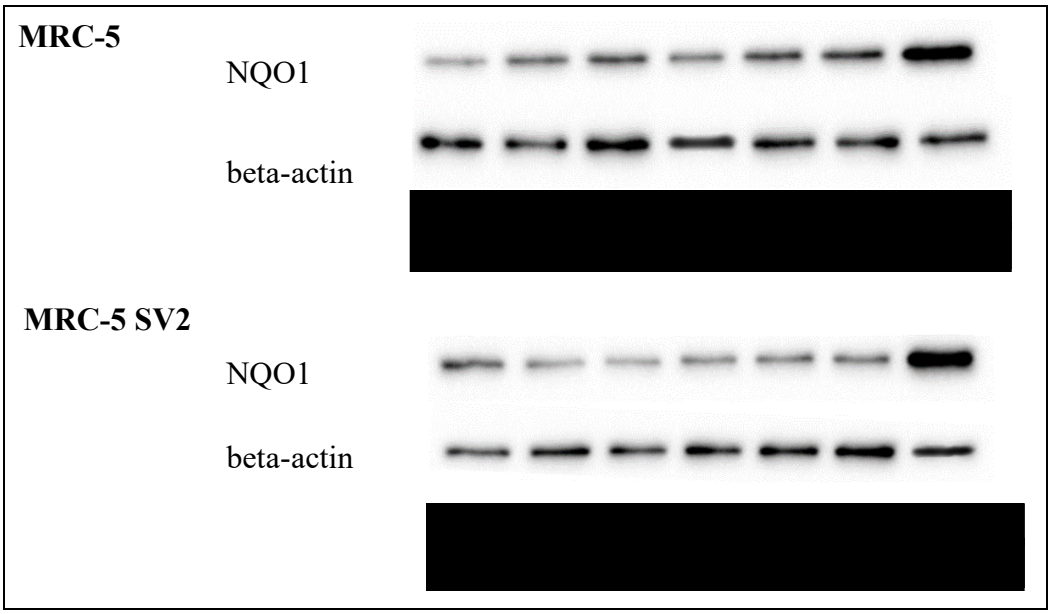

10- DMU-1113

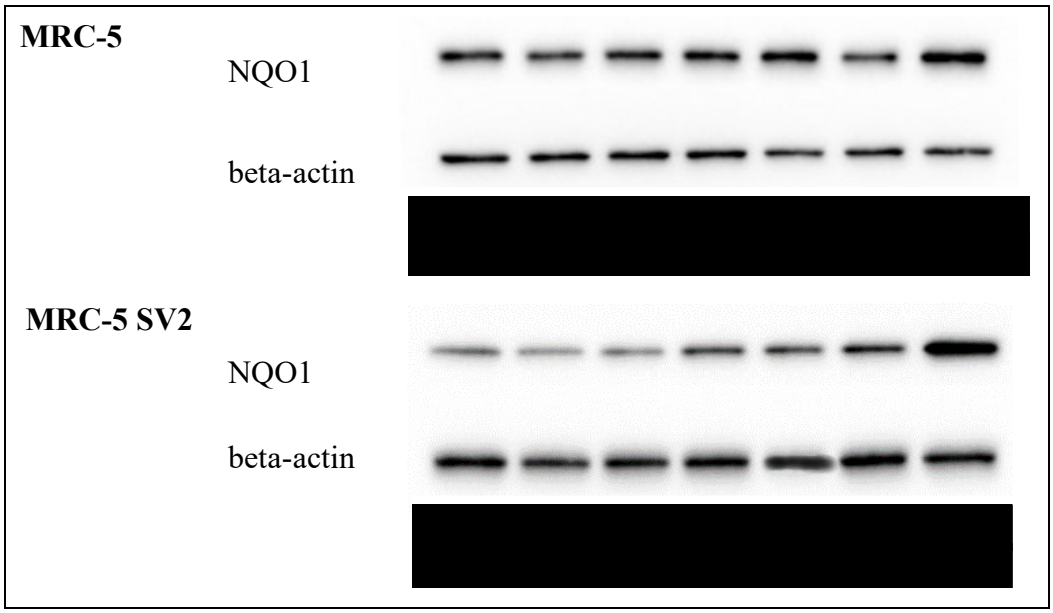

Figure 4.17 Time course of NQO1 protein level following chalcone (9) DMU-1119 and (10) DMU-1113 treatment. MRC5 and MRC5-SV2 cells were incubated with the indicated chalcones up to a maximum of 24 h before being harvested and then subjected to Western blotting (as detailed in methods section 2.2.7). Vehicle control (Control) (0.1% DMSO at 24 hours), *t*-BHQ (25 μM) was included as a positive control (24 h incubation)

11- DMU-2219

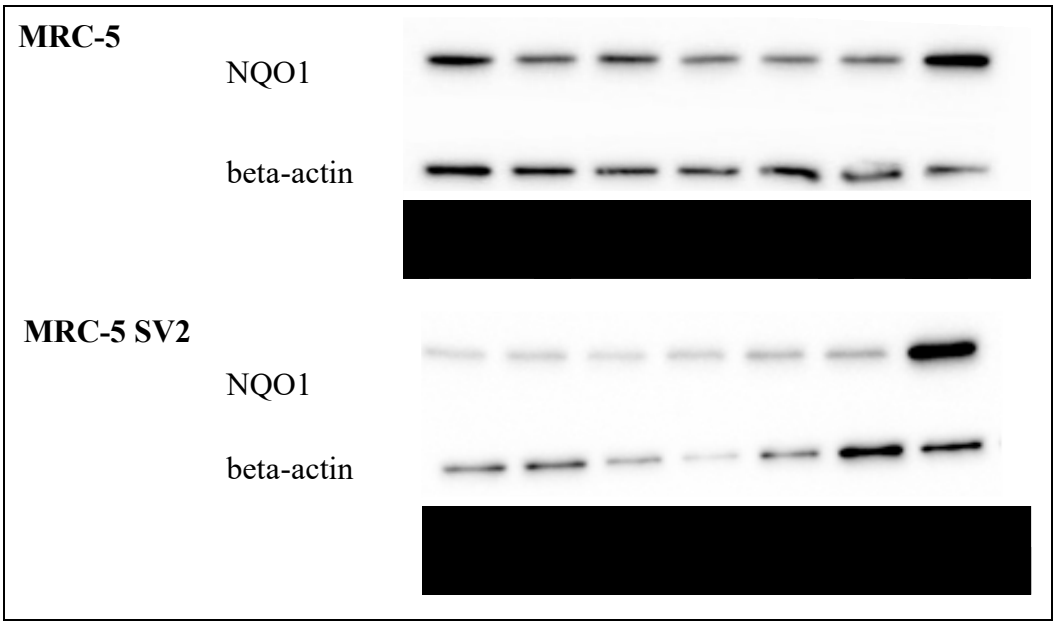

12- DMU-192

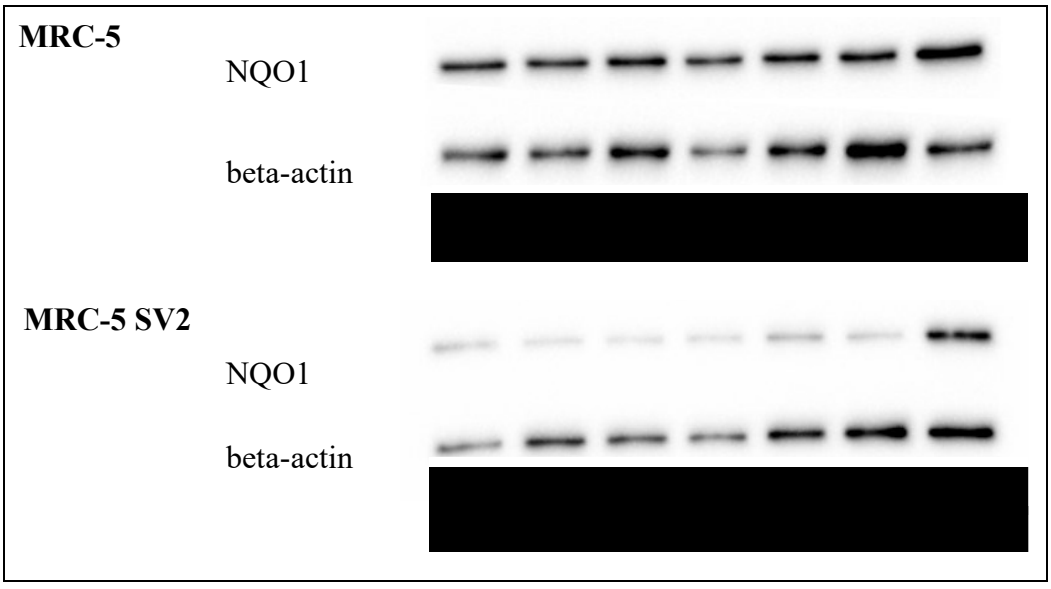

Figure 4.18 Time course of NQO1 protein level following chalcone (11) DMU-2210 and (12) DMU-1122 treatment. MRC5 and MRC5-SV2 cells were incubated with the indicated chalcones up to a maximum of 24 h before being harvested and then subjected to Western blotting (as detailed in methods section 2.2.7). Vehicle control (Control) (0.1% DMSO at 24 hours), *t*-BHQ (25 μM) was included as a positive control (24 h incubation)

Table 15 Summary the Western blotting results for increase NQO1 level on time posting

Chalcone	NQO1 protein level (hour)	
	MRC-5	MRC-5 SV2
DMU-2210	12, 24	24
DMU-1122	24	24
DMU-1103	24	24
DMU-2265	24	24
DMU-1112	No	12, 24
DMU-411	3, 6	24
DMU-2207	12, 24	24
DMU-2267	No	No
DMU-1119	No	No
DMU-1113	No	No
DMU-2219	No	No
DMU-192	No	No

The correlation between chalcone and Nrf2 is the remarkable outcome because DMU-2210 had increased Nrf2 activity in AREc32 cell by 16 fold induction (Section 3.2.2.), interestingly it can increase protein level at 12 and 24 h in MRC-5 and MRC-5 SV2 cells. Moreover, DMU-1122 and DMU-1103 had induced Nrf2 activity by 7 fold and DMU-2265 by 3 fold in AREc32, also they have induced Nfr2 in MRC-5 and MRC-5 SV2 at 24 h. In addition, DMU-1112 induce Nrf2 activity by 3 fold induction, DMU-411 and 2207 by 2 fold induction in AREc32 cell, all can increase Nrf2 activity in MRC-5 SV2 at 24 h.

It is thought that the ability of a chalcone to induce NQO1 protein level depends upon the inherent ability of the chalcone to disrupt the Nrf2-Keap1 complex. Chemically, chalcones have an α and β unsaturated site that reacts with thiol groups via a Micheal-addition reaction (Rozmer, 2014). The Keap1 protein contains cysteine residues, which are a rich source of thiols (Yamamoto *et al.*, 2018). It is speculated that as a result of chalcone-cysteine-thiol modification, associated Nrf2 is dissociated from the Nrf2-Keap1 complex and enters the nucleus then switches on *NRF2* gene expression (Albena *et al.*, 2002; Lau *et al.*, 2008; Kansanen *et al.*, 2013; Ma, 2013; Iso *et al.*, 2016; De Freitas Silva *et al.*, 2018).

In consideration of the structures of the rings of the chalcones, which contain two methoxy groups on both rings in DMU-2210 and 2207; an ethoxy group on ring B like DMU-1122; a methylene-dioxy group on ring B like DMU-411 and 2265; and a methylene-dioxy group on ring A like DMU-1112 and 1103; it might have been predicted that NQO1 protein level would have been found. The results presented here confirm this hypothesis and clearly show that chalcones containing different chemical groups on the rings affect the reactivity of the α and β unsaturated (C-8,7) positions and influence the ability to switch on cell defence genes via the Nrf2 pathway. Yang *et al.* (2017) have reported the position of methoxy might change the α, β unsaturated moiety reactivity.

Several studies have reported the potential of chalcones to act as chemopreventive agents via activation of Nrf2. Natural and synthetic compounds such as dimer chalcones, which are lophirones B **(23)** and C **(24)** (Ajiboye *et al.*, 2014), licochalcone A **(73)** (Liu, 2018), isoliquiritigenin **(56)** (Xiong, 2018), a novel chalcone-coumarin hybrid **(74)** (Lee *et al.*, 2018) and *trans*-chalcone **(25)** (Miranda-Sapla, 2019) have all been reported to possess the aforementioned ability to activate Nrf2.

These immunoblotting results are consistent with those of Kim *et al.* (2012), who report that licochalcone E **(75)** has the ability to activate the Nrf2 pathway and consequently increase NQO1 protein level in SH-SY5Y cells, which are a neuroblastoma cell. In addition, chalcones (*E*)-3-(4-hydroxy-3-methoxyphenyl)-1-(4-methoxyphenyl) prop-2-en-1-one **(76)** and 2-methoxy-4-((*E*)-3-(4-methoxyphenyl)-3-oxoprop-1-enyl) phenyl acrylate **(77)** have been reported to activate *NRF2* gene expression in PC12 cells (Jian-Zhang *et al.*, 2014). The correlation between α and β unsaturated sites in chalcones and Nrf2 induction are in accord with recent studies which report that cinnamic acid, which also has an α and β unsaturated group, can activate Nrf2 (Yao *et al.*, 2019). Moreover, xanthohumol (2′,4′,4-trihydroxy-6′-methoxy-3′-prenylchalcone) **(78)** from *Humulus lupulus* has been recently reported to possess the potential to prevent neurodegeneration as indicated by its ability to induce Nrf2 activation in PC12 (rat neuronal cells). This capacity is thought to be due to the presence of α and β unsaturated site in xanthohumol (Yao, 2015).

In conclusion, of the research reported here it is distinguished that chalcone DMU-1122 was non-toxic up to 20 μM in both cell lines. In addition DMU-2210, 1122, 1103 and 2265 have increased the level of NQO1 protein in both cell lines at 24 h.

There may be some possible limitations in Western blotting assay:

1- Despite using Bradford assay to quantify the amount of protein, sometimes the blotting results specially beta-actin (house-keeping) showed unquantifiable results.
2- Using stripping buffer to indicate another protein could remove all the proteins, which lead to lose the blot.
3- Moreover, using several steps like preparing sample, gel, buffer, blotting, blocking and detecting lead to inferior imaging.

Chapter 5 **Investigation into the chemopreventive capacity of chalcones to prevent malondialdehyde toxicity**

5.1 Introduction:

MDA is the product of lipid peroxidation, and it has been used as a biomarker of lung injuries (Kodavanti, 2014). Data from several sources have identified increased levels of MDA to be associated with different lung disease. For instance, increased MDA levels are found in lung and breast cancer patients (Gönenç *et al.*, 2001). In addition, it is also found to be increased in smokers, and individuals who suffer from the chronic obstructive pulmonary disorder, asthma, and bronchiectasis (Bartoli *et al.*, 2011; Waseem *et al.*, 2012).

Previous studies have considered the effect of natural or synthetic compounds as chemoprevention agents against MDA associated toxicity. Turgut *et al.* (2016) investigated the chemoprotective effect of naringin **(79)** in rats, and report that naringin can reduce the levels of MDA following bleomycin exposure. Moreover, MDA levels were also reduced in rats treated with chemopreventive agent 18β-glycyrrhetinic acid **(80)** following treatment with MDA inducing monocrotaline (Zhang *et al.*, 2019). MRC-5 and MRC-5 SV2 cell lines have used to examine the mutagenic effect of MDA using MRC-5 and MRC-5 SV2 (Yates *et al.*, 2019). Moreover, the MRC-5 cell line has used to investigate the chemopreventive effect of laminarin **(11)** and *Ribes nigrum L* against H_2O_2 (Liu *et al.*, 2017; Luo *et al.*, 2018).

Researchers have extracted MDA from different sources such as urine, plasma, amniotic fluid, wound secretions and tissue samples (Khoschsorur *et al.*, 2000), Different methods have been used to determine the level of MDA such as thiobarbituric acid reactive substances (TBARS) assay (Atasayar *et al.,* 2004), high performance liquid chromatography (HPLC) (Seljeskog *et al.*, 2006), gas chromatography/mass spectrometry (GC/MS), GC/MS/MS and liquid chromatography/mass spectrometry (LC/MS/MS) for accurate results (Ito *et al.*, 2019). For example, MDA-DNA adduct 8-

oxo-guanine can be detected by HPLC methods (Helbock *et al.*, 1998), M_1dG and M_1dA detect by GC/MS or LC/MS/MS (Hakala *et al.*, 1999; Marnett, 1999).

The TBARS assay, which was used in this project to determine the MDA concentrations, is the most common assay use to determine the lipid peroxidation products like MDA (Wheatley, 2000). In these assay, MDA can react with two thiobarbituric acid (TBA) under low pH and high temperature to generate a red coloured TBA_2-MDA adduct (Scheme 12) (Janero, 1990; Onyango and Baba, 2010). That can be measured by spectrophotometrically OD_{532} nm, or fluorimetrically ($\lambda_{exc\,532}$ nm and λ_{em553} nm). TBAR test is commonly used due to rapid and low-cost (Ito *et al.*, 2019).

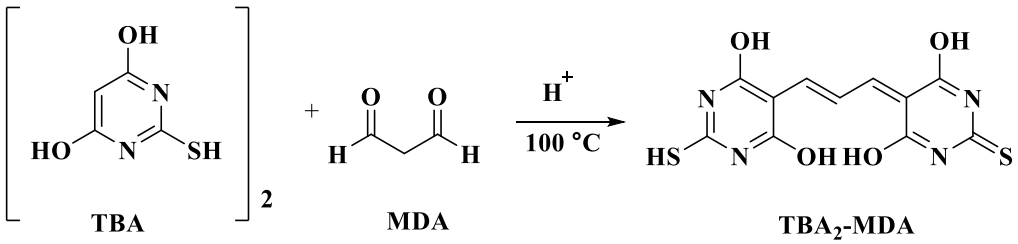

Scheme 12 Reaction of 2TBA with MDA to generate TBA_2-MDA, adapted from Atasayar *et al.* (2004)

5.1.1 The aims and objectives of this chapter:

One of the lipid peroxidation products that can induce lung cancer due to smoking cigarettes is MDA. To prevent the toxicity of MDA, the ability of the twelve selected chalcones were consequently investigated in MRC-5 and MRC-5SV2 lung cell lines. An initial study was thus conducted to determine the maximal concentration of each chalcone that could be used as pre-treatment before significant toxicity occurred. For that reason, the aims of this chapter are finding the range of MDA concentrations that have different toxicity levels and investigating if the pre-treated with the non-toxic concentration of chalcone can decrease the toxicity effect of MDA comparing with MDA alone. In consideration of the previous results, the objectives of this section were to investigate

1- Synthesis of MDA and determine the concentrations comparing with standard curve using TBARS assay.

2- The toxicity effect of MDA in different concentrations (rage of concentrations that were not kill all the cells) on two types of the lung cell line (MRC-5 and MRC-5 SV2) using MTT assay.

3- The ability of selected chalcones to prevent MDA toxicity in MRC-5 and MRC-5 SV2 cell lines using MTT assay.

5.2 Result and discussion

5.2.1 MDA standard

To confirm the MDA concentration, a TBARS assay has been assessed. The R^2 value of linear regression was 0.99 that indicated excellent linearity (Figure **5.1**).

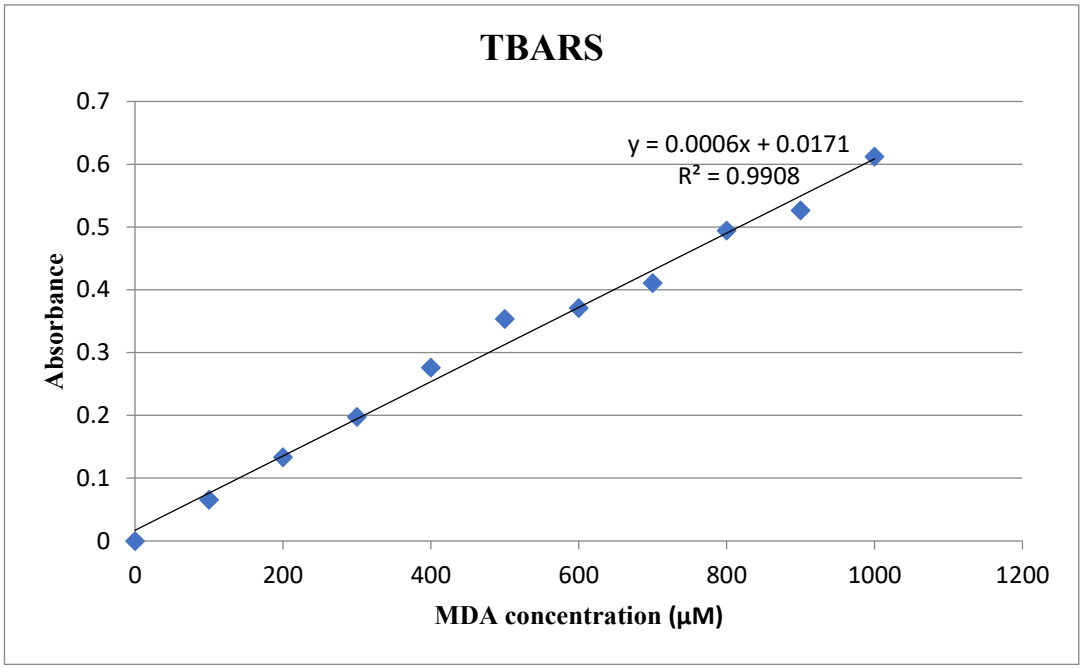

Figure 5.1 Standard curve of MDA (0-1000 µM) measured by a TBARS assay, at OD_{532} nm absorbance measured.

TBARS assay, have been commonly used due to quick and potent reaction (Ghani *et al.*, 2017). Several studies have used TBARS assay to determine lipid peroxidation products especially MDA in tissue (Qebesy *et al.*, 2015) plasma (Ramezani *et al.*, 2010) and cell culture (Hu *et al.*, 2019). In addition, the reaction between TBA and MDA under high temperature illustrate a red/pink colour.

5.2.2 Effect MDA on MRC-5 and MRC-5 SV2 cell viability

Figure **5.2** shows that MDA at the concentration of 100 µM was non-toxic in MCRC-5 and 50 µM in MRC-5 SV2. In addition, MDA illustrates significant toxicity by decreasing the cellular viability with increasing the MDA concentrations in both cell lines. These results are in agreement with earlier work by Yates (2015) which demonstrates that 100 µM MDA was more toxic on MRC-5 SV2 cell than MRC-5.

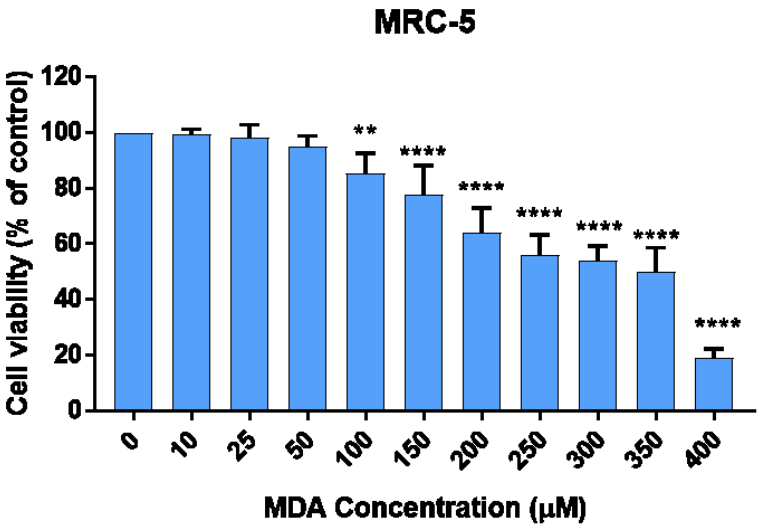

A

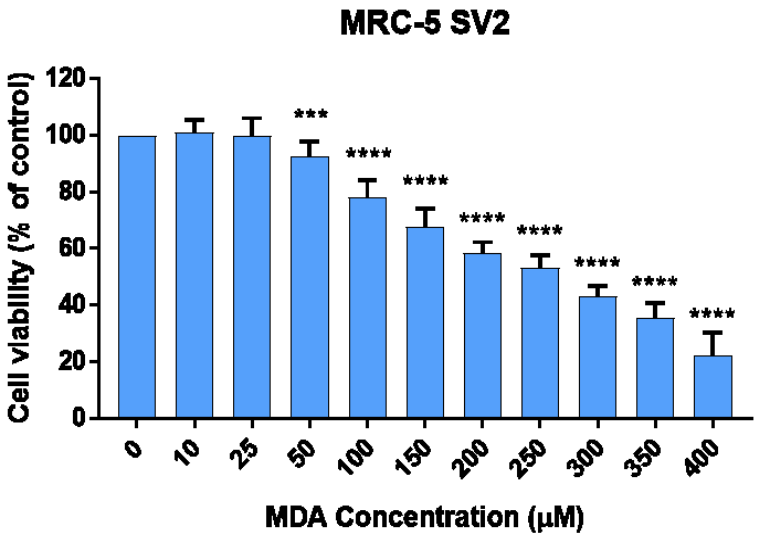

B

Figure 5.2 MRC-5 (A) and MRC-5 SV2 (B) cells were exposed to MDA for 24 h after which cell viability was determined using the MTT assay. Data are presented mean ± SD. (n=3), * for $p<0.05$, ** for $p<0.01$, *** for $p<0.001$ and **** for $p<0.0001$ significant compared to control

5.2.3 The protective effect of chalcones against MDA

Depending on the fold induction of luciferase in AREc32 reporter cell line that was used as an indicator of inducing Nrf2 signalling pathway, which was measured by luciferase assay (Section 3.6). Twelve chalcones out of thirty-one have induced luciferase at two fold induction or more, thus have been chosen to examine the potential effect of them to prevent MDA toxicity. Prevention of MDA induced cytotoxicity was investigated in MRC-5 and MRC-5 SV2 cell lines, using the previously determined non-toxic concentration of chalcones (Section 4.2.2).

The MRC-5 results show that DMU-1113 (Figure **5.3**), DMU-2265 (Figure **5.4**), DMU-2210 (Figure **5.5**), DMU-2267 (Figure **5.6**), DMU-1103 (Figure **5.7**), DMU-1122 (Figure **5.8**), and DMU-1119 (Figure **5.9**) have reduced MDA toxicity significantly, as well as they can increase the IC_{50} as shown in Table 16. However, DMU-1112 (Figure **5.10**), DMU-411 (Figure **5.11**), DMU-2207 (Figure **5.12**), DMU-2219 (Figure **5.13**) and DMU-192 (Figure **5.14**) have not reduced MDA toxicity. The MRC-5 SV2 results show that DMU-1113 (Figure **5.3**), DMU-2267 (Figure **5.6**), DMU-1103 (Figure **5.7**), DMU-1122 (Figure **5.8**) and DMU-1119 (Figure **5.9**) have decreased cell viability in presence of MDA significantly, as well as decrease the IC_{50} as shown in Table 16. Meanwhile, DMU-2265 (Figure **5.4**), DMU-2210 (Figure **5.5**), DMU-1112 (Figure **5.10**), DMU-411 (Figure **5.11**), DMU-2207 (Figure **5.12**), DMU-2219 (Figure **5.13**) and DMU-192 (Figure **5.14**) have not shown significant difference to MDA treatment.

1- DMU-1113

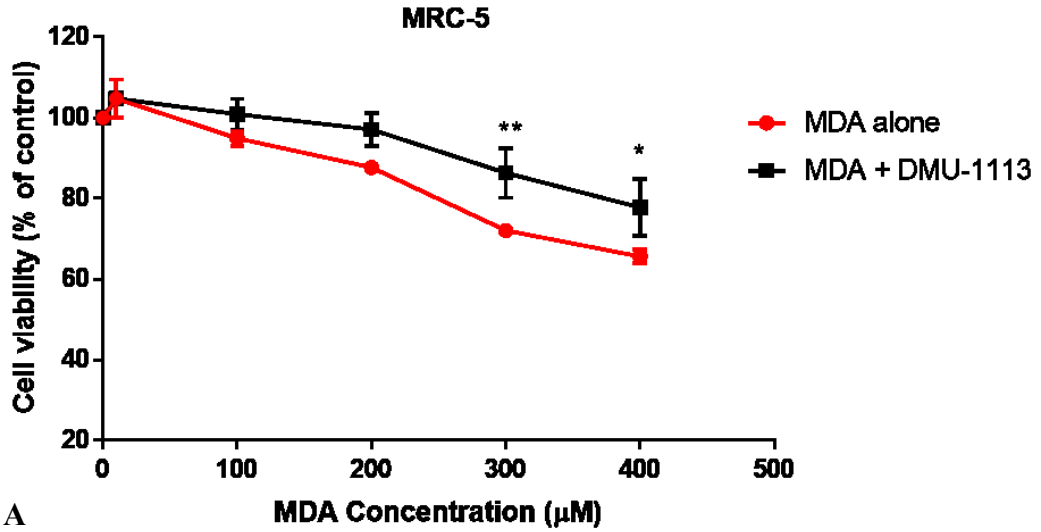

A

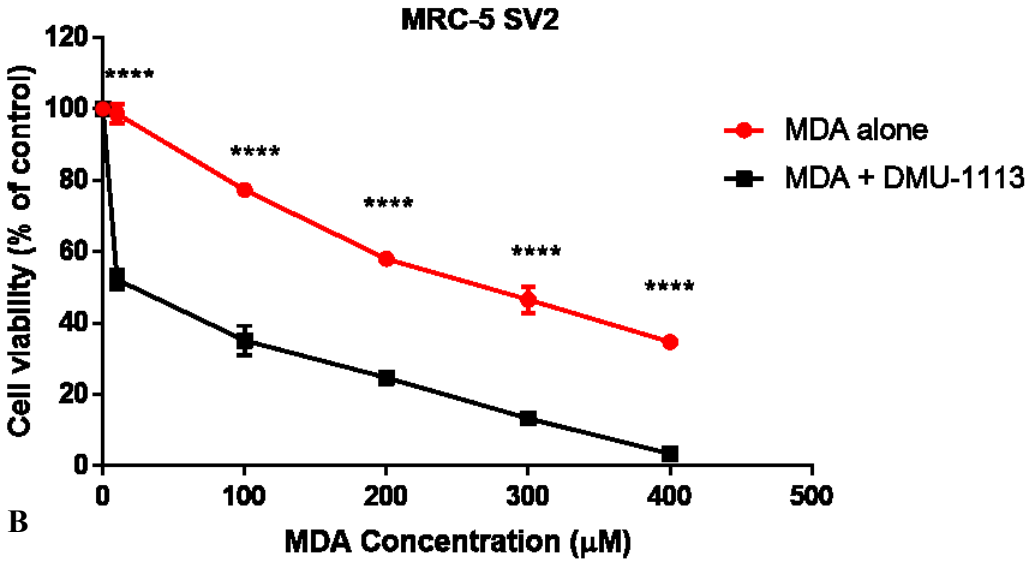

B

Figure 5.3 (A) MRC-5 and (B) MRC-5 SV2 were pretreated with chalcone DMU-1113 for 24 h then exposed to MDA for 24 h after which cell viability was determined using the MTT assay. Data are presented as mean ± SD. (n=3), * for $p<0.05$, ** for $p<0.01$ and **** for $p<0.0001$ significant compared to MDA as a control

2- DMU-2265

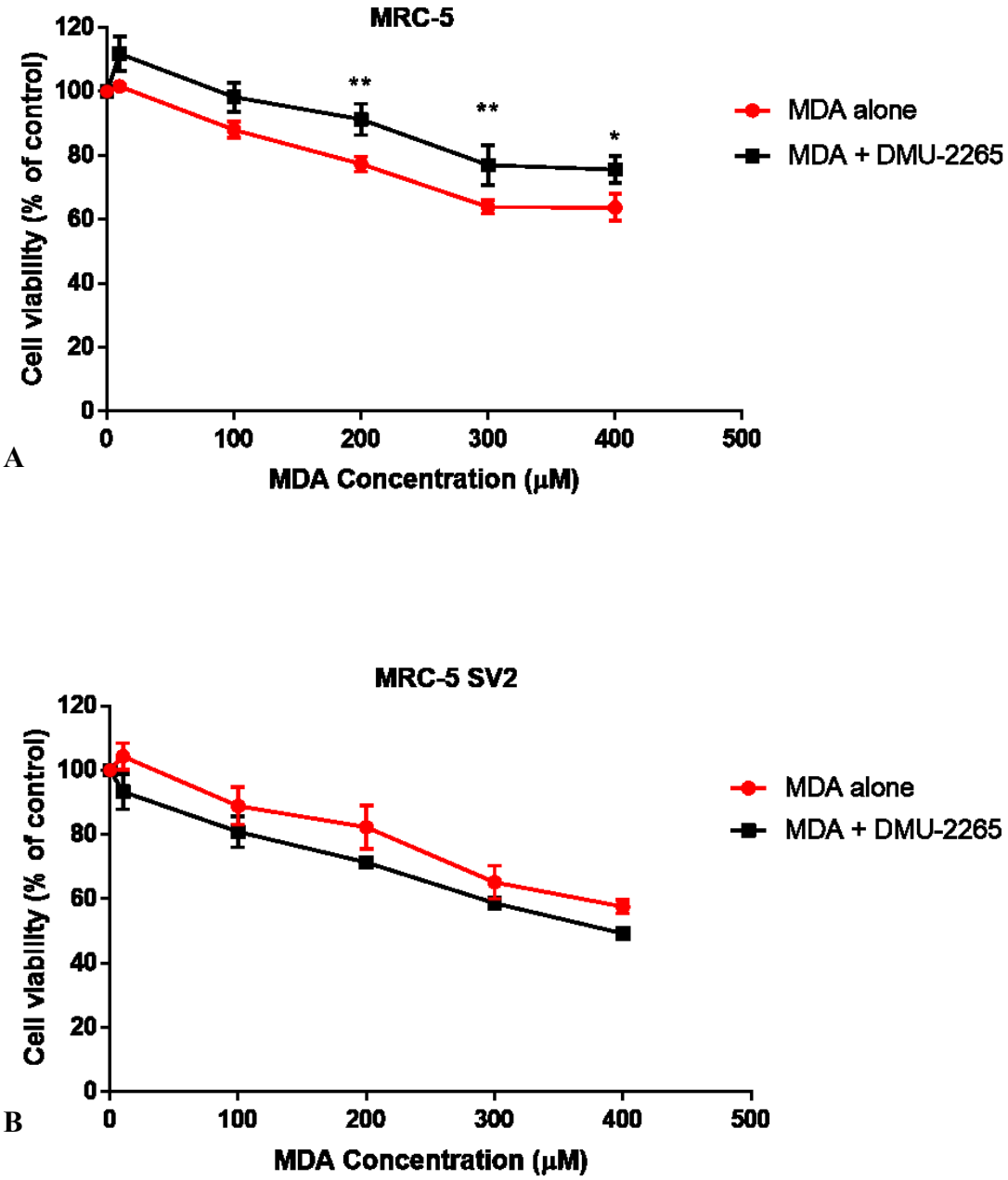

Figure 5.4 (A) MRC-5 and (B) MRC-5 SV2 were pretreated with chalcone DMU-2265 for 24 h then exposed to MDA for 24 h after which cell viability was determined using the MTT assay. Data are presented as mean ± SD. (n=3), * for $p<0.05$, ** for $p<0.01$, significant compared to MDA as a control

3- DMU-2210

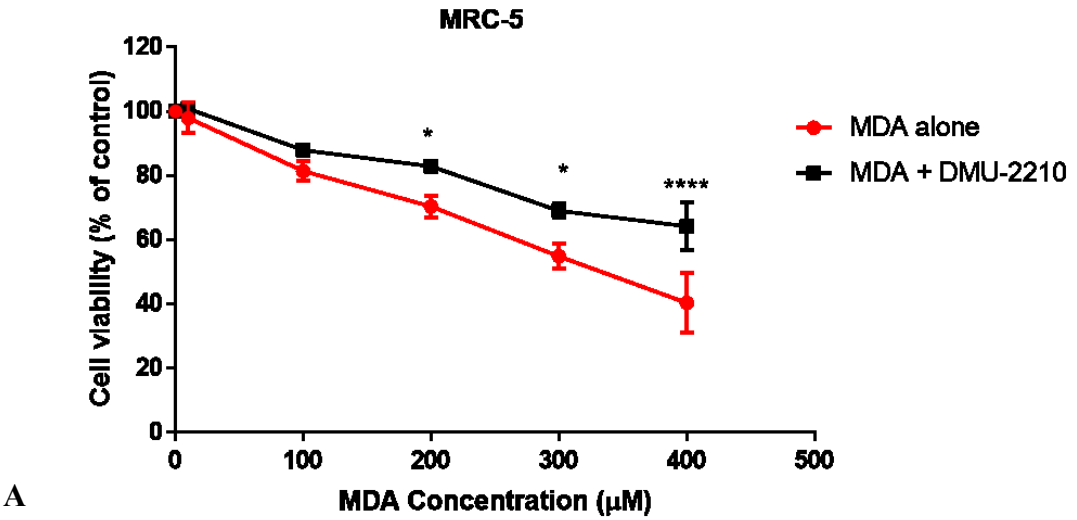

A

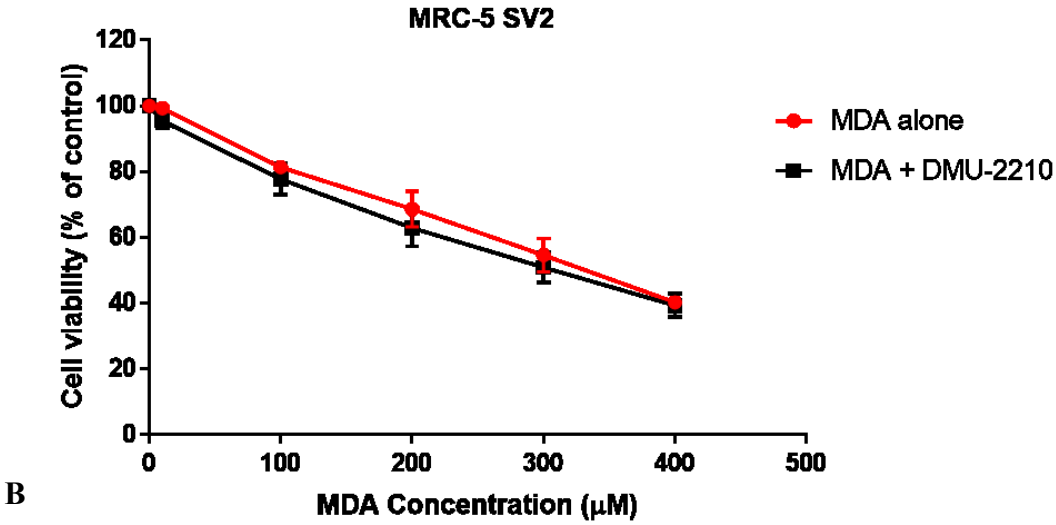

B

Figure 5.5 (A) MRC-5 and (B) MRC-5 SV2 were pretreated with chalcone DMU-2210 for 24 hours then exposed to MDA for 24 hours after which cell viability was determined using the MTT assay. Data are presented as mean ± SD. (n=3), * for $p<0.05$, and **** for $p<0.0001$ significant compared to MDA as a control

4- DMU-2267

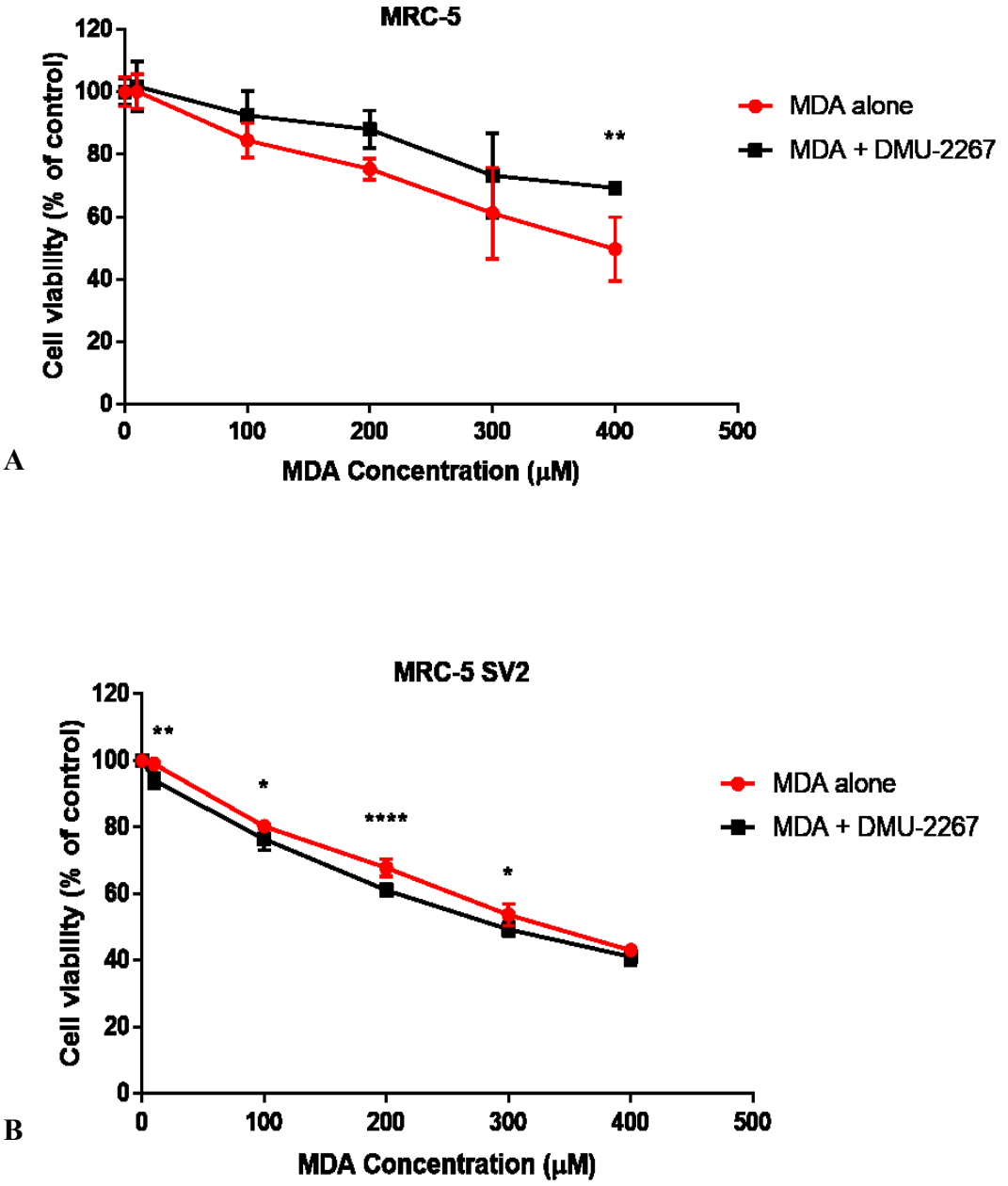

Figure 5.6 (A) MRC-5 and (B) MRC-5 SV2 were pretreated with chalcone DMU-2267 for 24 h then exposed to MDA for 24 h after which cell viability was determined using the MTT assay. Data are presented as mean ± SD. (n=3), * for $p<0.05$, ** for $p<0.01$, and **** for $p<0.0001$ significant compared to MDA as a control

5- DMU-1103

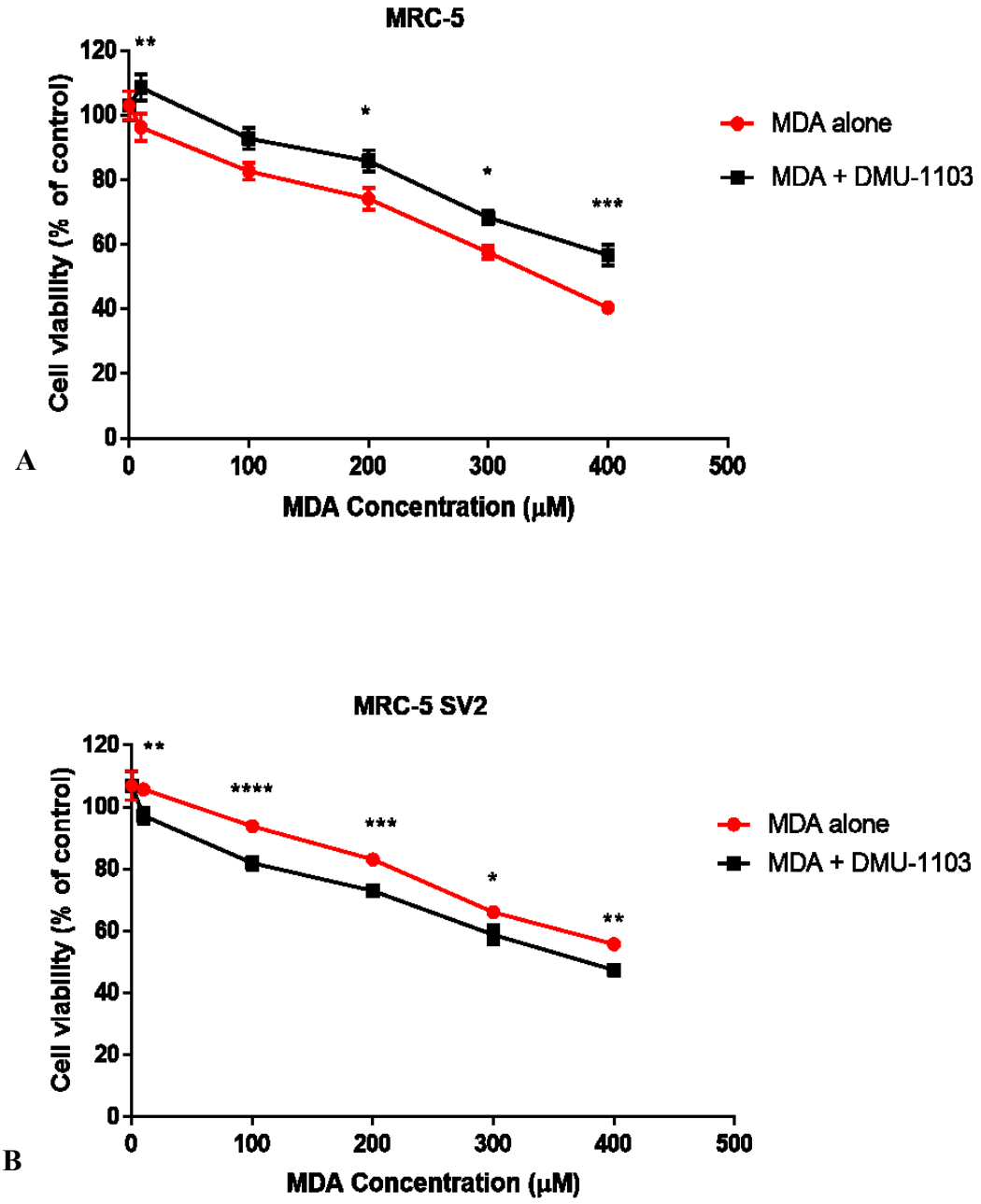

Figure 5.7 (A) MRC-5 and (B) MRC-5 SV2 were pretreated with chalcone DMU-1103 for 24 h then exposed to MDA for 24 h after which cell viability was determined using the MTT assay. Data are presented as mean ± SD. (n=3), * for $p<0.05$, ** for $p<0.01$, *** for $p<0.001$ and **** for $p<0.0001$ significant compared to MDA as a control

6- DMU-1122

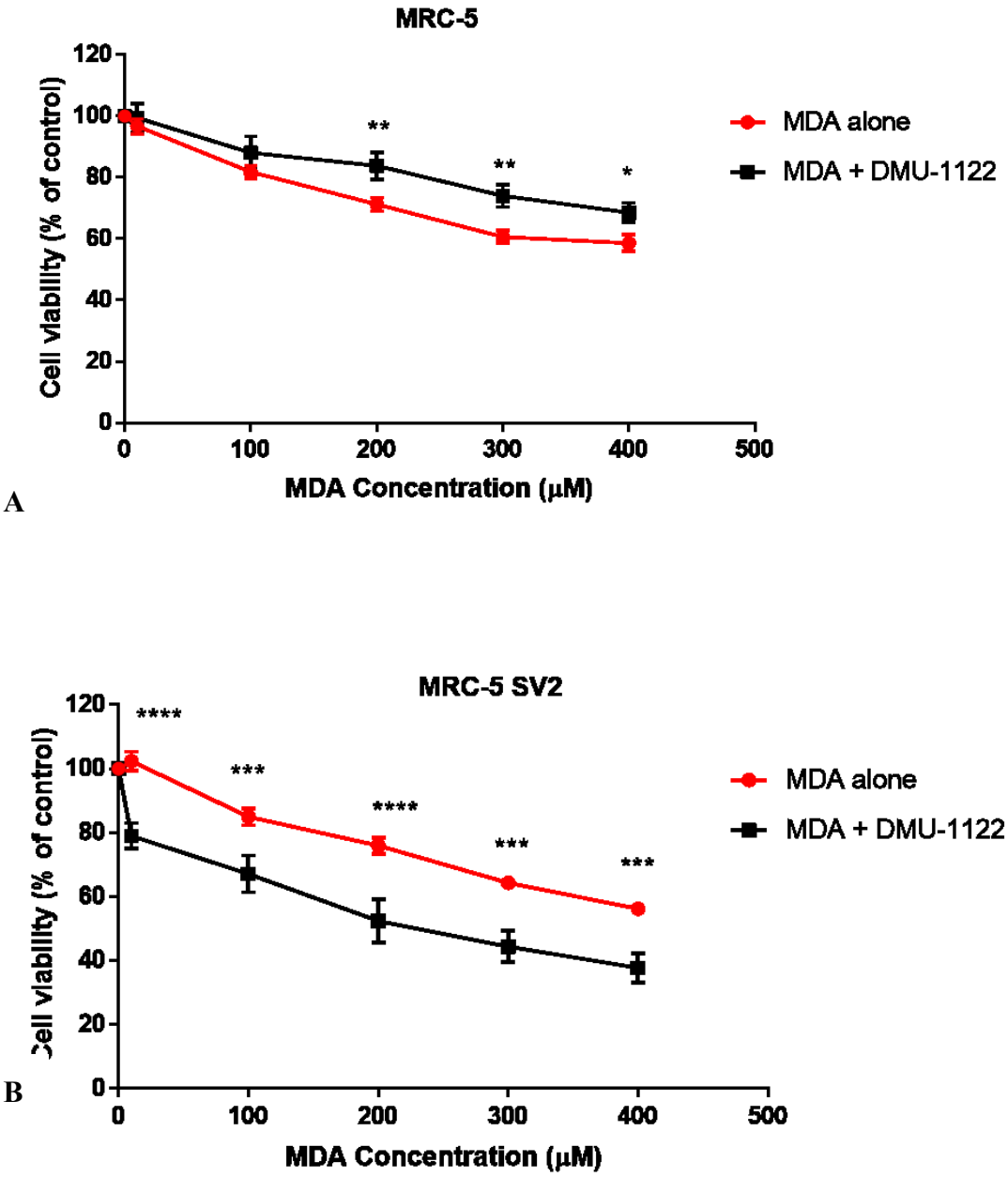

Figure 5.8 MRC-5 (A) and MRC-5 SV2 (B) were pretreated with chalcone DMU-1122 for 24 h then exposed to MDA for 24 h after which cell viability was determined using the MTT assay. Data are presented as mean ± SD. (n=3), * for $p<0.05$, ** for $p<0.01$, *** for $p<0.001$ and **** for $p<0.0001$ significant compared to MDA as a control

7- **DMU-1119**

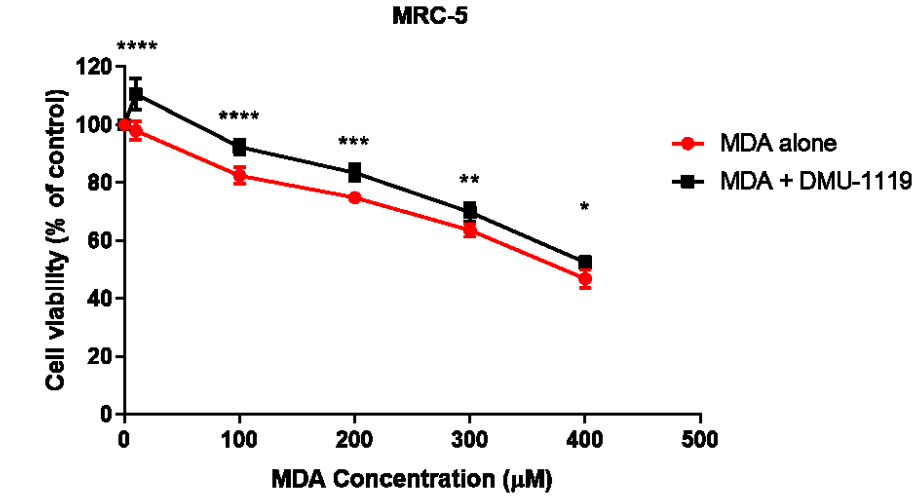

A

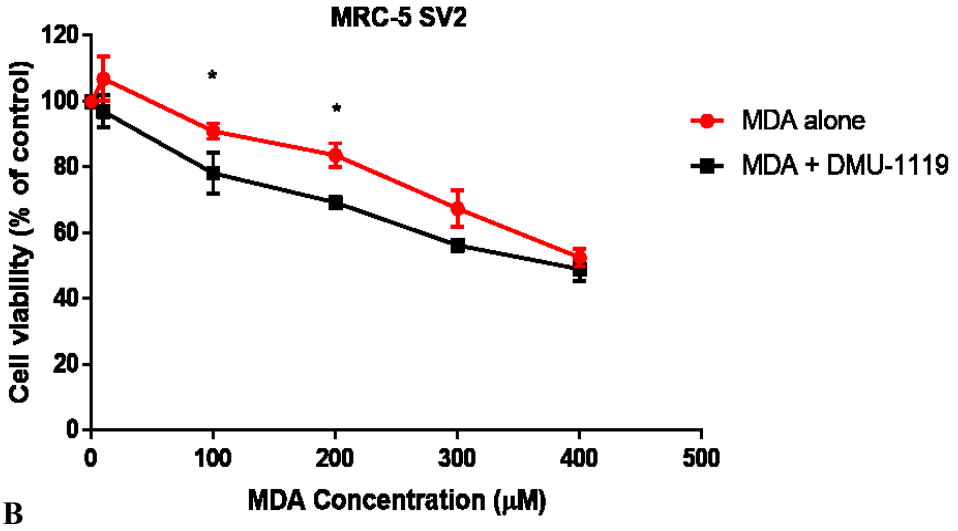

B

Figure 5.9 (A) MRC-5 and (B) MRC-5 SV2 were pretreated with chalcone DMU-1119 for 24 h then exposed to MDA for 24 h after which cell viability was determined using the MTT assay. Data are presented as mean ± SD. (n=3), * for $p<0.05$, ** for $p<0.01$, *** for $p<0.001$ and **** for $p<0.0001$ significant compared to MDA as a control

8- DMU-1112

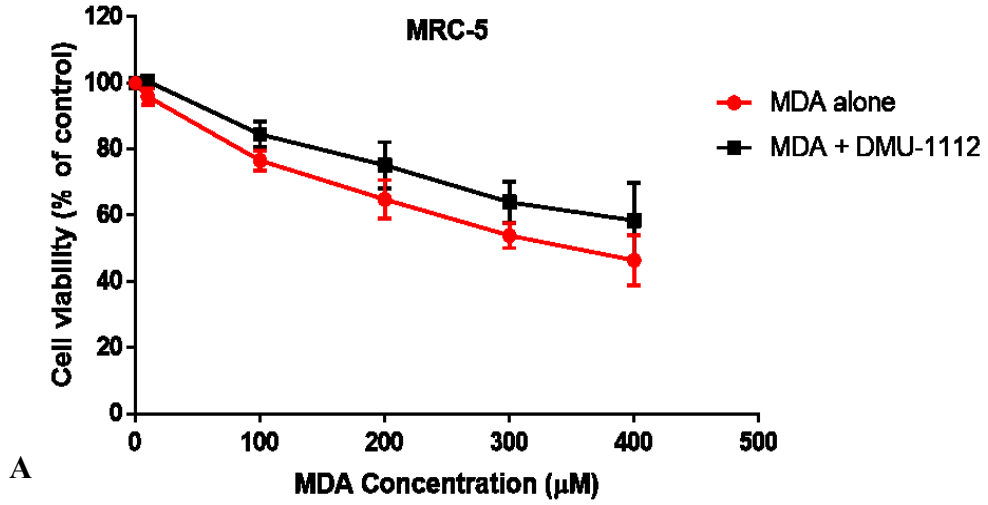

A

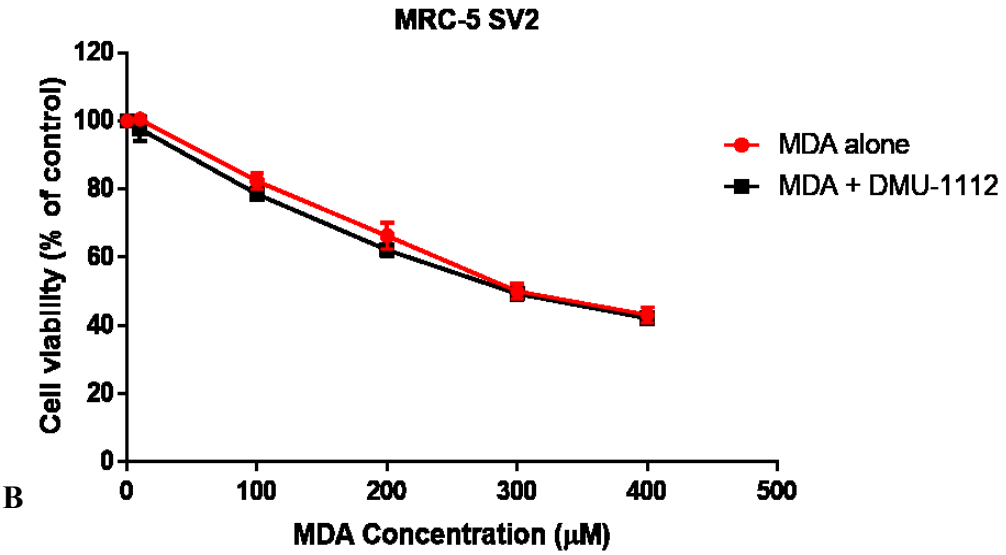

B

Figure 5.10 (A) MRC-5 and (B) MRC-5 SV2 were pretreated with chalcone DMU-1112 for 24 h then exposed to MDA for 24 h after which cell viability was determined using the MTT assay. Data are presented as mean ± SD. (n=3), compared to MDA as a control

9- DMU-411

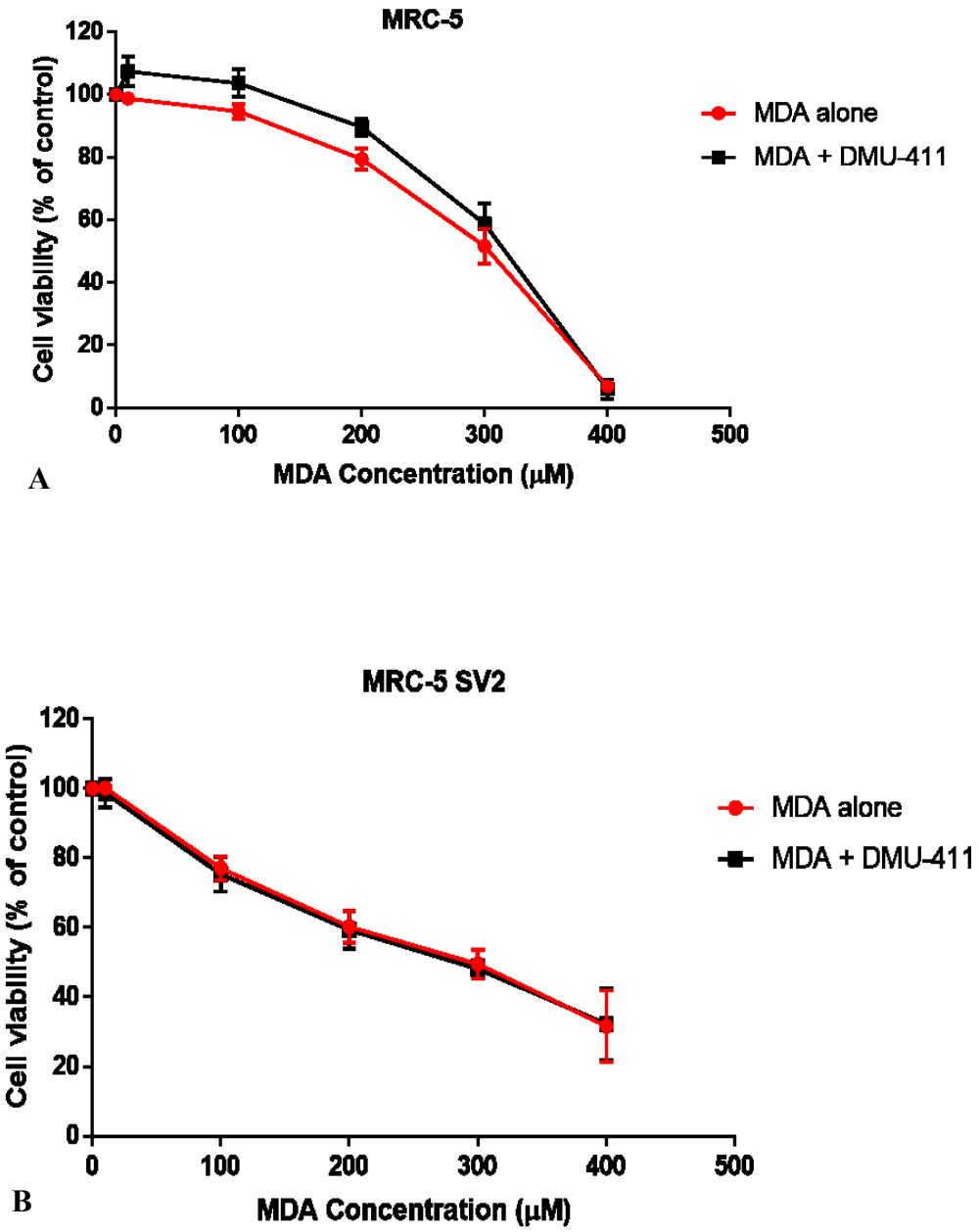

Figure 5.11 (A) MRC-5 and (B) MRC-5 SV2 were pretreated with chalcone DMU-411 for 24 h then exposed to MDA for 24 h after which cell viability was determined using the MTT assay. Data are presented as mean ± SD. (n=3), compared to MDA as a control

10- DMU-2207

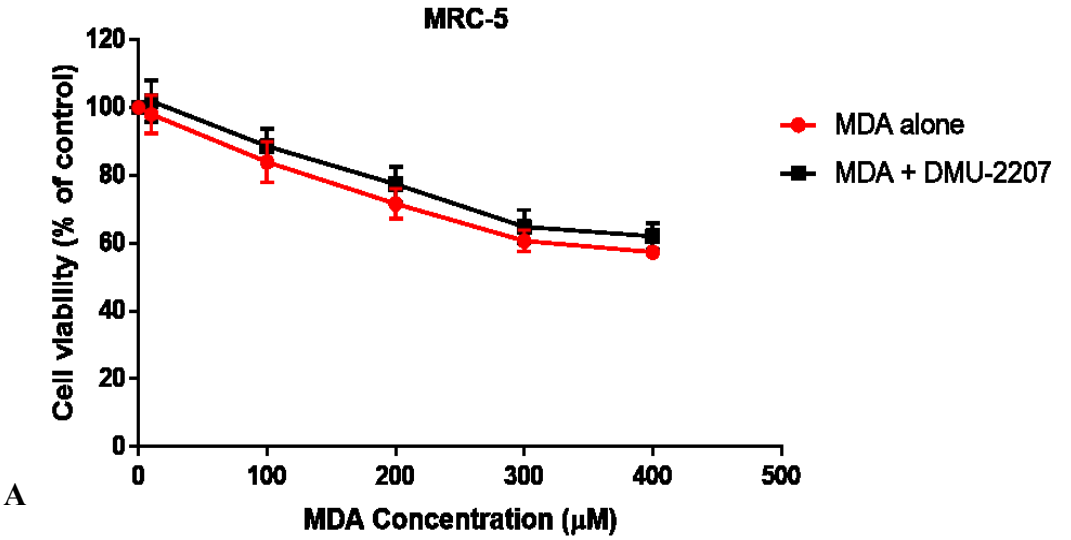

A

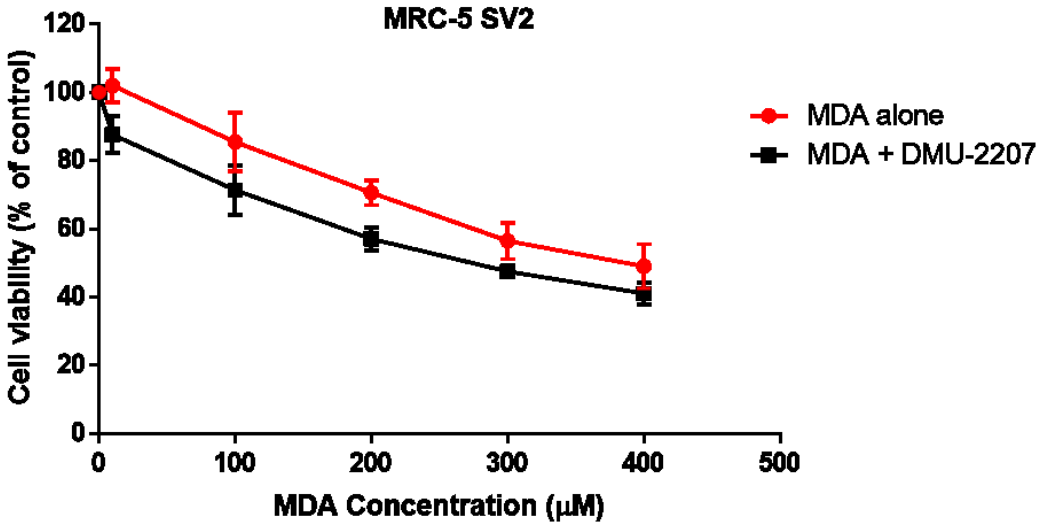

B

Figure 5.12 (A) MRC-5 and (B) MRC-5 SV2 were pretreated with chalcone DMU-2207 for 24 h than exposed to MDA for 24 h after which cell viability was determined using the MTT assay. Data are presented as mean ± SD. (n=3), compared to MDA as a control

11- DMU-2219

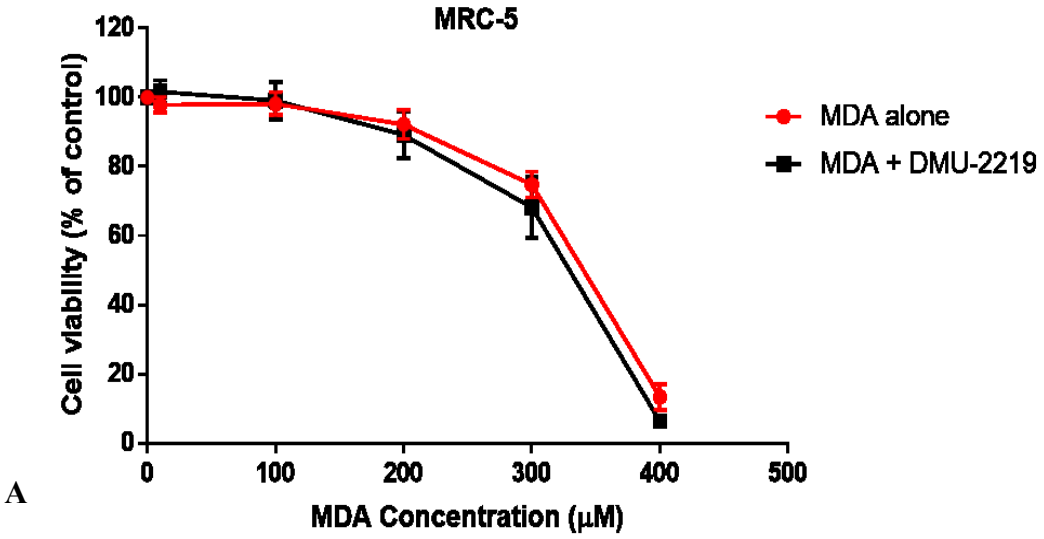

A

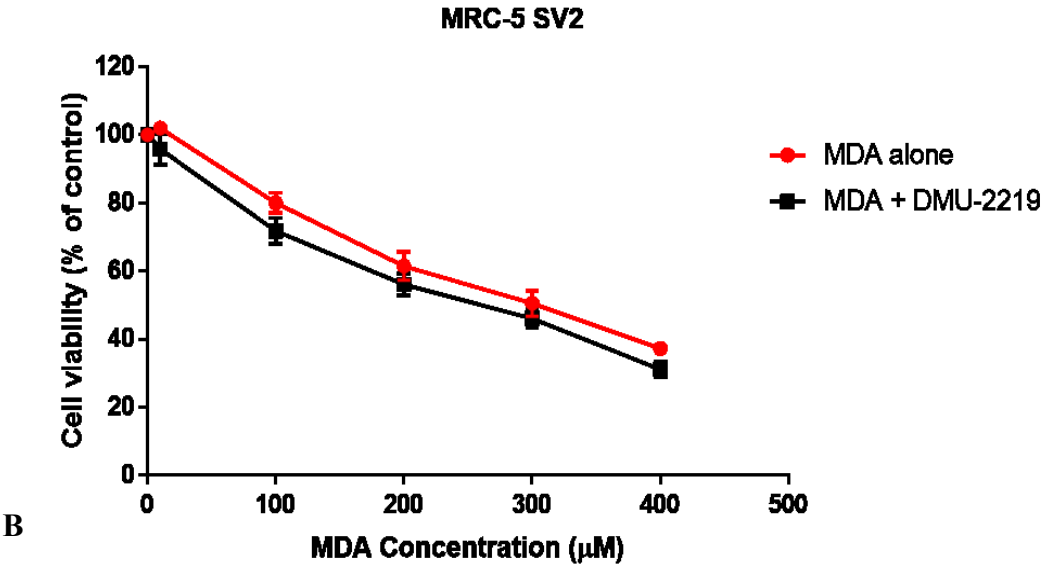

B

Figure 5.13 (A) MRC-5 and (B) MRC-5 SV2 were pretreated with chalcone DMU-2219 for 24 h then exposed to MDA for 24 h after which cell viability was determined using the MTT assay. Data are presented as mean ± SD. (n=3), compared to MDA as a control

12- DMU-192

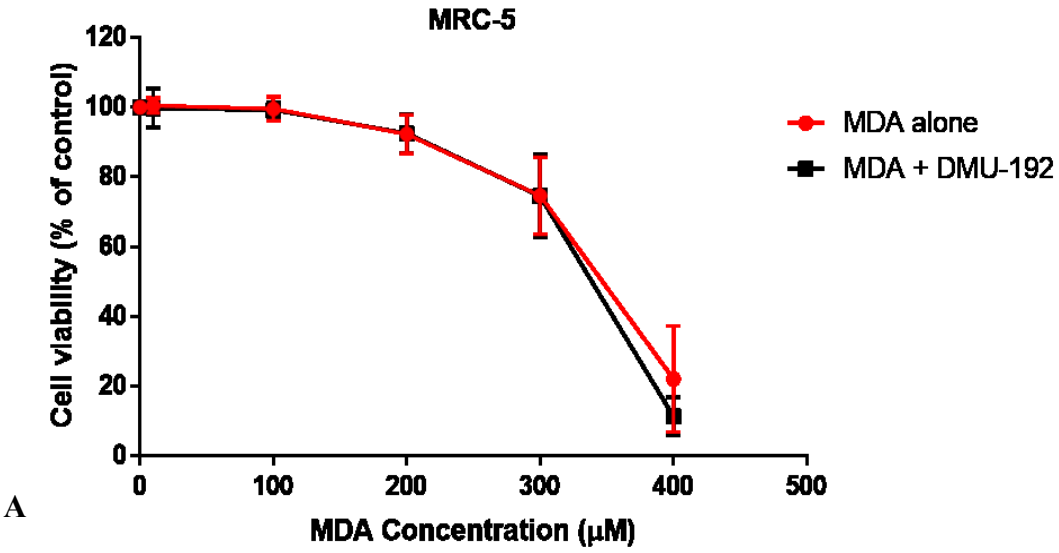

A

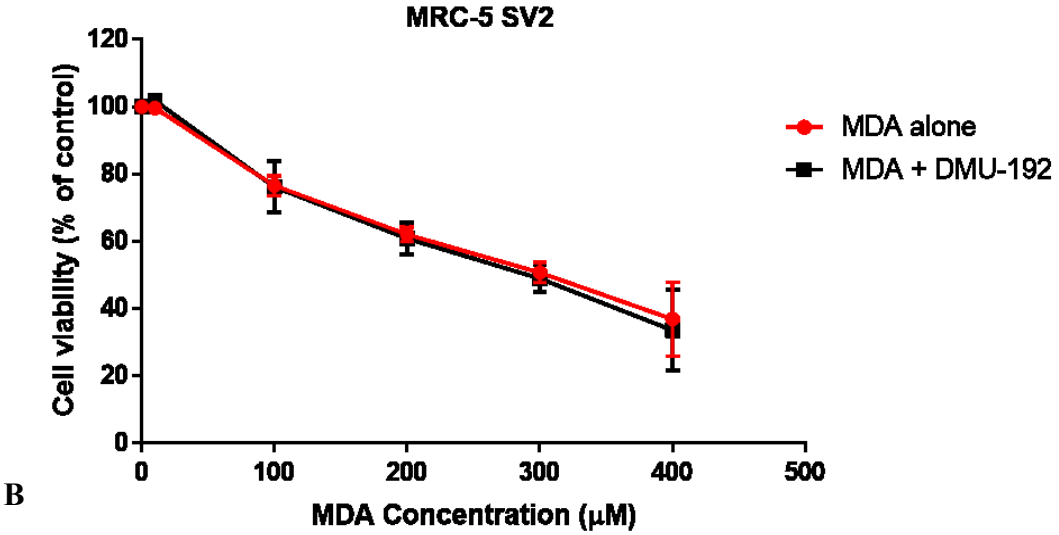

B

Figure 5.14 (A) MRC-5 and (B) MRC-5 SV2 were pretreated with chalcone DMU-192 for 24 h then exposed to MDA for 24 h after which cell viability was determined using the MTT assay. Data are presented as mean ± SD. (n=3), compared to MDA as a control

Table 16. The effect of selected chalcones on MDA induced toxicity in MRC-5 and MRC-5 SV2 cell lines.

Chalcone	MRC-5 (IC_{50})			MRC-5 SV2 (IC_{50})		
	MDA only	Chalcone + MDA	% change in IC_{50}	MDA only	Chalcone + MDA	% change in IC_{50}
DMU-1113	904.1	1978	+119 %	264.8	25.74	-90 %
DMU-2265	641.6	1331	+107 %	637	426.1	-33 %
DMU-2210	365.4	748.7	+105 %	357.4	307.6	-14 %
DMU-2267	480.5	975.1	+103 %	358.8	298.4	-17 %
DMU-1103	396.8	710.6	+79 %	658.6	431.2	-35 %
DMU-1122	501.4	885.1	+77 %	555.1	220.3	-60 %
DMU-1112	349.7	561.7	+61 %	343.9	312.2	-9 %
DMU-1119	466.2	659.3	+41 %	629.5	396.1	-37 %
DMU-411	300.2	376.8	+26 %	271	261.7	-3 %
DMU-2207	504.9	637.5	+26 %	430.7	264.6	-39 %
DMU-2219	471.4	399.4	+15 %	303	235.2	-22 %
DMU-192	529.5	465.5	+12 %	295.1	275.5	-7 %

MDA has been commonly used as a model carcinogen due to its toxicity and reactivity, it is also used as a biomarker of lipid peroxidation. Additionally, a considerable amount of literature has been published in the correlation between MDA and lung diseases. Therefore, one purpose of this study was to assess the potential of twelve chalcones to prevent MDA-induced toxicity in matched non-transformed (MRC-5) and transformed (MRC-5 SV2).

A one-way ANOVA reveals that there is a significant difference in cell viability between MDA alone and MDA pretreated with chalcones in both the cell lines but in different ways. In normal cells, the MRC-5 results showed that DMU-1113 (Figure **5.3**), DMU-2265 (Figure **5.4**), DMU-2210 (Figure **5.5**), DMU-2267 (Figure **5.6**), DMU-1103 (Figure **5.7**), DMU-1122 (Figure **5.8**), and DMU-1119 (Figure **5.9**) protected MRC-5 from MDA toxicity, as well as they were increased the IC_{50} as shown in Table 16.

Interestingly, in cancer cells, the MRC-5 SV2 results showed that DMU-1113 (Figure **5.3**), DMU-1122 (Figure **5.8**), DMU-2207 (Figure **5.12**) DMU-1119 (Figure **5.9**), DMU-1103 (Figure **5.7**) and DMU-2265 (Figure **5.4**) have chemopreventive activity. They showed growth inhibitory activity through decrease in cell viability in the presence of MDA, as well as decreased in the $IC_{50,}$ as shown in Table 16.

Several researchers have investigated chalcones as chemopreventive agents. Su (2011) found that 2′,4′-dihydroxy-6′-methoxy-3′,5′-dimethylchalcone **(81)** has the ability to prevent PC12 cells from H_2O_2-induced oxidative stress by reducing apoptosis. Moreover, *trans*-chalcone **(25)** has been reported as a protective agent on HepG2 (hepatocellular carcinoma) cell viability due to a decrease in lipid peroxidation production (Sikander, 2011).

Another group have reported that flavonoids can reduce lipid peroxidation in rat liver microsomes and have attributed the protective effect due to the presence of *α,β*-unsaturated sites in conjunction with a 4-keto function, which leads to stabilised the compounds through transferring electron and/or hydrogen (Popoola, 2015).

Zhao (2017) has reported that indolyl derivative chalcone can inhibit cancer growth activity through inducing Nrf2 and increasing cell apoptosis on A549 cells (lung carcinoma). Literature reveals that cellular proliferation has inhibited by different type of chalcones such as cyclohexenyl chalcones nicolaioidesin C **(82)** and panduratin A **(83)** on PC-3 human prostate cancer cells (Deb Majumdar, 2011), chalcones (E)-2-(4′-methoxybenzylidene)-1-benzosuberone **(84)** and (E)-2-(2′,4′-dimethoxybenzylidene)-1-tetralone **(85)** on Caco-2 cells (Kello *et al.*, 2016), para hydroxy meta methoxy chalcone **(86)** on T47 D (breast cancer cells) (Arianingrum *et al.*, 2016). Additionally, chalcone flavokawain B **(33)** has inhibited HSC-3 cell viability by inducing apoptosis and attributed that to upregulation of HO-1/Nrf2 (Hseu *et al.*, 2012). Echoing this finding the following chapter will now go on an investigate the cellular mechanism responsible for the protection provided from MDA toxicity by selected chalcones.

In conclusion, the results of this investigation showed that DMU-1113 (3,4,5,4′-OMe), 2265 (3,4-OCH_2O, 2′-OMe), 2210 (3,4,3′,4′-OMe), 2267 (2,4,2′,4′-OMe), 1103 (2,4-OMe, 3′,4′-OCH2O) and 1122 (4-OEt, 2′,4′-OMe) can increase cell prevention from the toxicity effect of MDA by increasing the IC_{50} in MRC-5. Whereas, DMU-1113 (3,4,5,4′-OMe), and 1122 (4-OEt, 2′,4′-OMe) have cell growth inhibition in the presence of MDA by decreasing in the IC_{50} in MRC-5 SV2, which means thus chalcones have a cytoprotective effect on normal cell and cytotoxic effect in transformed cells.

As with the majority of studies, the design of the current chapter is subject to limitations.

1- The limitation of MDA assay like preparing MDA or TBARS is related to preparation time and temperature that may reduce the linearity due to change the concentrations.
2- MDA are not a stable product, so it might be change during the incubation time.

Chapter 6 **Protective Effect of chalcones against DNA damage induced by MDA**

6.1 Introduction

DNA damage has the potential to occur through many mechanisms such as via endogenous toxic aldehydes (MDA) induced by endogenous sources such as ROS and lipid peroxides, originating from exogenous sources such as air pollution or diet (Gupta and Lutz, 1999; Ahmed Laskar and Younus, 2019). The most beneficial way to prevent cancer is to prevent DNA damage either through promoting the phase II enzymes (see the previous chapter) or by scavenging ROS (current chapter) (Rupasinghe *et al.*, 2014).

6.1.1 Reactive oxygen species (ROS)

It is known that ROS are an intracellular product with an important role in oxidising lipids, proteins, also damaging DNA and RNA (Wu and Yotnda, 2011). ROS generated by lipid hydroperoxide (LOOH), can be detect at λ_{exc}=488 nm and λ_{em}525 nm , through different methods such as spectrophotometry, electron spin resonance and fluorescent probes like dichlorofluorescein (DCF), which is the product of the oxidation of 2′,7′-dichlorofluorescin ($DCFH_2$) in the presence of intracellular ferrous iron (Fe^{2+}) (Scheme 13) (Girard-Lalancette *et al.*, 2009; Carniel *et al.*, 2015; Hseu *et al.*, 2017; Zhang *et al.*, 2018). This assays allows the determination of intracellular ROS levels and hence also the ability of chalcones to induce cell defence mechanism (via Nrf2 induction).

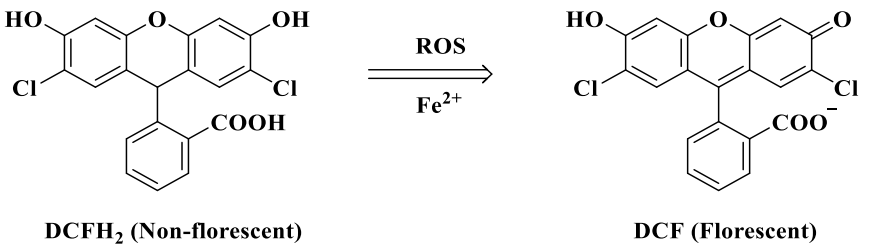

Scheme 13 The mechanism of conversion $DCFH_2$ (Non-florescent) to DCF (Florescent) product, adapted from Girard-Lalancette *et al.* (2009)

6.1.2 Single cell gel electrophoresis (Comet) assay

Various alkaline assays like unwinding, elution, and sucrose gradient sedimentation, are in use to measure overall DNA damage in the whole sample. However, single-cell gel electrophoresis, also known as comet assay, can be used to determine the DNA damage in an individual cell (Azqueta and Collins, 2006). Comet assay is one of the sensitive, versatile and simple detection methods of DNA damage. It has used *in vivo* and *in vitro* to detect the DNA double and single-strand damage and repair, DNA lesions and cross-link site to assess genotoxicity, human molecular and biomonitoring epidemiology, ecogenotoxicology, aging, carcinogenesis and to screen novel drugs and cosmetics (Singh *et al.*, 1988; Collins, 2004; Keohavong and Grant, 2005; Azqueta and Collins, 2013; Kyoya, 2018). DNA damage appears as a small nucleoid head and long tail (called a comet). This feature is generated by the relaxation of supercoiled DNA loops strand breaks through being placed in agarose gel, alkaline solution and then being exposed to an electrophoresis, moreover, the amount of DNA damage are indicated by the comet tail intensity due to unwinding loops (Azqueta and Collins, 2006).

6.1.3 The aims and objectives of this chapter

MRC-5 cell line has been chosen to continue the project due to the time and financial situation as well as it is better to look at chemoprevention in the non-cancer cell lines. Moreover, in consideration of the previous results (see previous chapters 4 and 5), three chalcones DMU-1122, 2210 and 1103 have been chosen to proceed further. These chalcones have induced NQO1 at 24 h treatment and have reduced the toxicity of MDA in MRC-5 cells. The induced NQO1 plays an important role in the antioxidant defence system and preventing DNA. Therefore, the aims of this chapter is to investigate the genotoxicity of selective chalcones, as well as the potential of these chalcones to reduce

ROS production and prevent DNA damage induced by MDA. These aims can be investigated by following objectives:

1- Determine the antioxidant effect of chalcone DMU-1122, 2210 and 1103 against MDA oxidative stress in MRC-5 cells, using ROS assay.

2- Scanning the genotoxic effect of chalcone DMU-1122, 2210 and 1103 in MRC-5 cells, using comet assay.

3- To assess the potential of this chalcones to prevent DNA damaged my MDA in MRC-5 cells, using comet assay.

6.2 Results and Discussion

6.2.1 Reactive oxygen species:

Initially, MRC-5 cell line have been pretreated with chalcones for 24 h and then with MDA for another 24 h. This was then treated with DCFH-DA for 30-60 minutes. On the contrary, MDA increases cell death during the incubation and causes change in live cell membrane characteristics. This reduces the cell's dye uptake capacity and results in lower generation of ROS induced by MDA in comparison to the control. Therefore, it has bene decided to use the dye before treating the cells with MDA. Moreover, the DCFH-DA dye has a short lifetime; therefore, in the current sets of experiments, MDA incubation time has been reduced to 4 h instead of 24 h. To determine the antioxidant effect of chalcones on the production of ROS induced by MDA, the MRC-5 cell line has been pretreated with DMU-1122 (Figure **6.1**), 2210 and DMU-1103 (Figure **6.2**) for 24 h, followed by treated with MDA for 4 h.

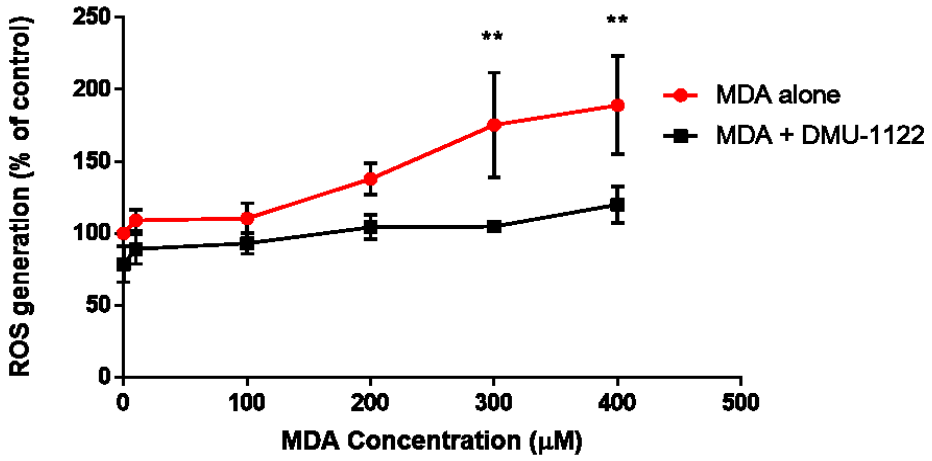

Figure 6.1 Effect of chalcones on intracellular ROS levels. MRC-5 cells were exposed to chalcone DMU-1122 for 24 h, after which MDA was added in the indicated concentrations for 4 h. ROS levels were then determined using the $DCFH_2$ assay. Data are presented mean ± SD. (n=3), * for $p<0.05$ and ** for $p<0.01$ significant compared to control (cells and MDA only) H_2O_2 was used a positive control for ROS generation (data not shown)

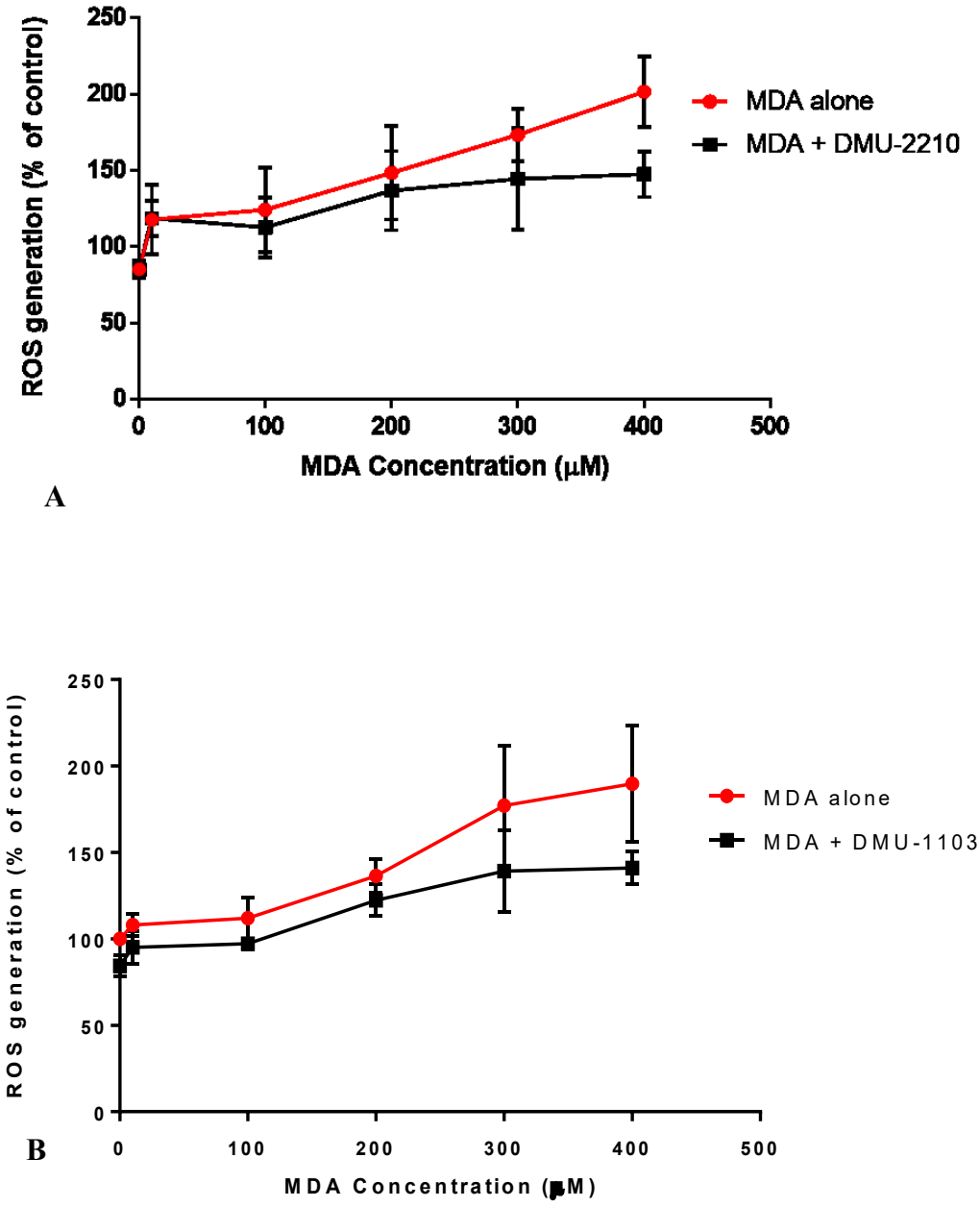

Figure 6.2 Effect of chalcones on intracellular ROS levels. MRC-5 cells were exposed to chalcone (A) DMU-2210 and (B) DMU-1103 for 24 h, after which MDA was added in the indicated concentrations for 4 h. ROS levels were then determined using the $DCFH_2$ assay. Data are presented mean ± SD. (n=3), compared to control (cells and MDA only) H_2O_2 was used a positive control for ROS generation (data not shown)

It can be observed from Figure **6.1** and Figure **6.2** that MDA increases the ROS content of the cells gradually with increasing concentration. Meanwhile, significantly less ROS levels are detected following treatment with DMU-1122. However, DMU-2210 and 1103 despite showing a trend to reduce intracellular ROS levels did not show statistically significant reductions. DMU-1122, therefore, has the potential to protect against MDA damage. This finding supports the earlier results that showed DMU-1122, has the ability to induce antioxidant enzyme like NQO1 (Chapter 4), which can prevent genotoxic damage through scavenging ROS. ROS in many cases has been associated with increased MDA. In addition, as a consequence of increased ROS, cells attempt to induce phase II cytoprotective enzyme like Nrf2 that can induce the antioxidant related enzyme like NQO1. The antioxidant enzyme has the ability to prevent DNA damage induced by MDA through electrophiles exclusion or detoxification.

Studies have shown that phytochemicals can potentially prevent the DNA damage caused by ROS and can promote DNA repair (Rupasinghe *et al.,* 2014). A natural chalcone xanthohumol **(78)** has chemoprevention activity by reducing the generation of ROS in MCF-7 at concentration 0.001 -0.01 μM (Blanquer-Rosselló *et al.*, 2013). Moreover, natural chalcones, lophirones B **(23)** and C **(24)** have extracted from *Lophira* show electrophiles elimination and detoxification of ROS through increase the expression of *NRF2* in rat liver (Ajiboye *et al.*, 2014).

Bukhari *et al.* (2014) have used a library of synthetic chalcones and they found chalcone (*Z*)-3-(4-diethylaminophenyl)-1-diphenyl-2-propen-1-one can prevent the production of ROS in human blood. Another study has used synthetic bis-coumarin chalcone hybrids as chemoprevetive agents against H_2O_2, and they found some chalcones could decrease microsomal lipid peroxidation, hydroxyl radicals and superoxide anions in microsome (Sashidhara *et al.*, 2011). Furthermore, 2′,4′-dihydroxy-6′-methoxy-3′,5′-

dimethylchalcone **(87),** found in *Cleistocalyx operculatus* buds, has cyropreventive activity via reducing ROS generated by H_2O_2 and also induces antioxidant defence enzymes like SOD and GSH in PC12 (Su *et al.*, 2010) in ECV-304 (Human umbilical vein endothelial) cells (Ye *et al.* 2013). Additionally, Martinez *et al.* (2015) found that hesperidin methyl chalcone **(26)** has antioxidant activity capable of reducing ROS generation induced by lipid peroxidation. Han *et al.* (2015) have extracted chalcone isosalipurposide (**88**) from *Corylopsis coreana Uyeki* and found this chalcone has switched on Nrf2-ARE pathway and reduced the production of ROS induced by *tert*-butyl hydroperoxide, which can generate MDA, in $HepG_2$. Likewise, licochalcone A (**73**) has protective activity by decreasing ROS and inducing Nrf2 pathway and subsequently increase antioxidant defence genes like Ho-1, NQO1 and GCL in primary human fibroblasts skin cells (Kühnl *et al.*, 2015), mice collagen- arthritis and human rheumatoid arthritis synovial fibroblasts (Su *et al.*, 2018).

Furthermore, it has been reported that chalcone lonchocarpine **(89)**, extracted from *Abrus precatorius*, has chemopreventive capability against H_2O_2 in brain glial cells by reducing the generation of ROS, in contrast it can up-regulate Nrf2 and consequently increase antioxidant enzyme such as NQO1, HO-1 and SOD (Jeong *et al.*, 2016). Synthetic chalcone (*E*)-1-(3,4-dihydroxyphenyl)-3-(2,5-dimethoxyphenyl)prop-2-en-1-one **(90)** has also been reported to have cytoprotective activity via Nrf2 pathway induction in PC12 cells (Wang *et al.*, 2019).

6.2.2 Single cell gel electrophoresis (Comet) assay

Below are representative examples of the visual results found with the comet assay (Figure **6.3** and Figure **6.4**). Quantitative analysis was undertaken using Tri-Tek Comet Score 2.0.0.38 software. The results of this analysis are shown in Figure **6.5** - Figure **6.7**.

6.2.2.1 Comet assay imaging

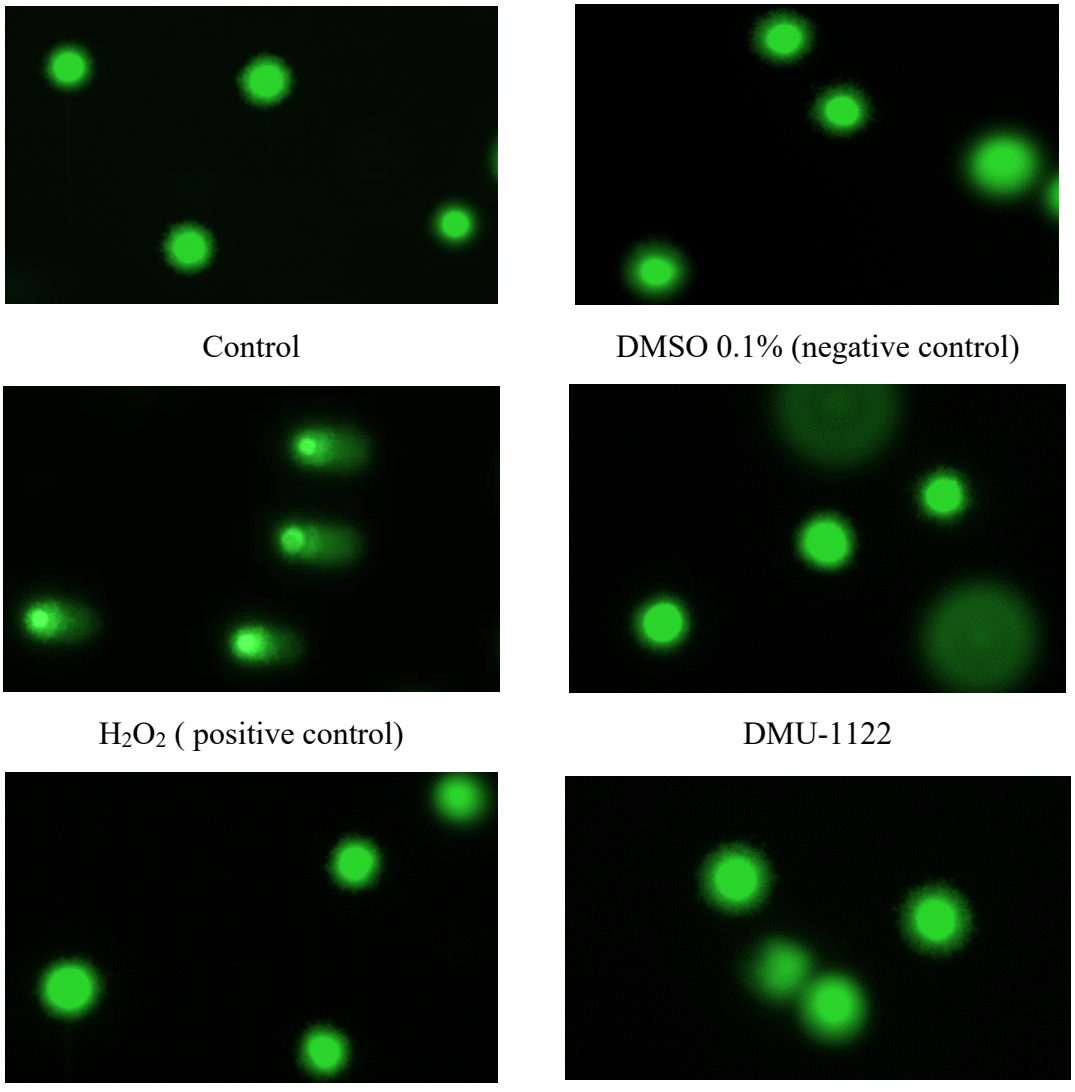

Figure 6.3 MRC-5 cells were treated with chalcone (DMU-1122, 2210 and 1103) for 24 h. Controls included no treatment, vehicle control (DMSO 0.1%) and positive control (H_2O_2 100 μM)

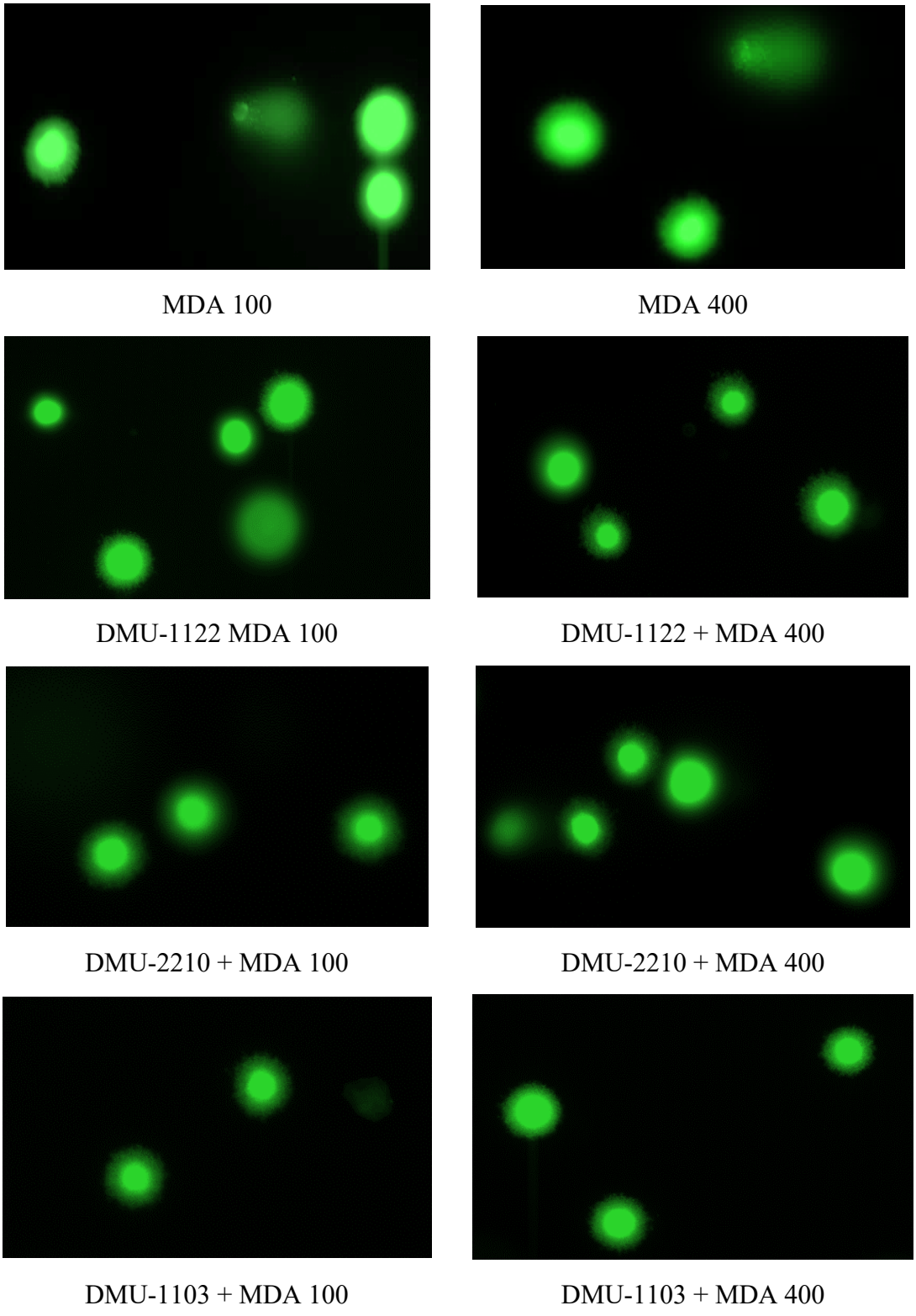

Figure 6.4 MRC-5 cells were either treated with MDA individually or pretreated with chalcone (DMU-1122, 2210 and 1103) for 24 hours before being exposed to MDA (100 and 400 μM) for 24 hours

Single cell gel electrophoresis fluorescent images are presented in Figure **6.3** and 6.5. Figure **6.3** illustrates the nuclear material attached in the matrix forming a spherical shape in the control (no treatment), negative control (DMSO 0.1%), and chalcones DMU-1122, DMU-2210 and DMU-1103 samples because of intact DNA. However, in the positive control (H_2O_2 at 100 μM) DNA damage is apparent (comet like appearance). During electrophoresis, undamaged DNA material is linked together, while damaged DNA moves from the cathode to anode side depending on the size of fragments. Azqueta and Collins (2006) have explained that the supercoiled loop of DNA can relax due to unwinding by alkaline solution.

Figure **6.4** shows the effect of MDA at 100 and 400 μM on MRC-5 cells for 24 h treatment. The figure demonstrates that some cells retain a spherical shape. However other cells have DNA damage induced by MDA and form the comet shape. Nevertheless, pre-treatment with chalcones DMU-1122 (20 μM), DMU-2210 (10 μM) and DMU-1103 (10 μM) reduced DNA damage, as most nuclear materials remained connected together in the head of the comet due to the chemopreventive activity of the chalcones under investigation.

6.2.2.2 Comet assay analysis data

Figure **6.5** - Figure **6.7** are present the results obtained from the analysis of comet assay using Tri-Tek Comet Score 2.0.0.38 software.

1- DMU-1122:

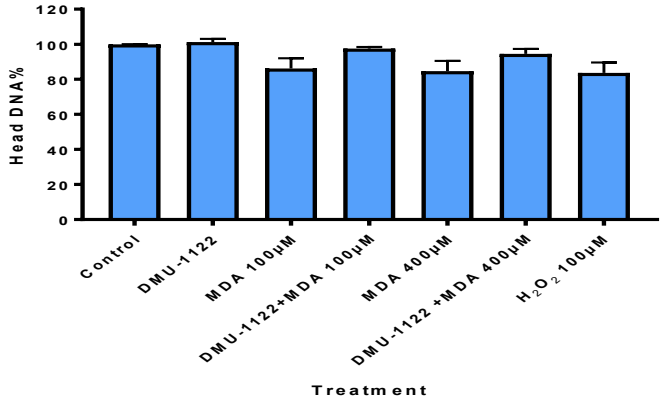

A

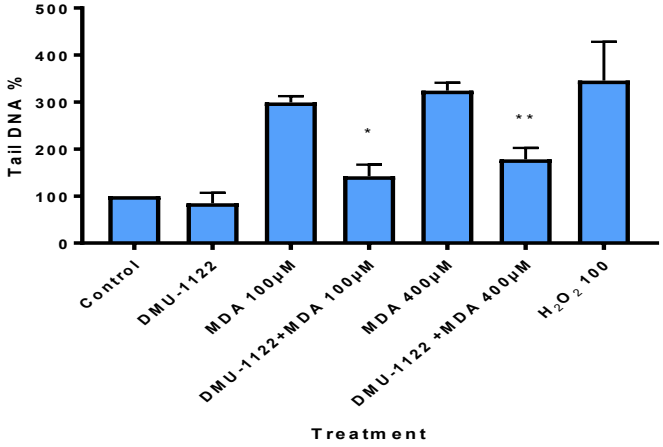

B

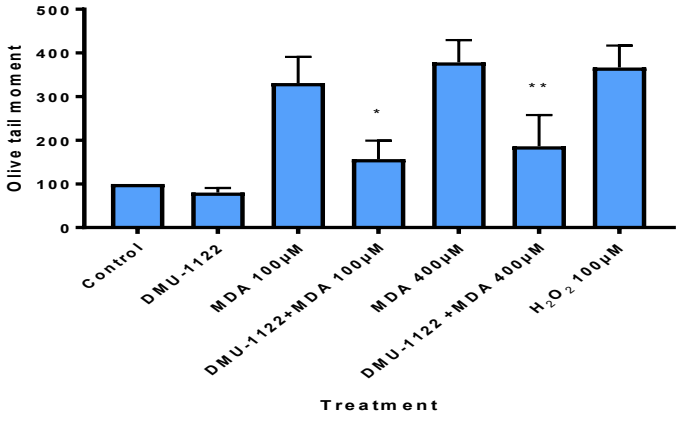

C

Figure 6.5 Assessment of the genotoxic and antigenotoxic activities of the DMU-1122 against different doses of MDA (100 and 400 uM) in MRC-5 cells using the comet assay assessed by (A) %DNA in Head and(B) tail and (C) Olive tail moment parameters. Data are presented mean ± SD. (n=3), * for $p<0.05$ and ** for $p<0.01$ significant compared to MDA.

2- DMU-2210

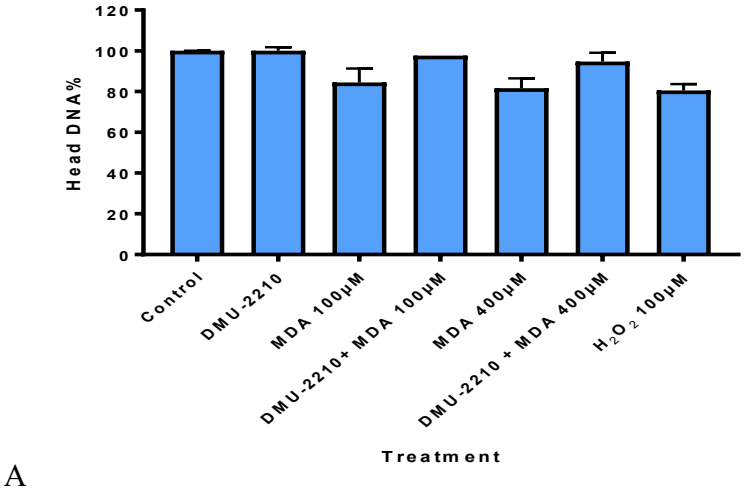

A

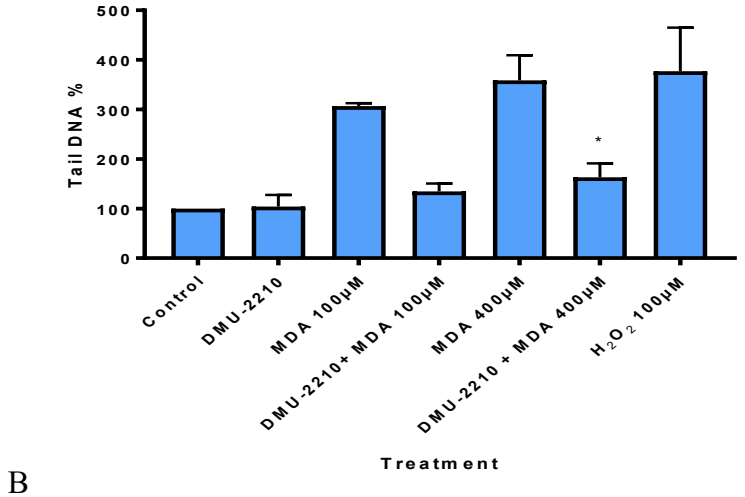

B

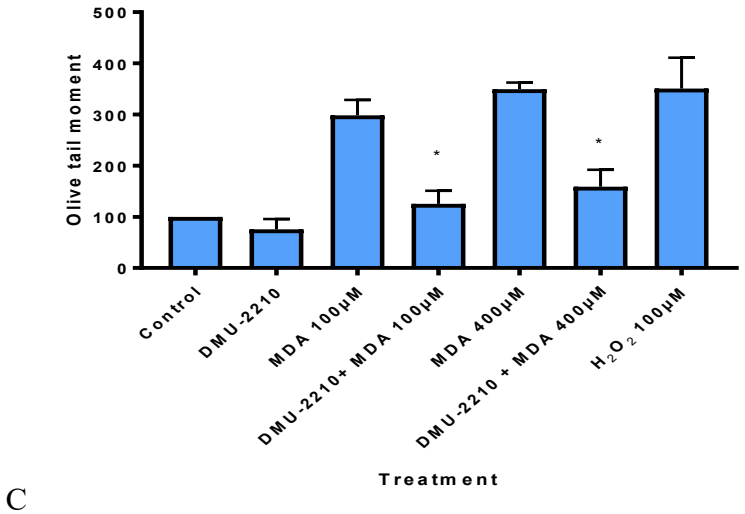

C

Figure 6.6 Assessment of the genotoxic and antigenotoxic activities of the DMU-2210 against different doses of MDA (100 and 400 uM) in MRC-5 cells using the comet assay assessed by (A) %DNA in Head and (B) tail and (C) Olive tail moment parameters. Data are presented mean ± SD. (n=3), * for $p<0.05$ significant compared to MDA.

3- DMU-1103

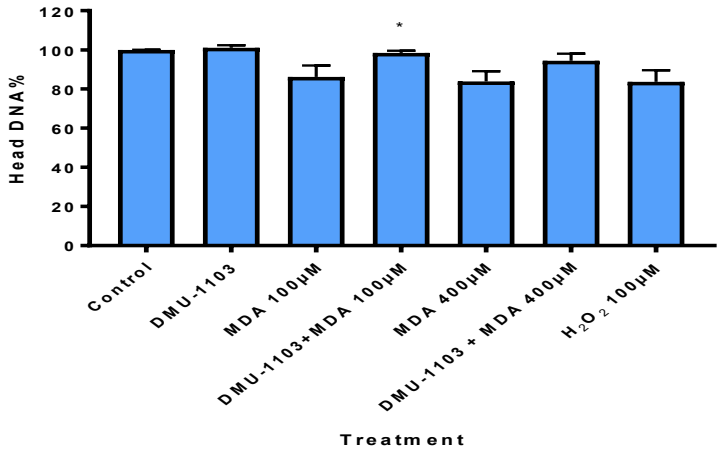

A

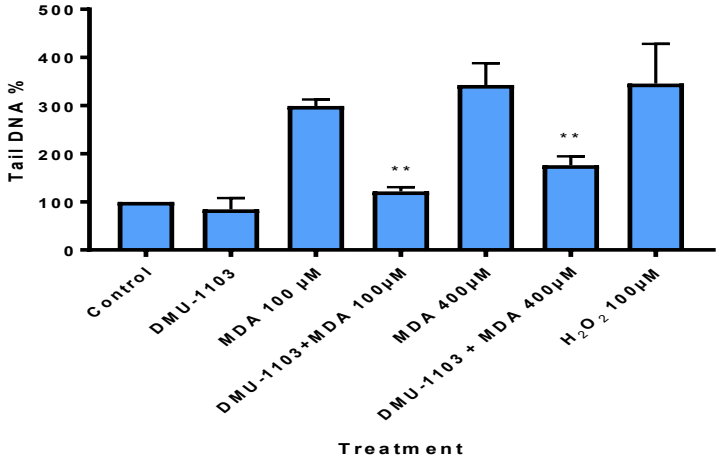

B

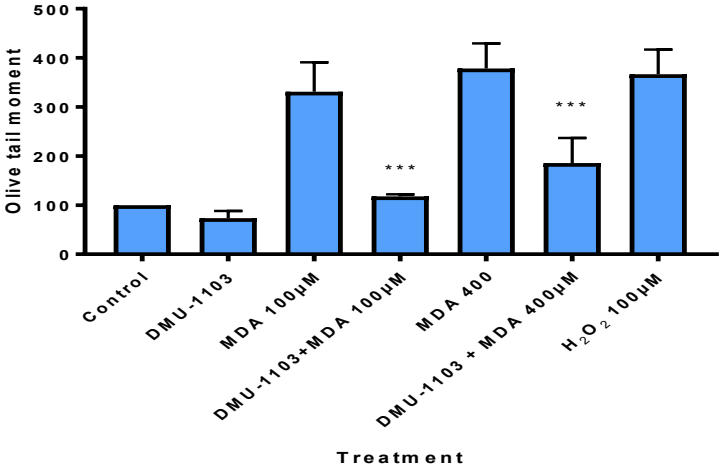

C

Figure 6.7 Assessment of the genotoxic and antigenotoxic activities of the DMU-1103 against different doses of MDA (100 and 400 uM) in MRC-5 cells using the comet assay assessed by %DNA in (A) Head and (B) tail and (C) Olive tail moment parameters. Data are presented mean ± SD. (n=3), * for $p<0.05$, ** for $p<0.01$ and *** for $p<0.001$ significant compared to MDA.

The results of DMU-1122, 2210 and 1103 were not showed genotoxic on MRC-5. However, the antigenotoxic activity of three chalcones showed significant differences with cells pretreated with chalcones before MDA exposure compared to cells being treated with MDA only. Although DMU-1122 and DMU-2210 were not show a significant difference in DNA head percentage, they illustrated a significant difference in DNA tail percentage and tail olive moment at 100 and 400 μM treatment by MDA. Furthermore, DMU-1103 had shown a significant difference in DNA tail percentage and tail olive moment at 100 and 400 μM as well as at 100 μM of MDA in DNA head percentage.

The results showed that chalcones can decrease the toxic effect of MDA by decreasing the percentage of the tail intensity and tail olive moment, which had been used as an indicator of DNA damage. Thus, chalcones can reduce DNA damage by preventing MDA toxicity. It might be the reason for that it was because chalcones have the ability to reduce the generation of ROS and consequently, reduce DNA damage. A positive correlation was found between the results of ROS and comet assay. Indeed, decreased ROS generation by chalcones lead to decrease in DNA damage by MDA (see Figure **6.5** - Figure **6.7**). Moreover, chalcones have induced the Nrf2/ARE pathway by promoting the antioxidant enzyme like NQO1.

The present findings seem to be consistent with other research which found carbazole chalcones **(91)** could prevent the oxidative DNA damage induce by 2,2′-azobis (2-amidinopropane hydrochloride) through scavenging ROS and as a result reducing DNA damage (Bandgar *et al.*, 2013). Furthermore, chalcone 2′,4′-dihydroxychalcone **(92)** was isolated from *Zuccagnia punctate,* could prevent DNA damage through inhibiting the toxicity effect of benzo(*a*)pyrene (Zampini, 2008).

Researchers have reported that xanthohumol **(78)** showed cytoprotective activity against benzo(a)pyrene and amino-3-methyl-imidazo[4,5-*f*]quinoline in HepG2 cells and rats, by decreasing the comet formation. It had been speculated that the suppression of DNA damage, reduction in DNA-adducts and decrease in the number of micronuclei was due to the induction of phase II enzyme like NAD(P)H: quinone oxidoreducatse (NQO1), modification of cell proliferation and induce DNA repair (Plazar *et al.*, 2007; Ferk *et al.*, 2010).

Other groups have reported that chalcone isoliquiritin apioside **(93)**, extracted from *Glycyrrhiza glabra*, has a potential of cancer chemoprevention activity through decreasing the tail moment generated by H_2O_2 and 4-nitroquinoline-N-oxide in human blood lymphocytes (Kaur *et al.*, 2009). Likewise, chestnut bee pollen extract, which counting *trans*-chalcone **(25)**, has reduce one-third of DNA damage by H_2O_2 in calf thymus DNA (Şahin and Karkar, 2019).

Moreover, a pre-treatment with (*E*)-3-(3,4,5-trimethoxyphenyl)-1-(pyridin-4-yl)prop-2-en-1-one (**94**) illustrated cytoprotective activity against benzo(a)pyrene in human HEK293 cells through reducing the cell DNA damage (Horley *et al.*, 2017). Also, chalcone (*E*)-1-(2-hydroxyphenyl)-3-(4-methylphenyl)-prop-2-en-1-one) **(54)** showed chemopreventive activity against cyclophosphamide, sodium azide and 4-nitroquinoline-1-oxide in mice, through decrease DNA damage and micronuclei frequency (Da Silva Lima *et al.*, 2017). The causes of reducing the mutagenic effect could be attributed to the reaction between *α,β*-unsaturation site in chalcone with a mutagenic factor like sodium azide and 4-nitroquinoline-1-oxide through the generation of a nucleophilic centre at *β*-carbon. Thus, leading to a reduction in ROS generation and consequently the prevention of DNA damage (Torigge *et al.*, 1983; Noroozi *et al.*, 1998).

In conclusion, the investigation of DNA damage prevention induced by MDA has shown that DMU-1122 can reduce the ROS level. However, all chalcones DMU-1122, 2210 and 1103 have decreased the percentage of DNA damage by MDA.

This section has potential limitations, briefly summarised below:

1- The time and financial constraints restricted the project with just one cell line MRC-5.
2- The incubation time of MDA in ROS detection was reduced to 4 h instead of 24 h due to the toxicity effect of MDA on cell membrane leading to reduced DCFH-DA uptake by live cells.
3- Comet assay was showing DNA damage, but it did not show the type of damage such as deletion, insertion and single or double strand breaks.

Chapter 7 **Chalcones and *NRF2* gene expression**

7.1 Introduction

Gene expression refers to the process of biological information being coded into an active molecule. During gene expression, the RNA template is transcribed from a DNA template and then translated to a specific protein (Hickey, 2007).

7.1.1 Gene expression using reverse transcription quantitative polymerase chain reaction

Since the discovery, the important role of reverse transcriptase is to convert the RNA template to cDNA, researchers have used Polymerase Chain Reaction (PCR) to quantify the transcriptional activity of a specific target gene (Bustin, 2004; Krebs *et al.*, 2018). PCR is an enzymatic amplification of nominated DNA sequences and it is frequently used in molecular biology and genetic disease (Chen and Janes, 2002). Real-time PCR is commonly used for amplifying, detecting, monitoring reactions by fluorescent dyes or probes, is also rapid and highly sensitive (Logan *et al.*, 2009). In addition one important application of real-time PCR named quantitative PCR (qPCR), which includes the reverse transcriptase (RT), a RNA dependent DNA polymerase, used to quantify the transcription of RNA (Kennedy and Oswald, 2011).

The cell has an extraordinary effective mechanism to protect itself against abnormal conditions. One of the essential genes that are responsible for inducing antioxidant defence gene is *NRF2* (Townsend and Tew, 2014). Several studies have determined the level of *NRF2* gene expression by using qPCR, such as NRF2 being induced by 2′,3′-dihydroxy-4′,6′-dimethoxy **(95)** in the PC12 cell line (Izumi *et al.*, 2012), hesperidin methyl chalcone **(26)** in mice (Martinez *et al.*, 2016) and *trans*-chalcone **(25)** in mice (Martinez *et al.*, 2017).

7.1.2 Knockdown *NRF2* gene

The study of gene function requires removal or silence the gene of interest to observe the outcome of that gene. One of essential technique is using to silence the specific gene called gene knockdown, which is refer to reduce the gene expression (reduce RNA and protein products). The knockdown techniques can be achieved by different methods, one of the most useful methods is RNA interference (RNAi). This method depends on two enzymes including Dicer, which can split the RNA strand into 21 bp fragments (siRNA), and RNA-induced silencing complex (RISC), which is used to discover, anneal and mark the specific mRNA fragments that are generated by Dicer, and destroy them. RNAi is targeted by double-stranded RNA (dsRNA), and the formation of a dsRNA molecule and hence downregulation of the gene of interest (Robert and Farrell, 2010; Krebs *et al*., 2018).

Gene knockdown is used to identifying the consequence of gene expression in cells, as well as to determine the functions of proteins. In addition, RNAi is commonly used to discover and develop the pharmaceuticals due to its ability to silence particular genes (Farrell, 2017).

Several studies have investigated *NRF2* gene expression using the gene silencing technique to determine the consequence of the absence of *NRF2*. For example, the silencing of the *NRF2* gene led to a down-regulation of NQO1 protein levels in SK-OV cells (Cho *et al.*, 2008), GPX in mice (Singh *et al.*, 2006), NQO1, GP, HO-1 and GCL in A549 cells (Homma *et al.*, 2009), Nrf2 protein in HepG2 (Li *et al.*, 2017) and effecting on ARE driven gene activity in PC12 (Izumi *et al.*, 2018).

7.1.3 The aims and objectives of this chapter

At the early stage of this research it has been found that NQO1 protein expression was induced by chalcones DMU-1122, 2210 and 1103. In addition, these chalcones also have the ability to reduce MDA toxicity, consistent with the induction of antioxidant defensive genes via the switch on Nrf2 signalling pathway. In consideration of this, the aims of this chapter is to identify the mechanism of chalcones to switch on Nrf2 pathway, also weather the chemopreventive of chalcones are related to induce *Nrf2* gene. These aims can be investigated by following objectives:

1- Determine the potential ability of selective chalcones to induce NRF2 gene expression and subsequently induce NQO1 gene, as a prototype of defence genes, in post time for detecting the gene starting time, using qPCR protocols.
2- Identify the toxicity, time and concentrations of siRNA reagent using MTT and qPCR assays.
3- Investigate the role of NRF2 gene in the prevention of MDA toxicity, by pre-treating with chalcones then MDA in present or absent (knockdown) of NRF2 gene, using Western blot, qPCR and MTT assays.

7.2 Results and Discussion

7.2.1 Chalcone induced *NRF2* gene expression

The fold induction of *NRF2* and *NQO1* gene expression in MRC-5 cell line that treated with chalcones DMU-1122 (Figure **7.1**), DMU-2210 (Figure **7.2**) and DMU-1103 (Figure **7.3**) are presented below.

1- DMU-1122

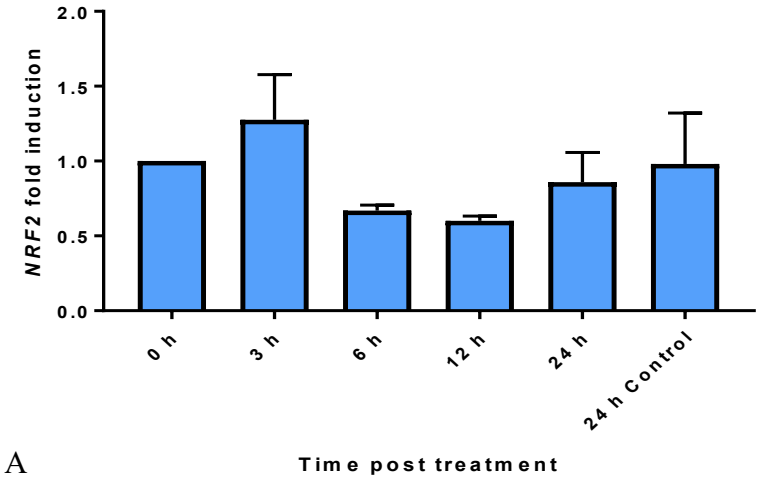

A

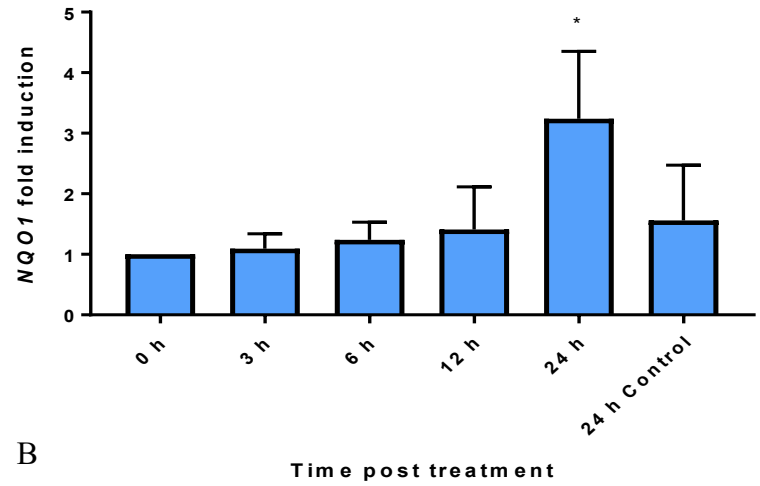

B

Figure 7.1 Induction of (A) *NRF2* (B) *NQO1* mRNA expression relative to the negative control and reference gene beta-actin, in cells treated with DMU-1122 (20 µM) for 24 h. Data are presented as mean ± SD (n=6), * for $p<0.05$, compared with control (0.1 % DMSO)

2- DMU-2210

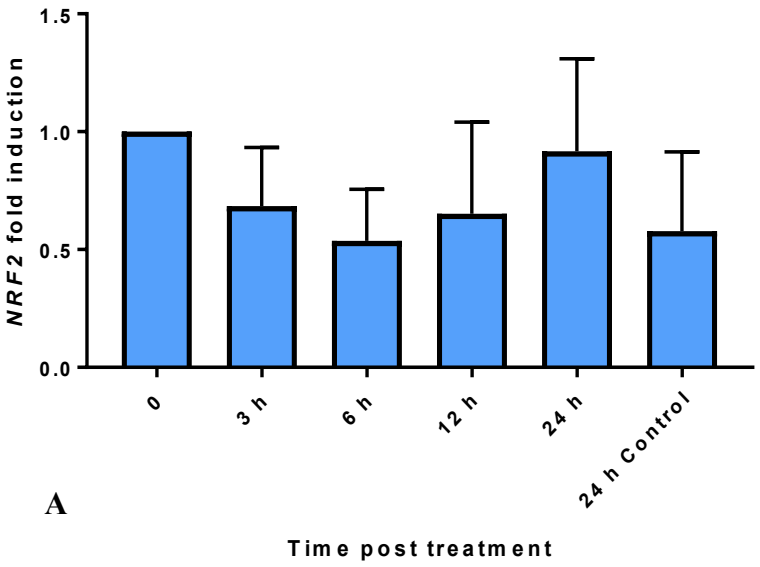

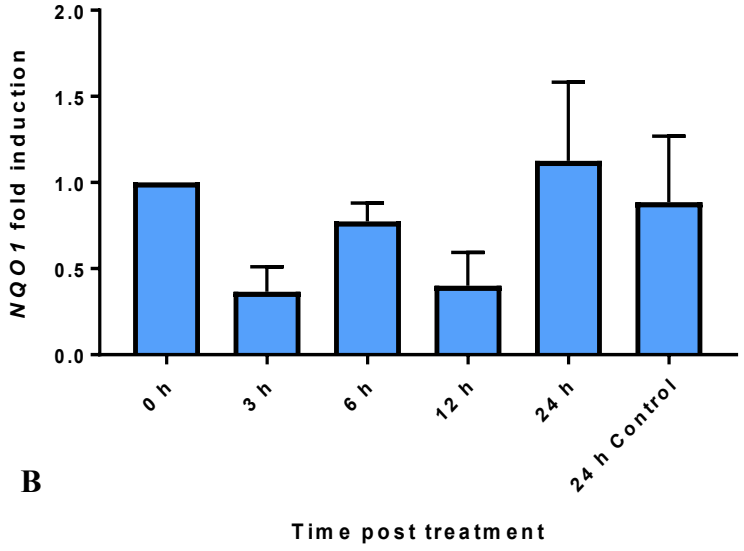

Figure 7.2 Induction of (A) *NRF2* (B) *NQO1* mRNA expression relative to the negative control and reference gene *beta-actin*, in cells treated with DMU-2210 (10 µM). Data are presented as mean ± SD (n=6), * for $p<0.05$, compared with control (0.1 % DMSO)

3- DMU-1103

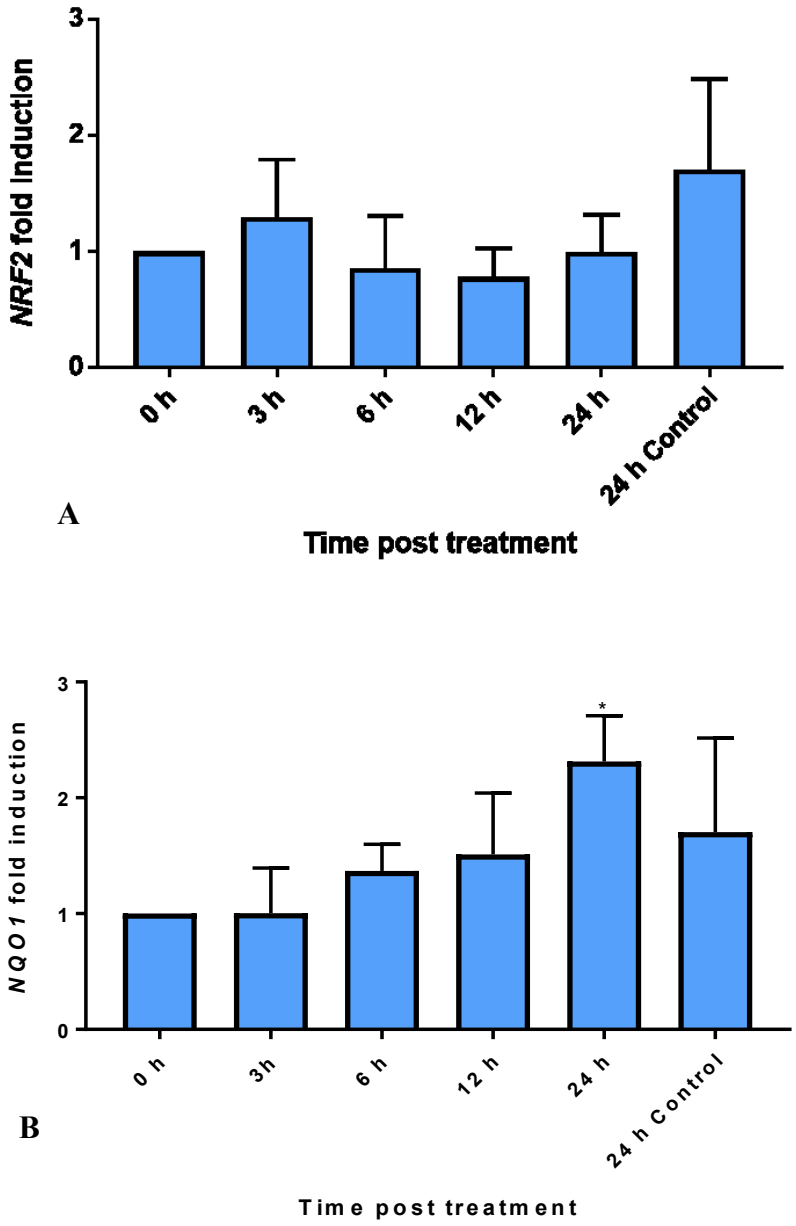

Figure 7.3 Induction of (A) *NRF2* (B) *NQO1* mRNA expression relative to the negative control and reference gene *beta-actin*, in cells treated with DMU-1103 (10 µM). Data are presented as mean ± SD (n=6), * for $p<0.05$, compared with control (0.1 % DMSO)

The expression of *NRF2* and *NQO1* mRNA in cells treated with chalcones DMU-1122, 2210 and 1103 were compared with the negative control (0. 1% DMSO). C_T values were determined for both genes of interest (*NRF2 and NQO1*) and reference gene (*beta-actin*). The latter was used to normalize the gene expression data. The fold induction of genes of interest was calculated by the $2^{-\Delta\Delta CT}$.

The results show that DMU-1122 (Figure **7.1**) and DMU-1103 (Figure **7.3**) have induced *NQO1* significantly after 24 h treatment, and suggest that DMU-1122 and 1103 have the ability to induce NQO1 protein expression via the Nrf2 pathway. However, DMU-2210 (Figure **7.2**) could not induce *NQO1* gene expression. The *NRF2* gene is responsible for inducing many antioxidant genes like *NQO1* (Kennedy and Oswald, 2011), thus play an essential role in the detoxification of reactive electrophiles (Ajiboye *et al.*, 2014). A study by (Krajka-Kuźniak *et al.*, 2013) reported that chalcone xanthohumol **(78)** can upregulate *NQO1* mRNA and protein in THLE-2 cells. Furthermore, Licochalcone E **(75)** has the ability to increase the level of NQO1 resulting in neuroprotective activity in mice (Kim *et al.*, 2012), due to the *α,β*-unsaturated motifs on the chalcone activating the *NRF2* gene with the consequent induction of antioxidant enzymes (Maydt *et al.*, 2013). These findings are close to those of (Mohan and Gupta, 2019) who found Nrf2 protein level was decreased at 14 h. However, NQO1 protein expression was increased at 24 h, this explains that NRF2 is time and treatment dependent (Schaap, 2015).

7.2.2 NRF2 knockdown studies

7.2.2.1 Determination of the concentration of silencing gene and the transfection reagent required

To determine the time and concentration of transfection reagent that can successfully knockdown the gene of interest. MRC-5 cell line was treated with 50 nM *NRF2* gene silencing with different concentrations of transfection reagent for 24 and 48 h. the fold induction of *NRF2* and *NQO1* gene expression were assessed by RT-PCR (Figure **7.4**).

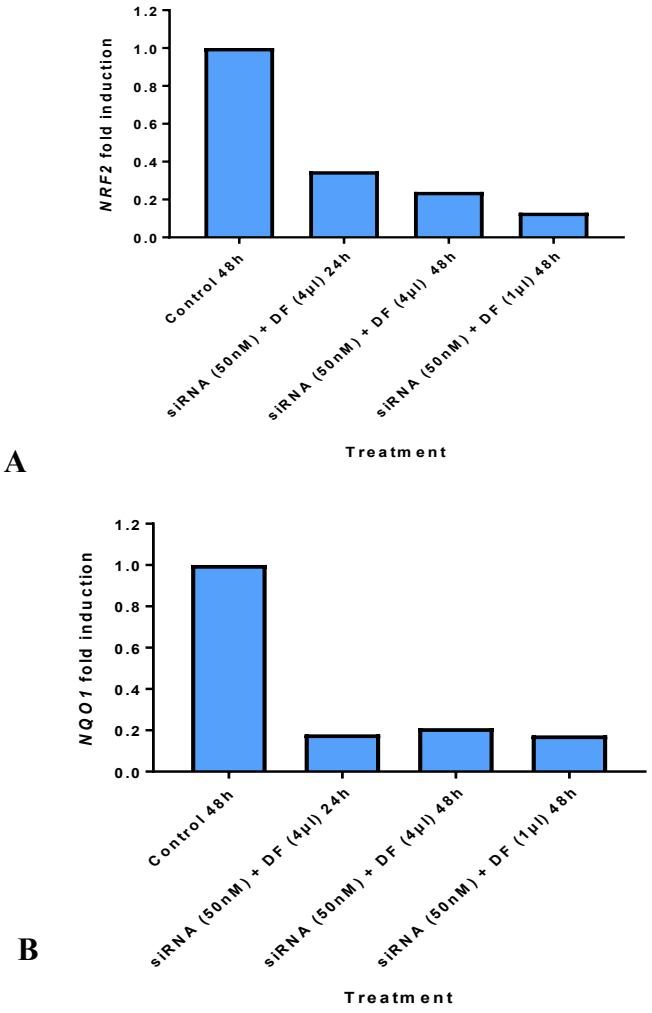

Figure 7.4 The fold induction of (A) *NRF2* (B) *NQO1* mRNA expression relative to the negative control and reference gene *beta-actin*, in cells treated with 50 nM *Nrf2* siRNA and different concentration of transfection reagent and different time incubation in MRC-5 cells

7.2.2.2 Identifying the nontoxic concentration of knockdown reagents:

To determine the toxicity of knockdown reagents that successfully silencing *NRF2* gene of interest (Section 7.2.2.1), MRC-5 cell line was treated with 0.1% transfection reagent, in addition to 50 nM of the target gene or non-target gene, then assessed by MTT assay (Figure **7.5**).

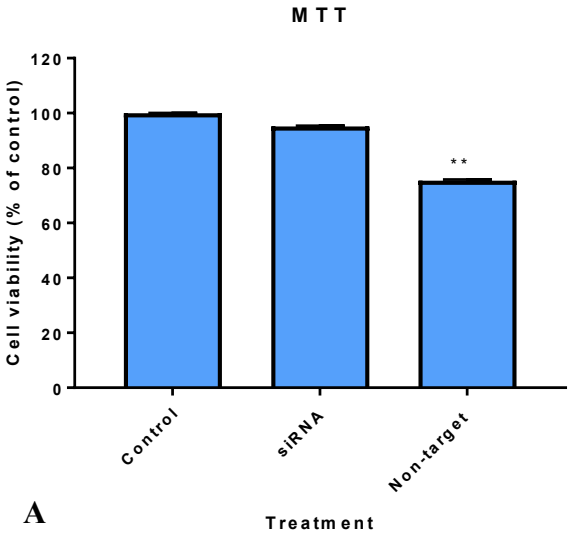

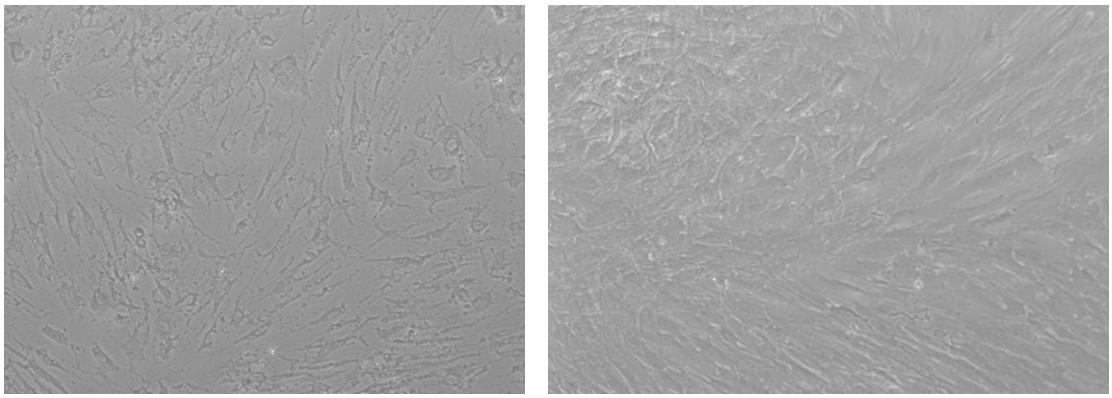

B Non-target gene Target gene

Figure 7.5 MRC-5 were exposed to knockdown reagents including 0.1% transfection reagent and 50 nM of siRNA or non-target gene for 24 h then incubated for 72 h and the results were compared to control (no treatment) (A) MTT assay result to determine the non-toxic concentration, (B) cell imaging after 72 h incubation. Data are presented as mean ± SD (n=6), * for $p<0.05$

Although several researchers have knocked down the gene in MRC-5 cells using SMARTpool: ON-TARGETplus siRNA and ON-TARGETplus non-targeting pool (Dharmacon) (Requena *et al.*, 2016; Dunphy *et al.*, 2018), they have not reported the toxicity of the reagents. However, the results were shown the non-targeting pool was more toxic than the targeting pool using MTT assay (Figure **7.5** A). The images (Figure **7.5** B) illustrate the shape of MRC-5 cell line after 72 h of incubation, which shows that non-targeting pool can change the cell morphology comparing with targeting pool. On that basis, it has searched for the reason that toxicity and it was found that the smart pool contained (UGGUUUACAUGUCGACUAA, UGGUUUACAUGUUGUGUGA, UGGUUUACAUGUUUUCUGA, UGGUUUACAUGUUUUCCUA) sequences. Fedorov *et al.* (2006) have reported that UUUUU, AUUUG, AUUUU, GUUUU, GUUUG and CUUUU sequences display toxicity during gene knockdown experiments. In consideration of this evidence we chose to use ON-TARGETplus Non-targeting Control siRNA as it contains UGGUUUACAUGUCGACUAA sequences, the result was showed no difference in cell viability in control (no treatment), *NRF2* siRNA gene (50 nM) and nan-target gene (50 nM) (Figure **7.6**).

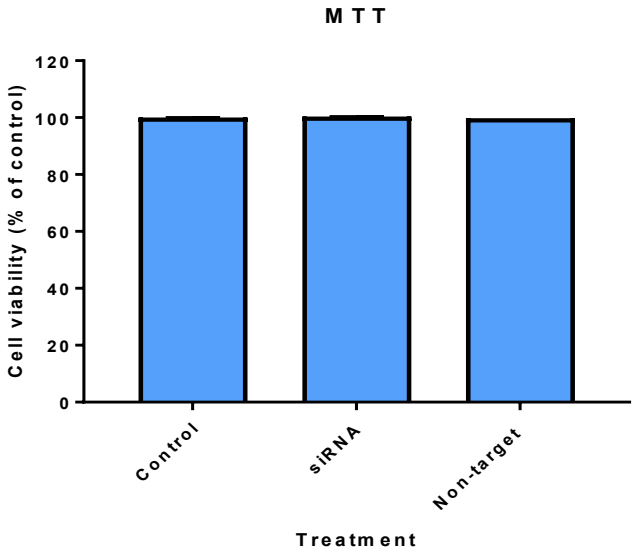

Figure 7.6 MRC-5 was exposed to 0.1 % transfection reagent and 50 nM of each *NRF2* siRNA gene and Non-target gene for 24 h then incubated for 72 h, after which cell viability was determined using the MTT assay. Data are presented as mean ± SD. (n=3). The results were compared to control (no treatment)

7.2.2.3 Assessment of the *NRF2* gene knockdown and there related to chalcone:

7.2.2.3.1 siRNA Western blotting results:

The level of NQO1 protein induction with and without *NRF2* gene silencing, also with chalcones and/or MDA was assessed using the western blotting assay (Figure **7.7**).

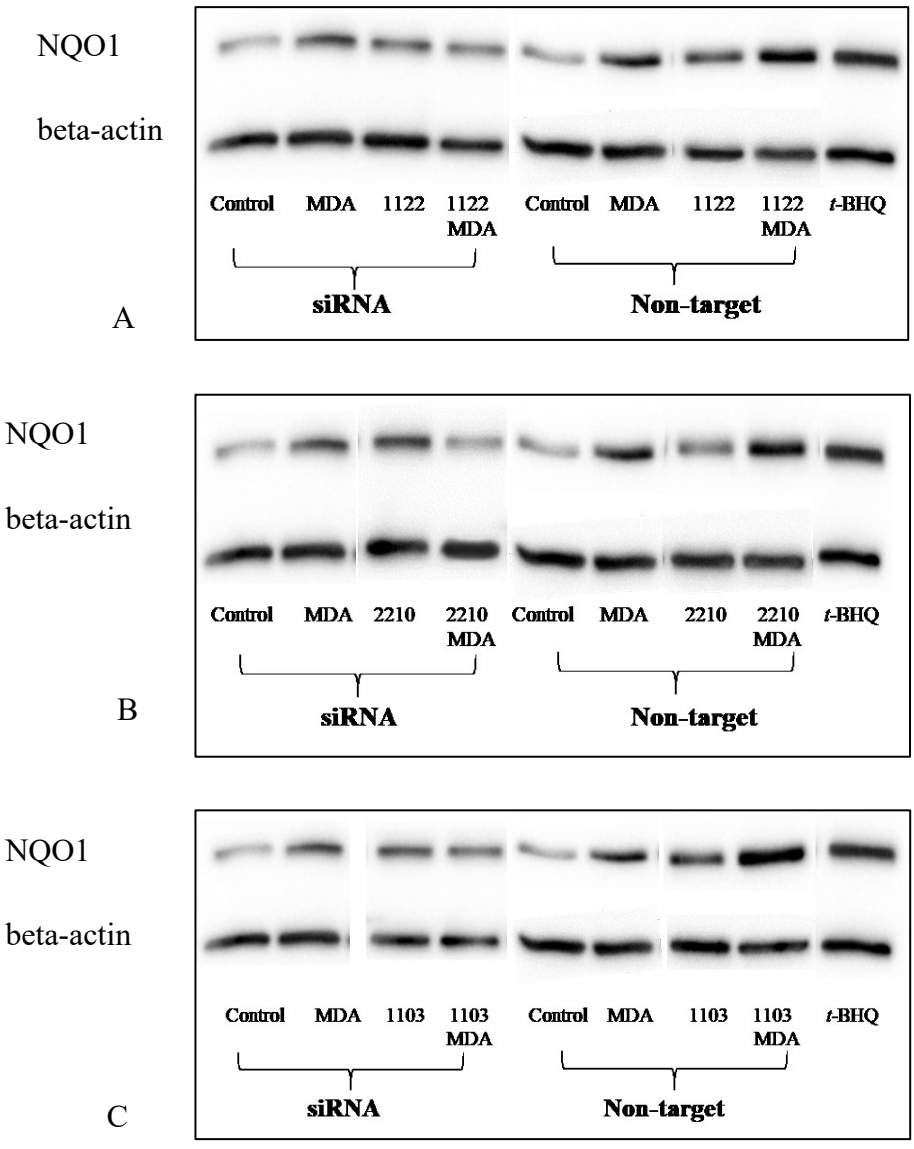

Figure 7.7 NQO1 protein expression following chalcone (A) DMU-1122, (B) DMU-2210 and (C) DMU-1103 treatment. MRC5 cells were knocked-down *NRF2* gene for 24 h then incubated with the indicated chalcones up to a maximum of 24 h. Thereafter, cells were incubated with 100 µM MDA before being harvested and then subjected to Western blotting. Vehicle control (Control) (0.1% DMSO at 24 hours). *t*-BHQ (25 µM) was included as a positive control (24 h incubation)

7.2.2.3.2 siRNA RT-PCR results:

The fold induction of *NRF2* and *NQO1* gene expression in MRC-5 cell line, which was knocked down *NRF2* gene, was treated with MDA and/or chalcones DMU-1122 (Figure **7.8**), DMU-2210 (Figure **7.9**) and DMU-1103 (Figure **7.10**).

1- DMU-1122

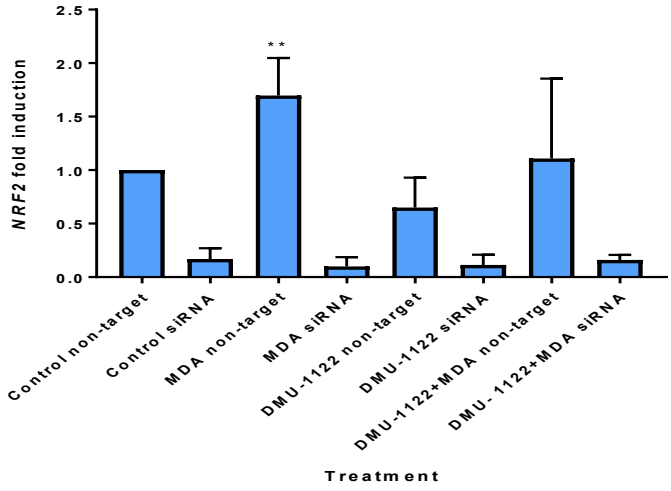

A

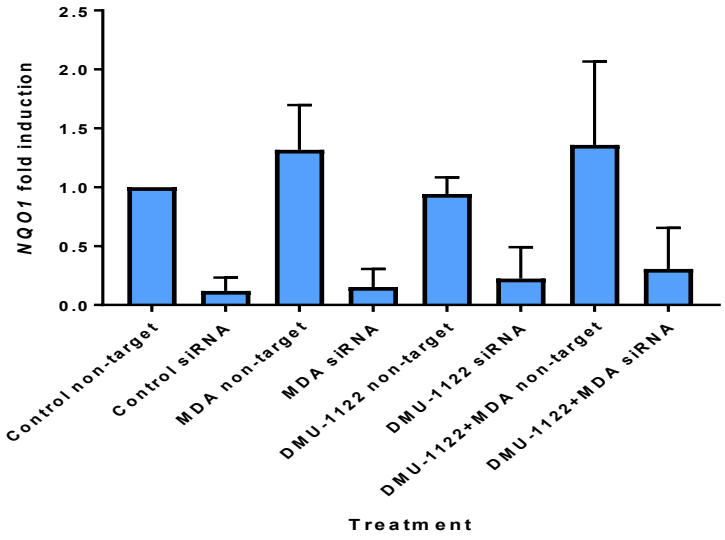

B

Figure 7.8 Induction of (A) *NRF2* (B) *NQO1* mRNA expression relative to the Non-target gene (no treatment) as a negative control and reference gene *beta-actin*, in MRC-5 cells have knocked down of the *NRF2* gene for 24 h followed by treatment with DMU-1122 (20 µM) for 24 h. Thereafter, treated with MDA 100 µM for 24 h before being harvested and then subjected to qPCR. Data are presented as mean ± SD. (n=4), ** for $p<0.01$ significant compared with non-target control

2- DMU-2210

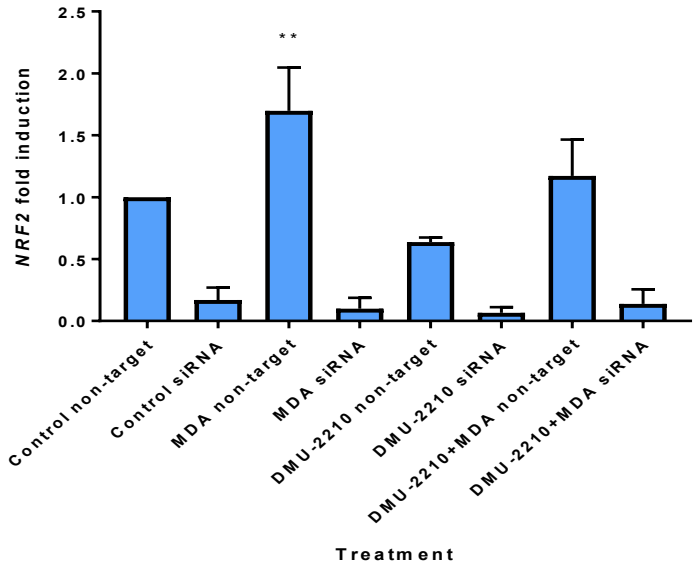

A

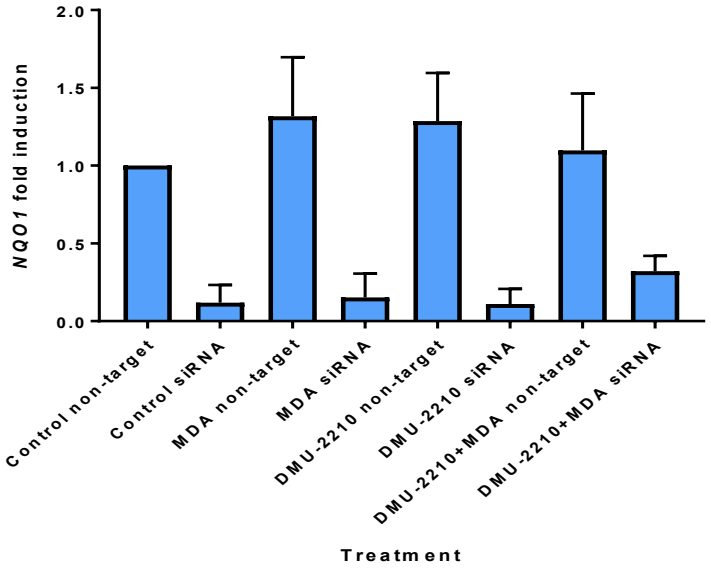

B

Figure 7.9 Induction of (A) *NRF2* (B) *NQO1* mRNA expression relative to the Non-target gene (no treatment) as a negative control and reference gene *beta-actin*, in MRC-5 cells following knocked down of the NRF2 gene for 24 h followed by treatment with DMU-2210 (10 µM) for 24 h. Thereafter, treated with MDA 100 µM for 24 h before being harvested and then subjected to qPCR. Data are presented as mean ± SD. (n=4), ** for $p<0.0$ significant compared with non-target control

3- DMU-1103

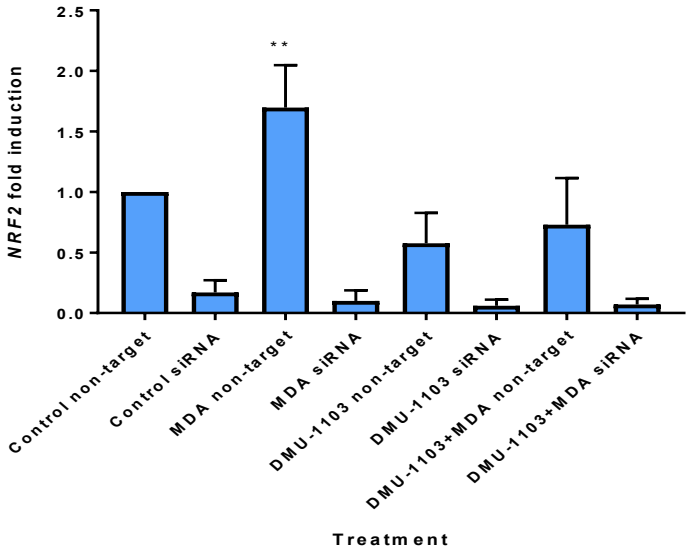

A

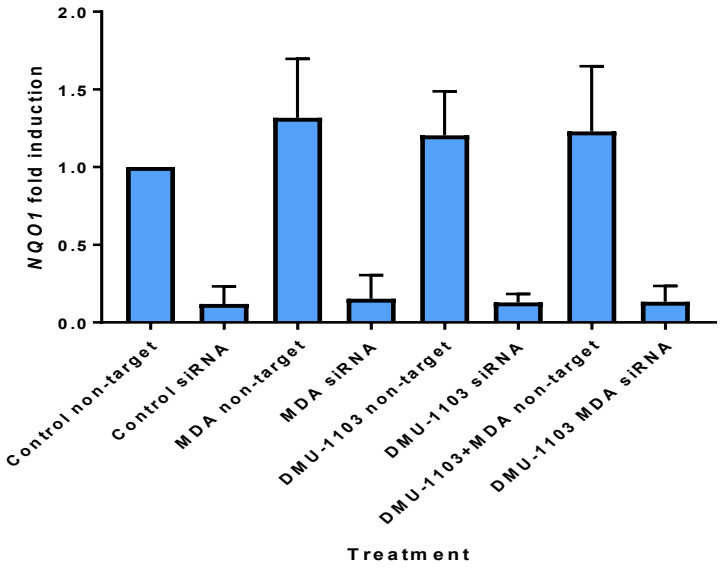

B

Figure 7.10 Induction of (A) *NRF2* (B) *NQO1* mRNA expression relative to the Non-target gene (no treatment) as a negative control and reference gene *beta-actin*, in MRC-5 cells have knocked down of the *NRF2* gene for 24 h followed by treatment with DMU-1103 (10 μM) for 24 h. Thereafter, treated with MDA 100 μM for 24 h before being harvested and then subjected to qPCR. Data are presented as mean ± SD. (n=4), ** for $p<0.01$ significant compared with non-target control

7.2.2.3.3 MTT assay:

To determine the correlation between *NRF2* as cell defence gene and the chemopreventive of DMA-1122 (Figure **7.11** A), DMU-2210 (Figure **7.11** B) and DMU-1103 (Figure **7.12**) against MDA toxicity, the MRC-5 was knocked down *NRF2* gene and then pretreated with chalcones followed by a range of MDA concentrations.

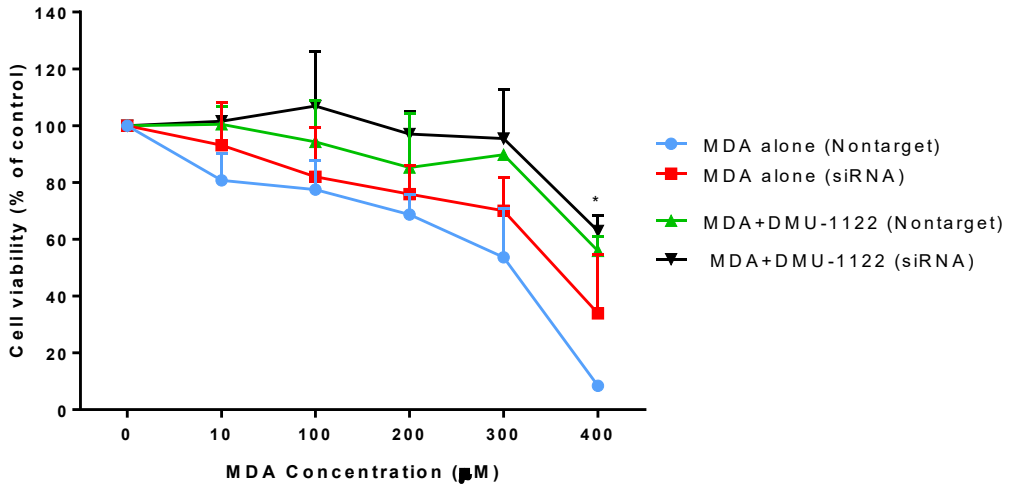

A

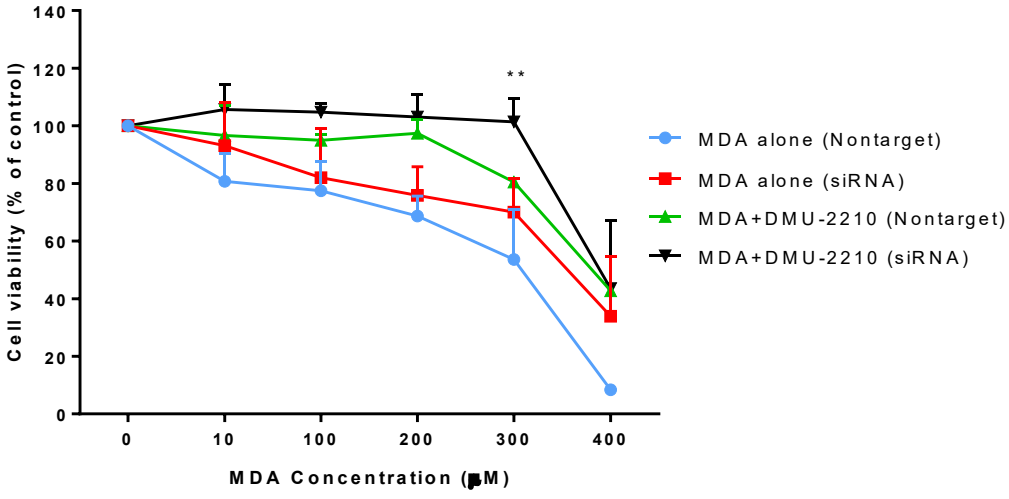

B

Figure 7.11 *NRF2* gene knockdown in MRC-5 cells followed by pretreatment with chalcone DMU-1122 (A), 2210 (B) for 24 h. Cells were then exposed to MDA for 24 h after which cell viability was determined using the MTT assay. Data are presented as mean ± SD. (n=3), * for $p<0.05$, ** for $p<0.01$, significant compared to MDA non-target as a control

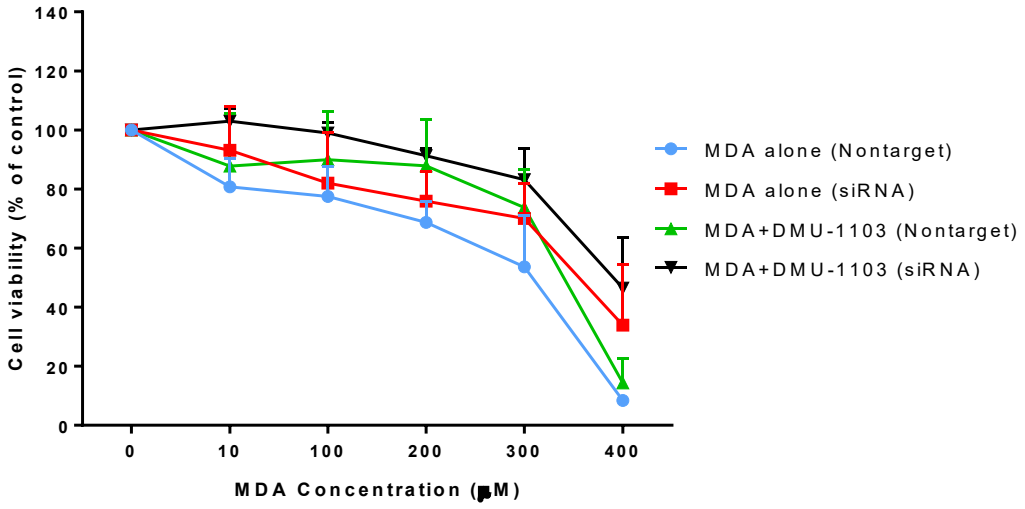

Figure 7.12 *NRF2* gene knockdown in MRC-5 cells followed by pretreatment with chalcone DMU- 1103 for 24 h. Cells were then exposed to MDA for 24 h after which cell viability was determined using the MTT assay. Data are presented as mean ± SD. (n=3), compared to MDA non-target as a control

To determine the correlation between chalcones as chemopreventive compounds and *NRF2* gene expression (antioxidant genes inducer), the *NRF2* gene was knocked down in MRC-5 cells using siRNA. Cells were then pretreated with chalcones for 24 h followed by treatment with MDA for another 24 h. Cells were also treated in the same process but using non-target gene instead of on target as a control. The results in Figure **7.7** presents the intercorrelations among the nine measures of NQO1 protein induction with and without *NRF2* gene silencing using the western blotting assay, and show that the NQO1 protein expression was reduced due to knock down *NRF2* gene comparing with the non-target gene. In addition, the Western blotting results of the non-target gene show that the combination of chalcone DMU-1122, DMU-2210 and DMU-1103 with MDA increased the level of NQO1 protein. Moreover, the RT-PCR results (Figure **7.8** - Figure **7.10**) show that *NRF2* gene was knocked down successfully, however, there were no significant

differences between treated the cell with chalcones alone or the combination with MDA using non-target gene in *NRF2* and *NQO1* gene expression. These differences between mRNA and protein expression can be explained by the variation among transcription and translation process, indeed several researchers have reviewed that transcription and translation process some times are not in a linearity relationship (Maier *et al.*, 2009). In addition current results seem to be consistent with other workers who report, a contrary direction between mRNA and protein expression (Cheng *et al.*, 2016).

Additionally, MDA alone illustrates the significant increase of *NRF2* gene expression (Figure **7.8**, 7.9 and 7.10). This might be due to the presence of MDA leading to the elevation of ROS and the latter initiating *NRF2* gene expression as an inducer of cell defence pathways against oxidative stress (Townsend and Tew, 2014).

Finally to determine the ultimate aim of this project and to verify that NRF2 was induced by chalcones thus leading to protection against MDA induced toxicity. *NRF2* was successfully knocked down, the cells pretreated with chalcones and then investigated for their ability to withstand MDA toxic insult. In spite of silencing the *NRF2* gene, the MTT results (Figure **7.11** and Figure **7.12**) show that pretreatment with chalcones lead to increased cell viability. The results illustrate a significant increase in cell viability at 400 µM MDA by DMU-1122 and 300 µM MDA by DMU-2210 comparing with the non-target gene, meaning that the chalcones retain the ability to prevent cell damage induced by MDA despite *NRF2* being knocked down. Consequently, the chalcones studied here, do have the ability to switch on the Nrf2 pathway (as shown by increased levels of NQO1 protein), but in its absence, these same chalcones still prevent MDA induced toxicity. There are several possible antioxidant enzymes not related to NRF2 which may be being switched by the chalcones:

1- Klotz and Steinbrenner (2017) have reported that the xenosensors such as Nrf2, arylhydrocarbon receptor (AhR), pregnane X receptor (PXR), constitutive androstane receptor (CAR) and peroxisome proliferator-activated receptors (PPARs) may possibly control ROS generation. In addition, they state that NQO1 may be upregulated by both Nrf2 and AhR.

2- Apostolova and Victor (2015) have reported that along with Nrf2 dependent enzymes such as SOD, TRX, GPX and CAT, a non-enzymatic products including GSH, ascorbic acid, a-tocopherol, ubiquinol and coenzyme Q also have an antioxidant activity.

3- Snezhkina *et al.* (2019) have reported that the prevention of oxidative stress may also be related to the induction of the enzyme of epoxide hydrolase 2 (EPHX2), as well as antioxidant genes like *ALDH4* and *TIGAR*.

Nonetheless, these results must be interpreted with caution and a number of limitations should be tolerate in mind, such as:

1- Using RNAi protocol might effect on cell viability due to using lipofectamine as a vector for knockdown gene of interest.

2- Despite of knockdown *NRF2* gene, chalcones remaining prevent the cell from MDA toxicity. And because of the project theory focused on Nrf2 pathway, it was ended with unknown prevention pathway induced by chalcones.

To conclude the result of this chapter, chalcone DMU-1122 and 1103 have increased the expression of NQO1 at 24 h. Also, the pretreated with the three chalcones have increased the level of NQO1 protein preventing the cell from MDA. Finally, the chemopreventive of chalcones not related to induce Nrf2 pathway, but it may be induce another preventive pathway.

Chapter 8 **Conclusions and future work**

8.1 Conclusions

The present study was designed to determine the ability of a library of thirty-one novel synthetic chalcones, kindly gifted by Prof Arroo from De Montfort University (DMU), to induce Nrf2 and as such act as a chemopreventive agent preventing malondialdehyde toxicity. Thus chalcones have tested for their cytotoxicity as an anticancer drug, however, in this research, they have tested for the first time as chemoprevention agents and in lung cell lines. Initially, the library has classified into two categories, including chalcones with alkoxy group and chalcones with methoxy, dioxy and dioxin group. Twelve chalcones have increased the fold induction of luciferase as a biomarker of inducing Nrf2 pathway in AREc32 reporter cell line. Then the twelve chalcones have tested in MRC-5 and MRC-5 SV2 lung cell lines, for determining the induction of antioxidant defence protein level like NQO1, resulted from switching on Nrf2 signalling pathway. The results showed chalcone DMU-2210, 1122, 1103 and 2265 ability to increase the NQO1 protein level in both cell lines.

To determine the chemopreventive activity, both lung cells have pretreated with a non-toxic concentrations of chalcones then with a range of concentrations of MDA. The results showed that chalcones DMU-1113, 2210, 2207 and 1122, which have alkoxy group, and DMU-2265 and 1103, which have methoxy and dioxy group, have the ability to prevent the normal cells from MDA toxicity. In contrast, DMU-1113 and 1122, which have alkoxy group, showed growth inhibition activity in transform cells agents MDA.

Based on previous results, NQO1 protein inducing chalcones can prevent MDA toxicity, such as DMU-2210 (3,4,3′,4′-OMe), DMU-1122 (4-OEt, 2′,4′-OMe) and DMU-1103 (2,4-OMe, 3′,4′-OCH_2O) that have been chosen to continue the project. Thus three chalcones have examined for their ability to prevent DNA damaged by MDA. Results pointed out that DMU-1122 can reduce the generation of ROS induced by MDA.

Furthermore, the three chalcones have indicated for their ability to prevent DNA damaged by MDA through decreasing the percentage of damaged DNA. To clarify the protective effect of chalcones related to switching on *NRF2* gene expression, DMU-1122 and DMU-1103 showed increasing in *NQO1* gene expression. Nevertheless, based on knockdown *NRF2* gene the three chalcones have remained preventing the cells against MDA.

The results of this investigation revealed that chalcones DMU-1122, 2210 and 1103 can afford cellular protection against MDA-induced toxicity. However, this protection was not diminished following silencing of the *NRF2* gene (Figure 8.1). It is therefore concluded that the identified chalcones may activat multiple pathways to prevent MDA-induced toxicity.

The development of chemoprevention drug has the target of efficiency protective agents and it has to be aware that this compound is not causing any harm to the major organs and metabolic pathways. Based on current investigation DMU-1122, 2210 and 1103 showed preventive activity against MDA as well as the used concentrations was not-toxic to the lung normal cell. That may assist decrease the risk of lung cancer development, specifically the smokers and non-smokers those exposed to smoking cigarette environmentally. Therefore to progress these finding as lung chemopreventive agents, the three chalcones have to investigate on different normal cell lines and also, in animal models to assure their safety.

Comparing chemopreventive agents such as *N*-acetylcysteine, α-tocopherol and β-carotene that seem having no chemopreventive activity against lung cancer, as well as β-carotene might have a negative effect on smokers (Bergan, 2001). DMU-1122, 2210 and 1103 chalcones showed non-toxicity and also, prevent MDA toxicity in a lung cell, which is possibly preferable to use as a lung cancer chemoprevention drug.

DMU-chalcones have examined in the current project as a chemopreventive agent. However, these chalcones could examine for their potential activity as an anticancer drug, such as DMU-1113 that have prevented the normal cell, on the same time increased the cytotoxic on transformed cell in the presence MDA. Moreover, several chalcones have examined for their bioactivities such as lophirone B (**23**) and C (**24**) as antibacterial (Ajiboye *et al*., 2019), flavokawain B (**33**) as antiprotozoal, anti-inflammatory and anticancer (Lin *et al.*, 2009; Rodrigues *et al.*, 2017; Hseu *et al.*, 2019), xanthoangelol (**18**) and 4-hydroxyderricin (**19**) as antidiabetic (Enoki *et al.*, 2007). In this case, DMU-chalcones probably can apply for treating infections, diabetic and tumours.

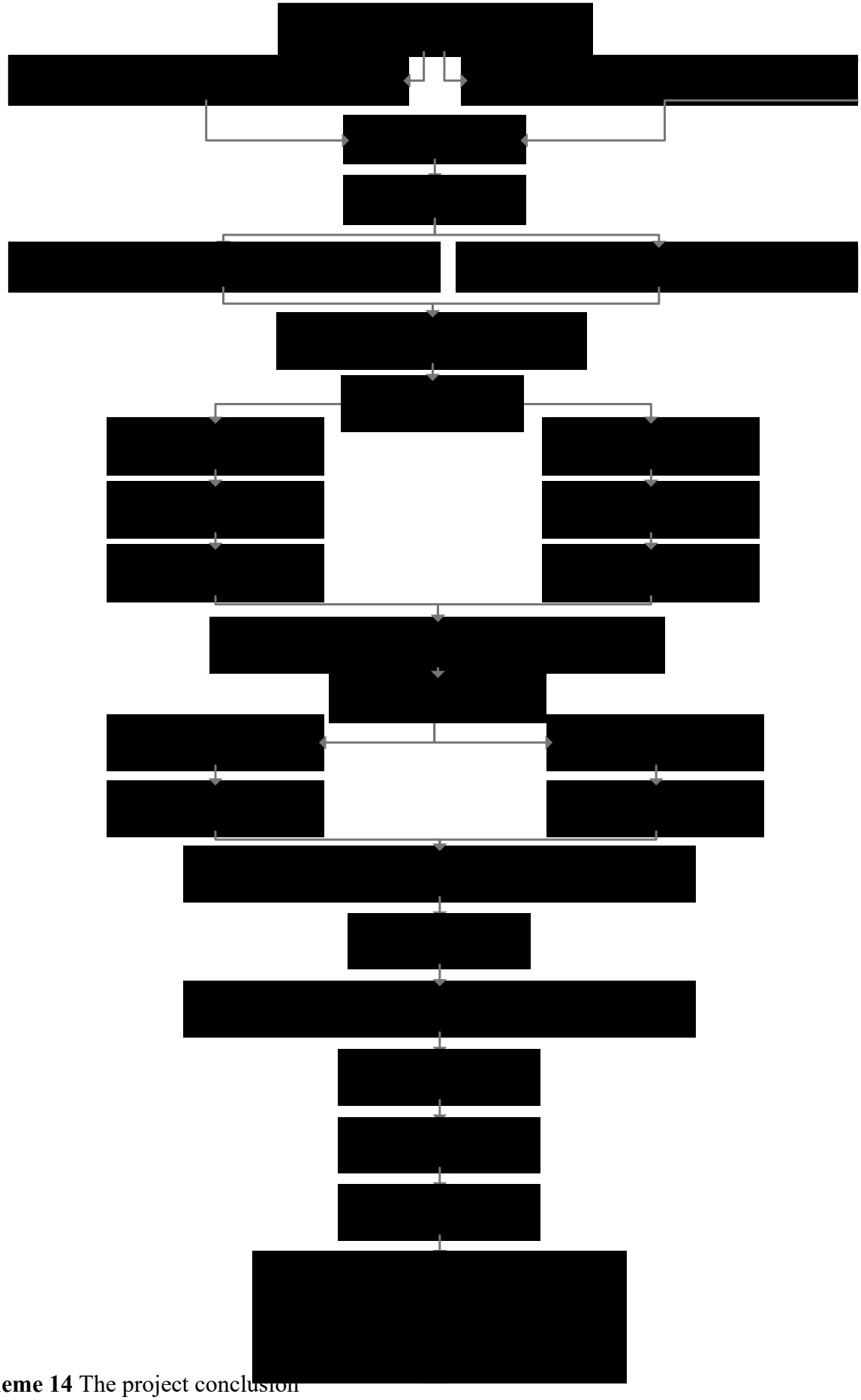

Scheme 14 The project conclusion

8.2 Future work

In the current project, a library of synthetic chalcones was carried out using different assays to determine the chemoprevention activity of thus chalcones due to switching on Nrf2 signalling pathway as a transcription factor, which controls the antioxidant defence enzyme and the drug-metabolism. A clear evidence has been found that three chalcones out of thirty-one have the ability to prevent DNA damaging by MDA. Nevertheless, further work might need to carry out to improve and complete these findings, such as:

1- Examine the library of chalcones with different applications like an antimicrobial, antidiabetic and anticancer.
2- Identify the cytotoxicity and the mechanism of action of DMU-1113 as an anticancer drug.
3- Investigate whether DMU-1122, 2210 and 1103 can prevent mutations, as well as DNA adducts that induce by MDA.
4- Examine DMU-1122, 2210 and 1103 on different cell lines and animal model to ensure they are safety in clinical use.
5- Evaluate DMU-1122, 2210 and 1103 in different preventive pathways.

Taken together, these findings suggest a role for DMU-1122, 2210 and 1103 chalcones in preventing DNA damage induced by carcinogens, as well as DMU-1113 and 1122 as anticancer products in lung cells. However, considerably more work will need to be done to determine the effect of these chalcones *in vivo* before they may be considered to human use.

References

Abbas, S.H., El-Hafeez, A.A.A., Shoman, M.E., Montano, M.M. and Hassan, H.A. (2019) New quinoline/chalcone hybrids as anti-cancer agents: design, synthesis, and evaluations of cytotoxicity and PI3K inhibitory activity. *Bioorganic Chemistry*, 82, 360-377.

Abu, N., Akhtar, M.N., Yeap, S.K., Lim, K.L., Ho, W.Y., Abdullah, M.P., Ho, C.L., Omar, A.R., Ismail, J. and Alitheen, N.B. (2016) Flavokawain B induced cytotoxicity in two breast cancer cell lines, MCF-7 and MDA-MB231 and inhibited the metastatic potential of MDA-MB231 via the regulation of several tyrosine kinases *in vitro*. *BMC Complementary and Alternative Medicine*, 16 (1), 86-100.

Ad, T., (2015) In Vitro Effects of Ascorbic Acid and Alpha-tocopherol on Serum Malondialdehyde formation in Diabetic Patients. *International Research Journal of Science and Engineering* , 3(1), 7–11.

Ahmad, S. (1995) *Oxidative stress and antioxidant defenses in biology*. Chapman & Hall.

Ahmed Laskar, A. and Younus, H. (2019) Aldehyde toxicity and metabolism: the role of aldehyde dehydrogenases in detoxification, drug resistance and carcinogenesis. *Drug Metabolism Reviews*, 51 (1), 42-64.

Ajiboye, T.O., Yakubu, M.T. and Oladiji, A.T. (2014) Electrophilic and Reactive Oxygen Species Detoxification Potentials of Chalcone Dimers is Mediated by Redox Transcription Factor Nrf-2. *Journal of Biochemical and Molecular Toxicology*, 28 (1), 11-22.

Ajiboye, T., Aliyu, N. and Ajala-Lawal, R. (2019) Lophirones B and C induce oxidative cellular death pathway in Acinetobacter baumannii by inhibiting DNA gyrase. *Microbial Pathogenesis*, 130, 226-231.

Akihisa, T., Tokuda, H., Hasegawa, D., Ukiya, M., Kimura, Y., Enjo, F., Suzuki, T. and Nishino, H. (2006) Chalcones and other compounds from the exudates of *Angelica keiskei* and their cancer chemopreventive effects. *Journal of Natural Products*, 69 (1), 38-42.

Aksöz, B.E. and Ertan, R. (2011) Chemical and structural properties of chalcones I. *FABAD J Pharm Sci*, 36, 223-242.

Albena, T.D.-K., Holtzclaw, W.D., Robert, N.C., Ken, I., Nobunao, W., Yasutake, K., Masayuki, Y. and Paul, T. (2002) Direct evidence that sulfhydryl groups of Keap1 are the sensors regulating induction of phase 2 enzymes that protect against carcinogens and

oxidants. *Proceedings of the National Academy of Sciences of the United States of America*, 99 (18), 11908.

Alberts, B., Bray, D., Hopkin, K., Johnson, A.D., Lewis, J., Raff, M., Roberts, K. and Walter, P. (2019) *Essential cell biology*. 5th ed. New York W.W. Norton and Company.

Ali, H., Assiri, M.A., Shearn, C.T. and Fritz, K.S. (2019) Lipid peroxidation derived reactive aldehydes in alcoholic liver disease. *Current opinion in toxicology*, 13, 110-117.

Aliyu, N.O., Ajala-Lawal, R.A. and Ajiboye, T.O. (2018) Lophirones B and C halt acetaminophen hepatotoxicity by upregulating redox transcription factor Nrf-2 through Akt, PI3K, and PKC pathways. *Journal of Biochemical and Molecular Toxicology*, 32 (6), e22055.

Allard, S.T. and Kopish, K. (2008) Luciferase reporter assays: powerful, adaptable tools for cell biology research. *Cell Notes*, 21, 23-26.

Altıntop, M.D., Sever, B., Çiftçi, G.A., Kucukoglu, K., Özdemir, A., Soleimani, S.S., Nadaroglu, H. and Kaplancıklı, Z.A. (2017) Synthesis and evaluation of new benzodioxole-based dithiocarbamate derivatives as potential anticancer agents and hCA-I and hCA-II inhibitors. *European Journal of Medicinal Chemistry*, 125, 190-196.

American Cancer Society (2018) *Global Cancer: Facts & Figures* [online]

Available at: https://www.cancer.org/content/dam/cancer-org/research/cancer-facts-and-statistics/annual-cancer-facts-and-figures/2018/cancer-facts-and-figures-2018.pdf

Ames, B.N. & Gold, L.S. (1998) The causes and prevention of cancer: the role of environment. *Biotherapy (Dordrecht, Netherlands)*, 11(2-3), 205–220.

Anand, P., Kunnumakara, A.B., Sundaram, C., Harikumar, K.B., Tharakan, S.T., Lai, O.S., Sung, B. and Aggarwal, B.B. (2008) Cancer is a preventable disease that requires major lifestyle changes. *Pharmaceutical Research*, 25 (9), 2097-2116.

Angel, C. and Mario, D. (2017) *Impact of Lipid Peroxidation on the Physiology and Pathophysiology of Cell Membranes*. Spain: Frontiers Media SA.

Apostolova, N. and Victor, V.M. (2015) Molecular strategies for targeting antioxidants to mitochondria: therapeutic implications. *Antioxidants and Redox Signaling*, 22 (8), 686-729.

Ardite, E., Peinado, V.I., Rabinovich, R.A., Fernández-Checa, J.C., Roca, J. and Barberà, J.A. (2006) Systemic effects of cigarette smoke exposure in the guinea pig. *Respiratory Medicine*, 100 (7), 1186-1194.

Arianingrum, R., Sunarminingsih, R., Meiyanto, E. and Mubarika, S. (2016) Cytotoxic and Apoptotic Effects of Para-Hydroxy Meta Methoxy Chalcone (pHmMC) on T47D Breast Cancer Cells. *International Journal of Pharmaceutical and Clinical Research*, 8 (5), 335-340.

Atasayar, S., Orhan, H. and Özgüneş, H. (2004) Malondialdehyde quantification in blood plasma of tobacco smokers and non-smokers. *FABAD Journal of Pharmaceutical Sciences*, 29 (1), 15-19.

Ayala, A., Muñoz, M.F. and Argüelles, S. (2014) Lipid Peroxidation: Production, Metabolism, and Signaling Mechanisms of Malondialdehyde and 4-Hydroxy-2-Nonenal. *Oxidative Medicine and Cellular Longevity*, 2014 (4).

Azqueta, A. and Collins, A.R. (2006) The comet assay: a sensitive and quantitative method for analysis of DNA damage. *Encyclopedia of Analytical Chemistry: Applications, Theory and Instrumentation*.

Azqueta, A. and Collins, A.R. (2013) The essential comet assay: a comprehensive guide to measuring DNA damage and repair. *Archives of Toxicology*, 87 (6), 949.

Azqueta, A., Slyskova, J., Langie, S.A.S., O'Neill Gaivão, I. and Collins, A. (2014) Comet assay to measure DNA repair: approach and applications. *Frontiers in Genetics*, 5, 288-288.

Bai, H., Chen, W., Wu, W., Ma, Z., Zhang, H., Jiang, T., Zhang, T., Zhou, Y., Du, L., Shen, Y. and Li, M. (2015) Discovery of a series of 2-phenylnaphthalenes as firefly luciferase inhibitors. *Royal Society of Chemistry Advances*, 5 (78), 63450-63457.

Baird, L. and Dinkova-Kostova, A.T. (2011) The cytoprotective role of the Keap1–Nrf2 pathway. *Archives of Toxicology*, 85 (4), 241-272.

Bandgar, B.P., Adsul, L.K., Lonikar, S.V., Chavan, H.V., Shringare, S.N., Patil, S.A., Jalde, S.S., Koti, B.A., Dhole, N.A. and Gacche, R.N. (2013) Synthesis of novel carbazole chalcones as radical scavenger, antimicrobial and cancer chemopreventive agents. *Journal of Enzyme Inhibition and Medicinal Chemistry*, 28 (3), 593-600.

Barrera-Rodríguez, R. (2018) Importance of the Keap1-Nrf2 pathway in NSCLC: Is it a possible biomarker? *Biomedical reports*, 9 (5), 375-382.

Bartoli, M.L., Novelli, F., Costa, F., Malagrinò, L., Melosini, L., Bacci, E., Cianchetti, S., Dente, F.L., Franco, A.D., Vagaggini, B. and Paggiaro, P.L. (2011) Malondialdehyde in Exhaled Breath Condensate as a Marker of Oxidative Stress in Different Pulmonary Diseases. *Mediators of Inflammation*, 2011 (2011).

Bartsch, H., Nair, J. and Owen, R.W. (1999) Dietary polyunsaturated fatty acids and cancers of the breast and colorectum: emerging evidence for their role as risk modifiers. *Carcinogenesis*, 20 (12), 2209-2218.

Beddowes, E.J., Faux, S.P. and Chipman, J.K. (2003) Chloroform, carbon tetrachloride and glutathione depletion induce secondary genotoxicity in liver cells via oxidative stress. *Toxicology*, 187 (2-3), 101-115.

Bergan, R.C. (2001) *Cancer chemoprevention*. London: Boston, Mass. Kluwer Academic.

Best, S.A. and Sutherland, K.D. (2018) "Keaping" a lid on lung cancer: the Keap1-Nrf2 pathway. *Cell Cycle*, 17 (14), 1696-1707.

Blair, I.A. (2008) DNA adducts with lipid peroxidation products. *Journal of Biological Chemistry*, 283 (23), 15545-15549.

Blanquer-Rosselló, M.M., Oliver, J., Valle, A. and Roca, P. (2013) Effect of xanthohumol and 8-prenylnaringenin on MCF-7 breast cancer cells oxidative stress and mitochondrial complexes expression. *Journal of Cellular Biochemistry*, 114 (12), 2785-2794.

Boelsterli, U.A. (2007) *Mechanistic toxicology : the molecular basis of how chemicals disrupt biological targets*. 2nd ed. London: Boca Raton, CRC Press.

Boerboom, A.-M.J., Vermeulen, M., van der Woude, H., Bremer, B.I., Lee-Hilz, Y.Y., Kampman, E., Van Bladeren, P.J., Rietjens, I.M. and Aarts, J.M. (2006) Newly constructed stable reporter cell lines for mechanistic studies on electrophile-responsive element-mediated gene expression reveal a role for flavonoid planarity. *Biochemical Pharmacology*, 72 (2), 217-226.

Bousquet, M.S., Ratnayake, R., Pope, J.L., Chen, Q.-Y., Zhu, F., Chen, S., Carney, T.J., Gharaibeh, R.Z., Jobin, C. and Paul, V.J. (2019) Seaweed natural products modify the host inflammatory response via Nrf2 signaling and alter colon microbiota composition and gene expression. *Free Radical Biology and Medicine*.

Bryan, H.K., Olayanju, A., Goldring, C.E. and Park, B.K. (2013) The Nrf2 cell defence pathway: Keap1-dependent and -independent mechanisms of regulation. *Biochemical Pharmacology*, 85 (6), 705-717.

Bukhari, S.N., Tajuddin, Y., Benedict, V.J., Lam, K.W., Jantan, I., Jalil, J. and Jasamai, M. (2014) Synthesis and evaluation of chalcone derivatives as inhibitors of neutrophils'

chemotaxis, phagocytosis and production of reactive oxygen species. *Chemical Biology and Drug Design*, 83 (2), 198-206.

Bustin, S.A. (2004) *A-Z of quantitative PCR*. La Jolla, CA: La Jolla, CA : International University Line.

Butler, M. (2004) *Animal cell culture and technology*. 2nd ed. London: BIOS Scientific Publishers.

Cancer Research UK (2019) [online]

Available at: https://www.cancerresearchuk.org/health-professional/cancer-statistics/worldwide-cancer

[Accessed: 18/09/2019]

Cancer Research UK. (2019) *Lung cancer statistics* [online]

Available at: https://www.cancerresearchuk.org/health-professional/cancer-statistics/statistics-by-cancer-type/lung-cancer#heading-Four

Carniel, F.C., Zanelli, D., Bertuzzi, S. and Tretiach, M. (2015) Desiccation tolerance and lichenization: a case study with the aeroterrestrial microalga *Trebouxia* sp.(Chlorophyta). *Planta*, 242 (2), 493-505.

Castello, A. (2012) Insights into RNA biology from an atlas of mammalian mRNA-binding proteins. *Cell*, 149 (6), 1393.

Cazarolli, L.H., Kappel, V.D., Zanatta, A.P., Suzuki, D.O.H., Yunes, R.A., Nunes, R.J., Pizzolatti, M.G. and Silva, F.R.M.B. (2013) Natural and synthetic chalcones: Tools for the study of targets of action - Insulin secretagogue or insulin mimetic? *Studies in Natural Products Chemistry*, 39, 47-89.

Champelovier, P., Mininno, M., Duchamp, E., Nicolle, E., Curri, V., Boumendjel, A. and Boutonnat, J. (2011) Cytotoxicity of chalcone derivatives towards glioblastoma. *Anticancer Research*, 31 (10), 3213-3218.

Chauhan, S.S., Singh, A.K., Meena, S., Lohani, M., Singh, A., Arya, R.K., Cheruvu, S.H., Sarkar, J., Gayen, J.R. and Datta, D. (2014) Synthesis of novel *β*-carboline based chalcones with high cytotoxic activity against breast cancer cells. *Bioorganic and Medicinal Chemistry Letters*, 24 (13), 2820-2824.

Chen, B.-Y. and Janes, H.W. (2002) *PCR cloning protocols*. Springer Science and Business Media.

Chen, C. and Kong, A.-N.T. (2004) Dietary chemopreventive compounds and ARE/EpRE signaling. *Free Radical Biology and Medicine*, 36 (12), 1505-1516.

Chen, C. and Kong, A.-N.T. (2005) Dietary cancer-chemopreventive compounds: from signaling and gene expression to pharmacological effects. *Trends in Pharmacological Sciences*, 26 (6), 318-326.

Chen, G., Zhou, D., Li, X.-Z., Jiang, Z., Tan, C., Wei, X.-Y., Ling, J., Jing, J., Liu, F. and Li, N. (2017) A natural chalcone induces apoptosis in lung cancer cells: 3D-QSAR, docking and an *in vivo/vitro* assay. *Scientific Reports*, 7 (1), 10729-10729.

Cheng, Z., Teo, G., Krueger, S., Rock, T.M., Koh, H.W., Choi, H. and Vogel, C. (2016) Differential dynamics of the mammalian mRNA and protein expression response to misfolding stress. *Molecular Systems Biology*, 12 (1).

Chiou, C.-C., Chang, P.-Y., Chan, E.-C., Wu, T.-L., Tsao, K.-C. and Wu, J.T. (2003) Urinary 8-hydroxydeoxyguanosine and its analogs as DNA marker of oxidative stress: development of an ELISA and measurement in both bladder and prostate cancers. *Clinica Chimica Acta*, 334 (1-2), 87-94.

Cho, J.-M., Manandhar, S., Lee, H.-R., Park, H.-M. and Kwak, M.-K. (2008) Role of the Nrf2-antioxidant system in cytotoxicity mediated by anticancer cisplatin: implication to cancer cell resistance. *Cancer Letters*, 260 (1-2), 96-108.

Clayden, J. (2002) *Organolithiums: selectivity for synthesis: Regioselective Synthesis of Organolithiums by Deprotonation*. Elsevier.

Collado, R., Ivars, D., Oliver, I., Tormos, C., Egea, M., Miguel, A., Sáez, G.T. and Carbonell, F. (2014) Increased oxidative damage associated with unfavorable cytogenetic subgroups in chronic lymphocytic leukemia. *BioMed Research International*, 2014.

Collins, A.R. (2004) The comet assay for DNA damage and repair. *Molecular Biotechnology*, 26 (3), 249.

Cooper, G.M. and Hausman, R.E. (2009) *The cell : a molecular approach*. 5th ed. Washington: Sunderland, Mass. : Sinauer Associates.

Corso, C.D., Rutter, C.E., Wilson, L.D., Kim, A.W., Decker, R.H. and Husain, Z.A. (2015) Re-evaluation of the role of postoperative radiotherapy and the impact of radiation dose for non–small-cell lung cancer using the National Cancer Database. *Journal of Thoracic Oncology*, 10 (1), 148-155.

Czauderna, C., Palestino-Dominguez, M., Castven, D., Becker, D., Zanon-Rodriguez, L., Hajduk, J., Mahn, F.L., Herr, M., Strand, D. and Strand, S. (2018) Ginkgo biloba induces different gene expression signatures and oncogenic pathways in malignant and non-malignant cells of the liver. *PLoS One*, 13 (12), e0209067.

Da Rocha, A.B., Lopes, R.M. and Schwartsmann, G. (2001) Natural products in anticancer therapy. *Current Opinion in Pharmacology*, 1 (4), 364-369.

Da Silva Lima, D.C., do Vale, C.R., Véras, J.H., Bernardes, A., Pérez, C.N. and Chen-Chen, L. (2017) Absence of genotoxic effects of the chalcone (E)-1-(2-hydroxyphenyl)-3-(4-methylphenyl)-prop-2-en-1-one) and its potential chemoprevention against DNA damage using *in vitro* and *in vivo* assays. *PLOS One*, 12 (2), e0171224. https://doi.org/0171210.0171371/journal.pone.0171224.

Dalle-Donne, I., Rossi, R., Giustarini, D., Milzani, A. and Colombo, R. (2003) Protein carbonyl groups as biomarkers of oxidative stress. *Clinica Chimica Acta*, 329 (1-2), 23-38.

Davis, C.D. and Ross, A. (2019) *Diet and Cancer Prevention*. 3rd ed. US: Taylor and Francis Group.

Day, D.B. (2017) *The Effects of Ozone Exposure on Cardiovascular Pathophysiology*thesis, Duke University.

De Bont, R. and van Larebeke, N. (2004) Endogenous DNA damage in humans: a review of quantitative data. *Mutagenesis*, 19 (3), 169-185.

De Freitas Silva, M., Pruccoli, L., Morroni, F., Sita, G., Seghetti, F., Viegas Jr, C. and Tarozzi, A. (2018) The Keap1/Nrf2-ARE pathway as a pharmacological target for chalcones. *Molecules*, 23 (7), 1803.

Deb Majumdar, I. (2011) Synthetic cyclohexenyl chalcone natural products possess cytotoxic activities against prostate cancer cells and inhibit cysteine cathepsins *in vitro*. *Biochemical and Biophysical Research Communications*, 416 (3-4), 397.

DeLuca, M. and McElroy, W.D. (1974) Kinetics of the Firefly Luciferase Catalyzed Reactions. *Biochemistry*, 13 (5), 921-925.

Ding, C., Fan, X. and Wu, G. (2017) Peroxiredoxin 1–an antioxidant enzyme in cancer. *Journal of Cellular and Molecular Medicine*, 21 (1), 193-202.

Dinkova-Kostova, A.T., Abeygunawardana, C. and Talalay, P. (1998) Chemoprotective properties of phenylpropenoids, bis (benzylidene) cycloalkanones, and related Michael

reaction acceptors: correlation of potencies as phase 2 enzyme inducers and radical scavengers. *Journal of Medicinal Chemistry*, 41 (26), 5287-5296.

Dinkova-Kostova, A.T. and Talalay, P. (2010) NAD(P)H:quinone acceptor oxidoreductase 1 (NQO1), a multifunctional antioxidant enzyme and exceptionally versatile cytoprotector. *Archives of Biochemistry and Biophysics*, 501 (1), 116-123.

Dong, J., Li, Y., Xiao, H., Luo, D., Zhang, S., Zhu, C., Jiang, M., Cui, M., Lu, L. and Fan, S. (2019) Cordycepin sensitizes breast cancer cells toward irradiation through elevating ROS production involving Nrf2. *Toxicology and Applied Pharmacology*, 364, 12-21.

Doyle, A. and Griffiths, J.B. (1998) *Cell and tissue culture: laboratory procedures in biotechnology*. Wiley.

Ducki, S., Rennison, D., Woo, M., Kendall, A., Chabert, J.F.D., McGown, A.T. and Lawrence, N.J. (2009) Combretastatin-like chalcones as inhibitors of microtubule polymerization. Part 1: Synthesis and biological evaluation of antivascular activity. *Bioorganic and Medicinal Chemistry*, 17 (22), 7698-7710.

Dunphy, G., Flannery, S.M., Almine, J.F., Connolly, D.J., Paulus, C., Jønsson, K.L., Jakobsen, M.R., Nevels, M.M., Bowie, A.G. and Unterholzner, L. (2018) Non-canonical activation of the DNA sensing adaptor STING by ATM and IFI16 mediates NF-κB signaling after nuclear DNA damage. *Molecular Cell*, 71 (5), 745-760. e745.

Elhalem, E., Recio, R., Werner, S., Lieder, F., Calderón-Montaño, J.M., López-Lázaro, M., Fernández, I. and Khiar, N. (2014) Sulforaphane homologues: Enantiodivergent synthesis of both enantiomers, activation of the Nrf2 transcription factor and selective cytotoxic activity. *European Journal of Medicinal Chemistry*, 87, 552-563.

Enoki, T., Ohnogi, H., Nagamine, K., Kudo, Y., Sugiyama, K., Tanabe, M., Kobayashi, E., Sagawa, H. and Kato, I. (2007) Antidiabetic activities of chalcones isolated from a Japanese herb, *Angelica keiskei*. *Journal of Agricultural and Food Chemistry*, 55 (15), 6013-6017.

Ezzat, S.M., El-Halawany, A.M., Hamed, A.R. and Abdel-Sattar, E. (2018) Role Phytochemicals Play in the Activation of Antioxidant Response Elements (AREs) and Phase II Enzymes and Their Relation to Cancer Progression and Prevention. In: *Studies in Natural Products Chemistry.* Elsevier. pp. 345-369.

Fahn, H.-J., Wang, L.-S., Kao, S.-H., Chang, S.-C., Huang, M.-H. and Wei, Y.-H. (1998) Smoking-associated mitochondrial DNA mutations and lipid peroxidation in human lung tissues. *American Journal of Respiratory Cell and Molecular Biology*, 19 (6), 901-909.

Farmer, P.B. (2004) DNA and protein adducts as markers of genotoxicity. *Toxicology Letters*, 149 (1-3), 3-9.

Farrell, R.E. (2017) *RNA methodologies : laboratory guide for isolation and characterization*. 5th ed. London : Academic Press.

Fay, L.B., Kussmann, M. and Royal Society of, C. (2010) *Mass spectrometry and nutrition research*. Cambridge: Royal Society of Chemistry.

Fedorov, Y., Anderson, E.M., Birmingham, A., Reynolds, A., Karpilow, J., Robinson, K., Leake, D., Marshall, W.S. and Khvorova, A. (2006) Off-target effects by siRNA can induce toxic phenotype. *RNA*, 12 (7), 1188-1196.

Ferk, F., Huber, W.W., Filipič, M., Bichler, J., Haslinger, E., Mišík, M., Nersesyan, A., Grasl-Kraupp, B., Žegura, B. and Knasmüller, S. (2010) Xanthohumol, a prenylated flavonoid contained in beer, prevents the induction of preneoplastic lesions and DNA damage in liver and colon induced by the heterocyclic aromatic amine amino-3-methyl-imidazo[4,5- f]quinoline (IQ). *Mutation Research - Fundamental and Molecular Mechanisms of Mutagenesis*, 691 (1-2), 17-22.

Fracasso, M.E., Perbellini, L., Soldà, S., Talamini, G. and Franceschetti, P. (2002) Lead induced DNA strand breaks in lymphocytes of exposed workers: role of reactive oxygen species and protein kinase C. *Mutation Research/Genetic Toxicology and Environmental Mutagenesis*, 515 (1-2), 159-169.

Franceschelli, S., Pesce, M., Vinciguerra, I., Ferrone, A., Riccioni, G., Antonia, P., Grilli, A., Felaco, M. and Speranza, L. (2011) Licocalchone-C extracted from Glycyrrhiza glabra inhibits lipopolysaccharide-interferon-γ inflammation by improving antioxidant conditions and regulating inducible nitric oxide synthase expression. *Molecules*, 16 (7), 5720-5734.

Franks, L.M. (1997) *Introduction to the cellular and molecular biology of cancer*. 3rd ed. Oxford Universty. Press.

Freshney, R.I. (2016) *Culture of animal cells : a manual of basic technique and specialized applications*. 7th ed. Hoboken, New Jersey : Wiley-Blackwell.

Gao, D., Liu, F., Li, Z. and Guan, Y. (2019) Isobavachalcone attenuates Sephadex-induced lung injury via activation of A20 and NRF2/HO-1 in rats. *European Journal of Pharmacology*, 848, 49-54.

Ghani, M.A., Barril, C., Bedgood Jr, D.R. and Prenzler, P.D. (2017) Measurement of antioxidant activity with the thiobarbituric acid reactive substances assay. *Food Chemistry*, 230, 195-207.

Ghribia, L., Ghouilaa, H., Omrib, A., Besbesb, M. and Janneta, H.B. (2014) Antioxidant and anti–acetylcholinesterase activities of extracts and secondary metabolites from *Acacia cyanophylla*. *Asian Pacific Journal of Tropical Biomedicine*, 4 (1), S417-S423.

Girard-Lalancette, K., Pichette, A. and Legault, J. (2009) Sensitive cell-based assay using DCFH oxidation for the determination of pro-and antioxidant properties of compounds and mixtures: Analysis of fruit and vegetable juices. *Food Chemistry*, 115 (2), 720-726.

Goldring, C., Kitteringham, N., Jenkins, R., Copple, I., Jeannin, J. and Park, B. (2006) Plasticity in cell defence: access to and reactivity of critical protein residues and DNA response elements. *Journal of Experimental Biology*, 209 (12), 2337-2343.

Gönenç, A., Özkan, Y., Torun, M. and Şimşek, B. (2001) Plasma malondialdehyde (MDA) levels in breast and lung cancer patients. *Journal of Clinical Pharmacy and Therapeutics*, 26 (2), 141-144.

Gong, H., Zhang, B.-k., Yan, M., Fang, P.-f., Hu, C.-p., Yang, Y., Cao, P., Jiang, P. and Fan, X.-r. (2015) A protective mechanism of licorice (Glycyrrhiza uralensis): isoliquiritigenin stimulates detoxification system via Nrf2 activation. *Journal of Ethnopharmacology*, 162, 134-139.

Gupta, D., Jain, D. and Trivedi, P. (2010) Recent advances in chalcones as antiinfective agents. *International Journal of Chemical Sciences*, 8 (1), 649-654.

Gupta, R.C. (2019) *Biomarkers in toxicology*. 2nd ed. Oxford, United Kingdom: Academic Press.

Gupta, R.C. and Lutz, W.K. (1999) Background DNA damage for endogenous and unavoidable exogenous carcinogens: a basis for spontaneous cancer incidence? *Mutation Research*, 424 (1-2), 1-8.

Gupte, A. and Mumper, R.J. (2009) Elevated copper and oxidative stress in cancer cells as a target for cancer treatment. *Cancer Treatment Reviews*, 35 (1), 32-46.

Gutierrez, R.M.P., Muñiz-Ramirez, A. and Sauceda, J.V. (2015) The potential of chalcones as a source of drugs. *African Journal of Pharmacy and Pharmacology*, 9 (8), 237-257.

Gwozdz, T. and Dorey, K. (2017) *Basic Science Methods for Clinical Researchers: Western Blot*. Jalali, M., Saldanha, F. Y. L. and Jalali, M. (ed.). London UK,.Elsevier, Academic Press.

Hakala, K., Auriola, S., Koivisto, A. and Lönnberg, H. (1999) Mass spectrometric (HPLC/ESI–MS/MS) quantification of pyrimido [1, 2-a] purin-10 (3H)-one, a guanine adduct formed by reaction of malondialdehyde with DNA. *Journal of Pharmaceutical and Biomedical Analysis*, 21 (5), 1053-1061.

Han, G.E., Kang, H., Chung, S., C., L., A., L.J., Jin-Hee Lee, J., Wooki Kim 5, Kim, S. and H., L.J. (2018) Novel Neohesperidin Dihydrochalcone Analogue Inhibits Adipogenic Differentiation of Human Adipose-Derived Stem Cells through the Nrf2 Pathway. *International Journal of Molecular Sciences*, 19 (8), 2215.

Han, J.Y., Cho, S.S., Yang, J.H., Kim, K.M., Jang, C.H., Park, D.E., Bang, J.S., Jung, Y.S. and Ki, S.H. (2015) The chalcone compound isosalipurposide (ISPP) exerts a cytoprotective effect against oxidative injury via Nrf2 activation. *Toxicology and Applied Pharmacology*, 287 (1), 77-85.

Harmastuti, N., Herowati, R., Susilowati, D., Pranowo, H.D. and Mubarika, S. (2012) Synthesis and cytotoxic activity of chalcone derivatives on human breast cancer cell lines. *Indonesian Journal of Chemistry*, 12 (3), 261-267.

Helbock, H.J., Beckman, K.B., Shigenaga, M.K., Walter, P.B., Woodall, A.A., Yeo, H.C. and Ames, B.N. (1998) DNA oxidation matters: the HPLC–electrochemical detection assay of 8-oxo-deoxyguanosine and 8-oxo-guanine. *Proceedings of the National Academy of Sciences*, 95 (1), 288-293.

Hickey, G.I. (2007) *Genetics*. 3rd ed. New York, Abingdon: Taylor and Francis Group.

Higdon, J. and Frei, B. (2004) *Vitamine C as a Cancer Chemopreventive Agent*. Cancer Chemoprevention. Ed. Kelloff, G.J., Hawk, E.T. and Sigman, C.C., V.1, Humana Press, Totowa, New Jersey.

Higgins, L.G. (2008) Induction of cancer chemopreventive enzymes by coffee is mediated by transcription factor Nrf2. Evidence that the coffee-specific diterpenes cafestol and kahweol confer protection against acrolein. *Toxicology and Applied Pharmacology*, 226 (3), 328-337.

Hininger, I., Chollat-Namy, A., Sauvaigo, S., Osman, M., Faure, H., Cadet, J., Favier, A. and Roussel, A.-M. (2004) Assessment of DNA damage by comet assay on frozen total blood: method and evaluation in smokers and non-smokers. *Mutation Research/Genetic Toxicology and Environmental Mutagenesis*, 558 (1-2), 75-80.

Ho, C.-Y., Lu, C.-C., Jhang, J.-J. and Yen, G.-C. (2017) Diallyl sulfide attenuates transforming growth factor-*β*-stimulated pulmonary fibrosis through Nrf2 activation in lung MRC-5 fibroblast. *Journal of Functional Foods*, 28, 314-320.

Homma, S., Ishii, Y., Morishima, Y., Yamadori, T., Matsuno, Y., Haraguchi, N., Kikuchi, N., Satoh, H., Sakamoto, T. and Hizawa, N. (2009) Nrf2 enhances cell proliferation and resistance to anticancer drugs in human lung cancer. *Clinical Cancer Research*, 15 (10), 3423-3432.

Hopkins, B.L., Nadler, M., Skoko, J.J., Bertomeu, T., Pelosi, A., Shafaei, P.M., Levine, K., Schempf, A., Pennarun, B. and Yang, B. (2018) A peroxidase peroxiredoxin 1-specific redox regulation of the novel FOXO3 microRNA target let-7. *Antioxidants and Redox Signaling*, 28 (1), 62-77.

Horley, N.J., Beresford, K.J., Kaduskar, S., Joshi, P., McCann, G.J., Ruparelia, K.C., Williams, I.S., Gatchie, L., Sonawane, V.R. and Bharate, S.B. (2017) (E)-3-(3, 4, 5-Trimethoxyphenyl)-1-(pyridin-4-yl) prop-2-en-1-one, a heterocyclic chalcone is a potent and selective CYP1A1 inhibitor and cancer chemopreventive agent. *Bioorganic and Medicinal Chemistry Letters*, 27 (24), 5409-5414.

Hseu, Y.-C., Tsai, T.-J., Korivi, M., Liu, J.-Y., Chen, H.-J., Lin, C.-M., Shen, Y.-C. and Yang, H.-L. (2017) Antitumor properties of Coenzyme Q 0 against human ovarian carcinoma cells via induction of ROS-mediated apoptosis and cytoprotective autophagy. *Scientific Reports*, 7 (1), 8062.

Hseu, Y., Lee, M.S., Wu, C.R., Cho, H., Lin, K., Lai, G., Wang, S., Kuo, Y., Kumar, K. and Yang, H.L. (2012) The Chalcone Flavokawain B Induces G(2)/M Cell-Cycle Arrest and Apoptosis in Human Oral Carcinoma HSC-3 Cells through the Intracellular ROS Generation and Downregulation of the Akt/p38 MAPK Signaling Pathway. *Journal of Agricultural and Food Chemistry*, 60 (9), 2385-2397.

Hseu, Y.C., Yang, T.Y., Li, M.L., Rajendran, P., Mathew, D.C., Tsai, C.H., Lin, R.W., Lee, C.C. and Yang, H.L. (2019) Chalcone flavokawain A attenuates TGF-β1-induced fibrotic pathology via inhibition of ROS/Smad3 signaling pathways and induction of Nrf2/ARE-mediated antioxidant genes in vascular smooth muscle cells. *Journal of Cellular and Molecular Medicine*, 23 (2), 775-788.

Hu, T., Linghu, K., Huang, S., Battino, M., Georgiev, M.I., Zengin, G., Li, D., Deng, Y., Wang, Y. and Cao, H. (2019) Flaxseed extract induces apoptosis in human breast cancer MCF-7 cells. *Food and Chemical Toxicology*, 127, 188-196.

Hunt, I., Muers, M.F. and Treasure, T. (2009) *ABC of lung cancer*. Chichester: Chichester : Wiley-Blackwell/BMJ.

Huschtscha, L. and Holliday, R. (1983) Limited and unlimited growth of SV40-transformed cells from human diploid MRC-5 fibroblasts. *Journal of Cell Science*, 63 (1), 77-99.

Hwa Yun, B., Guo, J., Bellamri, M. and Turesky, R.J. (2018) DNA adducts: Formation, biological effects, and new biospecimens for mass spectrometric measurements in humans. *Mass Spectrometry Reviews*.

International Agency for Research on Cancer (2004) *Tobacco smoke and involuntary smoking* [online]

Available at: http://smokefreeengland.co.uk/files/summary-evaluation.pdf

Irigaray, P., Newby, J.A., Clapp, R., Hardell, L., Howard, V., Montagnier, L., Epstein, S. and Belpomme, D. (2007) Lifestyle-related factors and environmental agents causing cancer: An overview. *Biomedicine & Pharmacotherapy*, 61 (10), 640-658.

Isik, B., Ceylan, A. and Isik, R. (2007) Oxidative stress in smokers and non-smokers. *Inhalation Toxicology*, 19 (9), 767-769.

Iso, T., Suzuki, T., Baird, L. and Yamamoto, M. (2016) Absolute amounts and status of the Nrf2-Keap1-Cul3 complex within cells. *Molecular and Cellular Biology*, 36 (24), 3100-3112.

Ito, F., Sono, Y. and Ito, T. (2019) Measurement and Clinical Significance of Lipid Peroxidation as a Biomarker of Oxidative Stress: Oxidative Stress in Diabetes, Atherosclerosis, and Chronic Inflammation. *Antioxidants (Basel, Switzerland)*, 8 (3).

Izumi, Y., Matsumura, A., Wakita, S., Akagi, K.-i., Fukuda, H., Kume, T., Irie, K., Takada-Takatori, Y., Sugimoto, H. and Hashimoto, T. (2012) Isolation, identification, and biological evaluation of Nrf2-ARE activator from the leaves of green perilla (Perilla frutescens var. crispa f. viridis). *Free Radical Biology and Medicine*, 53 (4), 669-679.

Izumi, Y., Kataoka, H., Inose, Y., Akaike, A., Koyama, Y. and Kume, T. (2018) Neuroprotective effect of an Nrf2-ARE activator identified from a chemical library on dopaminergic neurons. *European Journal of Pharmacology*, 818, 470-479.

Jacobs, J.P., Jones, C. and Baille, J. (1970) Characteristics of a human diploid cell designated MRC-5. *Nature*, 227 (5254), 168.

Jadoon, S. and Malik, A. (2017) A review article on the formation, mechanism and biochemistry of MDA and MDA as a biomarker of oxidative sresss. *International Journal of Advanced Research*, 5 (12), 811-818.

Jaiswal, A.K. (2000) Regulation of genes encoding NAD(P)H:quinone oxidoreductases. *Free Radical Biology and Medicine*, 29 (3-4), 254-262.

Janero, D.R. (1990) Malondialdehyde and thiobarbituric acid-reactivity as diagnostic indices of lipid peroxidation and peroxidative tissue injury. *Free Radical Biology and Medicine*, 9 (6), 515-540.

Jelic, M.D., Mandic, A.D., Maricic, S.M. and Srdjenovic, B.U. (2019) Oxidative stress and its role in cancer. *Journal of Cancer Research and Therapeutics*. http://www.cancerjournal.net/preprintarticle.asp?id=257463;type=0

Jeong, Y.-H., Park, J.-S., Kim, D.-H. and Kim, H.-S. (2016) Lonchocarpine increases Nrf2/ARE-mediated antioxidant enzyme expression by modulating AMPK and MAPK signaling in brain astrocytes. *Biomolecules and Therapeutics*, 24 (6), 581.

Jian-Zhang, W., Chan-Chan, C., Lai-Lai, S., Zhan-Kun, W., Shou-Biao, W., Wu-Lan, L., Su-Hua, C., Rong-Ping, Z. and Pei-Hong, Q. (2014) Synthetic Chalcones with Potent Antioxidant Ability on H_2O_2-Induced Apoptosis in PC12 Cells. *International Journal of Molecular Sciences*, 15 (10), 18525-18539.

Juvale, K., Pape, V.F.S. and Wiese, M. (2012) Investigation of chalcones and benzochalcones as inhibitors of breast cancer resistance protein. *Bioorganic and Medicinal Chemistry*, 20 (1), 346-355.

Ka, H., Park, H.-J., Jung, H.-J., Choi, J.-W., Cho, K.-S., Ha, J. and Lee, K.-T. (2003) Cinnamaldehyde induces apoptosis by ROS-mediated mitochondrial permeability transition in human promyelocytic leukemia HL-60 cells. *Cancer Letters*, 196 (2), 143-152.

Kachadourian, R., Day, B.J., Pugazhenti, S., Franklin, C.C., Genoux-Bastide, E., Mahaffey, G., Gauthier, C., Di Pietro, A. and Boumendjel, A. (2012) A synthetic chalcone as a potent inducer of glutathione biosynthesis. *Journal of Medicinal Chemistry*, 55 (3), 1382-1388.

Kansanen, E., Kuosmanen, S.M., Leinonen, H. and Levonen, A.-L. (2013) The Keap1-Nrf2 pathway: mechanisms of activation and dysregulation in cancer. *Redox Biology*, 1 (1), 45-49.

Kashinakunti, S.V., Kollur, P., Kallaganada, G.S., Rangappa, M. and Ingin, J.B. (2011) Comparative study of serum MDA and vitamin C levels in non-smokers, chronic smokers and chronic smokers with acute myocardial infarction in men. *Journal of research in medical sciences: the official journal of Isfahan University of Medical Sciences*, 16 (8), 993.

Katzke, V.A., Kaaks, R. and Kühn, T. (2015) Lifestyle and cancer risk. *The Cancer Journal*, 21 (2), 104-110.

Kaur, P., Kaur, S., Kumar, N., Singh, B. and Kumar, S. (2009) Evaluation of antigenotoxic activity of isoliquiritin apioside from Glycyrrhizaglabra L. *Toxicology in Vitro*, 23 (4), 680-686.

Kello, M., Drutovic, D., Pilatova, M.B., Tischlerova, V., Perjesi, P. and Mojzis, J. (2016) Chalcone derivatives cause accumulation of colon cancer cells in the G2/M phase and induce apoptosis. *Life Sciences*, 150, 32-38.

Kennedy, S. and Oswald, N. (2011) *PCR troubleshooting and optimization : the essential guide*. Norfolk: Caister Academic Press.

Keohavong, P. and Grant, S.G. (2005) *Molecular toxicology protocols / edited by Phouthone Keohavong, Stephen G. Grant*. Totowa, N.J.: Totowa, N.J., Humana Press.

Kheradvar, A., Groves, E.M., Falahatpisheh, A., Mofrad, M.K., Hamed Alavi, S., Tranquillo, R., Dasi, L.P., Simmons, C.A., Jane Grande-Allen, K., Goergen, C.J., Baaijens, F., Little, S.H., Canic, S. and Griffith, B. (2015) Emerging Trends in Heart Valve Engineering: Part IV. Computational Modeling and Experimental Studies. *Annals of Biomedical Engineering*, 43 (10), 2314-2333.

Khoschsorur, G., Winklhofer-Roob, B., Rabl, H., Auer, T., Peng, Z. and Schaur, R. (2000) Evaluation of a sensitive HPLC method for the determination of malondialdehyde, and application of the method to different biological materials. *Chromatographia*, 52 (3-4), 181-184.

Kim, S.S., Lim, J., Bang, Y., Gal, J., Lee, S.-U., Cho, Y.-C., Yoon, G., Kang, B.Y., Cheon, S.H. and Choi, H.J. (2012) Licochalcone E activates Nrf2/antioxidant response element signaling pathway in both neuronal and microglial cells: therapeutic relevance to neurodegenerative disease. *The Journal of Nutritional Biochemistry*, 23 (10), 1314-1323.

Kim, W., Lee, H., Kim, S., Joo, S., Jeong, S., Yoo, J.-W. and Jung, Y. (2019) Sofalcone, a gastroprotective drug, covalently binds to KEAP1 to activate Nrf2 resulting in anti-colitic activity. *European Journal of Pharmacology*, 172722.

King, R.J.B. and Robins, M.W. (2006) *Cancer biology*. Pearson Education.

Kinnula, V. (2005) Focus on antioxidant enzymes and antioxidant strategies in smoking related airway diseases. *Thorax*, 60 (8), 693-700.

Kisby, G.E., Muniz, J.F., Scherer, J., Lasarev, M.R., Koshy, M., Kow, Y.W. and McCauley, L. (2009) Oxidative stress and DNA damage in agricultural workers. *Journal of Agromedicine*, 14 (2), 206-214.

Klaassen, C.D. and Watkins, J.B. (2015) *Casarett & Doull's essentials of toxicology*. 3rd ed. New York: McGraw Hill Medical.

Klaunig, J.E., Kamendulis, L.M. and Hocevar, B.A. (2010) Oxidative stress and oxidative damage in carcinogenesis. *Toxicologic Pathology*, 38 (1), 96-109.

Kleinsmith, L.J. (2006) *Principles of cancer biology*. London: Pearson Benjamin Cummings.

Klotz, L.-O. and Steinbrenner, H. (2017) Cellular adaptation to xenobiotics: interplay between xenosensors, reactive oxygen species and FOXO transcription factors. *Redox Biology*, 13, 646-654.

Knowles, M.A. and Selby, P. (2005) *Introduction to the cellular and molecular biology of cancer*. 4th ed. Oxford: Oxford : Oxford University Press.

Kodavanti, U.P. (2014) *Biomarkers in Toxicology: Respiratory toxicity biomarkers*. Elsevier Science.

Końca, K., Lankoff, A., Banasik, A., Lisowska, H., Kuszewski, T., Góźdź, S., Koza, Z. and Wojcik, A. (2003) A cross-platform public domain PC image-analysis program for the comet assay. *Mutation Research -Genetic Toxicology and Environmental Mutagenesis*, 534 (1-2), 15-20.

Kostanecki, S. and Tambor, J. (1899) Ueber die sechs isomeren Monooxybenzalacetophenone (Monooxychalkone). *Berichte der deutschen chemischen Gesellschaft*, 32 (2), 1921-1926.

Krajka-Kuźniak, V., Paluszczak, J. and Baer-Dubowska, W. (2013) Xanthohumol induces phase II enzymes via Nrf2 in human hepatocytes in vitro. *Toxicology in Vitro*, 27 (1), 149-156.

Krebs, J.E., Goldstein, E.S. and Kilpatrick, S.T. (2018) *Lewin's genes XII*. Burlington, MA: Burlington, MA : Jones and Bartlett Learning.

Kühnl, J., Roggenkamp, D., Gehrke, S.A., Stäb, F., Wenck, H., Kolbe, L. and Neufang, G. (2015) Licochalcone A activates Nrf2 *in vitro* and contributes to licorice extract-induced lowered cutaneous oxidative stress *in vivo*. *Experimental dermatology*, 24 (1), 42-47.

Kulkarni, Y.A., Garud, M.S., Oza, M.J., Barve, K.H. and Gaikwad, A.B. (2016) Diabetes, diabetic complications, and flavonoids. In: (ed.) *Fruits, Vegetables, and Herbs.* Elsevier. pp. 77-104.

Kumar, H., Kim, I.-s., More, S.V., Kim, B.-w. and Choi, D.-k. (2013) Natural product-derived pharmacological modulators of Nrf2/ARE pathway for chronic diseases. *Natural Product Reports*, 31 (1), 109-139.

Kumar, R., Sharma, P., Shard, A., Tewary, D.K., Nadda, G. and Sinha, A.K. (2012) Chalcones as promising pesticidal agents against diamondback moth (Plutella xylostella): microwave-assisted synthesis and structure–activity relationship. *Medicinal Chemistry Research*, 21 (6), 922-931.

Kumar, V., Kumar, S., Hassan, M., Wu, H., Thimmulappa, R.K., Kumar, A., Sharma, S.K., Parmar, V.S., Biswal, S. and Malhotra, S.V. (2011) Novel chalcone derivatives as potent Nrf2 activators in mice and human lung epithelial cells. *Journal of Medicinal Chemistry*, 54 (12), 4147-4159.

Kumaravel, T.S. (2009) Comet Assay measurements: a perspective. *Cell Biology And Toxicology*, 25 (1), 53.

Kuo, Y.-F., Su, Y.-Z., Tseng, Y.-H., Wang, S.-Y., Wang, H.-M. and Chueh, P.J. (2010) Flavokawain B, a novel chalcone from Alpinia pricei Hayata with potent apoptotic activity: Involvement of ROS and GADD153 upstream of mitochondria-dependent apoptosis in HCT116 cells. *Free Radical Biology and Medicine*, 49 (2), 214-226.

Kurien, B.T. and Scofield, R.H. (2009) *Protein Blotting and Detection Methods and Protocols*. Totowa, NJ : Humana Press.

Kyoya, T. (2018) The effect of different methods and image analyzers on the results of the *in vivo* comet assay. *Genes & Environment: The Official Journal Of The Japanese Environmental Mutagen Society*, 40, 4.

Lally, B.E., Zelterman, D., Colasanto, J.M., Haffty, B.G., Detterbeck, F.C. and Wilson, L.D. (2006) Postoperative radiotherapy for stage II or III non-small-cell lung cancer using the surveillance, epidemiology, and end results database. *Journal of Clinical Oncology*, 24 (19), 2998-3006.

Lau, A., Villeneuve, N.F., Sun, Z., Wong, P.K. and Zhang, D.D. (2008) Dual roles of Nrf2 in cancer. *Pharmacological Research*, 58 (5-6), 262-270.

Lee, S.Y., Chiu, Y.J., Yang, S.M., Chen, C.M., Huang, C.C., Lee-Chen, G.J., Lin, W. and Chang, K.H. (2018) Novel synthetic chalcone-coumarin hybrid for Aβ aggregation reduction, antioxidation, and neuroprotection. *CNS Neuroscience and Therapeutics*, 24 (12), 1286-1298.

León, J., Sáenz, J.M., Artacho-Cordón, F., Fernández, M.F., Martin-Olmedo, P., Salamanca-Fernández, E., Gómez-Peña, C., Olea, N. and Arrebola, J.P. (2019) Contribution of sociodemographic, occupational, lifestyle and dietary characteristics to the oxidative stress microenvironment in adipose tissue. *Environmental Research*, 175, 52-62.

Lepetsos, P., Papavassiliou, K.A. and Papavassiliou, A.G. (2019) Redox and NF-κB signaling in osteoarthritis. *Free Radical Biology and Medicine*, 132, 90-100.

Lesk, A.M. (2017) *Introduction to genomics*. 3rd ed. Oxford: Oxford University Press.

Leuratti, C., Singh, R., Lagneau, C., Farmer, P.B., Plastaras, J.P., Marnett, L.J. and Shuker, D. (1998) Determination of malondialdehyde-induced DNA damage in human tissues using an immunoslot blot assay. *Carcinogenesis*, 19 (11), 1919-1924.

Li, D., Wang, N., Zhang, J., Ma, S., Zhao, Z. and Ellis, E.M. (2017) Hepatoprotective effect of 7-hydroxycoumarin against methyl glyoxal toxicity via activation of Nrf2. *Chemico-Biological Interactions*, 276, 203-209.

Li, N., Meng, D., Pan, Y., Cui, Q., Li, G., Ni, H., Sun, Y., Qing, D., Jia, X. and Pan, Y. (2015) Anti-neuroinflammatory and NQO1 inducing activity of natural phytochemicals from *Coreopsis tinctoria*. *Journal of Functional Foods*, 17, 837-846.

Li, W.W. (2004) Tumor angiogenesis as a target for early intervention and cancer prevention. In: (ed.) *Cancer Chemoprevention.* Springer. pp. 611-633.

Li, Z., Yulei, J., Yaqing, J., Jinmin, Z., Xinyong, L., Jing, G. and Min, L. (2019) Protective effects of tetramethylpyrazine analogue Z-11 on cerebral ischemia reperfusion injury. *European Journal of Pharmacology*, 844, 156-164.

Lienhart, W.D., Gudipati, V., Uhl, M.K., Binter, A., Pulido, S.A., Saf, R., Zangger, K., Gruber, K. and Macheroux, P. (2014) Collapse of the native structure caused by a single amino acid exchange in human NAD(P)H:quinone oxidoreductase1. *Federation of European Biochemical Societies Journal*, 281 (20), 4691-4704.

Lin, C.-T., Senthil Kumar, K.J., Tseng, Y.-H., Wang, Z.-J., Pan, M.-Y., Xiao, J.-H., Chien, S.-C. and Wang, S.-Y. (2009) Anti-inflammatory activity of Flavokawain B from Alpinia pricei Hayata. *Journal of Ogricultural and Food Chemistry*, 57 (14), 6060-6065.

Lin, Y., Kuang, Y., Li, K., Wang, S., Ji, S., Chen, K., Song, W., Qiao, X. and Ye, M. (2017) Nrf2 activators from Glycyrrhiza inflata and their hepatoprotective activities against CCl4-induced liver injury in mice. *Bioorganic and Medicinal Chemistry*, 25 (20), 5522-5530.

Liu, D. (2018) NF-κB and Nrf2 pathways contribute to the protective effect of Licochalcone A on dextran sulphate sodium-induced ulcerative colitis in mice. *Biomedicine and Pharmacotherapy*, 102, 922.

Liu, D. and Xu, Y. (2011) p53, oxidative stress, and aging. *Antioxidants and Redox signaling*, 15 (6), 1669-1678.

Liu, J., Zhang, L., Lou, J. and Wu, C. (2015) Chalcone derivative, chana 1 induces inhibition of cell proliferation and prevents metastasis of pancreatic carcinoma. *Advances in Biomedicine and Pharmacy*, 2, 115-119.

Liu, L., Zhang, Q., Feng, J., Deng, L., Zeng, N., Yang, A. and Zhang, W. (1996) The study of DNA oxidative damage in benzene-exposed workers. *Mutation Research/Genetic Toxicology*, 370 (3-4), 145-150.

Liu, X., Liu, H., Zhai, Y., Li, Y., Zhu, X. and Zhang, W. (2017) Laminarin protects against hydrogen peroxide-induced oxidative damage in MRC-5 cells possibly via regulating NRF2. *PeerJ*, 5, e3642.

Livak, K.J. and Schmittgen, T.D. (2001) Analysis of relative gene expression data using real-time quantitative PCR and the 2− ΔΔCT method. *Methods*, 25 (4), 402-408.

Lohr, L. (2018) Abemaciclib (verzenio™). *Oncology Times*, 40 (6), 12.

Logan, J., Edwards, K. and Saunders, N. (2009) *Real-time PCR : current technology and applications*. Norfolk: Caister Academic Press.

Lou, Y., Guo, Z., Zhu, Y., Kong, M., Zhang, R., Lu, L., Wu, F., Liu, Z. and Wu, J. (2019) Houttuynia cordata Thunb. and its bioactive compound 2-undecanone significantly suppress benzo (a) pyrene-induced lung tumorigenesis by activating the Nrf2-HO-1/NQO-1 signaling pathway. *Journal of Experimental and Clinical Cancer Research*, 38 (1), 242.

Luo, L., Wang, R., Wang, X., Ma, Z. and Li, N. (2012) Compounds from Angelica keiskei with NQO1 induction, DPPH scavenging and α-glucosidase inhibitory activities. *Food Chemistry*, 131 (3), 992-998.

Luo, X., Zhang, H., Duan, Y. and Chen, G. (2018) Protective effects of radish (*Raphanus sativus L.*) leaves extract against hydrogen peroxide-induced oxidative damage in human fetal lung fibroblast (MRC-5) cells. *Biomedicine and Pharmacotherapy*, 103, 406-414.

Ma, P., Wu, Y., Zeng, Q., Gan, Y., Chen, J., Ye, X. and Yang, X. (2013) Oxidative damage induced by chlorpyrifos in the hepatic and renal tissue of Kunming mice and the antioxidant role of vitamin E. *Food and Chemical Toxicology*, 58, 177-183.

Ma, Q. (2013) Role of nrf2 in oxidative stress and toxicity. *Annual Review of Pharmacology and Toxicology*, 53, 401-426.

Mahapatra, D.K., Bharti, S.K. and Asati, V. (2015) Chalcone scaffolds as anti-infective agents: Structural and molecular target perspectives. *European Journal of Medicinal Chemistry*, 101, 496-524.

Maier, T., Güell, M. and Serrano, L. (2009) Correlation of mRNA and protein in complex biological samples. *Federation of European Biochemical Societies Letters*, 583 (24), 3966-3973.

Marnett, L.J. (1991) Peroxyl free radicals: biological reactive intermediates produced during lipid oxidation. *Advances In Experimental Medicine and Biology*, 283, 65.

Marnett, L.J. (1999) Lipid peroxidation-DNA damage by malondialdehyde. *Mutation Research*, 424 (1-2), 83.

Martinez, R.M., Pinho-Ribeiro, F.A., Steffen, V.S., Caviglione, C.V., Pala, D., Baracat, M.M., Georgetti, S.R., Verri, W.A. and Casagrande, R. (2016) Topical formulation containing hesperidin methyl chalcone inhibits skin oxidative stress and inflammation induced by ultraviolet B irradiation. *Photochemical and Photobiological Sciences*, 15 (4), 554-563.

Martinez, R.M., Pinho-Ribeiro, F.A., Steffen, V.S., Caviglione, C.V., Vignoli, J.A., Baracat, M.M., Georgetti, S.R., Verri, W.A. and Casagrande, R. (2015) Hesperidin methyl chalcone inhibits oxidative stress and inflammation in a mouse model of ultraviolet B irradiation-induced skin damage. *Journal of Photochemistry and Photobiology, B: Biology*, 148, 145-153.

Martinez, R.M., Pinho-Ribeiro, F.A., Vale, D.L., Steffen, V.S., Vicentini, F.T., Vignoli, J.A., Baracat, M.M., Georgetti, S.R., Verri Jr, W.A. and Casagrande, R. (2017) Trans-chalcone added in topical formulation inhibits skin inflammation and oxidative stress in a model of ultraviolet B radiation skin damage in hairless mice. *Journal of Photochemistry and Photobiology B: Biology*, 171, 139-146.

Maydt, D., De Spirt, S., Muschelknautz, C., Stahl, W. and Müller, T.J. (2013) Chemical reactivity and biological activity of chalcones and other α, β-unsaturated carbonyl compounds. *Xenobiotica*, 43 (8), 711-718.

Mehta, R.G., Murillo, G., Naithani, R. and Peng, X. (2010) Cancer chemoprevention by natural products: how far have we come? *Pharmaceutical Research*, 27 (6), 950-961.

Memon, A.H., Ismail, Z., Aisha, A.F., Al-Suede, F.S.R., Hamil, M.S.R., Hashim, S., Saeed, M.A.A., Laghari, M., Majid, A. and Shah, A.M. (2014) Isolation, characterization, crystal structure elucidation, and anticancer study of dimethyl cardamonin, isolated from Syzygium campanulatum Korth. *Evidence-Based Complementary and Alternative Medicine*, 2014.

Menezo, Y.J.R., Silvestris, E., Dale, B. and Elder, K. (2016) Oxidative stress and alterations in DNA methylation: two sides of the same coin in reproduction. *Reproductive BioMedicine Online*, 33 (6), 668-683.

McCready, T. (2006) *An introduction to cancer care*. Chichester: Chichester : Whurr.

Miao, Q., Xu, Y., Zhang, H., Xu, P. and Ye, J. (2019) Cigarette smoke induces ROS mediated autophagy impairment in human corneal epithelial cells. *Environmental Pollution*, 245, 389-397.

Miller, K.D., Nogueira, L., Mariotto, A.B., Rowland, J.H., Yabroff, K.R., Alfano, C.M., Jemal, A., Kramer, J.L. and Siegel, R.L. (2019) Cancer treatment and survivorship statistics, 2019. *CA: A Cancer Journal for Clinicians*, 69 (5), 363-385.

Miranda-Sapla, M.M. (2019) *trans*-Chalcone modulates *Leishmania amazonensis* infection *in vitro* by *Nrf2* overexpression affecting iron availability. *European Journal of Pharmacology*, 853, 275-289.

Misthos, P., Katsaragakis, S., Milingos, N., Kakaris, S., Sepsas, E., Athanassiadi, K., Theodorou, D. and Skottis, I. (2005) Postresectional pulmonary oxidative stress in lung cancer patients. The role of one-lung ventilation. *European Journal of Cardio-thoracic Surgery*, 27 (3), 379-383.

Mohan, S. and Gupta, D. (2019) Role of Nrf2-antioxidant in radioprotection by root extract of Inula racemosa. *International Journal of Radiation Biology*, 1-13.

Mokhtari, R.B. (2010) *Dietary Chemoprevention Agent Sulforaphane Inhibits Growth, Survival and Tumorigenic Activity in Human Neuroblastoma*thesis.

Munnia, A. (2006) Bronchial malondialdehyde DNA adducts, tobacco smoking, and lung cancer. *Free Radical Biology and Medicine*, 41 (9), 1499.

Munnia, A., Enrica Amasio, M. and Peluso, M. (2004) Exocyclic malondialdehyde and aromatic DNA adducts in larynx tissues. *Free Radical Biology and Medicine*, 37 (6), 850-858.

Najafov, A. (2017) *Western Blotting Guru*. London, England : Academic Press.

NCBI. (2019) *NFE2L2* [online]

Available at: https://www.ncbi.nlm.nih.gov/gene/4780#gene-expression

Nguyen, T., Nioi, P. and Pickett, C.B. (2009) The Nrf2-antioxidant response element signaling pathway and its activation by oxidative stress. *Journal of Biological Chemistry*, 284 (20), 13291-13295.

Niedernhofer, L.J., Daniels, J.S., Rouzer, C.A., Greene, R.E. and Marnett, L.J. (2003) Malondialdehyde, a product of lipid peroxidation, is mutagenic in human cells. *Journal of Biological Chemistry*, 278 (33), 31426-31433.

Nishimoto, S., Suzuki, T., Koike, S., Yuan, B., Takagi, N. and Ogasawara, Y. (2016) Nrf2 activation ameliorates cytotoxic effects of arsenic trioxide in acute promyelocytic leukemia cells through increased glutathione levels and arsenic efflux from cells. *Toxicology and Applied Pharmacology*, 305 (C), 161-168.

Niture, S. and Jaiswal, A. (2010) *Comprehensive Toxicology: Antioxidant Induction of Gene Expression*. 2nd ed.: London, Elsevier.

Noroozi, M., Angerson, W.J. and Lean, M. (1998) Effects of flavonoids and vitamin C on oxidative DNA damage to human lymphocytes. *The American Journal of Clinical Nutrition*, 67 (6), 1210-1218.

Oie, H. and Gazdar, A. (2000) Initiation of cell cultures from lung tumor biopsies. In: Pass, H. I., Mitchell, J. B., Johnson, D. H., Turrisi, A. T. and Minna, J. D. (ed.) *Lung Cancer: Principles and Practice.* 2nd ed. Philadelphia, USA: Lippincott, Williams and Wilkins. pp. 337-346.

Olive, P.L. (1999) The Comet Assay in Clinical Practice. *Acta Oncologica*, 38 (7), 839-845.

Olive, P.L., Banáth, J.P. and Durand, R.E. (1990) Heterogeneity in radiation-induced DNA damage and repair in tumor and normal cells measured using the" comet" assay. *Radiation Research*, 122 (1), 86-94.

Oliveira, P.A., Colaço, A., Chaves, R., Guedes-Pinto, H., De-La-Cruz, P., Luis, F. and Lopes, C. (2007) Chemical carcinogenesis. *Anais da academia brasileira de ciências*, 79 (4), 593-616.

Onyango, A.N. and Baba, N. (2010) New hypotheses on the pathways of formation of malondialdehyde and isofurans. *Free Radical Biology and Medicine*, 49 (10), 1594-1600.

Orlikova, B., Tasdemir, D., Golais, F., Dicato, M. and Diederich, M. (2011) Dietary chalcones with chemopreventive and chemotherapeutic potential. *Genes and nutrition*, 6 (2), 125.

Palmieri, C., Bird, E. and Simcock, R. (2013) *ABC of cancer care*. Chichester, West Sussex, UK: Chichester, West Sussex, UK : Wiley-Blackwell : BMJ Books.

Parikh, M., Kelly, K., Lara Jr, P.N. and Smit, E.F. (2018) Treatment of Extensive-Stage Small Cell Lung Cancer. In: (ed.) *IASLC Thoracic Oncology*. Elsevier. pp. 525-535. e525.

Parkin, D.M., Boyd, L. and Walker, L. (2011) The fraction of cancer attributable to lifestyle and environmental factors in the UK in 2010. *British Journal of Cancer*, 105 (2), 77-81.

Peixoto, M.S., Da Silva Junior, F.C., de Oliveira Galvão, M.F., Roubicek, D.A., de Oliveira Alves, N. and Batistuzzo de Medeiros, S.R. (2019) Oxidative stress, mutagenic effects, and cell death induced by retene. *Chemosphere*, 231, 518-527.

Petrov, O., Ivanova, Y. and Gerova, M. (2008) SOCl2/EtOH: Catalytic system for synthesis of chalcones. *Catalysis Communications*, 9 (2), 315-316.

Petruzzelli, S., Hietanen, E., Bartsch, H., Camus, A.M., Mussi, A., Angeletti, C.A., Saracci, R. and Giuntini, C. (1990) Pulmonary lipid peroxidation in cigarette smokers and lung cancer patients. *Chest*, 98 (4), 930-935.

Pey, A.L., Megarity, C.F. and Timson, D.J. (2019) NAD(P)H quinone oxidoreductase (NQO1): an enzyme which needs just enough mobility, in just the right places. *Bioscience Reports*, 39 (1).

Pidugu, L.S.M., Mbimba, J.E., Ahmad, M., Pozharski, E., Sausville, E.A., Emadi, A. and Toth, E.A. (2016) A direct interaction between NQO1 and a chemotherapeutic dimeric naphthoquinone. *BMC Structural Biology*, 16 (1), 1.

Pipas, J.M. (2009) SV40: Cell transformation and tumorigenesis. *Virology*, 384 (2), 294-303.

Piperakis, S., Visvardis, E., Sagnou, M. and Tassiou, A. (1998) Effects of smoking and aging on oxidative DNA damage of human lymphocytes. *Carcinogenesis*, 19 (4), 695-698.

Plazar, J., Žegura, B., Lah, T.T. and Filipič, M. (2007) Protective effects of xanthohumol against the genotoxicity of benzo (a) pyrene (BaP), 2-amino-3-methylimidazo [4, 5-f]

quinoline (IQ) and tert-butyl hydroperoxide (t-BOOH) in HepG2 human hepatoma cells. *Mutation Research/Genetic Toxicology and Environmental Mutagenesis*, 632 (1-2), 1-8.

Plopper, G., Sharp, D., Sikorski, E. and Lewin, B. (2015) *Lewin's Cells*. 3rd ed. Burlington, MA: Jones and Bartlett Learning.

Pop, S., Enciu, A.M., Tarcomnicu, I., Gille, E. and Tanase, C. (2019) Phytochemicals in cancer prevention: modulating epigenetic alterations of DNA methylation. *Phytochemistry Reviews*, 1-20.

Popoola, O.K. (2015) Inhibition of Oxidative Stress and Skin Aging-Related Enzymes by Prenylated Chalcones and Other Flavonoids from Helichrysum teretifolium. *Molecules*, 20 (4), 7143-7156.

Protein Data Bank in Europe, (2019) *NAD(P)H dehydrogenase [quinone] 1*

[online], https://www.ebi.ac.uk/pdbe/pdbe-kb/proteins/P15559#structures

Qebesy, H.S., Zakhary, M.M., Abd-Alaziz, M.A., Ghany, A.A.A. and Maximus, D.W. (2015) Tissue levels of oxidative stress markers and antioxidants in breast cancer patients in relation to tumor grade. *Al-Azhar Assiut Medical Journal*, 13 (4), 10-17.

Raghavan, S., Manogaran, P., Kuppuswami, B.K., Venkatraman, G. and Narasimha, K.K.G. (2015) Synthesis and anticancer activity of chalcones derived from vanillin and isovanillin. *Medicinal Chemistry Research*, 24 (12), 4157-4165.

Rahman, I. and Adcock, I. (2006) Oxidative stress and redox regulation of lung inflammation in COPD. *European Respiratory Journal*, 28 (1), 219-242.

Rahman, T., Hosen, I., Islam, M.T. and Shekhar, H.U. (2012) Oxidative stress and human health. *Advances in Bioscience and Biotechnology*, 3 (07), 997.

Ramezani, F., Keshavarz, A., Jalali, M., Eshraghian, M. and Chameri, M. (2010) The effect of weight loss on plasma MDA, lipids profile and ApoA and ApoB in obese woman. *ARYA Atherosclerosis*, 4 (2).

Ramirez-Tagle, R., Escobar, C.A., Romero, V., Montorfano, I., Armisén, R., Borgna, V., Jeldes, E., Pizarro, L., Simon, F. and Echeverria, C. (2016) Chalcone-induced apoptosis through caspase-dependent intrinsic pathways in human hepatocellular carcinoma cells. *International Journal of Molecular Sciences*, 17 (2), 260-278.

Ramkumar, K.M., Sekar, T.V., Foygel, K., Elango, B. and Paulmurugan, R. (2013) Reporter protein complementation imaging assay to screen and study Nrf2 activators in cells and living animals. *Analytical Chemistry*, 85 (15), 7542-7549.

Repetto, M., Semprine, J. and Boveris, A. (2012) *Lipid peroxidation: chemical mechanism, biological implications and analytical determination*. Angel Catala (ed) National University of La Plata, Argentina. InTechOpen.

Requena, C.E., Pérez-Moreno, G., Horváth, A., Vértessy, B.G., Ruiz-Pérez, L.M., González-Pacanowska, D. and Vidal, A.E. (2016) The nucleotidohydrolases DCTPP1 and dUTPase are involved in the cellular response to decitabine. *Biochemical Journal*, 473 (17), 2635-2643.

Riss, T.L., Moravec, R.A., Niles, A.L., Benink, H.A., Worzella, T.J. and Minor, L. (2016) Cell Viability Assays.

Ritchie, K.J., Henderson, C.J., Wang, X.J., Vassieva, O., Carrie, D., Farmer, P.B., Gaskell, M., Park, K. and Wolf, C.R. (2007) Glutathione transferase pi plays a critical role in the development of lung carcinogenesis following exposure to tobacco-related carcinogens and urethane. *Cancer Research*, 67 (19), 9248.

Robert, A.W. (2015) *Cancer: Principles and overview*. 3rd ed. Burlington, MA: Jones and Bartlett Learning.

Robert E. Farrell, J. (2010) *RNAi-Chapter 23:Take a RISC – Role the Dicer*. Elsevier Inc.

Robledinos-Antón, N., Fernández-Ginés, R., Manda, G. and Cuadrado, A. (2019) Activators and inhibitors of NRF2: a review of their potential for clinical development. *Oxidative Medicine and Cellular Longevity*, 2019.

Rodrigues, D., Maniscalco, D., Silva, F., Chiari, B., Castelli, M., Isaac, V., Cicarelli, R. and Lopez, S. (2017) Trypanocidal Activity of Flavokawin B, a Component of Polygonum ferrugineum Wedd. *Planta Medica.*, 83 (3-4), 239-244.

Rodríguez-Zavala, J.S., Calleja, L.F., Moreno-Sánchez, R. and Yoval-Sánchez, B. (2019) Role of aldehyde dehydrogenases in physiopathological processes. *Chemical Research in Toxicology*, 32 (3), 405-420.

Roede, J.R., Stewart, B.J. and Petersen, D.R. (2010) Hepatotoxicity of Reactive Aldehydes. In: (ed.) *Reference Module in Biomedical Sciences.* Elsevier Ltd. pp. 581-594.

Rosa, G.P., Seca, A.M., Barreto, M.d.C., Silva, A. and Pinto, D.C. (2019) Chalcones and flavanones bearing hydroxyl and/or methoxyl groups: Synthesis and biological assessments. *Applied Sciences*, 9 (14), 2846.

Ross, D., Kepa, J.K., Winski, S.L., Beall, H.D., Anwar, A. and Siegel, D. (2000) NAD(P)H:quinone oxidoreductase 1 (NQO1): chemoprotection, bioactivation, gene regulation and genetic polymorphisms. *Chemico-Biological Interactions*, 129 (1-2), 77-97.

Ross, D. and Siegel, D. (2017) Functions of NQO1 in Cellular Protection and CoQ(10) Metabolism and its Potential Role as a Redox Sensitive Molecular Switch. *Frontiers in Physiology*, 8.

Rozmer, Z. (2014) *Investigation of molecular mechanism of cytotoxic and chemoprotective effects of cyclic chalcone analogues*thesis, University of Pécs.

Rubio-Navarro, A., Guerrero-Hue, M., Vazquez-Carballo, C., García-Caballero, C., Herencia, C., Eduardo, G., Yuste, C., Sevillano, A., Praga, M. and Egea, J. (2019) Nrf2 Plays a Protective Role Against Intravascular Hemolysis-Mediated Acute Kidney Injury. *Frontiers in Pharmacology*, 10, 740.

Rucker, H., Al-Rifai, N., Rascle, A., Gottfried, E., Brodziak-Jarosz, L., Gerhauser, C., Dick, T.P. and Amslinger, S. (2015) Enhancing the anti-inflammatory activity of chalcones by tuning the Michael acceptor site. *Organic and Biomolecular Chemistry*, 13 (10), 3040-3047.

Ruparelia, K.C., Zeka, K., Ijaz, T., Ankrett, D.N., Wilsher, N.E., Butler, P.C., Tan, H.L., Lodhi, S., Bhambra, A.S., Potter, G.A., Arroo, R.R.J. and Beresford, K.J.M. (2018) The synthesis of chalcones as anticancer prodrugs and their bioactivation in CYP1 expressing breast cancer cells. *Medicinal Chemistry*, 14 (4), 322-332.

Rupasinghe, H.V., Nair, S.V. and Robinson, R.A. (2014) Chemopreventive properties of fruit phenolic compounds and their possible mode of actions. In: (ed.) *Studies in Natural Products Chemistry.* Elsevier. pp. 229-266.

Şahin, S. and Karkar, B. (2019) The antioxidant properties of the chestnut bee pollen extract and its preventive action against oxidatively induced damage in DNA bases. *Journal of Food Biochemistry*, e12888.

Saini, J., Goyal, A.K. and Jangra, A. (2019) High-fat diet with alcohol elevate oxidative stress which cause hyperlipidemia by inducing mutation in the ANGPTL3 locus. *International Journal of Diabetes in Developing Countries*, 1-7.

Sajjad, S., Do, M.T., Shin, H.S., Yoon, T.S. and Kang, S. (2018) Rapid and efficient western blot assay by rotational cyclic draining and replenishing procedure. *Electrophoresis*, 39 (23), 2974-2978.

Sakagami, H., Masuda, Y., Tomomura, M., Yokose, S., Uesawa, Y., Ikezoe, N., Asahara, D., Takao, K., Kanamoto, T. and Terakubo, S. (2017) Quantitative structure–cytotoxicity relationship of chalcones. *Anticancer Research*, 37 (3), 1091-1098.

Sakaguchi, C., Miura, N., Ohara, H. and Nagata, Y. (2019) Effects of reduced exposure to cigarette smoking on changes in biomarkers of potential harm in adult smokers: results of combined analysis of two clinical studies. *Biomarkers*, 1-12.

Salonen, P., Kellokumpu-Lehtinen, P.L., Tarkka, M.T., Koivisto, A.M. and Kaunonen, M. (2011) Changes in quality of life in patients with breast cancer. *Journal of clinical Nursing*, 20 (1-2), 255-266.

Salvayre, R., Auge, N., Benoist, H. and Negre-Salvayre, A. (2002) Oxidized low-density lipoprotein-induced apoptosis. *Biochimica et Biophysica Acta -Molecular and Cell Biology of Lipids*, 1585 (2-3), 213-221.

Sampey, B.P., Korourian, S., Ronis, M.J., Badger, T.M. and Petersen, D.R. (2003) Immunohistochemical characterization of hepatic malondialdehyde and 4-hydroxynonenal modified proteins during early stages of ethanol-induced liver injury. *Alcoholism: Clinical and Experimental Research*, 27 (6), 1015-1022.

Sashidhara, K.V., Kumar, M., Modukuri, R.K., Sonkar, R., Bhatia, G., Khanna, A., Rai, S. and Shukla, R. (2011) Synthesis and anti-inflammatory activity of novel biscoumarin–chalcone hybrids. *Bioorganic and Medicinal Chemistry Letters*, 21 (15), 4480-4484.

Schaap, M. (2015) *The biological evaluation of inhibitors of the Keap1-Nrf2 protein-protein interaction*. UCL (University College London).

Scherlieb, R. (2011) The MTT assay as tool to evaluate and compare excipient toxicity *in vitro* on respiratory epithelial cells. *International Journal of Pharmaceutics*, 411 (1-2), 98-105.

Schmittgen, T.D. and Livak, K.J. (2008) Analyzing real-time PCR data by the comparative C T method. *Nature Protocols*, 3 (6), 1101.

Schuster, M., Nechansky, A. and Kircheis, R. (2006) Cancer immunotherapy. *Biotechnology Journal: Healthcare Nutrition Technology*, 1 (2), 138-147.

Schwartz, K. and Bochkariov, D. (2017) Novel chemiluminescent Western blot blocking and antibody incubation solution for enhanced antibody-antigen interaction and increased specificity. *Electrophoresis*, 38 (20), 2631-2637.

Sebti, S.d., Solhy, A., Smahi, A., Kossir, A. and Oumimoun, H. (2002) Dramatic activity enhancement of natural phosphate catalyst by lithium nitrate. An efficient synthesis of chalcones. *Catalysis Communications*, 3 (8), 335-339.

Seljeskog, E., Hervig, T. and Mansoor, M.A. (2006) A novel HPLC method for the measurement of thiobarbituric acid reactive substances (TBARS). A comparison with a commercially available kit. *Clinical Biochemistry*, 39 (9), 947-954.

Shan, L., Wang, D., Mao, Q. and Xia, H. (2019) Establishment of a DGKθ Endogenous Promoter Luciferase Reporter HepG2 Cell Line for Studying the Transcriptional Regulation of DGKθ Gene. *Applied biochemistry and biotechnology*, 187 (4), 1344-1355.

Shi, Y., Wu, W.-Z., Huo, A., Zhou, W. and Jin, X.-H. (2017) Isobavachalcone inhibits the proliferation and invasion of tongue squamous cell carcinoma cells. *Oncology Letters*, 14 (3), 2852-2858.

Shin, J.M., Lee, K.-M., Lee, H.J., Yun, J.H. and Nho, C.W. (2019) Physalin A regulates the Nrf2 pathway through ERK and p38 for induction of detoxifying enzymes. *BMC Complementary and Alternative Medicine*, 19 (1), 101.

Siegel, D. (2018) Redox modulation of NQO1. *PLOS One*, 13 (1), e0190717.

Sikander, M. (2011) Cytoprotective activity of a *trans*-chalcone against hydrogen peroxide induced toxicity in hepatocellular carcinoma (HepG2) cells. *Asian Pacific Journal of Cancer Prevention*, 12 (10), 2513.

Silverman, R.B. and Holladay, M.W. (2015) *The Organic Chemistry of Drug Design and Drug Action*. 3rd ed.

Singh, A., Rangasamy, T., Thimmulappa, R.K., Lee, H., Osburn, W.O., Brigelius-Flohé, R., Kensler, T.W., Yamamoto, M. and Biswal, S. (2006) Glutathione peroxidase 2, the major cigarette smoke–inducible isoform of GPX in lungs, is regulated by Nrf2. *American Journal of Respiratory Cell and Molecular Biology*, 35 (6), 639-650.

Singh, N.P., McCoy, M.T., Tice, R.R. and Schneider, E.L. (1988) A simple technique for quantitation of low levels of DNA damage in individual cells. *Experimental Cell Research*, 175 (1), 184-191.

Singh, Z., Karthigesu, I.P., Singh, P. and Rupinder, K. (2014) Use of malondialdehyde as a biomarker for assessing oxidative stress in different disease pathologies: a review. *Iranian Journal of Public Health*, 43 (3), 7-16.

Skelly, J.V., Sanderson, M.R., Suter, D.A., Baumann, U., Read, M.A., Gregory, D.S., Bennett, M., Hobbs, S.M. and Neidle, S. (1999) Crystal structure of human DT-

diaphorase: a model for interaction with the cytotoxic prodrug 5-(aziridin-1-yl)-2,4-dinitrobenzamide (CB1954). *Journal of Medicinal Chemistry*, 42 (21), 4325-4330.

Smart, R.C. and Hodgson, E. (2008) *Molecular and biochemical toxicology*. 4th ed. Hoboken, N.J.: Wiley.

Snezhkina, A.V., Kudryavtseva, A.V., Kardymon, O.L., Savvateeva, M.V., Melnikova, N.V., Krasnov, G.S. and Dmitriev, A.A. (2019) ROS Generation and Antioxidant Defense Systems in Normal and Malignant Cells. *Oxidative Medicine and Cellular Longevity*, 2019.

Sohretoglu, D. and Huang, S., (2018) *Ganoderma lucidum* polysaccharides as an anti-cancer agent. *Anti-Cancer Agents in Medicinal Chemistry (Formerly Current Medicinal Chemistry-Anti-Cancer Agents)*, 18(5), pp.667-674.
Steward, W. and Brown, K. (2013) Cancer chemoprevention: a rapidly evolving field. *British Journal of Cancer*, 109 (1), 1.

Soto-Perez-de-Celis, E. and Hurria, A. (2020) Cancer in the Elderly: Biology, Prevention, and Treatment. In: (ed.) *Abeloff's Clinical Oncology.* Elsevier. pp. 874-881. e873.

Stoddart, M.J. (2011) Cell viability assays: introduction. In: (ed.) *Mammalian Cell Viability.* Springer. pp. 1-6.

Su, M.Y. (2011) Protective effects of 2',4'-dihydroxy-6'-methoxy-3',5'-dimethylchalcone to PC12 cells against cytotoxicity induced by hydrogen peroxide. *Journal Of Agricultural and Food Chemistry*, 59 (2), 521.

Su, M.-Y., Huang, H.-Y., Li, L. and Lu, Y.-H. (2010) Protective effects of 2′, 4′-dihydroxy-6′-methoxy-3′, 5′-dimethylchalcone to PC12 cells against cytotoxicity induced by hydrogen peroxide. *Journal of agricultural and food chemistry*, 59 (2), 521-527.

Su, X., Li, T., Liu, Z., Huang, Q., Liao, K., Ren, R., Lu, L., Qi, X., Wang, M. and Chen, J. (2018) Licochalcone A activates Keap1-Nrf2 signaling to suppress arthritis via phosphorylation of p62 at serine 349. *Free Radical Biology and Medicine*, 115, 471-483.

Sumiyoshi, M., Taniguchi, M., Baba, K. and Kimura, Y. (2015) Antitumor and antimetastatic actions of xanthoangelol and 4-hydroxyderricin isolated from Angelica keiskei roots through the inhibited activation and differentiation of M2 macrophages. *Phytomedicine*, 22 (7-8), 759-767.

Sun, H., Liu, Z., Zhao, H. and Ang, E.L. (2015) Recent advances in combinatorial biosynthesis for drug discovery. *Drug Design, Development and Therapy*, 9, 823.

Surh, Y.-J. (2003) Cancer chemoprevention with dietary phytochemicals. *Nature Reviews Cancer*, 3 (10), 768.

Suwito, H., Jumina, A.N., Mustofa, N.N.T., Kristanti, N.N.T. and Puspaningsih, N.N.T. (2014) Chalcones: Synthesis, Structure diversity and pharmacological aspects. *Journal of Chemical and Pharmaceutical Research*, 6 (5), 1076-1088.

Talalay, P., De Long, M.J. and Prochaska, H.J. (1988) Identification of a common chemical signal regulating the induction of enzymes that protect against chemical carcinogenesis. *Proceedings of the National Academy of Sciences*, 85 (21), 8261-8265.

Tamamizu-Kato, S., Wong, J.Y., Jairam, V., Uchida, K., Raussens, V., Kato, H., Ruysschaert, J.-M. and Narayanaswami, V. (2007) Modification by acrolein, a component of tobacco smoke and age-related oxidative stress, mediates functional impairment of human apolipoprotein E. *Biochemistry*, 46 (28), 8392-8400.

Tang, Y., Simoneau, A.R., Xie, J., Shahandeh, B. and Zi, X. (2008) Effects of the kava chalcone flavokawain A differ in bladder cancer cells with wild-type versus mutant p53. *Cancer prevention research*, 1 (6), 439-451.

Tanoue, L. and Detterbeck, F.C. (2019) *Lung cancer : a practical approach to Evidence-based clinical evaluation and management*. St. Louis, Missouri : Elsevier.

Taso, O.V., Philippou, A., Moustogiannis, A., Zevolis, E. and Koutsilieris, M. (2019) Lipid peroxidation products and their role in neurodegenerative diseases. *Annals of Research Hospitals*, 3.

Tavakkoli, A., Iranshahi, M., Hasheminezhad, S.H., Hayes, A.W. and Karimi, G. (2019) The neuroprotective activities of natural products through the Nrf2 upregulation. *Phytotherapy Research*.

Thorat, J., Joshi, A., Sontakke, A. and Wingkar, K. (2019) Effect of vitamin C supplementation on serum Cotinine, MDA and vitamin C levels in smokeless Tobacco chewers. *International Journal of Research in Pharmaceutical Sciences*, 10 (2), 803-811.

Thurston, D.E. (2007) *Chemistry and Pharmacology of Anticancer Drugs*. USA: Taylor and Francis.

Torigge, T., Arisawa, M., Itoh, S., Fujiu, M. and Maruyama, H.B. (1983) Anti-mutagenic chalcones: Antagonizing the mutagenicity of benzo (a) pyrene on *Salmonella typhimurium*. *Biochemical and Biophysical Research Communications*, 112 (3), 833-842.

Townsend, D.M. and Tew, K.D. (2014) *Advances in cancer research : redox and cancer*. 1st ed. San Diego, CA : Elsevier.

Tran, P.-L., Kim, O., Tran, H.N.K., Tran, M.H., Min, B.-S., Hwangbo, C. and Lee, J.-H. (2019) Protective effects of extract of *Cleistocalyx operculatus* flower buds and its isolated major constituent against LPS-induced endotoxic shock by activating the Nrf2/HO-1 pathway. *Food and Chemical Toxicology*, 129, 125-137.

Tsikas, D. (2017) Assessment of lipid peroxidation by measuring malondialdehyde (MDA) and relatives in biological samples: Analytical and biological challenges. *Analytical Biochemistry*, 524, 13.

Tung, Y.-C., Chou, Y.-C., Hung, W.-L., Cheng, A.-C., Yu, R.-C., Ho, C.-T. and Pan, M.-H. (2019) Polymethoxyflavones: Chemistry and Molecular Mechanisms for Cancer Prevention and Treatment. *Current Pharmacology Reports*, 5 (2), 98-113.

Turgut, N.H., Kara, H., Elagoz, S., Deveci, K., Gungor, H. and Arslanbas, E. (2016) The protective effect of naringin against bleomycin-induced pulmonary fibrosis in Wistar rats. *Pulmonary Medicine*, 2016 (2016).

Velali, E., Pantazaki, A., Besis, A., Choli-Papadopoulou, T. and Samara, C. (2019) Oxidative stress, DNA damage, and mutagenicity induced by the extractable organic matter of airborne particulates on bacterial models.(Report). *Regulatory Toxicology and Pharmacology*, 104, 59.

Walker, J.M. (2002) *The protein protocols handbook*. 2nd ed. ed. Totowa, N.J.: Totowa, N.J. : Humana Press.

Wang, J., Huang, L., Cheng, C., Li, G., Xie, J., Shen, M., Chen, Q., Li, W., He, W., Qiu, P. and Wu, J. (2019) Design, synthesis and biological evaluation of chalcone analogues with novel dual antioxidant mechanisms as potential anti-ischemic stroke agents. *Acta Pharmaceutica Sinica B*, 9 (2), 335-350.

Wang, X.J., Hayes, J.D. and Wolf, C.R. (2006) Generation of a stable antioxidant response element-driven reporter gene cell line and its use to show redox-dependent activation of Nrf2 by cancer chemotherapeutic agents. *Cancer Research*, 66 (22), 10983-10994.

Waseem, S.M.A., Hussain, M.M., Ahmad, Z. and Islam, N. (2012) A study of pulmonary functions and lipid peroxidation biomarker in COPD: Correlation between malondialdehyde and lung functions. *Biomedical Research*, 23 (1), 66-71.

Wason, M.S. (2013) Sensitization of pancreatic cancer cells to radiation by cerium oxide nanoparticle-induced ROS production. *Nanomedicine: Nanotechnology, Biology, and Medicine*, 9 (4), 558.

Watson, R.R. (2017) *Nutrition and Functional Foods for Healthy Aging*. Arizona: Academic Press.

Wauchope, O.R., Beavers, W.N., Galligan, J.J., Mitchener, M.M., Kingsley, P.J. and Marnett, L.J. (2015) Nuclear oxidation of a major peroxidation DNA adduct, M_1dG, in the genome. *Chemical Research in Toxicology*, 28 (12), 2334-2342.

Wauchope, O.R., Mitchener, M.M., Beavers, W.N., Galligan, J.J., Camarillo, J.M., Sanders, W.D., Kingsley, P.J., Shim, H.-N., Blackwell, T. and Luong, T. (2018) Oxidative stress increases M_1dG, a major peroxidation-derived DNA adduct, in mitochondrial DNA. *Nucleic Acids Research*, 46 (7), 3458-3467.

Wermuth, C.G. (2008) *The Practice of Medicinal Chemistry*. 3rd ed. Elsevier Science.

Wheatley, R.A. (2000) Some recent trends in the analytical chemistry of lipid peroxidation. *TrAC Trends in Analytical Chemistry*, 19 (10), 617-628.

Whitford, D. (2005) *Proteins : structure and function*. Chichester: Chichester: John Wiley.

William, N.W., John, V.H., Edward, S.K. and Scott, M.L. (2009) Molecular targets for cancer chemoprevention. *Nature Reviews Drug Discovery*, 8 (3), 213.

Workman, P. and Collins, I. (2014) *Chapter 1 - Modern Cancer Drug Discovery: Integrating Targets, Technologies, and Treatments for Personalized Medicine*. Elsevier Inc.

World Health Organization (2014) *Global status report on alcohol and health, 2014* [online], Available at:

https://www.who.int/substance_abuse/publications/global_alcohol_report/msb_gsr_2014_1.pdf

World Health Organization (2018) *Latest global cancer data: Cancer burden rises to 18.1 million new cases and 9.6 million cancer deaths in 2018* [online]

Available at: https://www.who.int/cancer/PRGlobocanFinal.pdf

Wu, D. and Yotnda, P. (2011) Production and detection of reactive oxygen species (ROS) in cancers. *Journal of Visualized Experiments* (57), e3357.

Wu, K.C., McDonald, P.R., Liu, J. and Klaassen, C.D. (2014) Screening of natural compounds as activators of the keap1-nrf2 pathway. *Planta Medica*, 80 (1), 97-104.

Wu, X.J. (2005) The role of reactive oxygen species (ROS) production on diallyl disulfide (DADS) induced apoptosis and cell cycle arrest in human A549 lung carcinoma cells. *Mutation Research*, 579 (1-2), 115.

Xiong, D. (2018) Isoliquiritigenin alleviated the Ang II-induced hypertensive renal injury through suppressing inflammation cytokines and oxidative stress-induced apoptosis via Nrf2 and NF-κB pathways. *Biochemical and Biophysical Research Communications*, 506 (1), 161.

Xue, Y., Mou, J., Liu, Y., Gong, X., Yang, Y. and An, L. (2010) An ab initio simulation of the UV/Visible spectra of substituted chalcones. *Central European Journal of Chemistry*, 8 (4), 928-936.

Yagura, T., Motomiya, T., Ito, M., Honda, G., Iida, A., Kiuchi, F., Tokuda, H. and Nishino, H. (2008) Anticarcinogenic compounds in the Uzbek medicinal plant, Helichrysum maracandicum. *Journal of Natural Medicines*, 62 (2), 174.

Yamamoto, M., Kensler, T.W. and Motohashi, H. (2018) The KEAP1-NRF2 system: A thiol-based sensor-effector apparatus for maintaining redox homeostasis. *Physiological Reviews*, 98 (3), 1169-1203.

Yang, H., Du, Z., Wang, W., Song, M., Sanidad, K., Sukamtoh, E., Zheng, J., Tian, L., Xiao, H. and Liu, Z. (2017) Structure–activity relationship of curcumin: role of the methoxy group in anti-inflammatory and anticolitis effects of curcumin. *Journal of Agricultural and Food Chemistry*, 65 (22), 4509-4515.

Yang, L., Su, L., Cao, C., Xu, L., Zhong, D., Xu, L. and Liu, X. (2013) The chalcone 2′-hydroxy-4′, 5′-dimethoxychalcone activates death receptor 5 pathway and leads to apoptosis in human nonsmall cell lung cancer cells. *International Union of Biochemistry and Molecular Biology Life*, 65 (6), 533-543.

Yao, J. (2015) Xanthohumol, a polyphenol chalcone present in hops, activating Nrf2 enzymes to confer protection against oxidative damage in PC12 cells. *Journal Of Agricultural and Food Chemistry*, 63 (5), 1521.

Yao, J., Peng, S., Xu, J. and Fang, J. (2019) Reversing ROS-mediated neurotoxicity by chlorogenic acid involves its direct antioxidant activity and activation of Nrf2-ARE signaling pathway. *BioFactors*, 45 (4), 616-26.

Yao, Y., Zhang, J., Tian, P., Li, L., Huang, X., Nawutayi, M., Huang, Y. and Zhang, C. (2019) Passive smoking induces rat testicular injury via the FAS/FASL pathway. *Drug and Chemical Toxicology*, 1-9.

Yates, S.A. (2015) *The Cytotoxic Effects of Malondialdehyde on Human Lung Fibroblast Cells*thesis, Liverpool John Moores University

Yates, S.A., Murphy, M.F. and Moore, S.A. (2019) The effect of malondialdehyde is modified by simian virus 40 transformation in human lung fibroblast cells. *Toxicology*, 415, 1.

Ye, X. (2017) *Phytochemicals in Citrus: Applications in Functional Foods*. CRC Press.

Ye, C.-L., Liu, X.-G. and Huang, Q. (2013) Antioxidant activity and protection of human umbilical vein endothelial cells from hydrogen peroxide-induced injury by DMC, a chalcone from buds of Cleistocalyx operculatus. *South African Journal of Botany*, 86, 36-40.

Yildizhan, H., Barkan, N.P., Turan, S.K., Demiralp, Ö., Demiralp, F.D.Ö., Uslu, B. and Ōzkan, S.A. (2018) Treatment strategies in cancer from past to present. In: (ed.) *Drug Targeting and Stimuli Sensitive Drug Delivery Systems.* Elsevier. pp. 1-37.

Yosef, H.A.A., Ibrahima, N.M., El-Hussienya, M., RH, M., Mahrana, M.M.A. and Mahmoudb, A.E. (2016) Synthesis, stereochemistry and antitumor evaluation of some novel chalcone derivatives. *Journal of Chemical and Pharmaceutical Research*, 8 (7), 943-957.

Yoshizaki, Y., Mori, T., Ishigami-Yuasa, M., Kikuchi, E., Takahashi, D., Zeniya, M., Nomura, N., Mori, Y., Araki, Y. and Ando, F. (2017) Drug-repositioning screening for Keap1-Nrf2 binding inhibitors using fluorescence correlation spectroscopy. *Scientific Reports*, 7 (1), 3945.

Yu, J.B., Soulos, P.R., Cramer, L.D., Decker, R.H., Kim, A.W. and Gross, C.P. (2015) Comparative effectiveness of surgery and radiosurgery for stage I non–small cell lung cancer. *Cancer*, 121 (14), 2341-2349.

Yu, W.-D., Sun, G., Li, J., Xu, J. and Wang, X. (2019) Mechanisms and therapeutic potentials of cancer immunotherapy in combination with radiotherapy and/or chemotherapy. *Cancer Letters*, 452, 66-70.

Zampini, I.C. (2008) Evaluation of genotoxic and antigenotoxic effects of hydroalcoholic extracts of *Zuccagnia punctata* Cav. *Journal of Ethnopharmacology*, 115 (2), 330-336.

Zhang, H., Liu, Y.-y., Jiang, Q., Li, K.-r., Zhao, Y.-x., Cao, C. and Yao, J. (2014) Salvianolic acid A protects RPE cells against oxidative stress through activation of Nrf2/HO-1 signaling. *Free Radical Biology and Medicine*, 69, 219-228.

Zhang, M., Chang, Z., Zhao, F., Zhang, P., Hao, Y.-J., Yan, L., Liu, N., Wang, J.-L., Bo, L., Ma, P., Zhou, W., Ma, X., Xu, Q.-B. and Zhou, R. (2019) Protective Effects of 18[BETA]-Glycyrrhetinic Acid on Monocrotaline-Induced Pulmonary Arterial Hypertension in Rats. *Frontiers in Pharmacology*, 10.

Zhang, R., Humphreys, I., Sahu, R.P., Shi, Y. and Srivastava, S.K. (2008) *In vitro* and *in vivo* induction of apoptosis by capsaicin in pancreatic cancer cells is mediated through ROS generation and mitochondrial death pathway. *Apoptosis*, 13 (12), 1465-1478.

Zhang, Y., Dai, M. and Yuan, Z. (2018) Methods for the detection of reactive oxygen species. *Anal. Methods*, 10 (38), 4625-4638.

Zhang, Y., Hou, Y., Liu, C., Li, Y., Guo, W., Wu, J.-L., Xu, D., You, X., Pan, Y. and Chen, Y. (2016) Identification of an adaptor protein that facilitates Nrf2-Keap1 complex formation and modulates antioxidant response. *Free Radical Biology and Medicine*, 97, 38-49.

Zhao, X. (2017) Novel indolyl-chalcone derivatives inhibit A549 lung cancer cell growth through activating Nrf-2/HO-1 and inducing apoptosis *in vitro* and *in vivo*. *Scientific Reports*, 7 (1), 3919.

Zhao, X., Dong, W., Gao, Y., Shin, D.-S., Ye, Q., Su, L., Jiang, F., Zhao, B. and Miao, J. (2017) Novel indolyl-chalcone derivatives inhibit A549 lung cancer cell growth through activating Nrf-2/HO-1 and inducing apoptosis *in vitro* and *in vivo*. *Scientific Reports*, 7 (1), 3919.

Zhou, B. and Xing, C. (2015) Diverse molecular targets for chalcones with varied bioactivities. *Medicinal Chemistry*, 5 (8), 388.

Zhou, X. (2019) Peroxynitrite contributes to arsenic-induced PARP-1 inhibition through ROS/RNS generation. *Toxicology and Applied Pharmacology*, 378, 114602.

Zhuang, C., Zhang, W., Sheng, C., Zhang, W., Xing, C. and Miao, Z. (2017) Chalcone: a privileged structure in medicinal chemistry. *Chemical Reviews*, 117 (12), 7762-7810.

Zi, X. and Simoneau, A.R. (2005) Flavokawain A, a novel chalcone from kava extract, induces apoptosis in bladder cancer cells by involvement of Bax protein-dependent and mitochondria-dependent apoptotic pathway and tumor growth in mice. *Cancer Research*, 65 (8), 3479-3486.

LIST OF CONFERENCES

- Hiba Jasim, Professor Satya Sarker, Dr Sharon Moore and Dr Kenneth Ritchie. *Assessment of synthetic chalcones as cancer chemopreventive agents*, PSE Young Scantest Meeting 2017, Lille, France, (Oral).

- Hiba Jasim, Professor Satya Sarker, Dr Sharon Moore and Dr Kenneth Ritchie. *Assessment of synthetic chalcones as cancer chemopreventive agents*. The 9th MMU Postgraduate Research Conference 2017, Manchester, UK, (Poster).

- Hiba Jasim, Professor Satya Sarker, Dr Sharon Moore and Dr Kenneth Ritchie. *Assessment of synthetic chalcones as cancer chemopreventive agents*. The pharmaceutical analysis postgraduate research awards and careers symposium 2017, Royal Society of Chemistry, London, UK. (Poster).

- Hiba Jasim, Satyajit D Sarker, Sharon A. Moore, Ketan Ruparelia, Randolph Arroo and Kenneth Ritchie. *Evaluation of synthetic chalcones on MRC-5 and MRC-5 SV2 cell line viability*. Young Scientists' Meeting on Advances in Phytochemical Analysis (Trends in Natural Products Research), Phytochemical Society of Europe 2018, Liverpool, United Kingdom. (Poster).

- Hiba A. Jasim, Satyajit D Sarker, Sharon A. Moore, Ketan Ruparelia, Randolph Arroo and Kenneth J. Ritchie. *Chemopreventive effect of synthetic chalcones against MDA on MRC 5 cell line*. International PSE Symposium on Natural Products in Cancer Prevention and Therapy 2018, Naples, Italy. (Oral).

- Hiba A. Jasim, Satyajit D Sarker, Sharon A. Moore, Ketan Ruparelia, Randolph Arroo3 and Kenneth J. Ritchie. *Cytotoxic activity of Synthetic chalcones in MRC-5 SV2 cell line.* Natural Product Research – PSE-Young Scientists' Meeting Biochemistry, Molecular Aspects and Pharmacology of Bioactive Natural Products 2019, Budapest, Hungary. (Oral).